

GEOLOGY FOR SOCIETY

SINCE 1858



**GEOLOGICAL
SURVEY OF
NORWAY**

· NGU ·



REPORT

Report no.: 2019.031		ISSN: 0800-3416 (print) ISSN: 2387-3515 (online)	Grading: Open
Title: Geophysical and geological investigations of graphite occurrences in Vesterålen, Northern Norway, in 2018 and 2019			
Authors: J.S. Rønning, H. Gautneb, B.E. Larsen, V.C. Baranwal, B. Davidsen, A.K. Engvik, J. Gellein, J. Knežević, F. Ofstad, Xiuyan Ren & G. Viken.		Client: Nordland County Administration Geological Survey of Norway (NGU)	
County: Nordland		Municipality: Bø, Hadsel, Sortland and Øksnes	
Map-sheet name (M=1:250,000) Svolveær		Map-sheet no. and -name (M=1:50,000) 1131 I Austvågøya 1132 I Nykvåg, 1132 II Stokmarknes 1232 III Sortland, 1232 IV Myre	
Deposit name and grid-reference: WGS 84 UTM 33 Several, see report text for details.		Number of pages: 212 Price (NOK): 600,- Map enclosures:	
Fieldwork carried out: June and August 2018 August – September 2019	Date of report: 30.11.2019	Project no.: 371100	Person responsible: 
<p>Summary: Several potential graphite occurrences in Vesterålen were selected for follow-up work based on helicopter-borne geophysical data. The purpose for this is to confirm the existence of the graphite and next to briefly evaluate the quality and quantity of the graphite-bearing structures. The goal for the project, which is sponsored by Nordland county administration, is to increase the knowledge of each individual graphite occurrence. By doing so, the interest in graphite prospecting in Northern Norway may increase, effective prospecting can be implemented, and land planning can be developed with appropriate regard for areas with potential for economic graphite.</p> <p>NGU has, in the course of this project (2015 – 2019), visited 31 potential graphite occurrences in Vesterålen. Eleven were previously known and the knowledge of these has increased. 20 new occurrences were discovered and partly mapped. Low resistivity from helicopter-borne measurements in three locations is most likely explained by other reasons than graphite. No work was undertaken in areas where follow-up investigations (detailed geophysics, geological mapping, sampling and drilling) have previously been executed.</p> <p>Only reconnaissance geological work was performed in some of these 31 locations. Others were mapped by geophysical ground measurements, and shallow core drilling was undertaken in six locations. An evaluation of the graphite occurrences was performed based on all the new data. Seven occurrences were given grade A (>one million tons of flake graphite), three got the grade B (between 500,000 and 1,000,000 t), three got the grade C (between 200,000 and 500,000 t), six occurrences got the grade D (100,000 – 200,000 t flake graphite) and six grade E (< 100, 000 t graphite). Three objects are probably caused by non-graphitic material (Grade F). NGU would like to stress that these are to be considered as individual standardized evaluations of the graphite occurrences and not at all as a kind of resource estimation.</p> <p>Occurrences of grades C, D and E are probably not of any economic interest today. Occurrences of grades A and B are interesting, and these are recommended for further, more detailed investigations. These can be further geophysical measurements that are able to “see” deeper than the EM31 instrument and deeper core drilling. These investigations are expensive and must be financed by prospecting or mining companies.</p>			
Keywords: Graphite	Geology	Quality	
Geophysics	Electromagnetic	Electrical	
Mapping	Analytical methods	Scientific report	

Executive summary

Aim:

To increase the knowledge of known and previously unknown graphite occurrences in Vesterålen and to make the data available for prospecting companies. This report is regarded as an update and enhancement of the results released in 2017 (Gautneb et al. 2017, Rønning et al. 2017) and 2018 (Rønning et al. 2018).

Methods:

- Ground geophysical follow-up: electric (CP/SP and ERT/IP) and electromagnetic surveying (EM31) of the mineralised areas.
- Representative sampling of outcropping graphite-bearing rocks.
- Shallow core-drilling, sampling of graphite-bearing sections and analysis of these sections.
- Petrographical characterisation of the graphite bearing rock units.

Results:

A table summarizing the content of total carbon (TC %) in the different areas and localities is shown in Chapter 10.1 (cut-off 0.5% TC). Data from earlier investigations are included. A summary of average Total Carbon contents is given in the Table below.

The number of graphite-bearing zones and their strike lengths were estimated using the available geophysical and geological information from each locality. The thicknesses of the zones were estimated from detailed geophysical data, observations in the field and partly from drilling. The thicknesses used in the volume estimates below are corrected for the average dip. The tonnage of graphite ore is calculated using an average graphite schist density of 2.6 t/m³ and the tonnage of graphite by multiplying with the average TC content in the occurrences.

The importance of the occurrences is graded in the following manner:

Grade A: More than 1.0 million t graphite

Grade B: Between 0.5 and 1.0 million t graphite

Grade C: Between 0.2 and 0.5 million t graphite

Grade D: Between 0.1 and 0.2 million t graphite

Grade E: Less than 0.1 million t graphite.

Objects that most probably do not contain graphite are given grade F.

Area Locality	Estimated volume (m ³)	Average TC content (%)	Estimated tonnage of graphite ore (t)	Estimated tonnage of graphite (10 ⁶ t)	Occurrence importance (Ranking)	Comments. Data from?
Bø Municipality						
Haugsnæs	3 438 696	19,3	8 940 609	1,7	A	Many thin structures
Høgmyran	1 838 507	?	4 780 117	?	B	No graphite samples
Kjerkhaugen	989 949	6,5	2 573 869	0,17	D	Only two samples
Møklund	1 392 558	9,0	3 620 652	0,33	C	Many short structures
Sund	0		0	0	F	No graphite
Olsetvatnet	?	?		?	?	Uncertain, graphite?
Rise	76 604	7,9	199 172	0,02	E	Short structure
Sommarland	346 410	12,1	900 666	0,11	D	Many short structures
Øyjorda	0		0	0	F	No graphite

Area	Estimated volume (m ³)	Average TC content (%)	Estimated tonnage of graphite ore (t)	Estimated tonnage of graphite (10 ⁶ t)	Occurrence importance (Ranking)	Comments. Data from?
Sortland Municipality						
Brenna	3 247 595	10,1	8 443 748	0,86	B	Many structures
Evassåsen	866 025	7,4	2 251 666	0,17	D	Two folded structures
Vikeid East	2 047 880	?	5 324 488		B	No samples
Vikeid Central	3 637 307	13,8	9 456 997	1,30	A	Three structures
Vikeid West	12 124 356	10,4	31 523 325	3,28	A	Five structures
Reinsnesøya	0		0	0	F	No graphite
Sæterstranda	77 135	15,8	200 550	0,03	E	One short structure
Ånstad	86 603	39,1	225 167	0,09	E	One short structure
Øksnes Municipality						
Alsvåg	103 923	8,0	270 200	0,02	E	Three structures
Instøya	6 062 178	8,6	15 761 662	1,40	A	Three long structures
Myre	42 426 407	?			A	Great area, uncertain
Rødhamran	565 685	13,7	1 470 782	0,20	C	Four structures
Romset	3 939 231	14,7	10 242 001	1,50	A	Two structures
Skogsøya	579 555	19,0	1 506 844	0,29	C	No ground geophysics
Smines	7 727 407	7,1	20 091 257	1,40	A	Uncertain, few data
Steinland	?				?	Graphite?
Straumen	39 392	11,6	102 420	0,01	E	Three short structures (?)
Svinøya	69 282	23,4	180 133	0,04	E	Short, under sea?
Hadsel Municipality						
Korsodden	0		0	0	F	No graphite
Sellåter	984 808	6,3	2 560 500	0,16	D	One short structure
Sommarhus	300 000	24,1	780 000	0,19	D	Two bodies?
Morfjord mine	260 000	18,5	676 000	0,13	D	Three structures
Total	93 227 493		132 082 826	13,4		

The purpose of these tonnage estimations is to compare the amount of graphite in the different localities using a common approach.

Conclusions / Recommendations

The geophysical anomalies and the different localities associated with graphite in Vesterålen have been investigated to the degree of detail that is natural for NGU. NGU teams have identified localities that have indicated resources of several 100-thousands of tons of graphite. No reserve calculations are available, but a number of localities, graded A and B above, are targets recommended for further investigation by mining companies.

Future work by NGU will involve object-related follow-up work on new graphite localities that might be found or where we see that important data are lacking.

Sammendrag på norsk.

Som en del av prosjektet *Mineralressurser i Nord-Norge* (MINN) ble det i 2013 foretatt geofysiske målinger fra helikopter over hele Langøya og deler av Austvågøya i Vesterålen and Lofoten. Disse målingene viste flere markerte elektromagnetiske anomalier, delvis knyttet til kjente grafittforekomster og delvis på mulige nye hittil ukjente forekomster. For å øke kunnskapen om de enkelte mineraliseringene foreslo NGU i 2016 et oppfølgingsprosjekt der en ser nærmere på størrelse og kvalitet av de forskjellige forekomstene. Prosjektet har fått støtte fra Nordland Fylkeskommune både i 2015, 2016, 2017 og 2018. Undersøkelser gjennomført i 2015 og 2016 ble rapportert vinteren 2017 (Rønning et al. 2017, Gautneb et al. 2017). Undersøkelsene utført i 2017 ble rapportert våren 2018 (Rønning et al. 2018). Undersøkelsene fra 2018 og 2019 beskrives i denne rapporten. NGU anser med dette sitt arbeid i samarbeid med Nordland Fylkeskommune som avsluttet, og videre arbeid må komme i samarbeid med prospekteringselskaper.

For å gjøre dataene tilgjengelig for internasjonale selskaper er alle rapportene skrevet på engelsk og på et faglig nivå som krever kompetanse innenfor geologi og geofysikk. Bruksområder og marked for grafitt er ikke omtalt. Vår bruk av stedsnavn lokalt og regionalt er gjort i forhold til vårt behov og slik som området er kjent blant internasjonal gruve og prospekteringsindustri. Dette kan avvike fra den lokale navnebruken.

I 2018 ble det foretatt undersøkelser på følgende lokaliteter:

Bø kommune

1. Høgmyran
2. Rise - Olsetvatnet - Kjerkhaugen (ny 2018)
3. Øyjorda (ny 2018)
4. Møkland - Sund
5. Kvern fjorden

Sortland kommune

6. Brenna
7. Evassåsen (ny 2018)
8. Ånstad (ny 2018)
9. Sæterstranda (Ny 2019)
10. Vikeid (øst, midtre og vest)

11. Reinsnesøya (ny 2019)

Øksnes kommune

12. Smines
13. Romsetfjorden
14. Steinland (ny 2018)
15. Myre
16. Alsvåg – Instøya – Straumen (ny 2019)

Hadsel kommune

17. Korsodden (ny 2018),
18. Sellåter
19. Sommarhus

I tillegg er det tidligere avsluttet undersøkelser på elleve lokaliteter (Gautneb et al. 2017, Rønning et al. 2017, Rønning et al. 2018). I områder markert med (ny), er det tidligere ikke utført noe arbeid av NGU. I de andre områdene er resultatene fra tidligere undersøkelser (2016 – 2017) tatt med for å gjøre presentasjonene komplette. I 2018 er det utført oppfølgende geofysiske arbeider med instrumentet EM31 og resistivitetsmålinger i kombinasjon med Indusert Polarisasjon (ERT/IP). I tillegg er det utført noe geologisk rekognosering med prøvetaking og det er kjerneboret 5 korte hull på tre lokaliteter (Vikeid, Myre og Sommarhus). Utgangspunktet for de oppfølgende arbeidene er magnetiske og elektromagnetiske målinger fra helikopter utført av NGU i 2013.

Hovedresultater:

Hvis vi lister opp de estimerte volum og antar en egenvekt på 2.6 t/m³ og antar at våre analyser fra den enkelte lokalitet er representative, kan vi sette opp en oversikt over mengde malm og mengde grafitt i hver lokalitet.

Area Locality	Estimert volum (m ³)	Snitt karbon- innhold (%)	Estimert tonnasje grafittmalm (t)	Estimert tonnasje grafitt (10 ⁶ t)	Forekomst viktighet (Gradering)	Kommentarer. NGU-rapport med dokumentasjon
Bø Kommune						
Haugsnæs	3 438 696	19,3	8 940 609	1,7	A	2018.011
Høgmyran	1 838 507	?	4 780 117	?	B	Ingen prøver 2019.031
Kjerkhaugen	989 949	6,5	2 573 869	0,17	D	2019.031
Møkland	1 392 558	9,0	3 620 652	0,33	C	2017.014, 2017.015
Sund	0		0	0	F	Ikke grafitt 2019.031
Olsetvatnet	?	?	?	?	?	Usikker 2019.031
Rise	76 604	7,9	199 172	0,02	E	Ikke geofysikk 2019.031
Sommarland	346 410	12,1	900 666	0,11	D	2018.011
Øyjorda	0		0	0	F	2019.031
Sortland Kommune						
Brenna	3 247 595	10,1	8 443 748	0,86	B	2018.011, 2019.031
Evassåsen	866 025	7,4	2 251 666	0,17	D	2019.031
Vikeid East	2 047 880	?	5 324 488		B	Ikke prøve 2019.031
Vikeid Central	3 637 307	13,8	9 456 997	1,30	A	2019.031
Vikeid West	12 124 356	10,4	31 523 325	3,28	A	2019.031
Reinsnesøya	0		0	0	F	Ikke grafitt 2019.031
Sæterstranda	77 135	15,8	200 550	0,03	E	2019.031
Ånstad	86 603	39,1	225 167	0,09	E	2019.031
Øksnes Kommune						
Alsvåg	103 923	8,0	270 200	0,02	E	2019.031
Instøya	6 062 178	8,6	15 761 662	1,40	A	2019.031
Myre	42 426 407	?			A	Stor, få data 2019.031
Rødhamran	565 685	13,7	1 470 782	0,20	C	2018.011
Romset	3 939 231	14,7	10 242 001	1,50	A	2019.031
Skogsøya	579 555	19,0	1 506 844	0,29	C	2017.015
Smines	7 727 407	7,1	20 091 257	1,40	A	Usikker, få data 2019.031
Steinland	?				?	Ingen prøver 2019.031
Straumen	39 392	11,6	102 420	0,01	E	2019.031
Svinøya	69 282	23,4	180 133	0,04	E	2017.015
Hadsel Kommune						
Korsodden	0		0	0	F	Ikke grafitt 2019.031
Sellåter	984 808	6,3	2 560 500	0,16	D	2019.031
Sommarhus	300 000	24,1	780 000	0,19	D	2019.031
Morfjord gruve	260 000	18,5	676 000	0,13	D	2018.011
Totalt	93 mill.		132 mill.	13,4		

Usikre anslag viser at det i Vesterålen kan finnes ca. 132 millioner tonn grafittmalm med et gjennomsnittlig grafittinnhold på 13,2 % eller i overkant av 13 millioner tonn grafitt. Usikre forekomster er da ikke regnet med. Av i alt 31 undersøkte forekomster har ti fått graderingen A eller B (henholdsvis større enn 1 mill. tonn og 0,5 mill. tonn grafitt). Disse er interessante for mer detaljerte undersøkelser, og kan være av nasjonal eller internasjonal betydning i henhold til dagens klassifisering (Dahl et al. 2014). Forekomster av nasjonal eller internasjonal betydning skal tas hensyn til ved kommunenes arealforvaltning.

Contents

Executive summary	3
1. INTRODUCTION	13
1.1 Physiography and landownership.....	15
2. GEOLOGICAL SETTING	15
3. HISTORICAL BACKGROUND, PREVIOUS AND ONGOING INVESTIGATIONS	17
4. GEOPHYSICAL AND GEOLOGICAL METHODS	18
4.1 Geophysical methods.....	18
4.1.1 Helicopter-borne Electromagnetic Measurements	18
4.1.2 Ground EM and magnetic methods (Modified EM31).....	20
4.1.3 Charged Potential and Self Potential methods.....	21
4.1.4 2D resistivity (ERT) and Induced Polarization (IP).....	23
4.1.5 Resistivity Drill-hole logging	25
4.2 Geological methods.....	25
4.2.1 Definitions of graphite types.....	25
4.2.2 Analytical methods	27
4.2.3 Core drilling, sampling and analyses	28
5. SELECTION OF FOLLOW-UP OCCURRENCES	30
5.1 Petrophysical properties of graphite	30
5.2 Data from helicopter-borne measurements at Langøya, Vesterålen.....	31
5.3 Data from helicopter-borne measurements at Austvågøya, Lofoten.....	37
5.4 Selected areas for follow-up work.....	40
6. RESULTS OF FOLLOW-UP WORK IN BØ MUNICIPALITY	41
6.1 Høgmyran.....	42
6.1.1 Geophysical work, EM31.....	42
6.1.2 Geophysical work, ERT/IP	44
6.1.3 Høgmyran summary	46
6.2 Rise – Olsetvatnet - Kjerkhaugen	46
6.2.1 Geophysical work, EM31.....	46
6.2.2 Geophysical work, ERT/IP	48
6.2.3 Geological work, sampling	49
6.2.4 Summary Rise – Olsetvatnet - Kjerkhaugen	49
6.3 Øyjorda	51
6.3.1 Geophysical work, ERT/IP	51
6.3.2 Summary Øyjorda.....	52

6.4	Møkland-Sund	53
6.4.1	Geophysical work, EM31	53
6.4.2	Geophysical work, ERT/IP	53
6.4.3	Summary, Møkland - Sund	56
6.5	Kvern fjorden	57
6.5.1	Geophysical and geological work in 2016 and 2017	57
6.5.2	Geophysical work in 2018, EM31	59
6.5.3	Summary Kvern fjorden.....	59
7.	RESULTS OF THE FOLLOW-UP WORK IN SORTLAND MUNICIPALITY	62
7.1	Brenna	63
7.1.1	Geophysical work, EM31.....	63
7.1.2	Geophysical work, ERT/IP	63
7.1.3	Geological work, Sampling.....	65
7.1.4	Brenna summary.	66
7.2	Ånstad.....	68
7.2.1	Geophysical work, EM31.....	68
7.2.2	Geological work, sampling and analysis.....	68
7.2.3	Geophysical work, ERT/IP	71
7.2.4	Summary Ånstad	71
7.3	Evassåsen	72
7.3.1	Geophysical work, EM31.....	72
7.3.2	Geological work, sampling	72
7.3.3	Geophysical work, ERT/IP	74
7.3.4	Summary Evassåsen.....	76
7.4	Vikeid East (Storelvbukta).....	76
7.4.1	Geophysical work, EM31.....	76
7.4.2	Geophysical work, ERT/IP	78
7.4.3	Summary Vikeid East	79
7.5	Central Vikeid (Vedåsen).....	79
7.5.1	Geophysical work, EM31.....	79
7.5.2	Geophysical work, ERT/IP	81
7.5.3	Geological work, sampling and analyses.....	82
7.5.4	Summary Vikeid Central area	82
7.6	Vikeid West (Vikeidet)	84
7.6.1	Geophysical work, EM31.....	84
7.6.2	Geophysical work, ERT/IP	86
7.6.3	Geophysical work, CP/SP	87
7.6.4	3D Inversion of helicopter-borne EM data	91
7.6.5	Geological work, sampling and analysis.....	94

7.6.6	Geological work, core drilling	94
7.6.7	Summary Vikeid West	96
7.7	Reinsnesøya.....	97
7.7.1	Geophysical work, EM31.....	97
7.7.2	Reinesøya summary.....	97
7.8	Sæterstranda.....	98
8.	RESULTS FROM THE FOLLOW-UP WORK IN ØKSNES MUNICIPALITY ...	100
8.1	Smines.....	101
8.1.1	Geophysical work, EM31.....	101
8.1.2	Geophysical work, CP/SP	103
8.1.3	Geophysical work, ERT/IP	105
8.1.4	Geological work, outcrops, samples and analysis.....	106
8.1.5	Summary Smines	107
8.2	Romsetfjorden	107
8.2.1	Geophysical work, EM31.....	107
8.2.2	Geological work, observations, sampling analysis.....	110
8.2.3	Summary Romsetfjorden.....	111
8.3	Steinland.....	113
8.3.1	Geophysical work, EM31.....	113
8.3.2	Geophysical work, ERT/IP	115
8.3.3	Summary Steinland	116
8.4	Myre.....	116
8.4.1	Geophysical work, EM31.....	117
8.4.2	Geophysical work, ERT/IP	117
8.4.3	Geological work, core drilling	122
8.4.4	Discussion and summary, Myre	124
8.5	Instøya – Alsvåg - Straumen.....	124
8.5.1	Instøya	125
8.5.2	Alsvåg	126
8.5.3	Straumen	130
8.5.4	Summary, Alsvåg – Instøya – Straumen	132
9.	RESULTS OF THE FOLLOW-UP WORK IN HADSEL MUNICIPALITY	133
9.1	Korsodden	134
9.1.1	Geophysical work, EM31.....	134
9.1.2	Geophysical work, ERT/IP	136
9.1.3	Summary Korsodden.....	137
9.2	Sellåter.....	137
9.2.1	Geophysical work, EM31.....	137

9.2.2	Geological work, sampling	139
9.2.3	Summary Sellåter	139
9.3	Sommarhus	141
9.3.1	Geophysical work, EM31.....	141
9.3.2	Geophysical work, ERT/IP	144
9.3.3	Geological work, sampling	145
9.3.4	Geological work, core drilling	145
9.3.5	Summary Sommarhus.....	148
10.	SUMMARY OF GRAPHITE QUALITY AND QUANTITY.....	150
10.1	Petrography of the graphite schist and associated rocks	150
10.1.1	Examples of thin sections.....	150
10.1.2	Particle analysis of graphite crystals.....	154
10.2	Summary of Carbon analysis, updated table	156
10.3	Summary of geometric information.....	159
10.4	Summary of tonnage estimates	161
11.	CONCLUSIONS AND RECOMMENDATIONS	163
12.	REFERENCES.....	164

APPENDICES

Appendix 1: Drill-core geology, log description

Appendix 2: Drill-core pictures

Appendix 3: Analysis of total sulphur (TS) and Total Carbon (TS) on drill-cores

Appendix 4: Portable XRF analysis of drill-cores.

Appendix 5: Electric conductivity (resistivity) from drill-hole logging.

Appendix 6: Complete list of analysed samples for TS, TC and TOC from 1990-2019

1. INTRODUCTION

Norway has been a major producer of graphite for more than 100 years and the geology in many places in the country favours the formation of flake graphite deposits. Graphite is a common mineral in Norwegian rocks. It is, however, rare to find it enriched in economically interesting amounts. There are more than 70 registered graphite occurrences in Norway. They are located in four graphite provinces (Figure 1.1). There has been historic graphite mining in all of these provinces. Today only one deposit, the Skaland graphite mine on the island of Senja, is in operation, producing ca. 10,000 tons of concentrate per year. The Lofoten-Vesterålen area and the island of Senja has numerous additional graphite occurrences.

In this report we will present the data and results from recent graphite exploration in ten potentially important graphite occurrences in Vesterålen and Lofoten. We will also give a brief review of the earlier work carried out in the area. In every chapter we will limit our descriptions to what is regarded relevant for the graphite mineralisation. More academic studies of the general geology and metamorphic petrology are reported by others elsewhere (Engvik et al. 2016, Griffin et al. 1978).

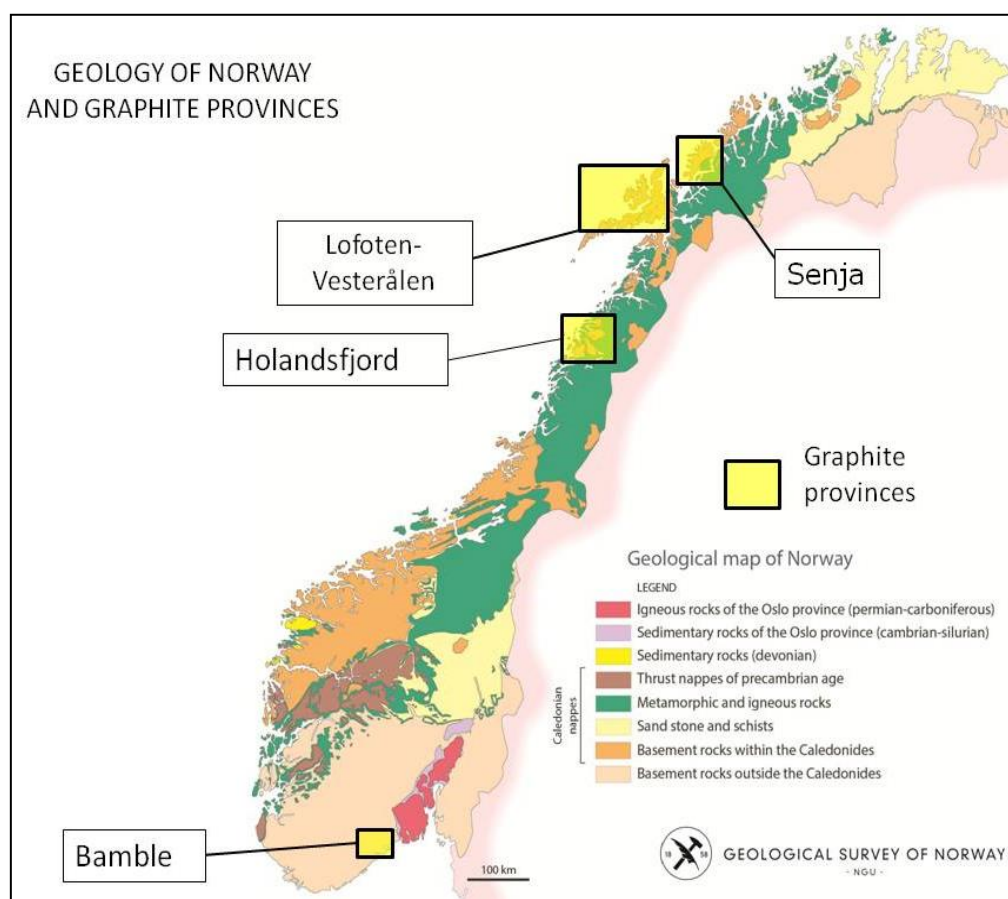


Figure 1.1: Geology and graphite provinces of Norway.

The investigations, which were planned for three years, are financially supported by Nordland County Administration. In the third year (2018), the investigations were concentrated at (easting and northing, WGS84 UTM Zone 33 N).

• Høgmyran, Bø Municipality	480700 - 7622400
• Rise, Bø Municipality	483200 - 7623000
• Kjerkhaugen, Bø Municipality	484000 - 7622200
• Øyjorda, Bø Municipality	480000 - 7619400
• Møklund - Sund, Bø Municipality	485400 - 7626000
• Kvern fjorden, Bø Municipality	488500 - 7621300
• Brenna, Sortland Municipality	502200 - 7628800
• Evassåsen, Sortland Municipality	514900 - 7622000
• Ånstad, Sortland Municipality	515600 - 7623400
• Vikeid East, (Storelvbukta) Sortland Municipality	511000 - 7628500
• Vikeid Central (Vedåsen), Sortland Municipality	511000 - 7628500
• Vikeid West (Vikeidet), Sortland Municipality	509800 - 7627800
• Reinsnesøya, Sortland Municipality	518394 – 7699216
• Sæterstranda, Sortland Municipality	514266 - 7638389
• Romsetfjorden, Sortland Municipality	500600 – 7633500
• Smines, Øksnes Municipality	499000 - 7639000
• Steinland, Øksnes Municipality	506600 - 7638100
• Myre, Øksnes Municipality	506500 - 7643800
• Alsvågen, Øksnes Municipality	511154 - 7643640
• Instøya, Øksnes Municipality	512291 - 7644071
• Straumen, Øksnes Municipality	513074 - 7644785
• Korsodden, Hadsel Municipality	483900 - 7591100
• Sellåter, Hadsel Municipality	487850 - 7589200
• Sommarhus, Hadsel Municipality	487000 - 7589000

During the work the following people have contributed with their different areas of expertise:

- Vikas C. Baranwal: Interpretation of airborne magnetic and EM data.
- Børre Davidsen: Bedrock geology, mapping, sampling and analysis.
- Ane K. Engvik: Bedrock geology, mapping, sampling and analysis.
- Håvard Gautneb: Graphite geology, core drilling, analysis and petrography, responsible field geologist.
- Jomar Gellein: Ground follow-up geophysics.
- Janja Knežević: Graphite geology, core logging, sample preparation, petrography.
- Bjørn Eskil Larsen: Ground follow-up geophysics, processing of data, GIS.
- NGU-lab: All chemical analysis.
- Frode Ofstad: Airborne and ground follow-up geophysics, electronics.
- Xiuyan Ren: 3D inversion of electromagnetic (EM) data
- Geir Viken: Core drilling.
- Jan Steinar Rønning: Responsible geophysicist, reporting, report editing and project leader.

The authors thank Ron Boyd and Marco Brönnner (both NGU) for improving the English language.

1.1 Physiography and land ownership

The cadastral map of the area can be seen at www.seeiendom.no. During normal annual snow conditions all parts of the investigated areas can be accessed from the middle of May to the end of October. Snow can be expected on the mountain tops from mid-October. Prospectors interested in this area should check the web sites of the Norwegian Directorate of Mining (www.dirmin.no) for Norwegian mining regulations and possible rights to the graphite mineralisation.

2. GEOLOGICAL SETTING

The Lofoten-Vesterålen area in northern Norway is normally considered to be a part of the Baltic Shield. The graphite-bearing rocks in Vesterålen occur in sequences belonging to a Precambrian domain comprising Lofoten, Vesterålen and the western islands of Troms County (see Figure 2.1).

The general outlines of the geology were established in the 1960s and 1970s, following work by Heier (1960) and Griffin et al. (1978, and references therein). In broad terms, the area is composed of an Archaean to possibly Early Proterozoic basement of magmatic and metasedimentary rocks, intruded by an Early Proterozoic magmatic suite composed of anorthosite-mangerite-charnockite-granite (AMCG) rocks. Subsequent radiometric dating has confirmed the presence of Archaean and Early Proterozoic rocks (Corfu 2004 and 2007, Davidsen & Skår 2004). Most of the AMCG suite was intruded into the basement within a relatively narrow time interval from 1800 to 1790 Ma (Corfu 2004).

The supracrustal sequences are distributed as patches intermingled with the Archaean domains, with graphite-bearing rocks occurring with marbles, quartzites, banded iron formations and presumed felsic and mafic volcanic rocks. Polyphase high-grade metamorphism and deformation have obliterated most of the primary supracrustal features, and the sequence is now represented by various schists, gneisses and migmatites (Griffin et al. 1978, and references therein). The metamorphic event(s) reached peak conditions at $P = 0.8\text{--}0.9$ GPa and $T = 860\text{--}880$ °C (Engvik et al. 2016). The metasedimentary rocks and associated graphitic schists were thought to be of Early Proterozoic age (Griffin et al. 1978) but results from ongoing studies are less conclusive and hold open the possibility of an Archaean age for this sequence. The mapping resulted in the publication of the 1:250,000 map sheet Svolvær, covering the Lofoten and Vesterålen area (Tveten, 1978).

NGU has, subsequent to the studies of W. L. Griffin and co-workers, continued local mapping activities, leading to the publication of the preliminary 1:50,000 map sheet Sortland (Tveten 1990) and the 1:250,000 map sheet Andøy (Tveten and Henningsen, 1998). In 1988 most of the island of Langøya was measured with airborne geophysics (Mogaard et al. 1988). A number of the graphite localities described in this report were discovered during geological mapping.

Some of these activities were conducted as a part of the exploration for graphite resources in Vesterålen (Gautneb & Tveten, 1992, Gautneb, 1992, 1993 & 1995). This work was reviewed by Gautneb & Tveten (2000).

Renewed activities in the Vesterålen area started in 2011 under the MINN program at NGU (**M**ineral resources **I**n **N**orthern **N**orway), comprising general bedrock mapping and studies, helicopter-borne geophysics (Rodionov et al. 2013 a & b), and targeted mineral exploration. These activities have led to the discovery of several new graphite occurrences.

The units containing the graphite-bearing rocks are thus believed to be intermingled with Archaean rocks. This relationship is, however, not easy to observe in the field. Polyphased deformation combined with granulite-facies metamorphism, locally with anatexis, has obscured most primary contacts. The supracrustal units containing the graphite schists are also often intruded by younger intrusions. These field relationships are important as they have the consequence that the graphite layers and lenses in Lofoten – Vesterålen, even though airborne geophysical data can indicate a considerable size, are commonly cut by later intrusions and folds into segments with a limited size (areal extent). However, aggregated areas commonly represent economically interesting dimensions and conditions such as the metamorphic grade are favourable for high-quality graphite formation.

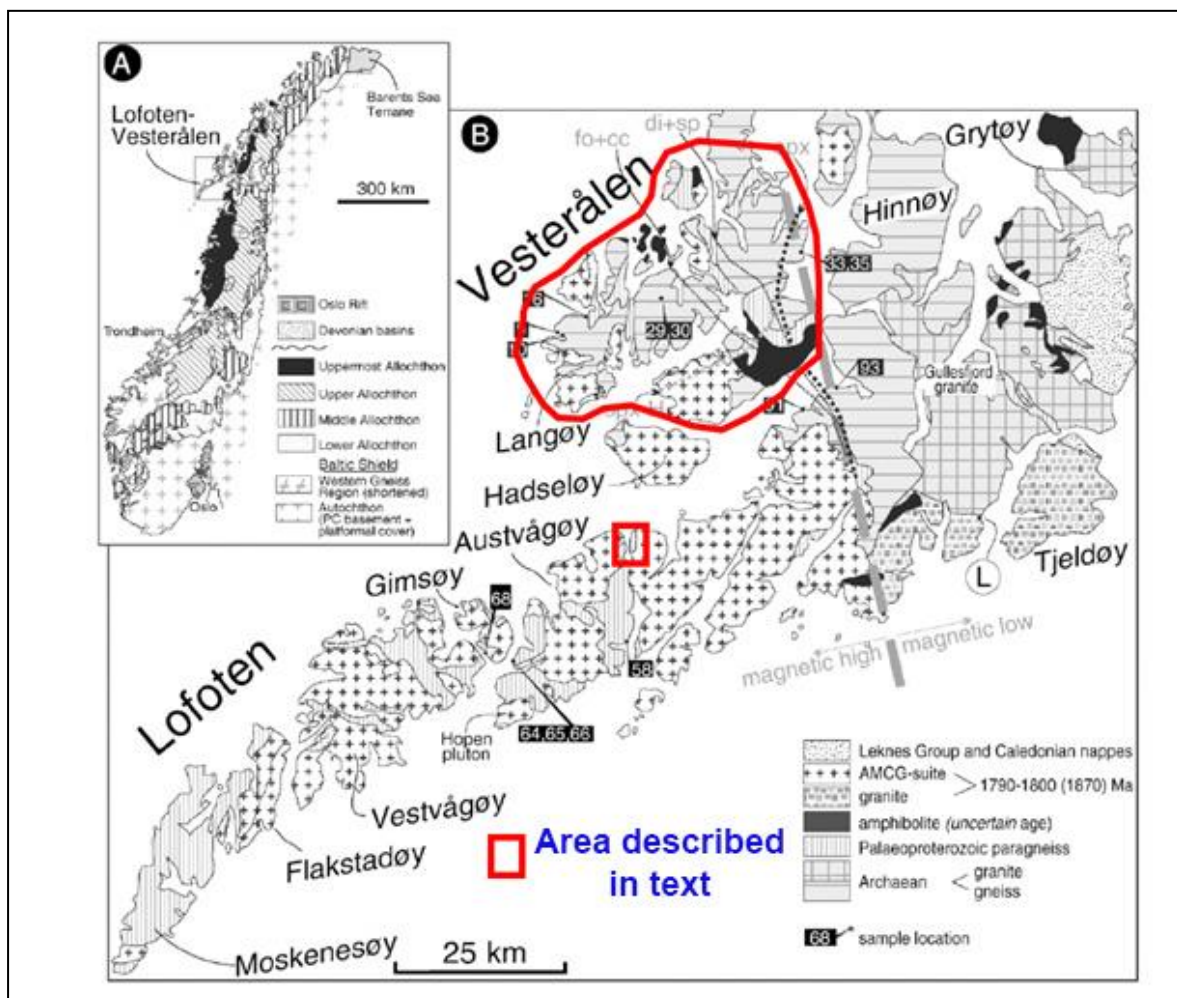


Figure 2.1: Simplified geological map of the Lofoten-Vesterålen islands (modified from Corfu 2007).

3. HISTORICAL BACKGROUND, PREVIOUS AND ON-GOING INVESTIGATIONS

The graphite deposits of Vesterålen were among the first in Norway to be described by geologists. Keilhau (1844) and Helland (1887) described several graphite deposits in Lofoten and Vesterålen. These occurrences had probably, by then, been known for some time. The British company, Anglo-Norwegian Mining, started mining in the Jennestad area around 1890 and the mine was in operation until 1914. Several other occurrences were explored and subjected to test mining during the same period. The Møklund, Sommarland and Morfjord occurrences were trenched and put into small-scale test production in this period.

All known graphite occurrences in Northern Norway were investigated in the early 1950s with respect to the occasional co-occurrence of uranium with graphite. The results were negative for most graphite occurrences with regard to the content of uranium (Neumann 1952).

The Jennestad graphite mines were in operation again from 1949 to 1960. Approximately 700 m of tunnels were mined out during this period. Unpublished reports describe the geology in the mines and their surroundings (Skjeseth 1952, Vokes 1954). Heier (1960) described the regional geology.

W.L. Griffin et al. (1978) investigated the crustal evolution of the Lofoten-Vesterålen rocks in the 1970s. They concluded that the graphite-bearing rocks were part of a supracrustal sequence comprising marbles, acid and basic volcanic rocks, banded iron formations and graphite schist. Polyphase high-grade (up to granulite facies) metamorphism and deformation have obscured most of the characteristics of the primary supracrustal rocks and they are now mapped as various types of gneisses and migmatites (Griffin et al. 1978 and references therein).

Part of Langøya was measured with airborne geophysics in 1988 (Mogaard et al. 1988). Only a part of this survey included electromagnetic measurements. Graphite occurrences in the Jennestad area were re-investigated with sampling, drilling and ground geophysics in the period 1990-1994. A total 1100 m of drilling was carried out on 15 different drill holes. At the Hornvann sub-locality proven reserves of 240,000 tons with a grade of 25 % graphitic carbon (Cg) were mapped (Gautneb & Tveten 1992, Dalsegg 1994, Gautneb 1993 & 1995, Rønning 1991 & 1993). This work was reviewed by Gautneb & Tveten (2000).

Corfu (2004 & 2007) performed radiometric dating, reviewed earlier work and studied the metamorphic evolution of selected rocks units in the Lofoten-Vesterålen area.

The junior company *Norwegian graphite* re-investigated the Jennestad area (Koven and Golia) by mapping and drilling in 2012 – 2013 (Sletten 2013). A total of 1365 m were core-drilled, distributed in 14 holes. Eleven parallel graphite lenses in Koven and two in the Golia area were mapped, extending 600 and 430 m along strike respectively. The structures are interpreted to dip 49 degrees to the north-northwest. The company found indicated reserves of 3.7 Mt with 9.6 % graphitic carbon. The thickness of the graphite-bearing units is reported to be up to 34 metres. *Norwegian graphite* was liquidated in 2016. Their reports are available and can be obtained from NGU (Håvard Gautneb) upon request.

NGU, as part of the MINN program (<http://www.ngu.no/prosjekter/minn>), carried out a new airborne geophysical survey, including electromagnetic measurements over the whole of Langøya (Rodionov et al. 2013a) and parts of Austvågøya in 2013 (Rodionov et al. 2013b). These surveys resulted in a large extension of the area with potential graphite deposits, with numerous new geophysical anomalies, and is the basis for the investigations in this project. The airborne geophysical survey is reviewed in more detail in Chapter 4.1.1.

Based on the helicopter-borne geophysics, ground based graphite investigations were performed in the area during 2015 and 2016 (Gautneb et al. 2017, Rønning et al. 2017), in 2017 (Rønning et al. 2018) and in 2018 (this report).

Parallel with our graphite exploration bedrock mapping, geochronology and metamorphic studies have been systematic undertaken by NGU staff. Unfortunately, little of this information is currently available apart from a few abstracts (Davidsen & Skår 2004, Engvik et al. 2016).

4. GEOPHYSICAL AND GEOLOGICAL METHODS

The resolution of helicopter-borne electromagnetic measurements is low and detailed ground measurements are necessary in order to achieve a good knowledge of the graphite deposits. Here we describe the methods used in the graphite investigations in 2016 and 2018.

4.1 Geophysical methods

The following geophysical methods were used in the graphite investigations in Vesterålen: Helicopter-borne electromagnetic (HEM), Charged Potential (CP), Self Potential (SP), 2D Resistivity (also called ERT), 2D Induced Polarisation (IP) and downhole logging of electric conductivity.

4.1.1 Helicopter-borne Electromagnetic Measurements

A new helicopter-borne geophysical survey was performed in Vesterålen in 2013, with a total of 5,650 line-km covering 1,050 km². The full technical description, including details of processing of the data collected, was reported by Rodionov et al. (2013a). The survey was performed using the instrumentation listed in Table. 4.1. A similar survey (1956 line-km, 390 km²) was performed in Lofoten in 2013 (Rodionov et al. 2013b).

The Electromagnetic (EM) instrumentation, Geotech Hummingbird (Geotech 1997), is able to map variations in electric conductivity in the ground and is the most useful method in graphite exploration. Details of frequencies, coil orientations and coil separation are shown in Table 4.2.

Table 4.1: Instrumentations used in the helicopter-borne geophysical surveys.

Instrument	Producer/Model	Accuracy	Sampling frequency
Magnetometer	Scintrex Cs-2	0,002 nT	5 Hz
Base magnetometer	GEM GSM-19	0.1 nT	0.33 Hz
Electromagnetic	Geotech Hummingbird	1 – 2 ppm	10 Hz
Gamma spectrometer	Radiation Solutions RSX-5	1024 ch's, 16 litres down, 4 litres up	1 Hz
Radar altimeter	Bendix/King KRA 405B	± 3 % 0 – 500 feet ± 5 % 500 –2500 feet	1 Hz
Pressure/temperature	Honeywell PPT	± 0,03 % FS	1 Hz
Navigation	Topcon GPS-receiver	± 5 metres	1 Hz
Acquisition system	NGU in house software		

Table 4.2: Configuration and frequencies of the Hummingbird EM equipment.

Coils:	Frequency	Orientation	Coil separation
A	7001 Hz	Coaxial	6.20 m
B	6600 Hz	Coplanar	6.20 m
C	980 Hz	Coaxial	6.025 m
D	880 Hz	Coplanar	6.025 m
E	34000 Hz	Coplanar	4.87 m

The apparent resistivity for each frequency was calculated based on "In phase" and "Out of phase" components of the EM data, using a half-space model of the earth (HEM-module, Geosoft 1997). Data can also be presented as profile maps, on which "In Phase" and "Out of phase" components for each frequency are plotted along the flight path.



Figure 4.1: Equipment used in the helicopter-borne geophysical survey in Vesterålen.

Inverted resistivity sections can be produced based on the measured "In phase" and "Out of phase" components for all frequencies. Available software for inversion of HEM data are EM1DFM (ElectroMagnetic 1D Frequency Measurements, UBC 2000) and AarhusInv (formerly called em1Dinv, AarhusInv 2013). These inversion codes create 2D images based, in principle, on 1D inversion. and, with vertical conducting structures, misleading images may be constructed. In one area (Vikeid West) the helicopter-borne EM data are inverted using the 3D HEM code published by Liu et al. (2018).

The main result from the geophysical surveys was a large extension of the area with potential for new graphite mineralisation, and a better definition of the areal extent of the known occurrences. This was the basis for defining new graphite targets to be followed up by ground investigations. Some of the occurrences described in this report were known previously, but the mineralised area is larger than previously known. Several new objects are derived from the interpretation of the new airborne geophysical data.

All the data from the helicopter survey can be downloaded from www.ngu.no as jpg-maps or as geo-referenced data sets (geotiff-files).

4.1.2 Ground EM and magnetic methods (Modified EM31)

Electromagnetic measurements from helicopter in the Lofoten and Vesterålen area (Rodionov et al. 2013a and 2013b) show many anomalies that might be caused by graphite. Some of these coincided with known graphite showings, others did not. The area is largely covered by soil and vegetation, so detailed geophysical measurements were necessary in order to locate possible new graphite mineralisation. In the first attempt to map known and possibly unknown graphite deposits, a ground conductivity meter Geonics EM31 (Geonics 1984) was used. This instrument is calibrated such that it measures the apparent electric conductivity directly in mS/m down to 6 – 7 m. The instrument has normally horizontal coplanar coils separated by 3.8 m and working at a frequency of 9,800 Hz.

NGU modified this instrument during the winter of 2017, including a GPS positioning system, magnetic sensor and a data logger. This made the measurements more effective and the quality of data were improved by continuous sampling and simultaneous registration of the magnetic field. Normal operation of the instrument produces one reading of apparent electric conductivity for each second. Measured apparent conductivity are presented as colour-coded dots where high electric conductivity is plotted on top of lower conductivities. In cases of dense measurements, this may give an over-representation of high apparent conductivities and details can be hidden. To overcome this problem, EM31 data in selected areas are plotted as profile curves. Apparent resistivity can be calculated as the inverse value of apparent conductivity.



Figure 4.2: Geonics EM31 used in graphite investigations in Vesterålen.

The EM31 is a very effective instrument for locating unexposed graphite deposits. We experienced a success rate of almost 100 % when excavating targets indicated by the instrument. Trenches were excavated based on the EM31 data and the underlying graphite deposits were revealed. However, EM31 like any other electric and electromagnetic instruments cannot discriminate between sulphides and graphite. Its penetration depth is a strong limitation and where the graphite mineralisation extends to a depth exceeding 10 m, the graphite mineralisation is hardly “discovered”.

Measurements with EM31 may, in some cases, show a negative apparent conductivity. This may happen when there is a vertical structure that is thinner than the coil separation of 3.8 m. In these cases, the apparent conductivity is read as -2 mS/m and given as black dots in the data presentation and labelled “Peak” in the legend.

4.1.3 Charged Potential and Self Potential methods

Charged Potential (CP) measurements are acquired by connecting a current electrode directly to the conductive body and locating the other remote electrode at a considerable distance to ensure that its effect is virtually non-existent in the survey area. The current can be injected through a surface outcrop or a drill-hole if no outcrops are available. The potential between two non-polarizable electrodes is then measured on the surface around the conductive body in a sequence of connected measurement-points. As long as the electric conductivity of the mineralisation is more than 1,000 times higher than that in the surrounding host rock, the electrical potential will, in practice, stay constant above the mineralisation, and then drop down when the measurements are outside the body (Figure 4.3). The body's length, dip and size can be mapped by measuring the potential around a known graphite body. In addition, an outline of unknown bodies can be mapped.

A practical way of interpreting the depth extent of nearly vertical electric conductive bodies from CP data is presented by Kihle & Eidsvig (1978).

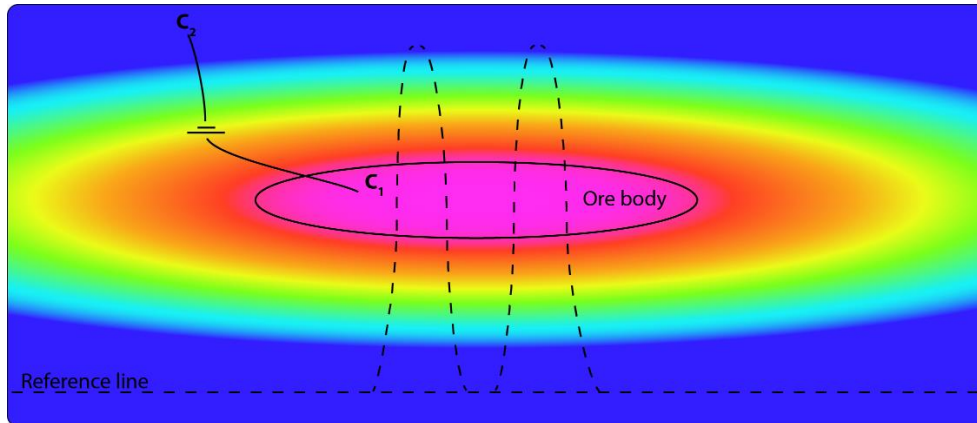


Figure 4.3: Conceptual illustration of the CP- method. The current electrode (C1) is connected to the ore body and the remote electrode (C2) is placed far outside the survey area. The colour indicates the strength of the charged potential above an orebody. The dashed line shows the survey paths along which the entire body will eventually be covered.

Self Potential (SP) is measured simultaneously with CP. SP is a natural potential in the ground created by electrochemical processes in connection with electronically conducting minerals (graphite, sulphides and oxides) (Sato & Mooney 1960). In order to separate data from the two methods, the transmitting and measuring sequence is controlled by GPS time. SP is measured just before a current pulse while both CP and SP are measured during a current pulse. SP is not dependant on exposed graphite for current injection and can be a very useful tool if there are several conductive bodies in the area of investigation.

SP may give negative potential values of 1000 mV or even more above graphite mineralisation. SP signals less than 100 mV are not regarded as anomalies in mineral prospecting.

The equipment used for **combined CP and SP** measurements was developed at NGU in 2014. It consists of an immobile current transmitter and a mobile receiver (Voltmeter). The transmitter sends current between the ore electrode (C1 in Figure 4.3) and the remote electrode (C2 in Figure 4.3) and charges the ore body. The current is transmitted in pulses of two seconds on and two seconds off. The pulses are synchronized through GPS-time enabling the receiver to "know" when the ore body is charged. SP is measured when the current is switched off and CP+SP is measured with the current on, and then, in order to get the pure CP, SP is subtracted from the CP+SP measurement. All of this is done automatically during the measuring procedure. Each measurement is the potential between the two mobile electrodes. This means that every measurement has to be added consecutively to a total potential sum. The position of each measured point is given by a GPS recorder at the position of the receiver. The accuracy of the positioning is +/- 5 m.



Figure 4.4: Establishing CP ore-grounding point (left) and data acquisition in combined CP and SP data (right).

4.1.4 2D resistivity (ERT) and Induced Polarization (IP)

Detailed 2D Electric Resistivity Traversing (ERT) and Induced Polarisation (IP) sections give valuable information in the evaluation of graphite mineralisation.

Data acquisition

The 2D resistivity and IP methods are carried out by injecting current into the ground with the use of two electrodes and by measuring the voltage between two separate electrodes. Based on measured resistance (measured voltage / injected current) and a geometrical factor dependent on the electrode positions, the apparent resistivity and IP effect can then be calculated.

The 2D ERT/IP measurements were performed using the Lund cable system (Dahlin 1993) and the instrument ABEM Terrameter LS (ABEM 2012) was used to acquire data. As seen in Figure 4.5, four multi-electrode cables can be used, and for the surveys presented in this report, a Multiple Gradient electrode configuration (Dahlin & Zhou 2006) was applied. Once the electrodes are connected to the ground and the measuring instrument, an automatic measuring procedure starts transmitting current at one electrode pair and measures electric potential at up to four electrode pairs simultaneously. Resistivity is measured when current is on, while IP-effect is measured shortly after cutting the electric current. The electrode separation can be 2 m, 5 m and even 10 m. The penetration depths are ca. 20 m, ca. 60 m and ca. 120 m respectively. Penetration depth is, however, dependent on the resistivity in the ground. The resolution decreases with depth and deeper parts of the resistivity sections are, by experience, of low reliability.

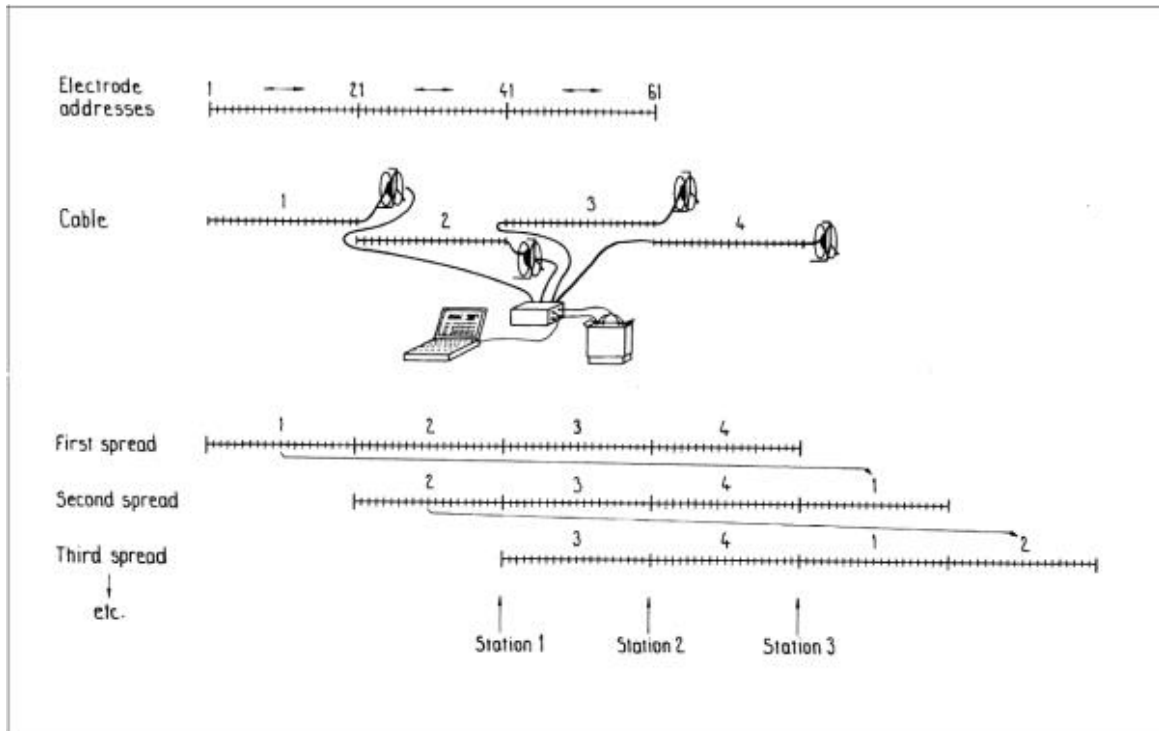


Figure 4.5: Diagram of measuring procedure illustrating the set-up of the Lund System and the roll-along method for performing as many measurements as required. (From ABEM 2012).

Data inversion

Almost all resistivity and IP measurements give an apparent resistivity and IP value. The apparent values represent a weighted average resistivity which resulted from resistivity of each heterogeneous volume in the surroundings of the measurement points. The data are inverted in order to find the specific resistivity of each part of the heterogeneous investigated volume. This is done by dividing the profile into blocks, each characterised by specific resistivity values; these are adjusted following an iterative procedure until a theoretical model fits the measured data.

Resistivity measurements were inverted using the computer program RES2DINV with robust data constraint, version 4.0 for the 2016 data and version 4.8.9 for the 2018 data (Loke, 2014, Loke, 2018).

Data quality

The quality of 2D ERT/IP data is dependent on current strength, resistivity in the ground and noise level in the area. Some data have too high standard deviation during inversion according to the methods guidelines. These data points will be removed from the dataset before the inversion.

The data inversion quality can be evaluated by looking at the absolute error (Abs. error) calculated as the difference between the measured data and a calculated response from the final inverted 2D resistivity section. Absolute error of < 5 % is very good; 5 – 15 % is good and between 15 and 30 % of acceptable quality. Absolute error > 30 % is not acceptable inverted data.

Data interpretation

Graphite is an electronically conducting mineral, and the resistivity in massive graphite ore bodies is commonly less than 2 Ωm , or electric conductivity higher than 500 mS/m, (Dalsegg, 1994, Rønning et al. 2012, Rønning et al. 2014). This can be used to distinguish between resistivity anomalies caused by graphite mineralisation and other ionic conducting geological materials such as porous rock filled with saline water, marine clay deposits and even sulphide deposits (resistivity less than 10 Ωm).

Induced Polarization responds to electronic conducting minerals which are not in electrical contact. This means that massive graphite deposits give no IP effect on massive graphite bodies. High IP effects are often seen in the contacts between graphite bodies and surrounding host rock where graphite grains are not connected (disseminated ore).

Unfortunately, 2D ERT/IP measurement may be disturbed by artificial conductivity effects interfering with responses from two or more sub-vertical conducting graphite bodies (Rønning et al. 2014). The effect of this is a continuous image despite there being two or more vertical structures.

4.1.5 Resistivity drill-hole logging

The resistivity values in drill-holes were logged using the ABEM SAS-LOG 200 equipment (ABEM 1993). Resistivity was measured each 25 cm with the Short Normal (SN) electrode configuration. This is a pole-pole configuration where distance between the drill-hole current and the drill-hole potential electrode is 40 cm. This configuration measures the apparent conductivity within a distance of ca. 20 cm into the surrounding rock.

4.2 Geological methods

In this section we define different types of graphite and describe the analytical methods and drilling equipment used.

4.2.1 Definitions of graphite types

There are differences between scientists and the industry in the terminology related to graphite and carbonaceous materials. Scientists base their classification on the crystallinity of the graphite crystals, using XRD and Raman spectroscopy. The International Committee for Coal and Organic Petrology (ICCP) divides graphitic material into graphite and semi-graphite (see Kwiecińska & Petersen 2004 for details). Rantitsch et al. (2016) and Palosaary et al. (2016) showed that graphite from Skaland and Jennestad respectively, are of fully ordered and crystalline flake graphite, free of internal defects. The nature of the graphite crystallinity has only been studied from two localities, but the metamorphic conditions are such that the graphite is most probably fully crystalline at other localities in Vesterålen also.

The industry on the other hand, bases its classification on the grain size, grain properties and on the use of the graphite. The terms, flake graphite, amorphous graphite and vein (lump) graphite are industrial terms, that we will clarify as follows:

Graphite is a mineral with the chemical composition C (pure carbon) in which the carbon atoms are arranged in sheets where hexagonal rings of C atoms are bonded together (Figure 4.6). These layers are again stacked in sheets that make up the graphite crystals. The industry distinguishes between flake, amorphous, and vein (lump) graphite.

Flake graphite is defined as graphite in which the crystals occur in well-defined flakes with a silvery or steel-like colour. Individual crystal sizes are usually from 0.1 mm up to several mm in diameter. Individual flakes are easily distinguished from each other with the eye only. Flake graphite usually occurs in metasedimentary rocks of high metamorphic grade (granulite facies).

Amorphous graphite is a micro-crystalline graphite with a black colour and in which the individual graphite crystals are indistinguishable to the eye. Amorphous graphite occurs where metasedimentary rocks have been subjected to lower degrees of metamorphism (greenschist to amphibolite facies) or in areas with contact metamorphism.

Vein (lump) graphite is a rare graphite type: economic deposits occur only on Sri Lanka. They are formed where pure carbon is deposited from hydrothermal solutions. This type of graphite occurs as massive lumps of pure carbon. On a small scale and as geological curiosities vein-type graphite is probably not uncommon and has been described from many places in addition to Sri Lanka. We have identified several localities where vein-type graphite occurs as local geological curiosities in Vesterålen but will not go into further detail in this report.

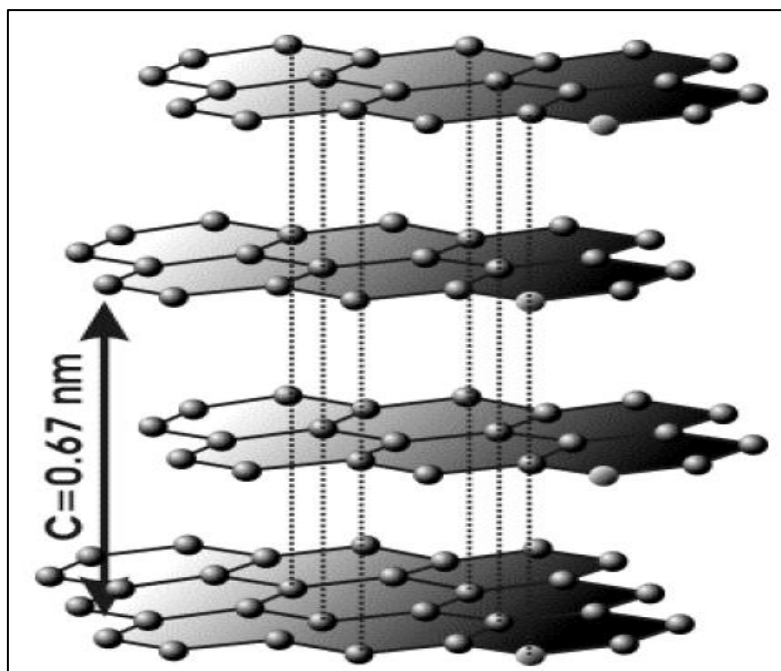


Figure 4.6: Crystalline structure of graphite with C atoms in a hexagonal sheet arrangement.

When we use the term “grade” we mean “content” and not metamorphic grade (facies). Stating, in this report, that the rock is a “medium-grade graphite schist” means that it is a graphite schist with an intermediate content of graphite based on observations in the field.

4.2.2 Analytical methods

The investigated area is partly covered in soil, but there are numerous outcrops, particularly on the mountain tops. We sampled the graphite schist when found in these areas and coordinates for every sampling point were recorded. We tried to obtain as representative samples as possible and from as large an area as possible. The usual sample size was about 1-2 kg. The samples were analysed further at the NGU laboratory.

Samples from different outcrops were crushed using standard methods. The powders were analysed for total carbon (TC) and total sulphur (TS) using a Leco SC-632 analyser. The detection limits are 0.06 % and 0.02 % for carbon and sulphur respectively. The analytical uncertainty at 2 σ level is +/-15 % relative. The aggregate results for all samples are shown and are also reported under each area description in chapters 6 to 9.

The graphite industry uses the term “carbon graphitic” (Cg) when reporting graphite occurrences. This type of analysis is essentially the same as “total organic carbon” (TOC) but includes an extra step in which organic matter is removed in a roasting step before Leco analyses. In rock types with little or no carbonate minerals and organic matter, analyses of TC would be similar or close to TOC and Cg but the former is much less expensive and faster. For samples where TC and TOC are reported together, these values usually differ only within the analytical uncertainty, justifying that TC is a good measure for the graphite content in the rock (see In Appendix 6). The commercial laboratory procedures for TC, TOC and Cg analyses are described by, e.g. www.alsglobal.com

A number of standard thin sections were made from different occurrences. The modal content of graphite in the thin sections was measured using the *ZEN 2 pro* program from Zeiss. The measurement involves the following steps:

- 1) A micro-photo mosaic covering a whole standard thin section is collected.
- 2) Using image-processing software, that involves several steps of colour segmentation, removal of “noise” and other adjustments and corrections, the total area percentage of graphite is calculated. In addition, the area, perimeter, diameter plus a number of other parameters are calculated for each individual graphite grain, in the measured thin sections. All data is available on request.

When we use this method to describe the particle size, we use the “diameter” of individual grains, which is the diameter of a circle with the same area as the area of the measured individual particles ($\text{diameter} = 2(\text{area of particle}/\pi)^{0.5}$).

The image processing of micro-photos to quantify the content and particle size of graphite in a thin section, has some shortcomings and errors. These are:

- 1) Individual particles that touch each other, will be regarded as one big grain, the same with mineral aggregates. The degree to which this can be compensated for varies from thin section to thin section.
- 2) Minerals with the same colour as graphite will be regarded as graphite: this problem can be checked and to a certain degree compensated for.
- 3) Image processing cannot distinguish between flake and amorphous graphite: this is done by visual inspection of hand samples.
- 4) A thin section represents a 2x3 cm large area and may not be representative for the hand sample or the locality
- 5) Grain size in situ in a rock cannot be directly used as a proxy for the grain size obtained after ore dressing.

Image-processing methods are, however, much more accurate than standard manual point-counting methods or simple visual in section of a thin section. When one looks at area % of graphite in relation to grain size distribution, there are always a few large grains that make up a large part of the total area % of graphite. The grain size of the graphite can also be readily estimated by visual examination in thin section

4.2.3 Core drilling, sampling and analyses

NGU has a truck-mounted drilling rig as shown in Figure 4.7. When the 4x4 wheel drive truck can drive into an area, core drilling can be performed. The core diameter is 36 mm. The core length is limited to ca. 50 m.

Three localities were chosen for core drilling:

- 1) Vikeid, Sortland Municipality, one drill-hole (Chapter 7.6.6)
- 2) Myre, Øksnes Municipality, two drill-holes (Chapter 8.4.3)
- 3) Sommarhus, Hadsel Municipality, two drill-holes (Chapter 9.3.4).

The purpose of the drilling was as follows:

- 1) To obtain a continuous section through the graphite-bearing units and their country rock.
- 2) To obtain information on the thickness and grade of graphite schists, on localities where there exists detailed ground geophysical information on the surface.



Figure 4.7: NGU's truck-mounted drilling gear in operation.

The drilling undertaken is not sufficiently detailed to permit estimation of a meaningful resource tonnage. Drilling was limited to localities accessible with the truck and the maximum drilling depth is ca. 50 m.

The drill core was logged, described, sampled, analysed and reported in the following manner:

- a) Lithological logs and descriptions of cores (Appendix 1).
- b) All drill cores were photographed dry and wet (Appendix 2).
- c) Measured with Portable XRF, one point/0.25 m. (Appendix 4).
- d) Splitting of core in 3 parts, one half and 2 quarter-cuts of the core.
- e) At selected intervals, where visual logging shows the occurrence of graphite, sampling of 2 m intervals was made.
- f) The most graphite-rich intervals were analysed for TC and TS (Appendix 3).
- g) Areas of high electric conductivity were identified using simple drill-hole resistivity logging, Appendix 5 (ABEM 1993).

5. SELECTION OF FOLLOW-UP OCCURRENCES

The selection of follow-up graphite occurrences was based on results from the helicopter-borne geophysics performed in 2013. This was dominantly Electro-magnetic data (EM), but was also based on the magnetic data. Data acquisition, processing and visualisation were described by Rodionov et al. (2013a and 2013b).

5.1 Petrophysical properties of graphite

The electronic conductivity of pure graphite is reported to be ca. $10^{-3} \Omega\text{m}$ (Telford et al. 1976). Graphite occurs, in most cases, together with other minerals: our experience demonstrates that the resistivity of graphite mineralisation may be ca. $1 \Omega\text{m}$ (see Chapter 4.1.4 for details).

Graphite is reported to be a diamagnetic mineral which means that graphite has a negative magnetic susceptibility and may reduce the earth's magnetic field (Reynolds, 2011). NGU has, within this project, tested laboratory measurements of magnetic susceptibility on 125 graphite samples (Rønning et al. 2018). However, the method employed here for measuring magnetic susceptibility is an electromagnetic method which will fail on electronically conductive graphite. Due to this, the measured results cannot be treated with confidence.

Sulphur, occurring as the magnetic mineral pyrrhotite, can have the opposite effect since this mineral normally has a higher magnetic susceptibility. This means that a low magnetic field in an area may indicate a lack of pyrrhotite in the bedrock.

Apparent resistivity and magnetic anomaly fields have been studied empirically from helicopter-borne measurements in a graphite-bearing area west of the town of Sortland (Figure 5.1). Areas which show up with low resistivity and exposed graphite mineralisation also display a low magnetic field. It is currently unclear whether the latter is caused by the diamagnetic effect of graphite, nonmagnetic host-rock or even remnant magnetisation of the host-rock. This will be studied later in a separate research project. If it is the diamagnetic effect that is indeed causing the low magnetic field, this would suggest the presence of extensive amounts of graphite.

A low magnetic field coinciding with low resistivity may be an indicator of good quality graphite. NGU has therefore developed a method to identify areas with low resistivity and low magnetic field from helicopter-borne geophysical measurements. In this study we use this method to identify potentially good quality graphite, both for the Langøya area in Vesterålen and for parts of the Austvågøya area in Lofoten.

It is necessary, in order to calculate the total tonnage of graphite ore, to know the density of the mineralisation. The density was measured at 141 samples from the area (Rønning et al. 2018, Appendix 6). The average density of these is 2.39 t/m^3 . These are, however, surface samples which may be weathered. In our tonnage estimations (Chapter 10.4) we used densities from fresh drill core samples at 2.6 t/m^3 .

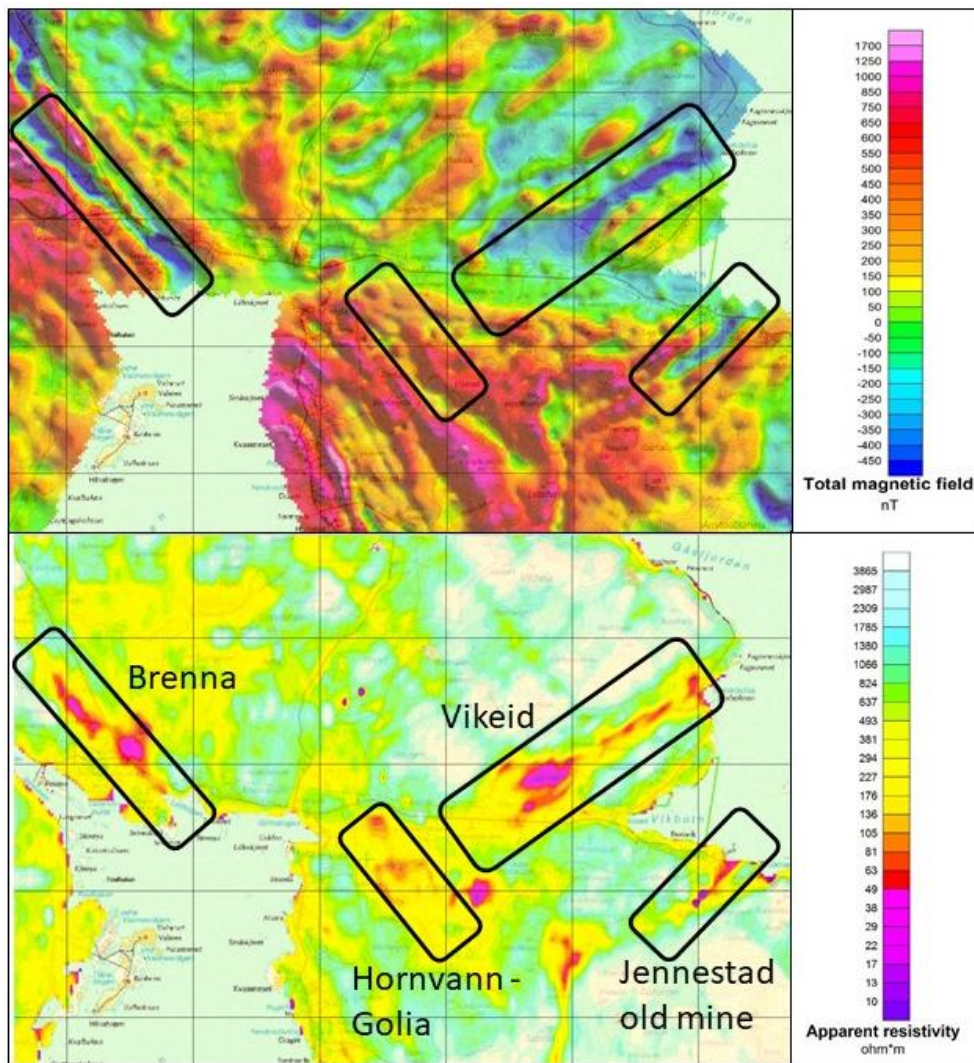


Figure 5.1: Magnetic anomaly field and apparent resistivity (7 kHz coaxial coils) from helicopter-borne measurements in the Jennestad area, west of Sortland town (modified from Rodionov et al. 2013a).

5.2 Data from helicopter-borne measurements on Langøya, Vesterålen

Helicopter-borne geophysical measurements produce data on the magnetic anomaly field, electromagnetic data at five frequencies and the concentrations of uranium, thorium and potassium. All of these data are relevant for graphite prospecting.

Electromagnetic data can pinpoint potential graphite deposits directly since the electric conductivity of graphite is quite high (low resistivity).

As described in the previous section, low magnetic field and low resistivity can be a good indicator of good quality graphite. However, in combination with iron-rich minerals, this effect can be cancelled out by magnetic minerals (iron oxides, pyrrhotite and others).

The acquisition of radiometric data from the helicopter-borne measurements is important in graphite exploration because radioactive elements such as uranium and thorium can be an environmental problem during graphite extraction.

Based on this, examples of electromagnetic data, magnetic data and radiometric data are presented as a basis for selecting ground follow-up investigations on potential graphite objects.

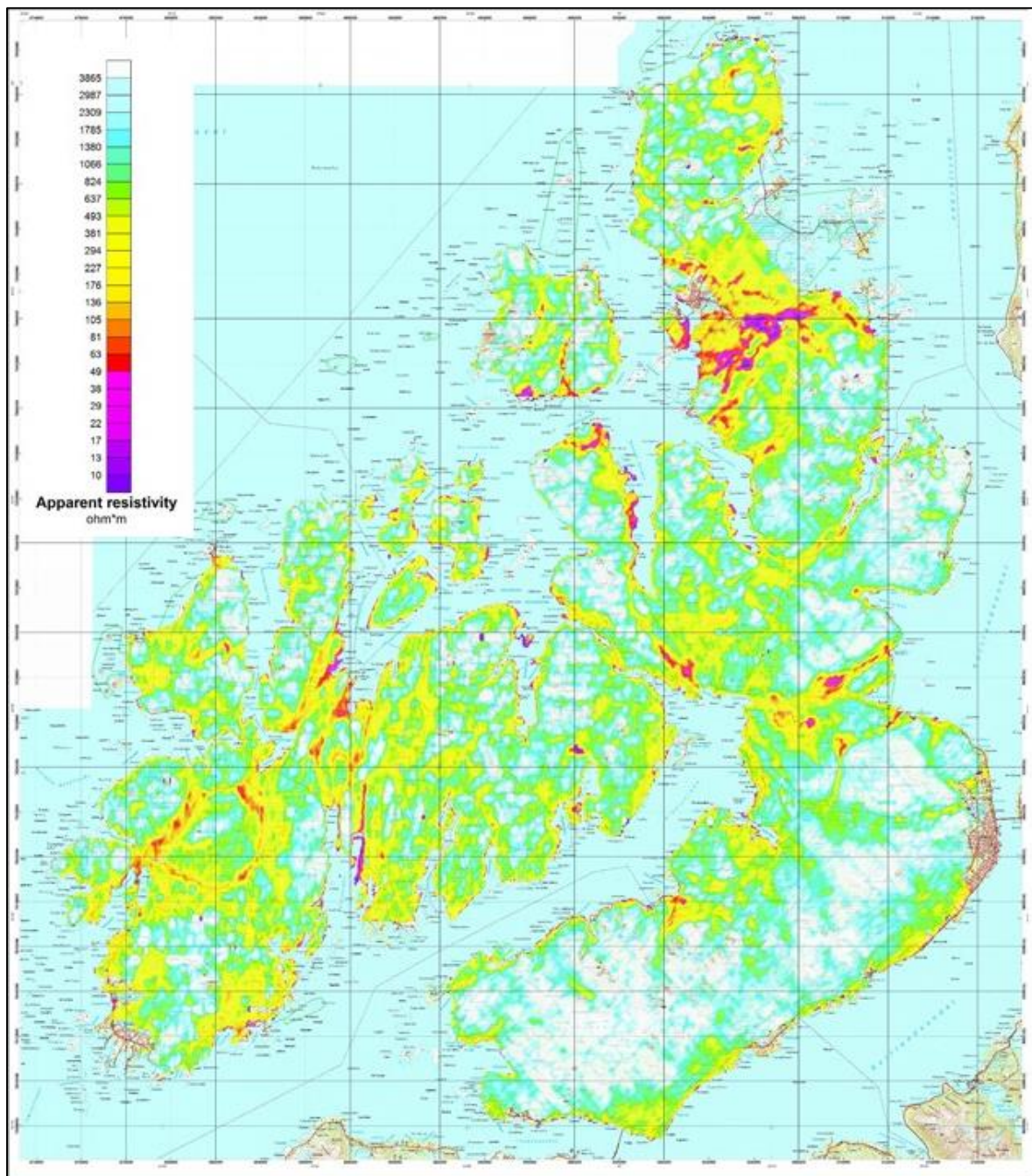


Figure 5.2: Apparent resistivity calculated from EM 7 kHz Coaxial coil configuration at Langøya in Vesterålen (from Rodionov et al. 2013a).

An example of the electromagnetic data from Langøya is presented in Figure 5.2. Yellow colours represent moderately anomalous low apparent resistivity. Orange, red and violet colours represent low apparent resistivity ($< 100 \Omega\text{m}$, high apparent conductivity). Note that these apparent values represent an average of a greater volume, and that smaller structures inside this volume might have lower resistivities (higher conductivities). The cause of the low resistivity may be graphite, sulphides, iron oxides and salt-water in porous soils and rocks.

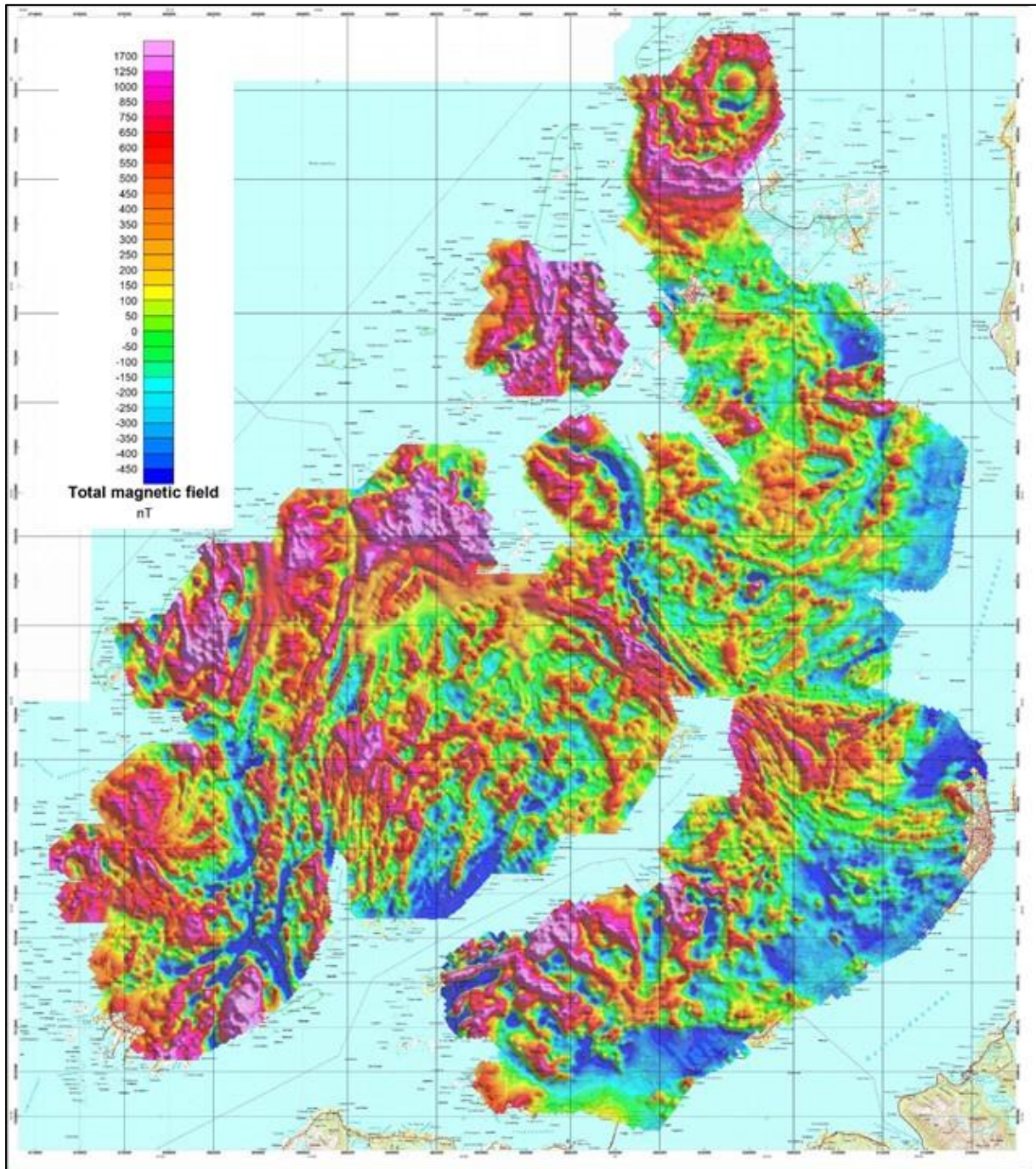


Figure 5.3: Magnetic anomaly field on Langøya, Vesterålen (from Rodionov et al. 2013a).

The magnetic anomaly field at Langøya (Figure 5.3) is produced by subtracting the International Geomagnetic Reference Field (IGRF 2015) from the diurnal corrected magnetic total field. The magnetic anomaly field shows strong positive anomalies (> 1700 nT) but also areas where the magnetic field is very low (< -300 nT, blue colours). Low magnetic field may indicate, as discussed above, good quality graphite, but also bedrock with low iron content (low magnetic susceptibility) and rocks with remanent (permanent) magnetisation.

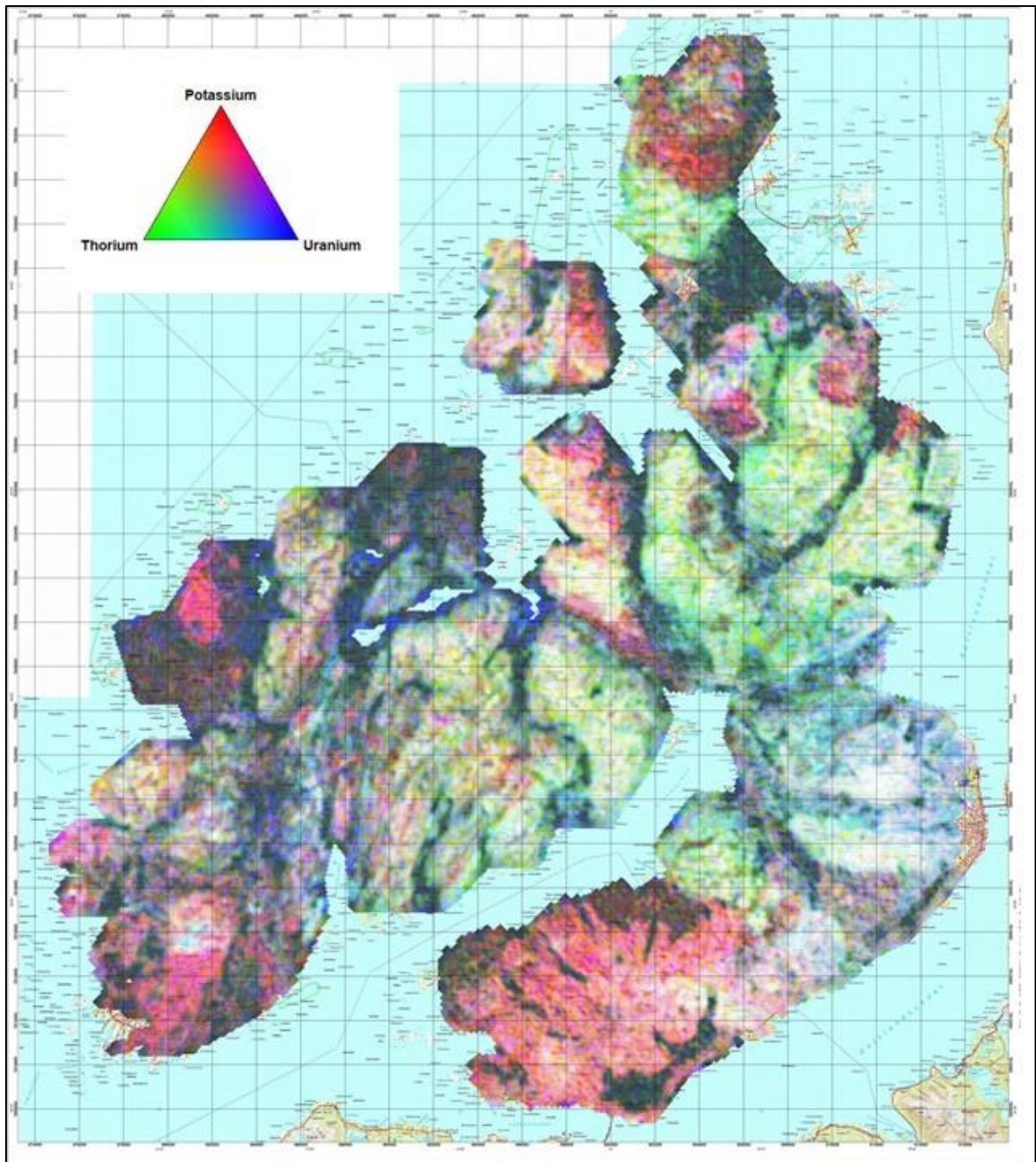


Figure 5.4: Radiometric ternary map (combined eU, eTh and K) of Langøya in Vesterålen (from Rodionov et al. 2013a).

The concentrations of the radioactive elements uranium and thorium are generally low on Langøya. The helicopter-borne measurements show a uranium concentration <2 ppm and a thorium concentration <10 ppm. These values must be looked upon as apparent values since they represent a weighted average value over a “footprint” of ca. 150m x 180m. Inside each footprint the values may be higher. For detailed element concentrations (U, Th and K), see the processing report (Rodionov et al. 2013a).

In the ternary map (Figure 5.4), the red colour represents potassium, green represents thorium and blue represents uranium. Dark colours represent low levels in all three elements whereas white indicates higher values in all three elements.

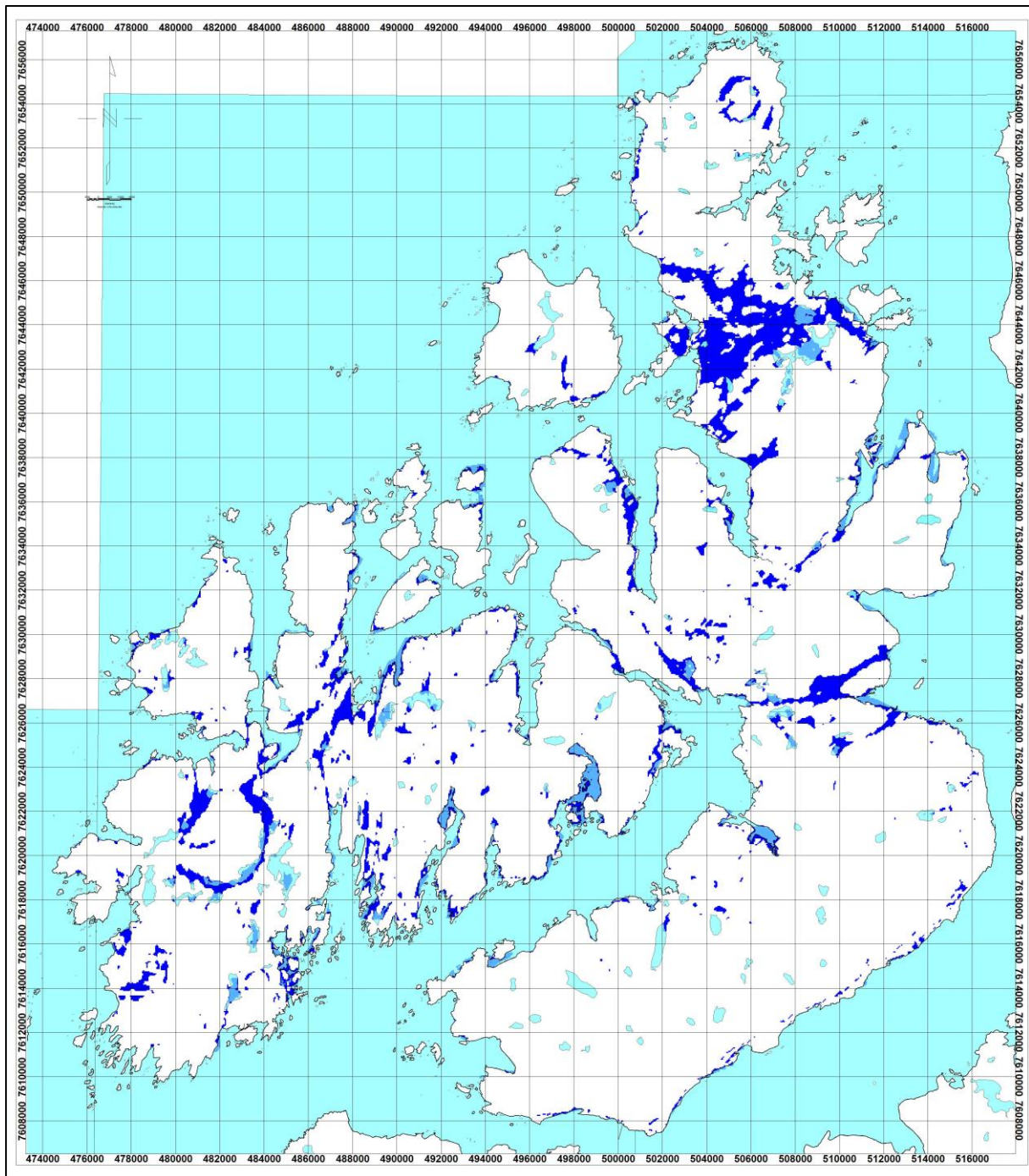


Figure 5.5: The blue colour shows areas on Langøya where apparent resistivity from EM 7 kHz coaxial coils is $< 300 \Omega\text{m}$ and magnetic total field is $< \text{IGRF} + 300 \text{ nT}$.

NGU has developed a new method for integrated interpretation of magnetic and electromagnetic methods. The blue colours in Figure 5.5 show areas where the apparent resistivity is $< 300 \Omega\text{m}$ and the magnetic anomaly field is $< 300 \text{ nT}$ (total field minus IGRF $< 300 \text{ nT}$). These are, according to the assumptions presented here, potential areas for extensive volumes of high-quality graphite. Figure 5.6 shows the same figure with the locations of sampled graphite schists.

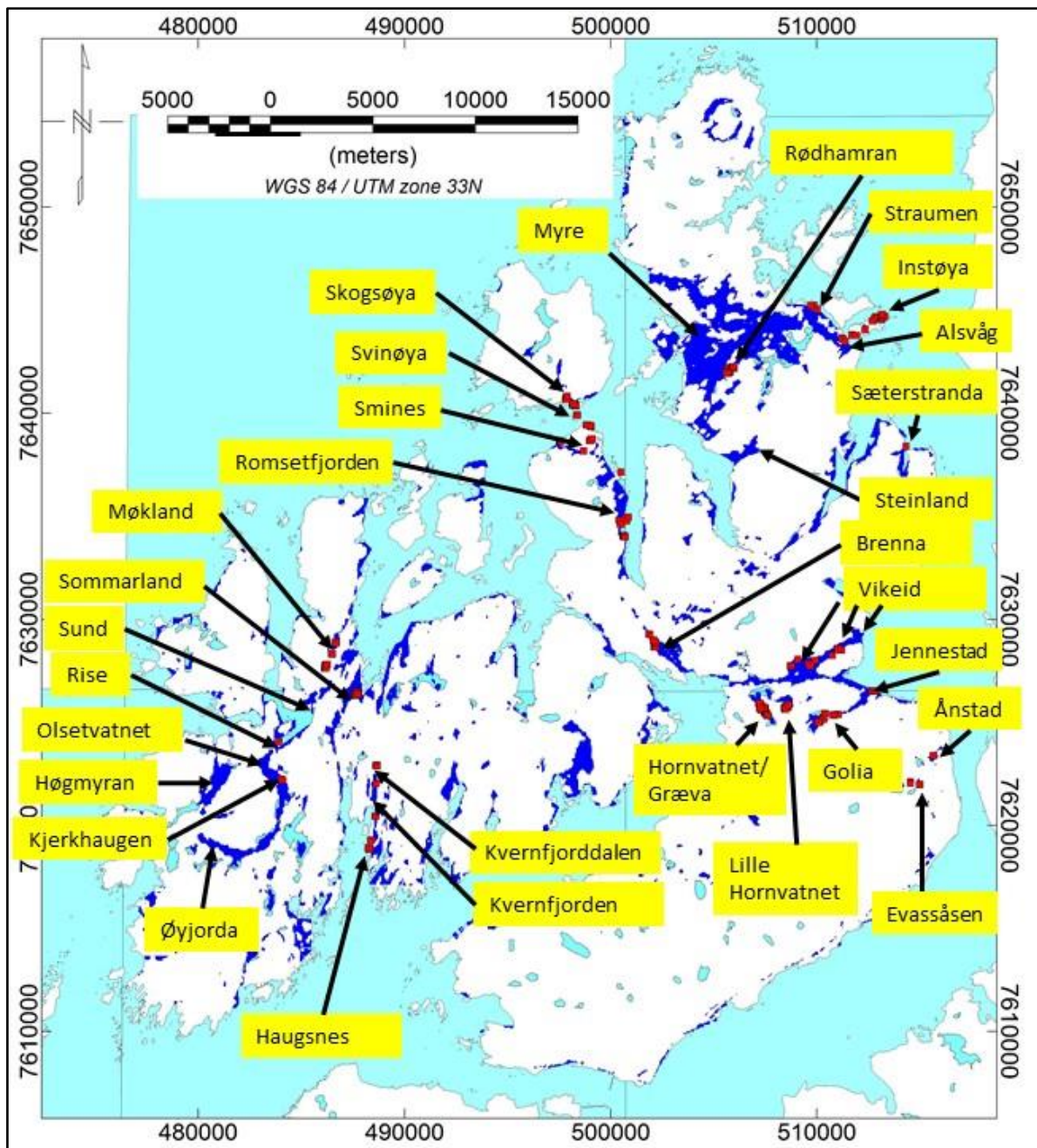


Figure 5.6: The blue colour shows areas on Langøya where apparent resistivity from EM 7 kHz coaxial coils is $< 300 \Omega\text{m}$ and the magnetic anomaly field is $< 300 \text{ nT}$. The red squares show sample locations of graphite-bearing rock.

The areas called Hornvatnet, Græva, Lille Hornvatnet, Golia, Jennestad, Viketid and Rødhamran were investigated in the 1990s (see Chapter 3). Some follow-up work was performed at Møkland, Skogsøya, Svinøya and Smines during 2013-2014. In 2015 and 2016 NGU carried out investigations at Møkland, Sommarland, Kvern fjorddalen, Haugsnes, Smines and Rødhamran (Gautneb et al. 2017, Rønning et al. 2017). During the field season of 2017, NGU carried out additional work at Høgmyran, Rise, Sund, Sommarland, Haugsnes, Brenna, Viketid, Rødhamran and east of Myre (Rønning et al. 2018). This report presents follow-up work undertaken in 2018 and 2019 at Høgmyran, Rise, Kjerkhaugen, Øyjorda, Møkland-Sund, Kvern fjorden, Evassåsen, Ånstad, Viketid, Reinsnesøya, Smines, Romsetfjorden, Steinland, Myre, Alsvåg-Instøya-Straumen and Sæterstranda.

5.3 Data from helicopter-borne measurements at Austvågøya, Lofoten

The same helicopter-borne geophysical measurements that were performed at Langøya (Rodionov et al. 2013b) were also undertaken on parts of Austvågøya. The processed data are presented in Figures 5.7, 5.8 and 5.9.

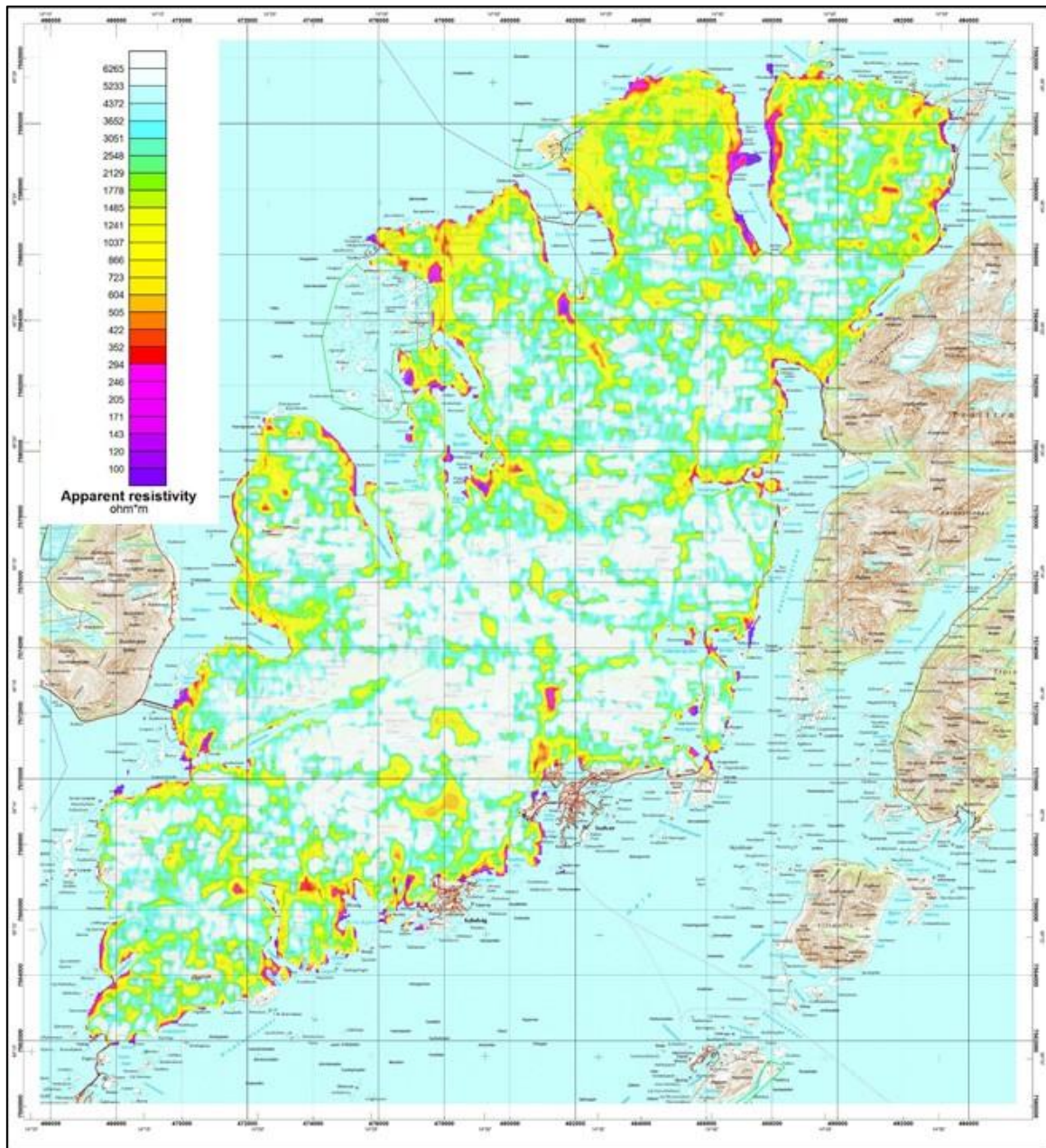


Figure 5.7: Apparent resistivity calculated from EM 7 kHz Coaxial coil configuration on parts of Austvågøya, Lofoten (from Rodionov et al. 2013b).

An example of the electromagnetic data from Austvågøya is presented in Figure 5.7. Yellow colours represent moderate anomalously low apparent resistivity. Orange, red and violet colours represent low apparent resistivity (high apparent conductivity). Note that these apparent values represent an average of a greater volume, and that smaller structures inside this volume may have lower resistivities (higher conductivities). The causes of low resistivity may be graphite, sulphides, iron oxides and salt-water in porous soils and rocks.

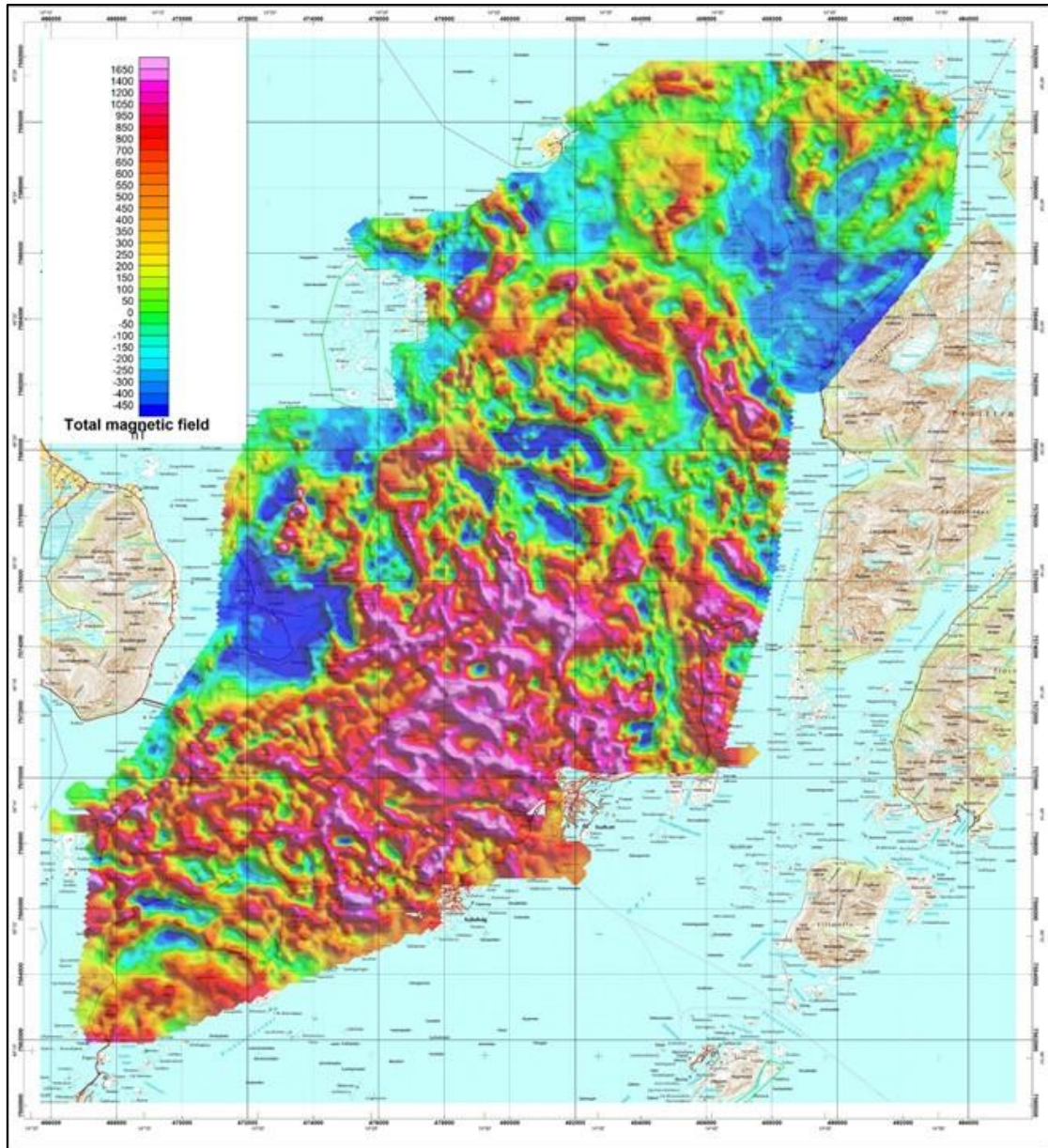


Figure 5.8: Magnetic anomaly field in parts of Austvågøya, Lofoten (from Rodionov et al. 2013b).

The map of magnetic anomaly field in parts of Austvågøya (Figure 5.8) was produced by subtracting the International Geomagnetic Reference Field (IGRF 2015) from the diurnal corrected magnetic total field. The magnetic anomaly field shows strong positive anomalies (> 1600 nT) but also areas where the magnetic field is very low (< -300 nT, blue colours). These areas may, potentially, as already discussed, contain graphite of good quality.

The concentrations of the radioactive elements uranium and thorium are also generally low on Austvågøya. The helicopter-borne measurements (Rodionov et al. 2013b) show a uranium concentration of <3 ppm and a thorium concentration of <11 ppm. These values must be considered as apparent values since they represent a weighted average value over a “footprint” of ca. $150\text{ m} \times 180\text{ m}$. Inside each footprint individual values may be higher. For detailed element concentrations (U, Th and K), see the processing report (Rodionov et al. 2013b).

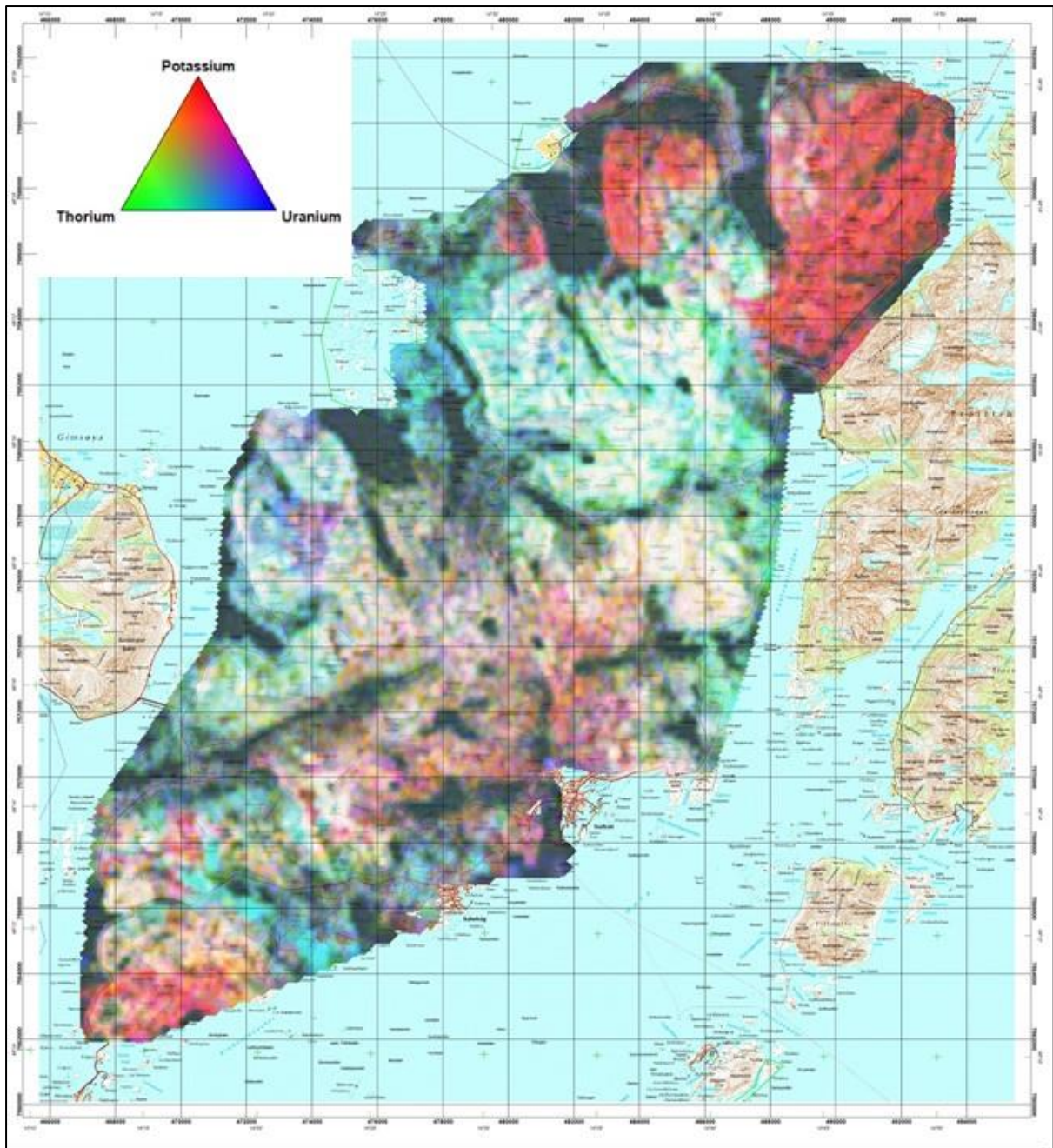


Figure 5.9: Radiometric ternary map (eU, eTh and K) from Austvågøya, Lofoten (from Rodionov et al. 2013b).

The ternary map (Figure 5.9) shows potassium (red), thorium (green) and uranium (blue). Dark colours represent low values in all three elements while white indicates high values in all three elements. Few areas are dominated by uranium.

NGU has developed a new method for joint interpretation of magnetic and electromagnetic methods. In Figure 5.10 blue colours show areas where the apparent resistivity is $<300 \Omega\text{m}$ and the magnetic total field is $<300 \text{ nT}$. According to this new method, these are areas with potentially extensive volumes of high-quality graphite.

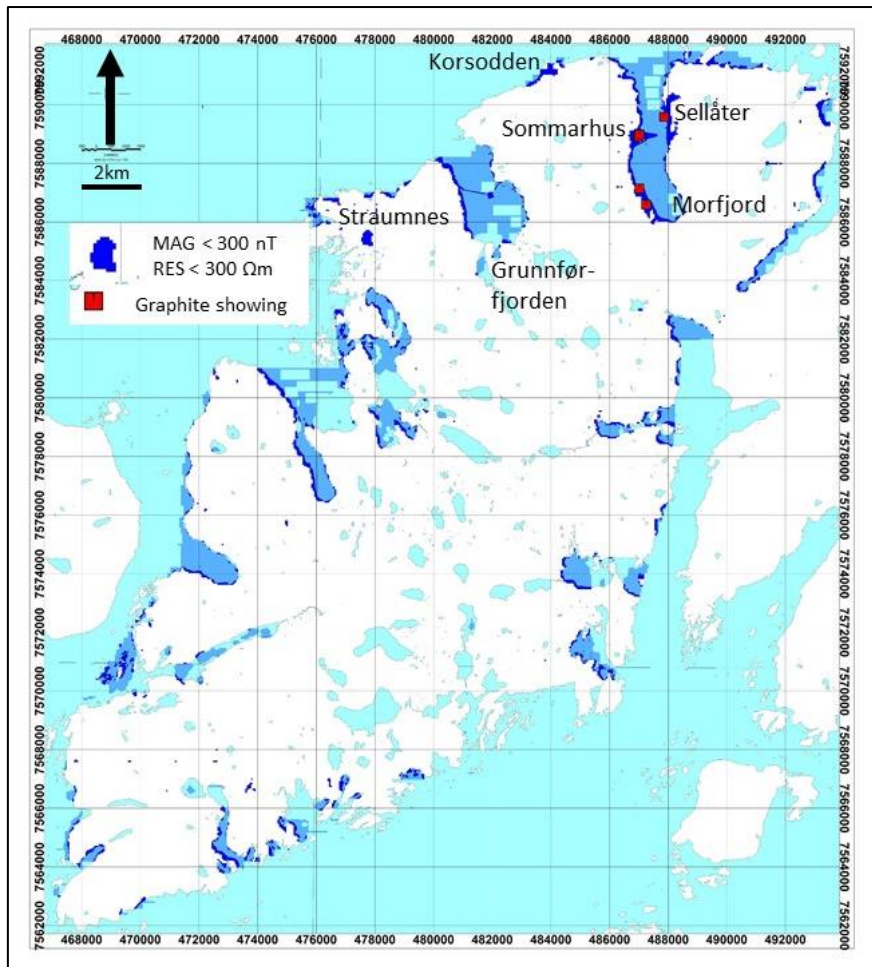


Figure 5.10: The blue colours shows areas on Austvågøya where apparent resistivity from EM 7 kHz coaxial coils is < 300 Ωm and magnetic total field is < IGRF 2015 + 300 nT. The red squares are samples of graphite-bearing rock.

In the Lofoten area, the most pronounced areas where there is a potential for graphite of high quality are at Morfjord (abandoned mine), Sommarhus, Sellåter and Korsodden. Follow-up work was performed in three of these areas in 2017 and graphite mineralisation were located (Rønning et al. 2018). The areas of Straumsnes and Grunnfjørden are less interesting due to their small size and their geological environment (see figure 5.8). Follow-up work was performed at Korsodden, Sellåter and Sommarhus in 2018, and the results are presented in this report.

5.4 Selected areas for follow-up work

In 2018 / 2019, ground geophysical and geological investigations were performed at

- Høgmyran, Rise-Olsetvatnet-Kjerkhaugen, Øyjorda, Møkland-Sund and Kvernfjorden, (Bø Municipality), Western Vesterålen (see Figure 5.6).
- Brenna, Evassåsen, Vikeid (East, Central and West) Reinsnesøya, Sæterstranda and Ånstad (Sortland Municipality, see Figure 5.6).
- Romsetfjorden, Smines, Steinland, Myre and Alsvåg-Instøya-Straumen Øksnes Municipality (see Figure 5.6).
- Korsodden, Sommarhus and Sellåter, Hadsel Municipality (see Figure 5.10).

6. RESULTS OF FOLLOW-UP WORK IN BØ MUNICIPALITY

In the Western part of Vesterålen, Bø Municipality, follow-up work was undertaken in 2018 in six areas; Høgmyran, Rise, Olsetvatnet-Kjerkhaugen, Øyjorda, Møkland-Sund and Kvern fjorden (See Figure 6.1). The areas Høgmyran, Olsetvatnet and Møkland were also investigated in 2016 and 2017 (Rønning et al. 2017 and 2018). To make the results complete, data from these investigations are included in this report. NGU has previously investigated the areas Sommarland, Sommarland East, Sommarland South, Kvern fjorddalen and Haugsnes (Rønning et al. 2018).

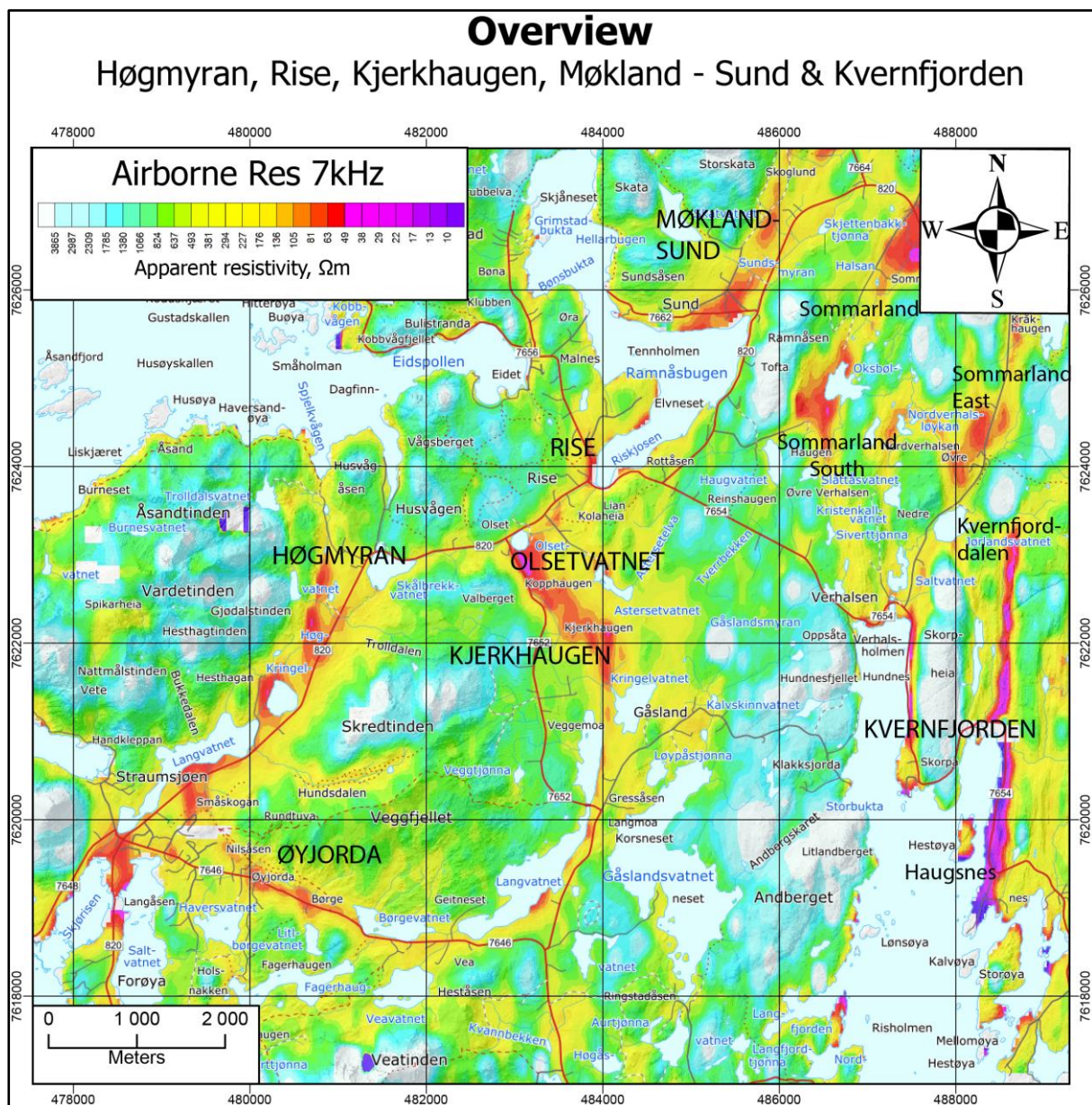


Figure 6.1: Overview map of Bø Municipality. Follow-up work was performed in 2018 in the areas Høgmyran, Rise-Olsetvatnet-Kjerkhaugen, Øyjorda, Møkland-Sund and Kvern fjorden.

6.1 Høgmyran

The Høgmyran area lies at the northern end of a nearly 4 km long anomaly of low resistivity from the helicopter-borne EM measurements, extending from Straume in the south to Høgmyran in the north (Figure 6.1). No information about any graphite occurrences is known in this area. Some follow-up work with EM31 was undertaken in 2017 (Rønning et al. 2018). In 2018 the entire area was covered with EM31 measurements and one ERT/IP profile was measured. The area has few outcrops of bedrock (Figure 6.2).



Figure 6.2: The area Høgmyran is nearly 100 % peat covered. Picture is along the ERT/IP profile 2018-2 (Figure 6.4).

6.1.1 Geophysical work, EM31

Figure 6.3 shows the results from EM31 measurements. Apparent conductivity higher than 100 mS/m (apparent resistivity less than 10 Ω m) shows up on the western flank of the EM anomaly from helicopter-borne EM measurements. Apparent conductivity of this order indicates graphite or sulphide mineralisation. Lack of EM31 high conductivity in the central part of the helicopter-borne EM anomaly may be caused by a dip towards the east in such a way that EM31 is not reaching down to the conductive material. Also, in the northern and southern parts of the helicopter-borne EM anomaly, high apparent conductivity values are absent. This is probably caused by a thicker soil cover. In all, conductive potential graphite mineralisation can be followed for about 1.6 km. The EM31 data indicate two conductive structures separated by ca. 40 m. The maximum width from EM31 data is ca. 20 m, and an average value of 15 m. However, internal quality variations are likely. Single peak EM31 values (black dots) are most likely caused by electric fences.

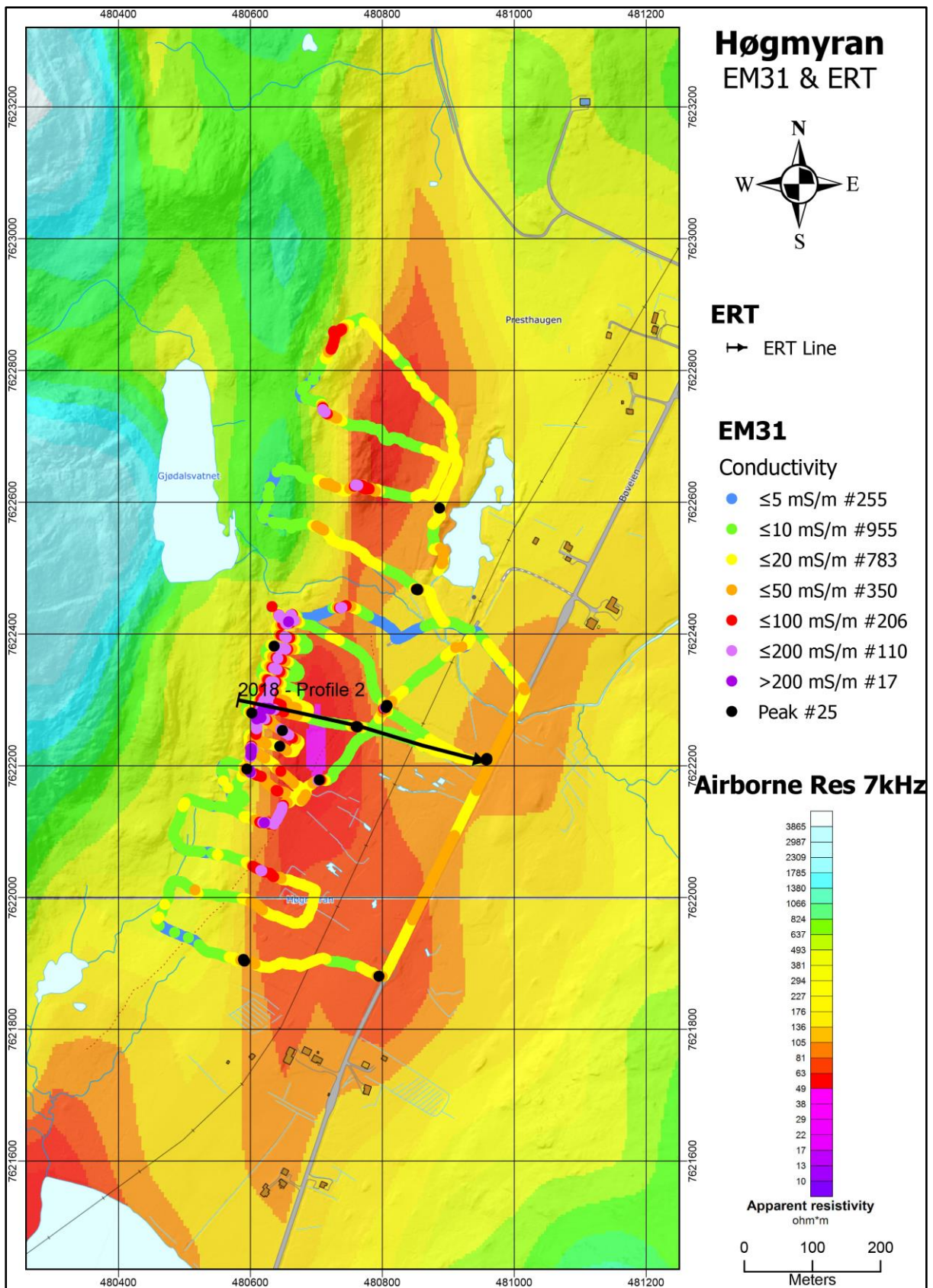


Figure 6.3: Results of EM31 measurements at Høgmyran superposed on apparent resistivity (7 kHz, from Rodionov et al. 2013a). Location of 2D ERT/IP profile is shown as a black line.

6.1.2 Geophysical work, ERT/IP

The location of the ERT/IP profile at Høgmyran is shown in Figure 6.3. Results of the combined 2D resistivity and Induced Polarisation measurements are shown in Figure 6.4. Electrode spacing was 5 m and the other acquisition and inversion parameters are as described in Chapter 4.1.4. The quality of the data and the inversion is characterized as good (see Table 6.1), with absolute error <10 % for both methods.

Table 6.1: Quality of 2D resistivity (ERT) and IP data at Høgmyran. Number of measured, removed and remaining data points for inversion, and observed “Absolute error” from the inversion of resistivity and IP data.

Profile name	Location	Measured data points	Removed data points	Inverted points	Abs. error ERT (%)	Abs. error IP (%)
2018-2	Høgmyran	1168	23	1145	9.6	8.5

In the central part of the profile (Figure 6.4), where low resistivity was expected, the resistivity lies mostly between 200 and 1200 Ωm and there is practically no IP effect. No graphite of good quality is likely to be found here. However, in the western part of the profile, the resistivity is less than 5 Ωm and there is an IP effect that suggests graphite. The resistivity indicates an apparent dip towards the east that may be as low as 20°, which is in accordance with measured dips (25 – 60°) in outcrops and confirms the indicated dip from EM31 measurements. At least two good conducting structures are indicated, almost outcropping, at ca. positions 40 and 80 along the resistivity section. Conductive material between these two may be an artificial effect (Rønning et al. 2014).

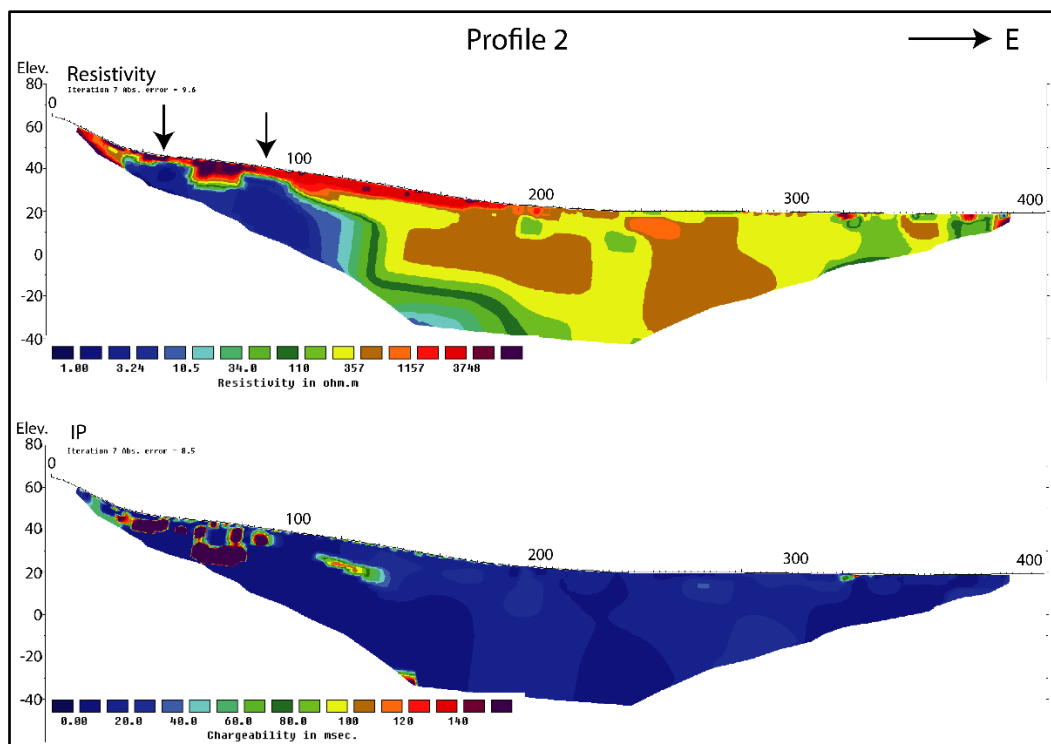


Figure 6.4: 2D resistivity (top) and IP (bottom) results along profile 2018-2 at Høgmyran. No graphite outcrops are observed. Potential (interpreted) graphite zones are indicated with black arrows.

A combined interpretation of near-surface potential graphite structures based on ground EM31, helicopter-borne EM and ERT/IP data is shown in Figure 6.5. Here, “near surface” means shallower than ca. 10 m. The total length of potential graphite structures is ca. 1.5 km.

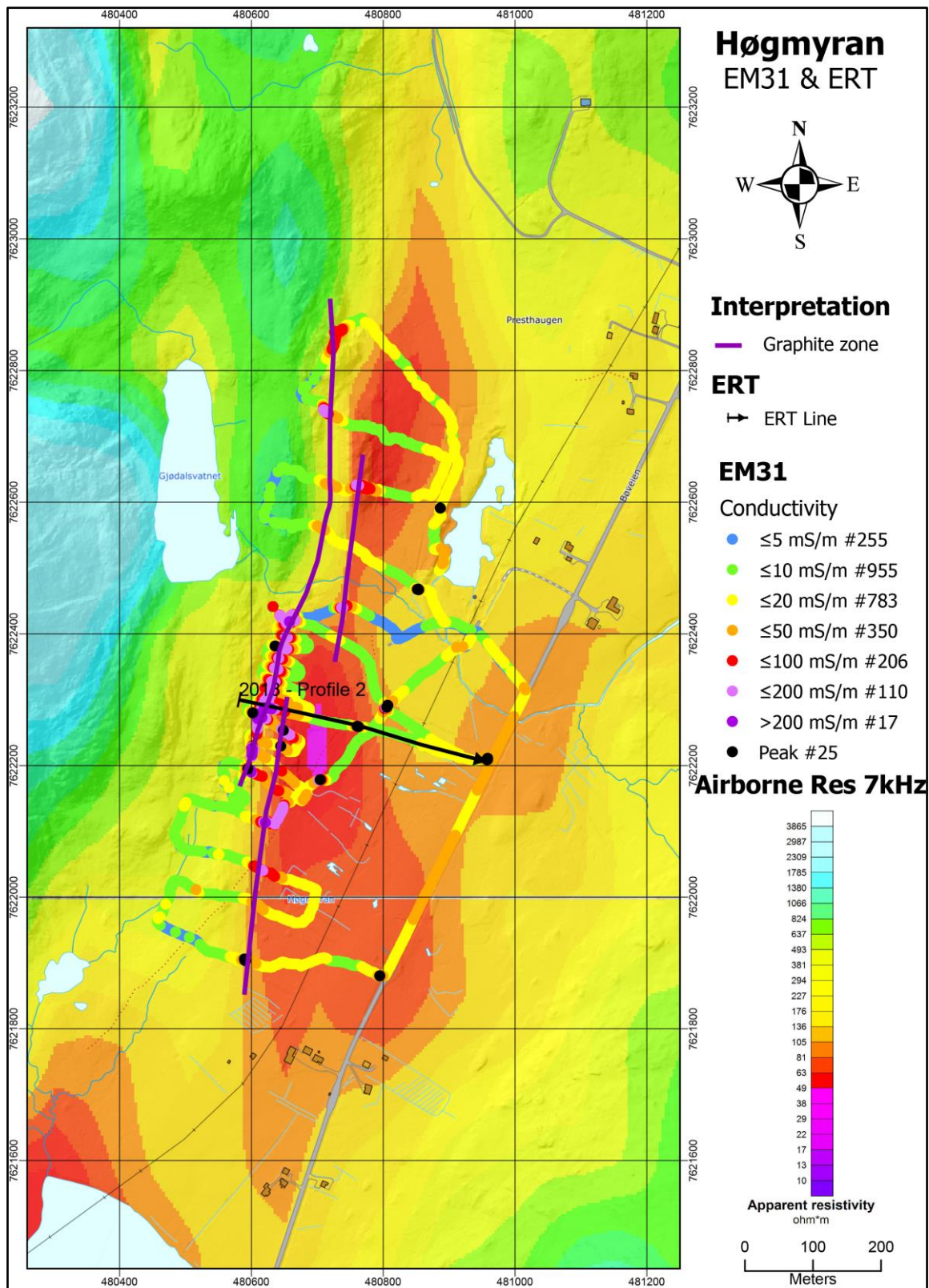


Figure 6.5: The Høgmyran area. Interpreted near-surface graphite structures based on ground and helicopter-borne EM geophysical data.

6.1.3 Høgmyran summary

At Høgmyran, a 1.5 km long conductive structure is detected from helicopter-borne EM data. This structure seems to be a part of a 4 km discontinuous structure extending from Straume to Høgmyran. Detailed EM31 data indicate three individual ca. 15m - thick structures with a total length of 1.6 km. The structures seem to be plunging to the S-SE. The combination of electric resistivity (conductivity) and IP effect indicates graphite or sulphide mineralisation. The area has few outcrops and graphite exposure has not been found. Due to this, no information on the quality of the mineralisation is available.

6.2 Rise – Olsetvatnet - Kjerkhaugen

The areas Rise, Olsetvatnet and Kjerkhaugen are located about 6 km NE of Straume (Figure 6.1). The Olsetvatnet area (earlier called Rise, Rønning et al. 2018) is farmland with few exposures (Figure 6.6). Some EM31 profiling and one ERT/IP line were measured in 2018 (Figure 6.6). As a result of the follow-up work in 2018, graphite mineralisation was discovered at Kjerkhaugen and ca. 200 m N of the road junction at Rise (Figure 6.7). The latter indicates a total length of ca. 250 m in the helicopter-borne EM data, and no geophysical follow-up work was performed.



Figure 6.6: The area Olsetvatnet are nearly 100 % covered farmland. Picture along the ERT/IP profile 2018-5 (location is shown in Figure 6.7).

6.2.1 Geophysical work, EM31

At Olsetvatnet, only a few EM31 profiles were measured (Figure 6.7). No conductivity anomalies appeared that could indicate outcropping or nearly outcropping graphite mineralisation. The reason for this is most likely the soil cover which may be more than ten metres thick.

At Kjerkhaugen, several profiles were measured using EM31 (Figure 6.7). At the northern end of EM anomaly, high apparent conductivity values were measured (> 100 mS/m, resistivity $< 10 \Omega\text{m}$), and graphite was observed here in 2018.

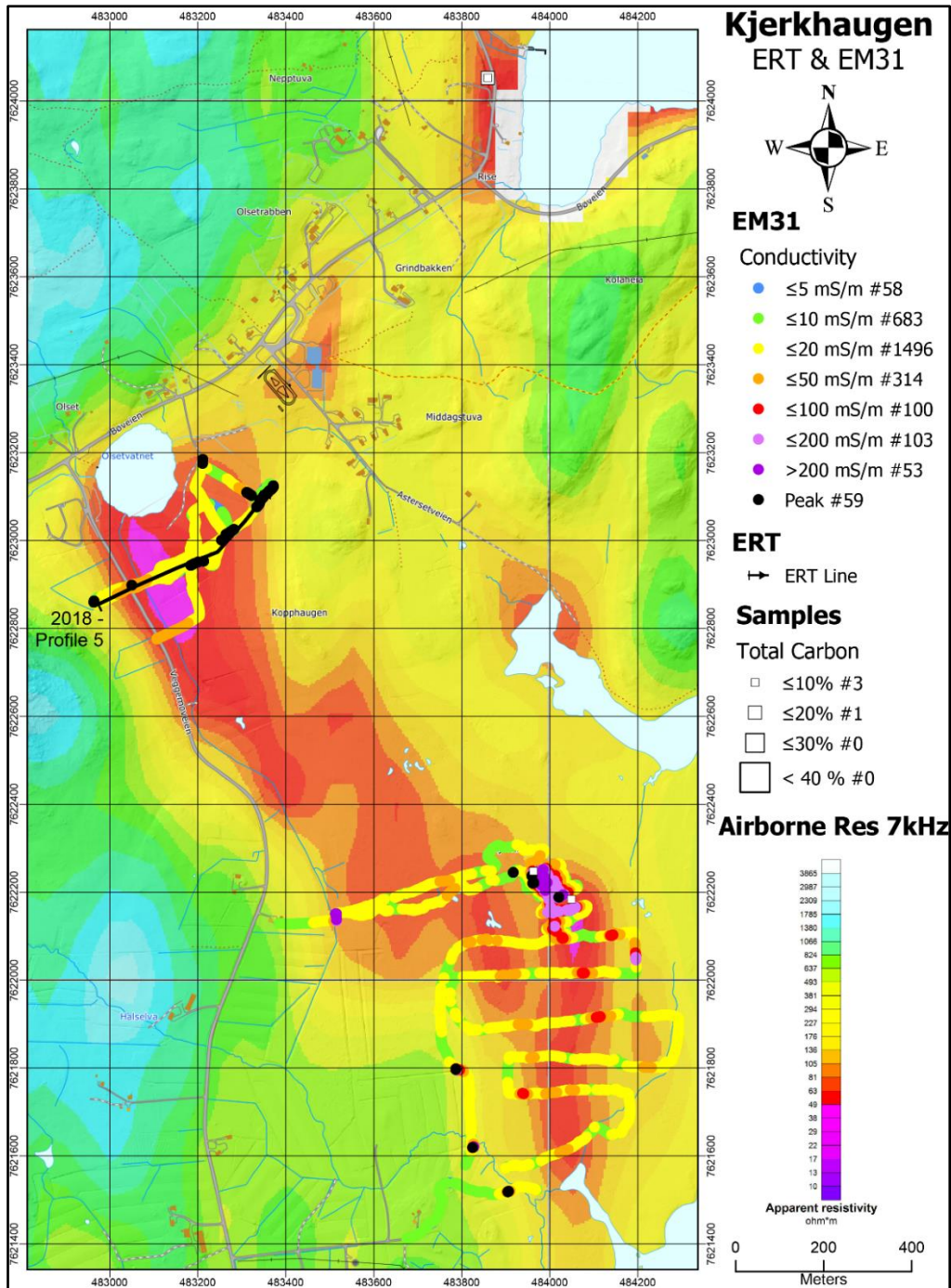


Figure 6.7: Results of EM31 measurements at Olsetvatnet and Kjerkhaugen superposed on apparent resistivity (7 kHz, from Rodionov et al. 2013a). Location of graphite samples and their Total Carbon grade is given as white squares. Location of 2D ERT/IP profile is shown as a black line.

The EM31 anomaly can be followed in a length of ca. 500 m, but the anomaly from the helicopter-borne EM indicates a total length of ca. 700 metres. It looks like this structure is plunging towards south. The EM31 data indicate a parallel structure ca. 200 m to the west. Here, the EM31 data show lower values (20 – 50 mS/m, resistivity 50 – 20 Ωm) which can be caused by thicker soil cover.

Single peak EM31 values (black dots) in both areas (Olsetvatnet and Kjerkhaugen) are most likely caused by metallic installations.

An interpretation of graphite and uncertain graphite structures based on geophysical data and the exposure is shown in Figure 6.9. Two structures are indicated, and the total length is ca. 1.5 km. Between the two areas called Olsetvatnet and Kjerkhaugen, the helicopter-borne data indicate (folded?) conductive structures and graphite is probably present here too. The length of this structure is ca. 800 m. The average thickness of the potential graphite structures, based on EM31 data, is ca. 20 m.

6.2.2 Geophysical work, ERT/IP

The location of the ERT/IP profile at Rise is shown in Figure 6.7. Results of the combined 2D resistivity and Induced Polarisation measurement are shown in Figure 6.8. Electrode spacing was 5 m and the other acquisition and inversion parameters are as described in Chapter 4.1.4. The quality of the inverted resistivity data is acceptable while the quality of IP inversion is good (see Table 6.2).

Table 6.2: Quality of 2D resistivity and IP data at Rise. Number of measured, removed and remaining data points for inversion, and observed “Absolute error” from the inversion of resistivity and IP data.

Profile name	Location	Measured data points	Removed data points	Inverted points	Abs. error ERT (%)	Abs. Error IP (%)
2018-2	Rise	1627	60	1567	18.9	5.8

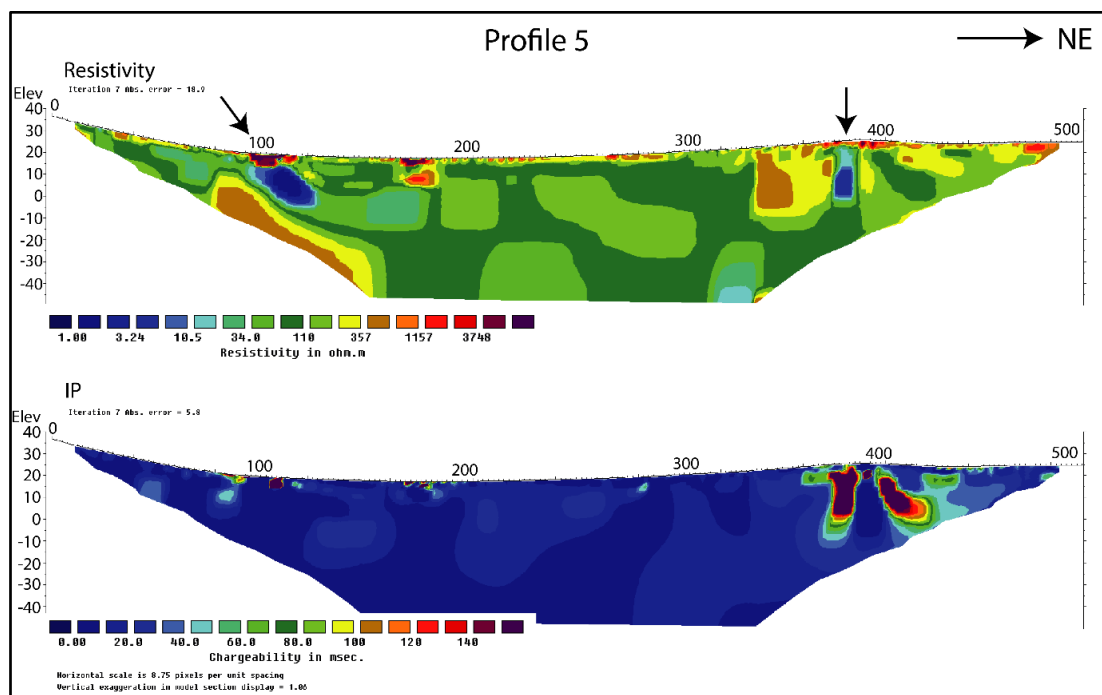


Figure 6.8: Olsetvatnet. 2D resistivity (top) and IP (bottom) results along profile 2018-5. No graphite outcrops are observed, but potential (interpreted) graphite zones are indicated with black arrows.

The resistivity section (upper part of Figure 6.8) shows a resistivity between 30 and 200 Ω m in large part of the profile. This may be interpreted as low-grade graphite, but there is no IP-effect (lower part of Figure 6.8). Most likely this material is a porous bedrock filled with salt/brackish water and is of the same kind as found at Møkland-Sund (this report) and at Møkland (Rønning et al. 2017). This bedrock is not observed

and confirmed in the field. At ca. positions 100 and 390 the resistivity is <10 Ωm (partly < 3 Ωm) and high IP effects appear here. The materials causing these anomalies are interpreted to be graphite or sulphides. The extension of these structures towards depth seems to be limited. The generally moderate resistivity along the entire profile explains the moderate EM31 anomalies.

6.2.3 Geological work, sampling

In 2018, graphite was observed in the Kjerkhaugen area and two samples were collected, one from a small (30 cm x 30 cm) exposure and one from a blue-grey sand nearby. The graphite occurs as disseminated medium to coarse-grained flakes (0.3-1 mm) in a foliated biotite-rich granulite gneiss with plagioclase and orthopyroxene.

At Rise (see Figure 6.7), 2 km further north, two samples were collected at a small EM-anomaly (ca. 250 m long) in fresh road cuts. The presence of graphite at this locality was known from previous mapping (field notes of Einar Tveten, 1976). The graphite occurs as disseminated medium to coarse-grained flakes (0,3-1,5 mm) in a granoblastic mafic granulite gneiss (containing plagioclase and orthopyroxene), that is also rich in pyrite / pyrrhotite.

Sample details are given in Appendix 6, while TC contents are given in Table 6.3.

Table 6.3: Total Carbon (TC) data from 4 surface samples from Kjerkhaugen and Rise. Note that sample 1 from Kjerkhaugen is sand, and not bedrock.

Rise - Kjerkhaugen	N	Average TC (%)	Max (%)	Min (%)	St. Dev (%)	Median (%)
Kjerkhaugen	2	6.5	10.0	2.9	-	-
Rise	2	7.9	11.1	4.7	-	-
Rise - Kjerkhaugen Total	4	7.2	11.1	2.9	4.0	7.4

6.2.4 Summary Rise – Olsetvatnet - Kjerkhaugen

The presence of graphite at Rise was known from previous mapping. In 2018, graphite was also discovered at Kjerkhaugen, ca. 1.8 km further to the south. At Kjerkhaugen, a folded graphite structure can be interpreted in a total length of ca. 700 m. West of this, a new structure is indicated, but most likely underneath a 10 m or more thick soil cover. The length of this is ca. 800 m. The average thickness of the potential graphite structures, based on EM31 data, is ca. 20 m. Graphite in this area is occurring as medium to coarse-grained flakes (0.3-1.5 mm), apparently with good crystallinity. At Rise the occurrence is associated with high contents of iron sulphides.

In the investigated area called Olsetvatnet, the helicopter-borne EM anomaly is most likely caused by porous bedrock filled by salt/brackish water, and only two small potential graphite structures are indicated. However, between Olsetvatnet and Kjerkhaugen, no information exists, and the area is a potential location of graphite mineralisation.

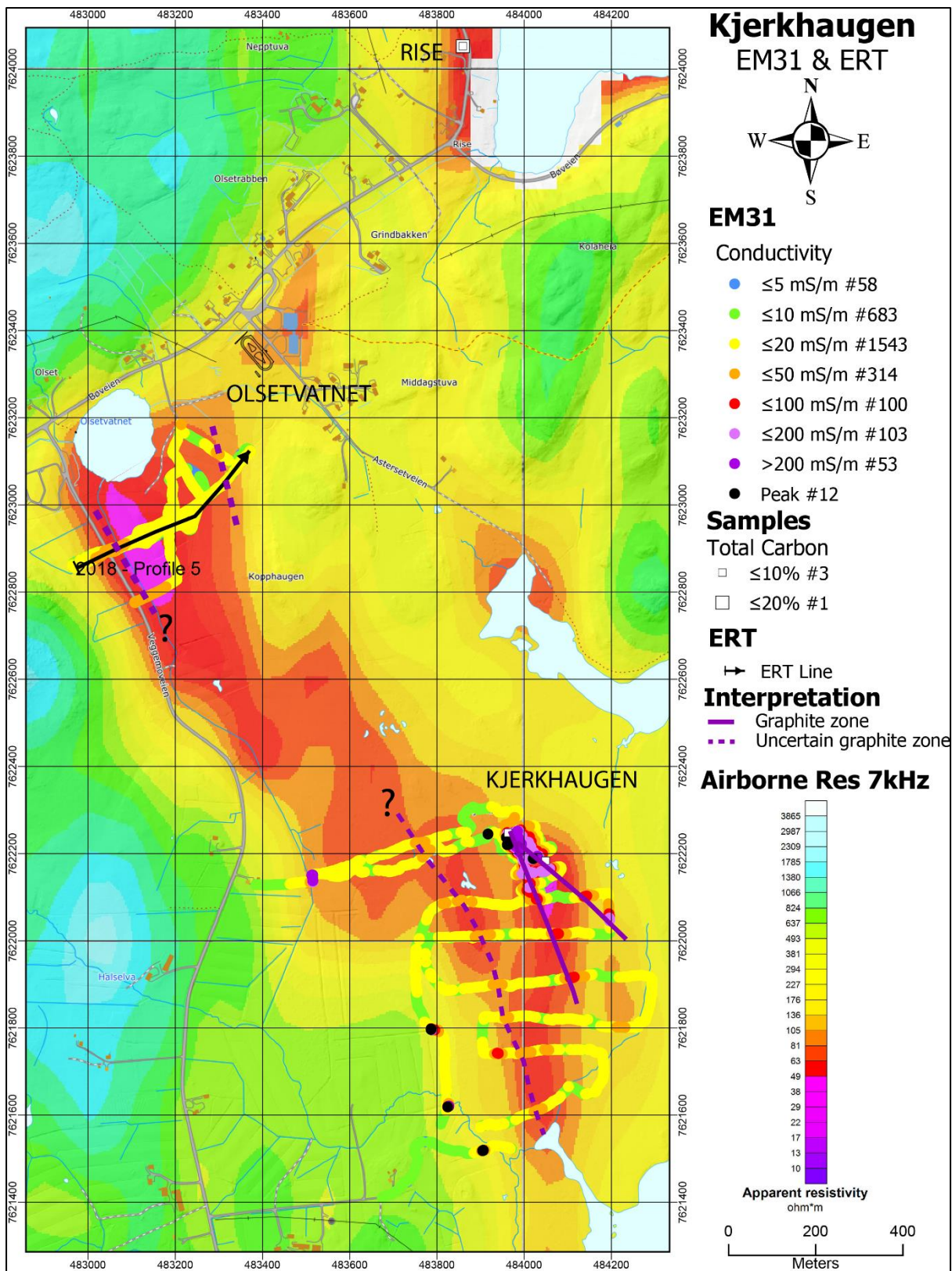


Figure 6.9: Rise, Olsetvatnet and Kjerkhaugen area. Interpreted near surface graphite structures based on ground and helicopter-based EM geophysical data and some exposures. Location of graphite samples and their TC content are shown as white squares.

6.3 Øyjorda

The Øyjorda area is located 3 km south of the Høgmyran and 2 km east of Straume (Figure 6.1). Øyjorda area seems to be a part of the same geological sequence as Høgmyran, Rise and Kjerkhaugen following the lowland around Skretinden and Veggfjellet mountains. The Øyjorda area is extensively covered. One ERT/IP profile was measured to see if the ca. 400 m long EM-anomaly from helicopter-borne measurements could be explained by graphite mineralisation. The apparent resistivity of this anomaly is ca. 100 Ω m. No further work was undertaken.

6.3.1 Geophysical work, ERT/IP

The location of the ERT/IP profile at Øyjorda is shown in Figure 6.10. Results of the combined 2D resistivity and Induced Polarisation measurement are shown in Figure 6.11. Electrode spacing was 5 m and the other acquisition and inversion parameters as described in Chapter 4.1.4. The quality of the inverted resistivity and IP sections are very good (see Table 6.4).

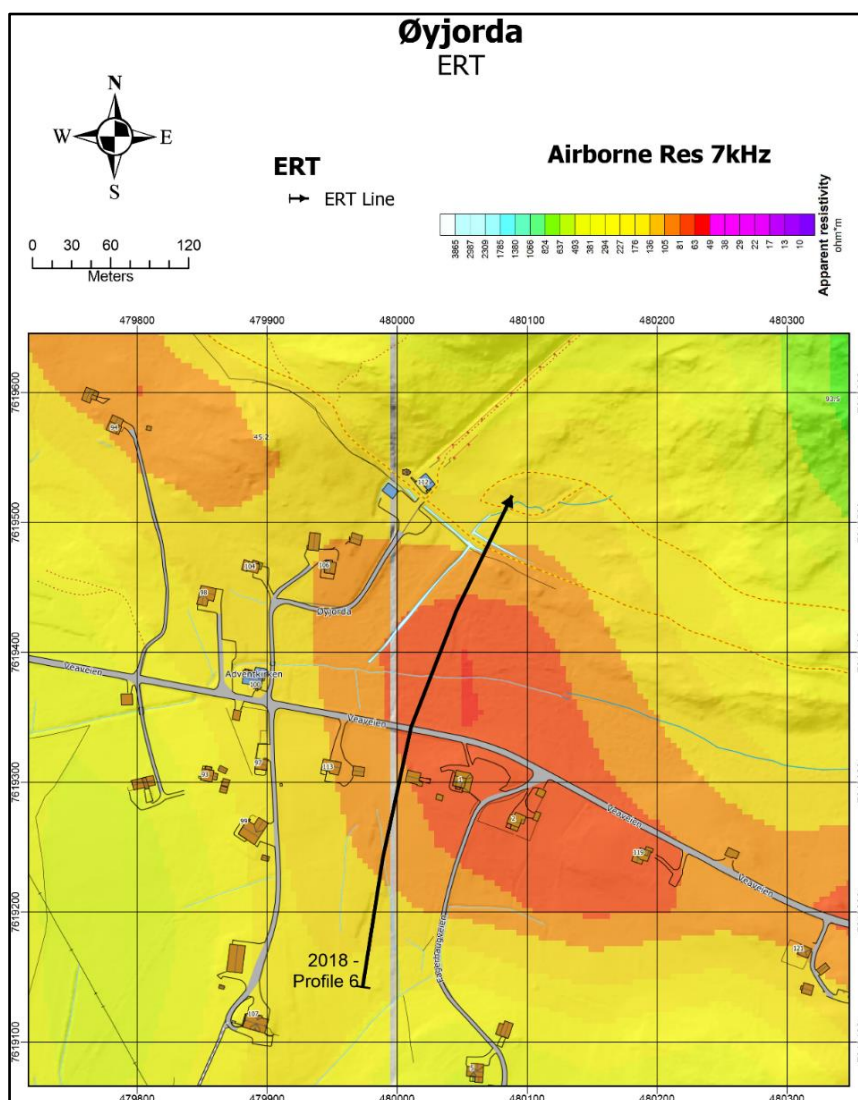


Figure 6.10: The location of the ERT/IP profile at Øyjorda superposed on apparent resistivity (7 kHz, from Rodionov et al. 2013a).

Table 6.4: Quality of 2D resistivity and IP data at Øyjorda. Number of measured, removed and remaining data points for inversion, and observed “Absolute error” from the inversion of resistivity and IP data.

Profile name	Location	Measured data points	Removed data points	Inverted points	Abs. error ERT (%)	Abs. Error IP (%)
2018-6	Øyjorda	1168	9	1159	2.9	5.3

The resistivity section (upper part of Figure 6.11) shows resistivity values between 30 and 200 Ωm in a large part of the profile. This may be interpreted as low-grade graphite, but there is no IP-effect (lower part of Figure 6.11). Most likely this material is a porous bedrock filled with salt/brackish water and is of the same kind as found at Rise, Møkland-Sund (this report) and at Møkland north (Rønning et al. 2017). This bedrock is not observed and confirmed in the field.

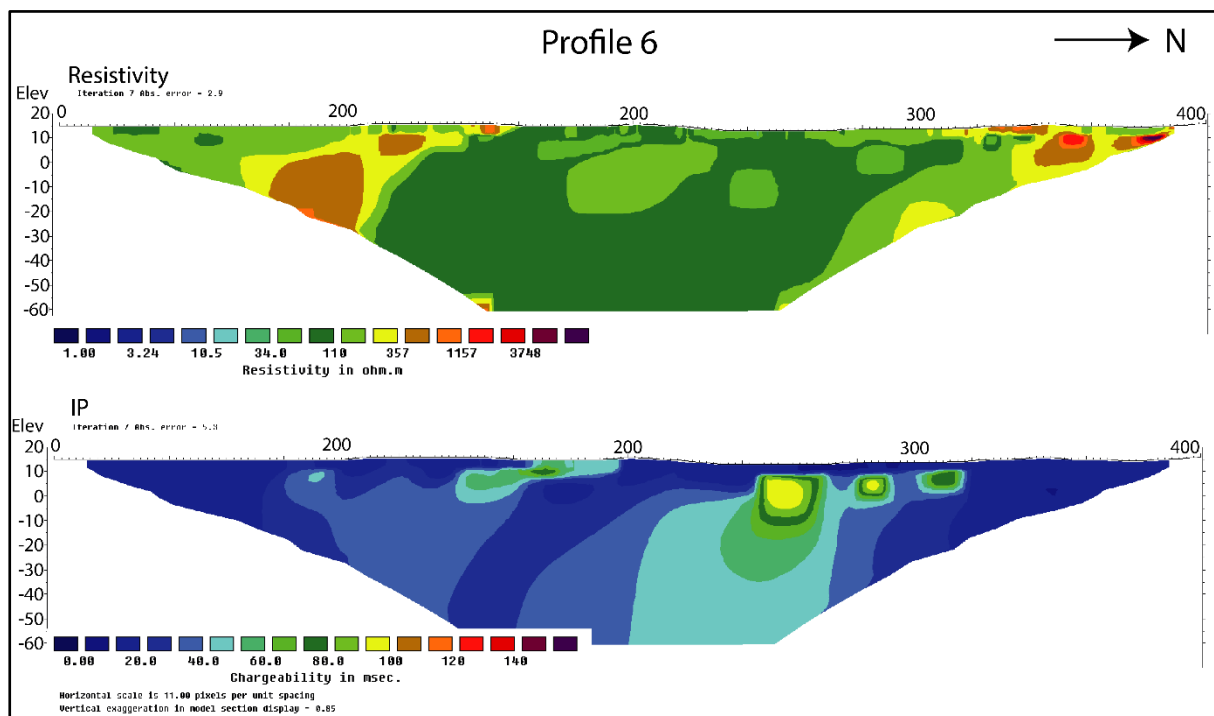


Figure 6.11: 2D resistivity (top) and IP (bottom) results along profile 2018-6 at Øyjorda. No graphite outcrops are observed.

6.3.2 Summary Øyjorda

Interesting graphite mineralisation at Øyjorda is less likely. Helicopter-borne EM anomaly is probably caused by porous bedrock filled with salt/brackish water or moderately conducting soil.

6.4 Møkland-Sund

The Møkland-Sund area, earlier called Møkland South, is located 3 km north-east of Rise and ca. 10 km north-east of Straume (Figure 6.1). The area has few outcrops, none with graphite. The northern part of the Møkland area is previously investigated by NGU (Gautneb et al. 2017, Rønning et al. 2017). Some EM31 profiling was undertaken in the southern part of Møkland area in 2017 (Rønning et al. 2018). In 2018, one ERT/IP profile was measured next to Sund (see Figure 6.13) to see if EM-anomaly from helicopter-borne measurements could be explained by graphite mineralisation. Along the same line, EM31 was measured on both sides of the local road. To make the results complete, data from 2017 investigations are included in this report.

6.4.1 Geophysical work, EM31

The data from EM31 profiling in 2017 are shown in Figure 6.12 together with apparent resistivity from helicopter-borne EM measurements. The latter show apparent resistivity in some places less than 100 Ωm . In the northern part of the presented data, graphite of relatively good quality was observed in trenches in 2016 (Gautneb et al. 2017). The thickness of the graphite structures was 5 m – 8 m but the length along strike was relatively short. Eight samples from trench 3-2016 (see Appendix 6) showed an average Total Carbon (TC) content of 14.0 % and a maximum value of 22.3 %.

In 2017, a conductive structure was mapped over more than 400 m strike length from coordinate 486080 - 7627400 in the north to 486400 - 7627000 in the south (Figure 6.12). This structure may also continue southwards. The apparent conductivity is as high as > 200 mS/m (apparent resistivity < 5 Ωm). Since this anomaly forms the continuation of the proven graphite layers further to the north, we assume that this anomaly also represents graphite. Single peak EM31 values are most likely caused by metallic installations.

In the southernmost part of this area, next to the fjord at Sund, the apparent resistivity from helicopter-borne EM measurements improves and is locally < 63 Ωm . The length of this structure is ca. 700 m and it is up to 200 m wide (Figure 6.12). To investigate the potential for good quality graphite in this area, one ERT/IP profile in combination with EM31 measurements was undertaken in 2018.

The EM31 measurements from 2018 (Figure 6.13) show an apparent conductivity mostly less than 50 mS/m. Only one measured point exceeds this value and is most likely caused by a technical installation. Since the low electric conductivity may be caused by thick soil cover, graphite mineralisation cannot be excluded, it was decided to measure one ERT/IP line.

6.4.2 Geophysical work, ERT/IP

The location of the ERT/IP profile at Møkland South is shown in Figure 6.13. Results of the combined 2D resistivity and Induced Polarisation measurement are shown in Figure 6.14. Electrode spacing was 5 m and the other acquisition and inversion parameters are as described in Chapter 4.1.4. The quality of the inverted resistivity and IP sections are acceptable and good respectively (see Table 6.5).

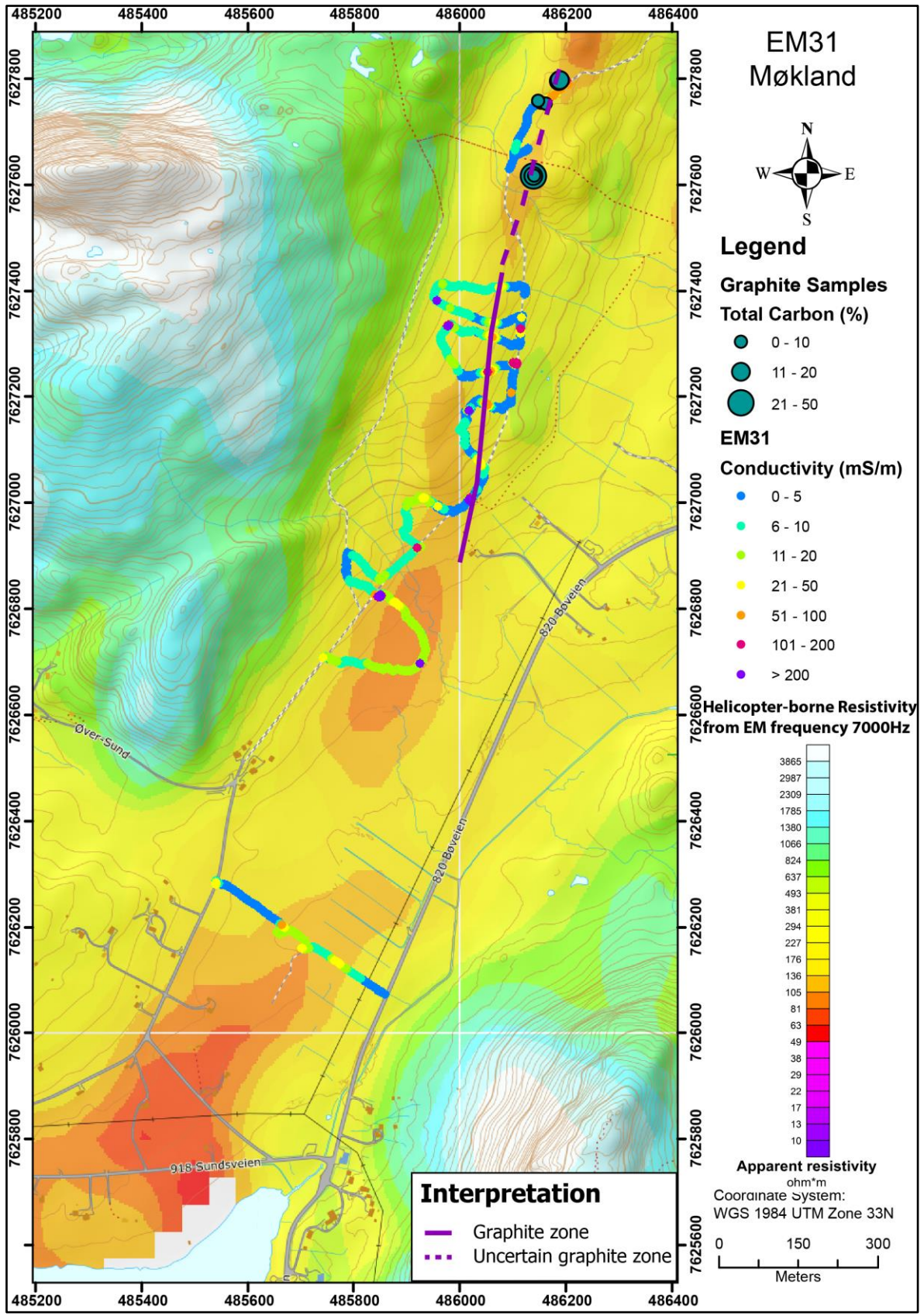


Figure 6.12: Results of EM31 measurements in the southern part of the Møklund area undertaken in 2017 superposed on apparent resistivity (7 kHz, from Rodionov et al. 2013a). Locations of graphite samples and their Total Carbon grade are shown with green circles (from Rønning et al. 2018).

Table 6.5: Quality of 2D resistivity and IP data at Møkland-Sund. Number of measured, removed and remaining data points for inversion, and observed “Absolute error” from the inversion of resistivity and IP data.

Profile name	Location	Measured data points	Removed data points	Inverted points	Abs. error ERT (%)	Abs. error IP (%)
2018-3	Møkland-Sund	1168	78	1090	17,9	12,4

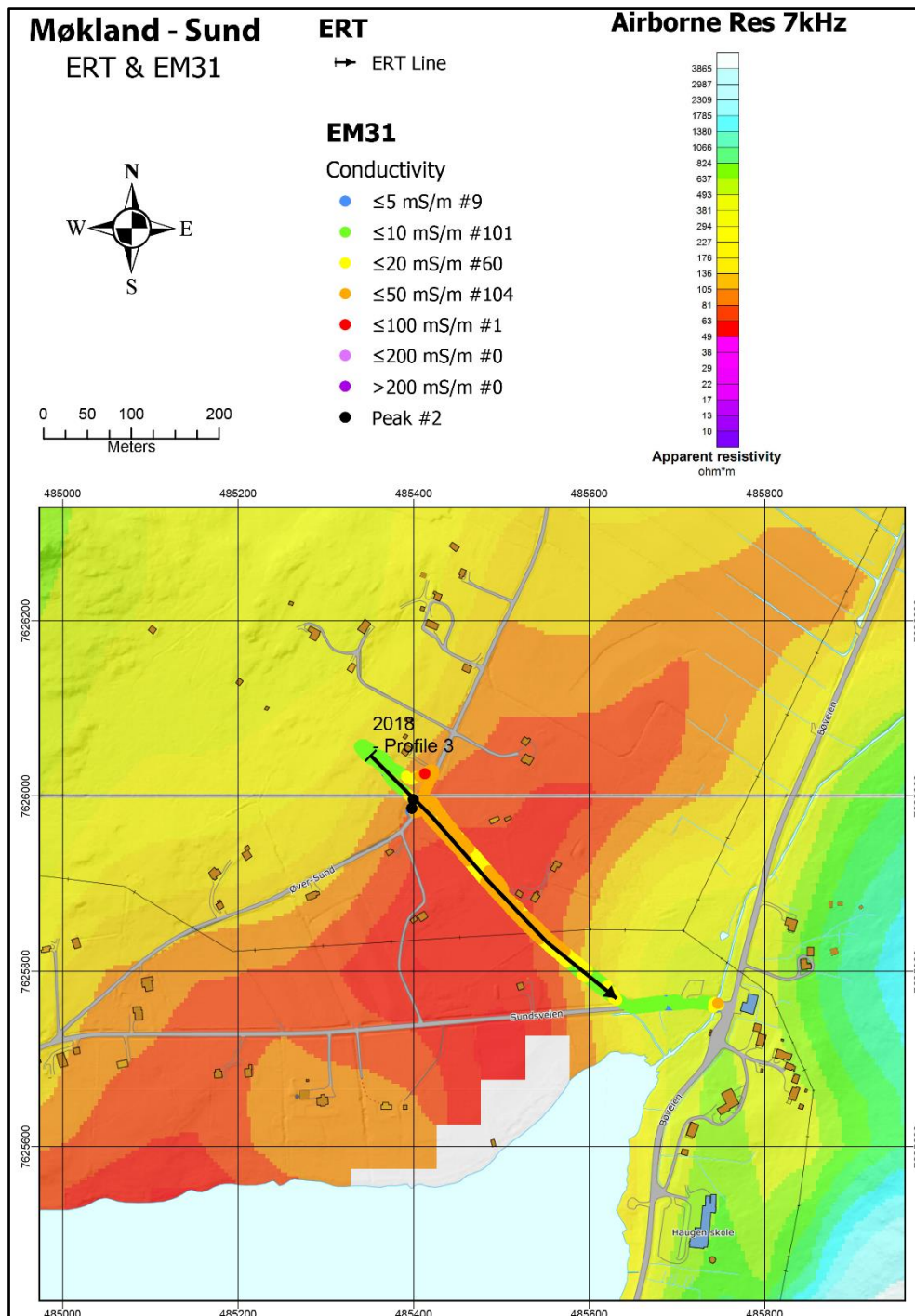


Figure 6.13: Results of EM31 measurements at Sund (southern part of Møkland area) superposed on apparent resistivity (7 kHz, from Rodionov et al. 2013a). Location of 2D ERT/IP profile is shown as a black line.

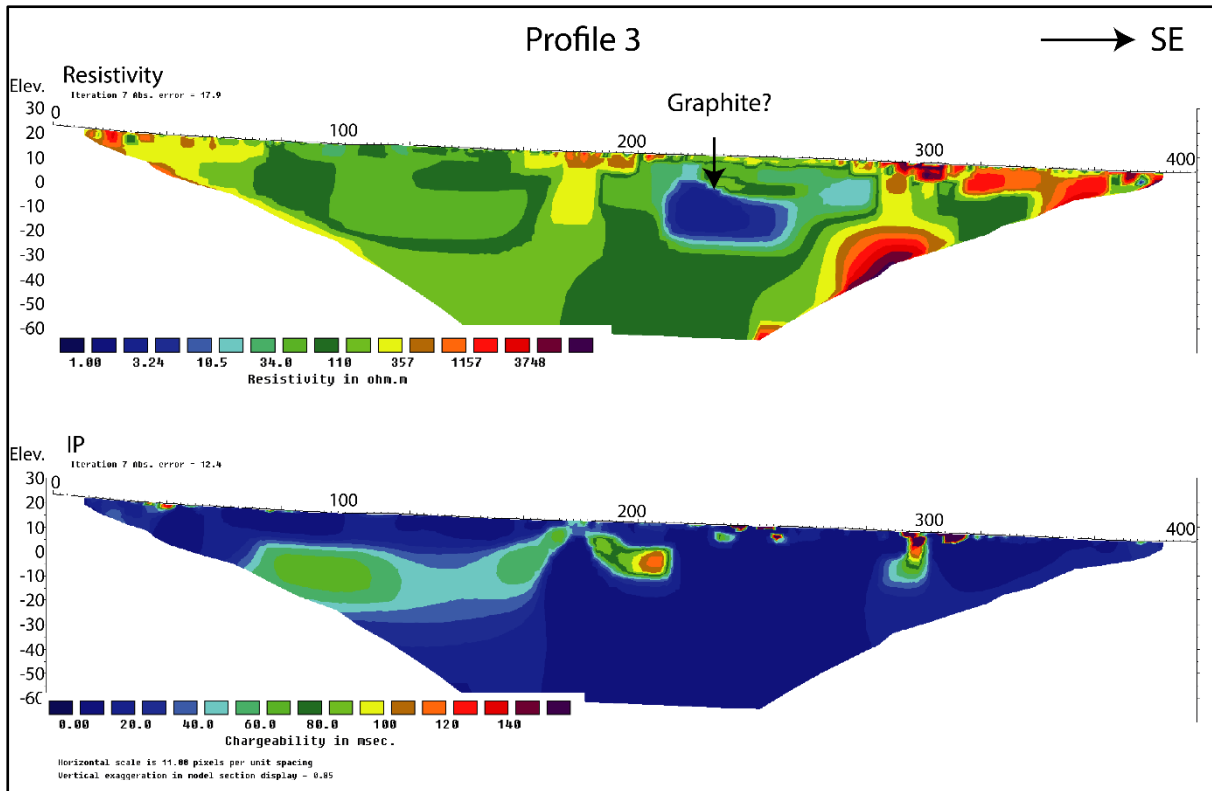


Figure 6.14: Møkland-Sund area. 2D resistivity (top) and IP (bottom) results along profile 2018-3. No graphite outcrops are observed.

The resistivity section (upper part of Figure 6.14) shows resistivity values between 30 and 200 Ωm in large parts of the profile. This may be interpreted as low-grade graphite, but there is almost no IP-effect (lower part of Figure 6.14). Most likely this material is a porous fractured bedrock filled with conducting water/clay and is of the same kind as indicated at Rise, Øyjorda (this report) and at Møkland North (Rønning et al. 2017). One local resistivity anomaly (blue colours in the central part of the section) may suggest graphite mineralisation but a strong IP effect is missing.

6.4.3 Summary, Møkland - Sund

A ca. 700 m by 200 m anomalous area from helicopter-borne EM measurements is investigated. The apparent resistivity anomaly is slightly higher than in the area further to the north where graphite of relatively good quality was observed in trenches. However, detailed EM31 measurements and one ERT/IP profile from 2018 do not show anomalies that may suggest graphite. Large amount of graphite of good quality is less likely at Sund south of the Møkland area.

6.5 Kvern fjorden

In the Kvern fjorden area, a resistivity anomaly from helicopter-borne EM measurements can be followed for about 5 km (Figures 5.2 and 6.1). This anomaly is previously investigated and called Kvern fjorddalen in the north (Gautneb et al 2017, Rønning et al. 2017) and Haugsnes in the south (Rønning et al. 2018). In the combined electromagnetic (EM) and magnetic studies shown in Figure 5.6, the southern part of Kvern fjorddalen shows up as a more interesting area. SP is previously measured in the area (Rønning et al. 2017). In 2018 EM31 measurements were undertaken. To make the data complete, results from earlier investigations are included here.

6.5.1 Geophysical and geological work in 2016 and 2017

The results from SP measurements in Kvern fjorddalen in 2016 (Rønning et al. 2017), are shown in Figure 6.15. Numerous SP lines cross a continuous ca. 2.5 km-long EM anomaly from the helicopter measurements. Several of these, show an SP anomaly higher than 800 mV while others show lower anomalies. This is typical for graphite mineralisation which are not continuous. At some crosspoints, two anomalies are indicated, telling us that the mineralisation may be more complex than shown in the helicopter-borne EM measurements.

In the northern part of the Kvern fjorddalen area, graphite is exposed and sampled (Gautneb et al. 2017). Nine samples show an average Total Carbon (TC) content of 5.3 % with a maximum value of 14,2 % (Table 6.6). CP measurements failed in the area. One ERT/IP profile showed typical anomalies for graphite mineralisation and at least two structures were observed (Rønning et al.2017).

Graphite is also exposed in the Haugsnes area further to the south (Gautneb et al. 2017, Rønning et al. 2018). Eleven samples show an average TC of 19.3 % and a maximum value 33.8 % (Table 6.6). However, analyses of drill-cores from the area show a lower content (Rønning et al. 2018).

Table 6.6: Total Carbon (TC) data from 15 surface samples from the Kvern fjorddalen and Haugsnes area.

Kvern fjorden - Haugsnes	N	Average TC (%)	Max (%)	Min (%)	StDev (%)	Median (%)
Haugsneset	11	19.3	33.8	10.6	9.4	14.7
Kvern fjorddalen	9	5.3	14.2	0.1	6.1	2.3
Kvern fjorden-Haugsn Total	20	13.0	33.8	0.1	10.7	13.2

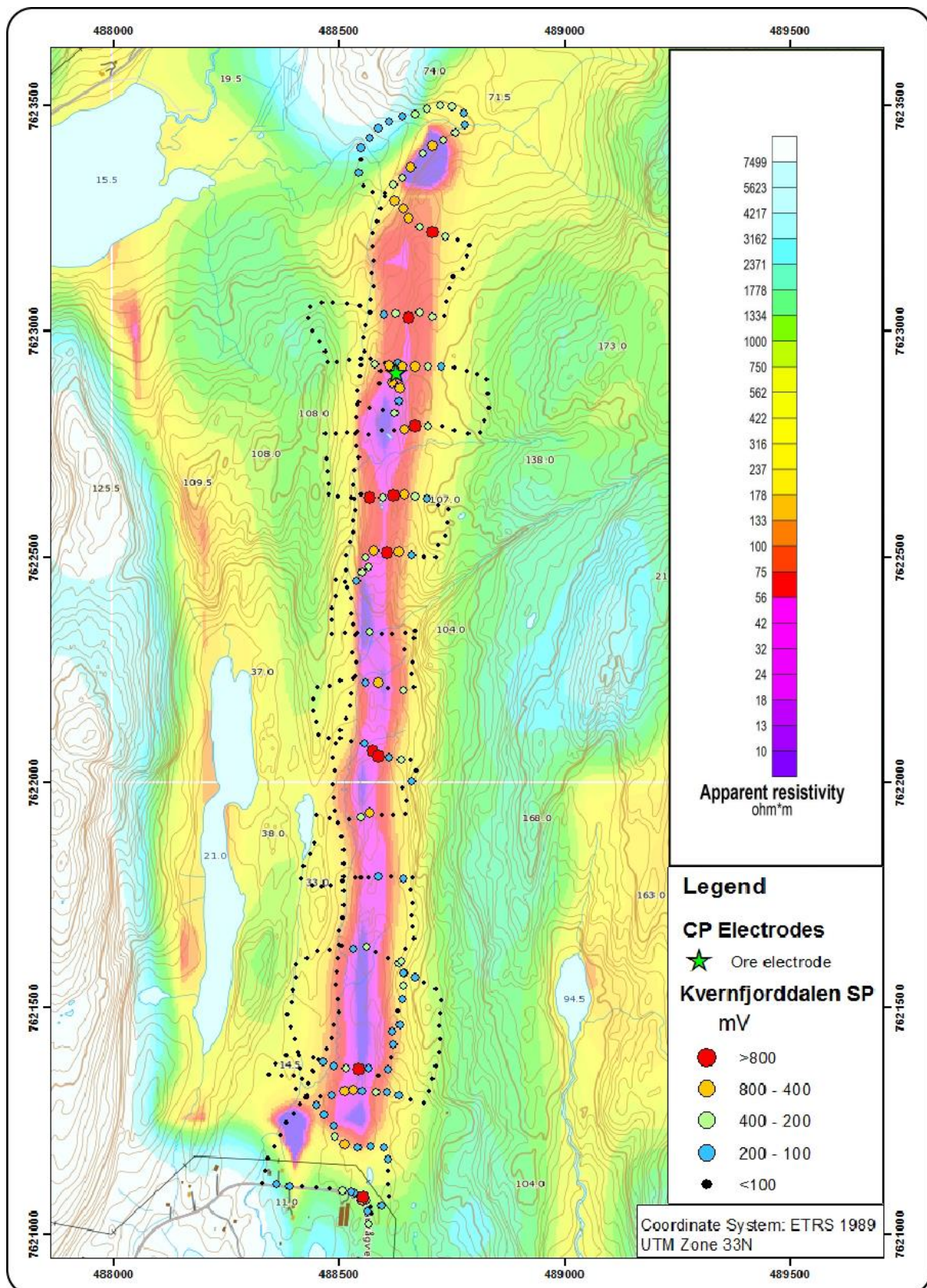


Figure 6.15: Kvern fjorddalen. SP anomalies superposed on airborne apparent resistivity calculated from 6600 Hz coplanar coils (from Rønning et al. 2017).

6.5.2 Geophysical work in 2018, EM31

The EM31 results from 2018 shown in Figure 6.16, confirm the EM anomaly from the helicopter-borne measurements and the SP results from 2016 (Rønning et al. 2017). The EM31 data is much more detailed and indicates two conducting structures in a total length of at least 500 m. The EM31 data indicate a total thickness of these structures to be from 20 to 30 m. West of these, another ca. 400 m long conducting and ca. 5 m thick structure appears. The apparent conductivity of this is less (20 – 50 mS/m, apparent resistivity between 20 and 50 Ω m) which can be caused by a deeper (> 10 m) graphite structure. The structures are open in both ends and may continue into the known graphite mineralisation in the area called Kvern fjorddalen in the north (Gautneb et al. 2017, Rønning et al. 2017) and into the area called Haugsnes to the south (Rønning et al. 2018). An interpretation of potential graphite structures at Kvern fjorden is shown in Figure 6.17.

Graphite is not observed in the area shown in Figure 6.16. However, since graphite is exposed, both north and south of the area and since the apparent conductivity is partly higher than 100 mS/m (resistivity < 10 Ω m), it is reasonable to conclude that the two conducting structures are caused by graphite schist. The apparent resistivity from helicopter-borne measurements is varying towards the north, and the quality of the graphite may also vary accordingly.

6.5.3 Summary Kvern fjorden.

From Kvern fjorden and to the north, a continuous linear helicopter-borne EM anomaly showing very low resistivity values can be followed for ca. 2.5 km. In the southern part, this resistivity anomaly coincides with low magnetic field (see Figure 5.6). The EM anomaly from helicopter-borne measurements is confirmed by EM31 and SP measurements. The EM31 data in the southern part (Kvern fjorden) indicates three parallel structures in a length of at least 500 m each. The thickness of these appears to be from 20 to 30 metres.

No graphite exposures are discovered in the Kvern fjorden area. Graphite is exposed north of the area (Kvern fjorddalen, Gautneb et al. 2017) and to the south (Haugsnæs, Rønning et al. 2018)., and most likely this is a continuous graphite structure. In Kvern fjorddalen, graphite schist is observed only in two small localities with average Total Carbon content of 5.3 %. The geophysical anomalies improve towards the south, and this can indicate a better quality. The graphite is of the same type as elsewhere in Vesterålen, typical flake graphite.

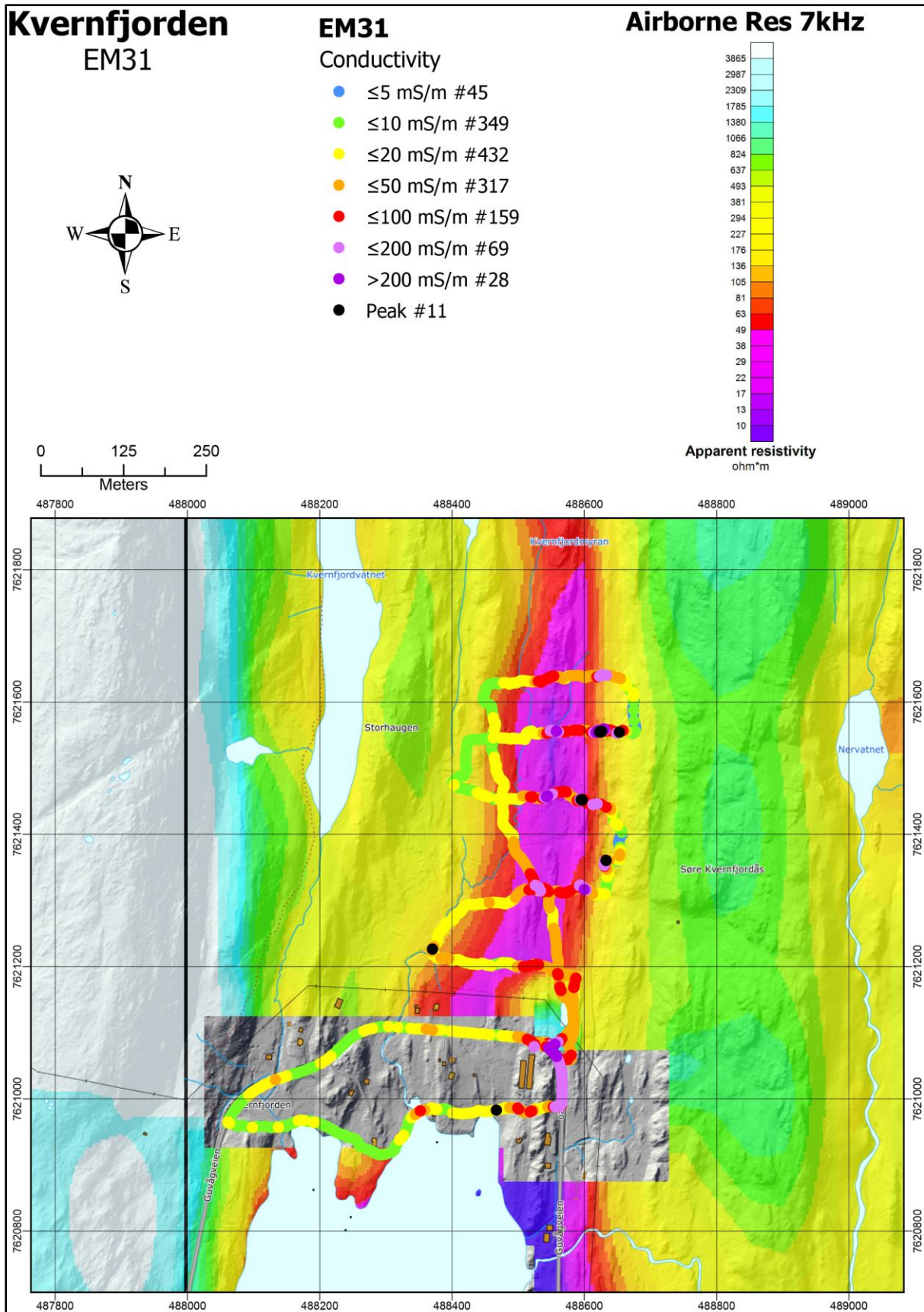


Figure 6.16: Results of EM31 measurements at Kvernfjorden superposed on apparent resistivity (7 kHz, from Rodionov et al. 2013a).

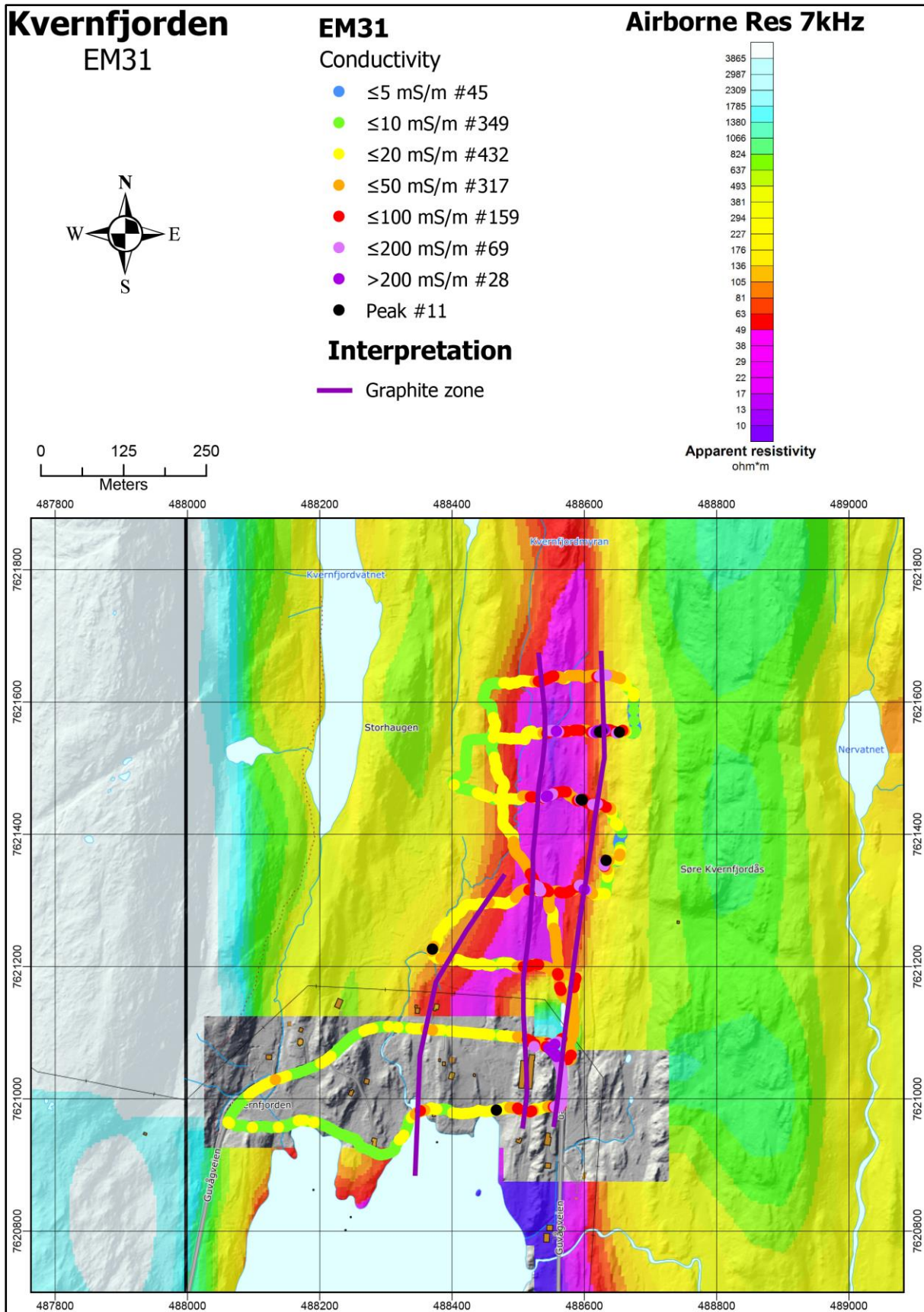


Figure 6.17: Kvernfjorden area. Interpreted near surface graphite structures based on helicopter-borne and ground-based EM geophysical data.

7. RESULTS OF THE FOLLOW-UP WORK IN SORTLAND MUNICIPALITY

In the Eastern part of Vesterålen, Sortland Municipality, follow-up work is undertaken in 2018 in four areas; Brenna, Vikeid, Ånstad and Evassåsen (see Figure 7.1). Late in 2019, the small island Reinsnesøya and Sæterstranda further to the north was visited for reconnaissance work. The areas Brenna and Vikeid were also investigated in 2017 (Rønning et al. 2018). To make the results complete, data from the 2017 are included in this report. Graphite occurrences in the Jennestad – Hornvann areas, have previously been investigated (see Chapter 3).

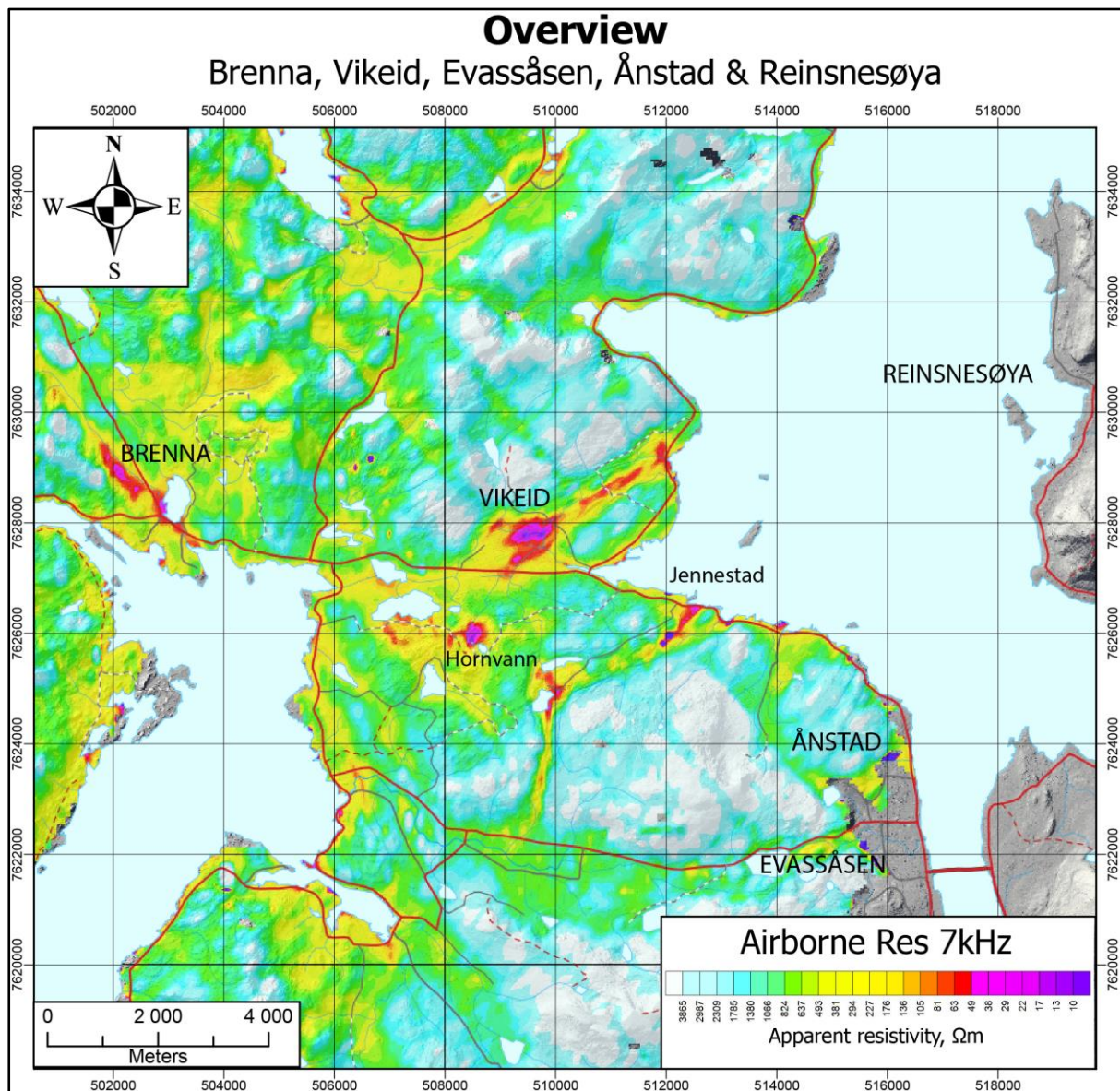


Figure 7.1: Overview map Sortland Municipality, Sortland Municipality. Follow-up work was performed in 2018 and 2019 in the areas Brenna, Vikeid, Ånstad, Evassåsen and Reinsnesøya.

7.1 Brenna

Graphite mineralisation was discovered in the Brenna area (previously called Grønorda), 2.5 km west of Frøskeland in the Sortland municipality (Figure 7.1), on a forest road and was sampled in 2016 (Gautneb et al. 2017). Some EM31 profiles and two ERT/IP profiles were measured in 2017 (Rønning et al. 2018). Additional EM31 profiling was performed in 2018. To make the presentation of the area complete, all data are reported here.

7.1.1 Geophysical work, EM31

The EM31 data from 2017 and 2018 are merged and presented together with apparent resistivity calculated from helicopter-borne EM measurements with 7 kHz coaxial coils in Figure 7.2. Several high-conductive structures (apparent conductivity > 100 mS/m, apparent resistivity < 10 Ω m) were mapped, partly where exposed graphite mineralisation occurs. An interpretation of graphite structures at Brenna is shown in Figure 7.5. Interpreted thicknesses of the structures based on EM31 data vary from 10 to 20 metres.

7.1.2 Geophysical work, ERT/IP

The locations of the two ERT/IP profiles at Brenna are shown in Figure 7.2. Results from the combined 2D resistivity and Induced Polarisation measurements are shown in Figures 7.3 and 7.4. Electrode spacing was 5 m and the other acquisition and inversion parameters as described in Chapter 4.1.4. The quality of the inverted resistivities is good/acceptable but the IP data are not acceptable (see Table 7.1).

Table 7.1: Quality of 2D resistivity and IP data at Brenna. Number of measured, removed and remaining data points for inversion, and observed “Absolute error” from the inversion of resistivity and IP data.

Profile name	Location	Measured data points	Removed data points	Inverted points	Abs. error ERT (%)	Abs. error IP (%)
2017-3	Brenna	676	91	585	13.3	41.8
2017-6	Brenna	676	218	458	20.5	Useless

ERT/IP profile 2017-3 intersects the EM anomalies perpendicularly. The soil cover is interpreted to be ca. 2 m - 8 m thick (Figure 7.3). Underneath this top layer, resistivity values of less than 10 Ω m and partly less than 3 Ω m appear along nearly the entire profile. This may be an artificial effect of several sub-vertical conducting structures. This is especially observed between positions 120 and 220, where moderate resistivity values are bending down. This can be a shielding effect of two conductors located at the two positions (see modelling in Rønning et al. 2014).

Resistivity profile 6, presented in figure 7.4, is parallel to the strike of the graphite mineralisation. The IP data are affected by a lot of noise and these data are therefore not presented. Low resistivity values (< 10 Ω m) are observed along almost the entire profile, indicating the presence of graphite. The graphite between positions 100 and 150 appears to be outcropping. In other areas the soil cover can be as much as ca. 10 m.

The combined resistivity and IP data indicate graphite or sulphide mineralisation.

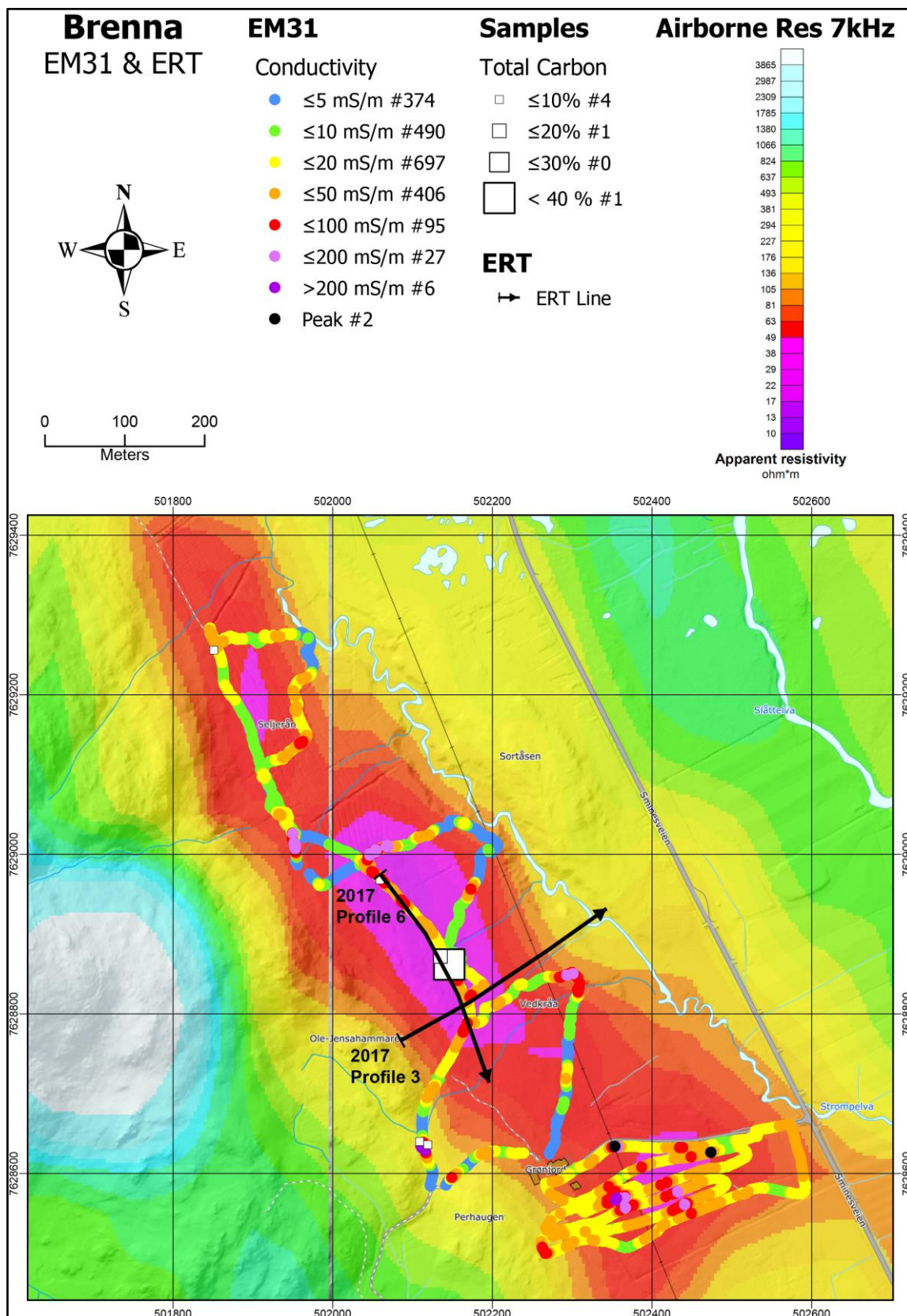


Figure 7.2: The Brenna area. The results from the EM31 measurements superposed on apparent resistivity (EM 7 kHz coaxial coil configuration, Rodionov et al. 2013a). Black lines show the locations of ERT/IP profiles. The locations of graphite samples and their TC content are shown as white squares.

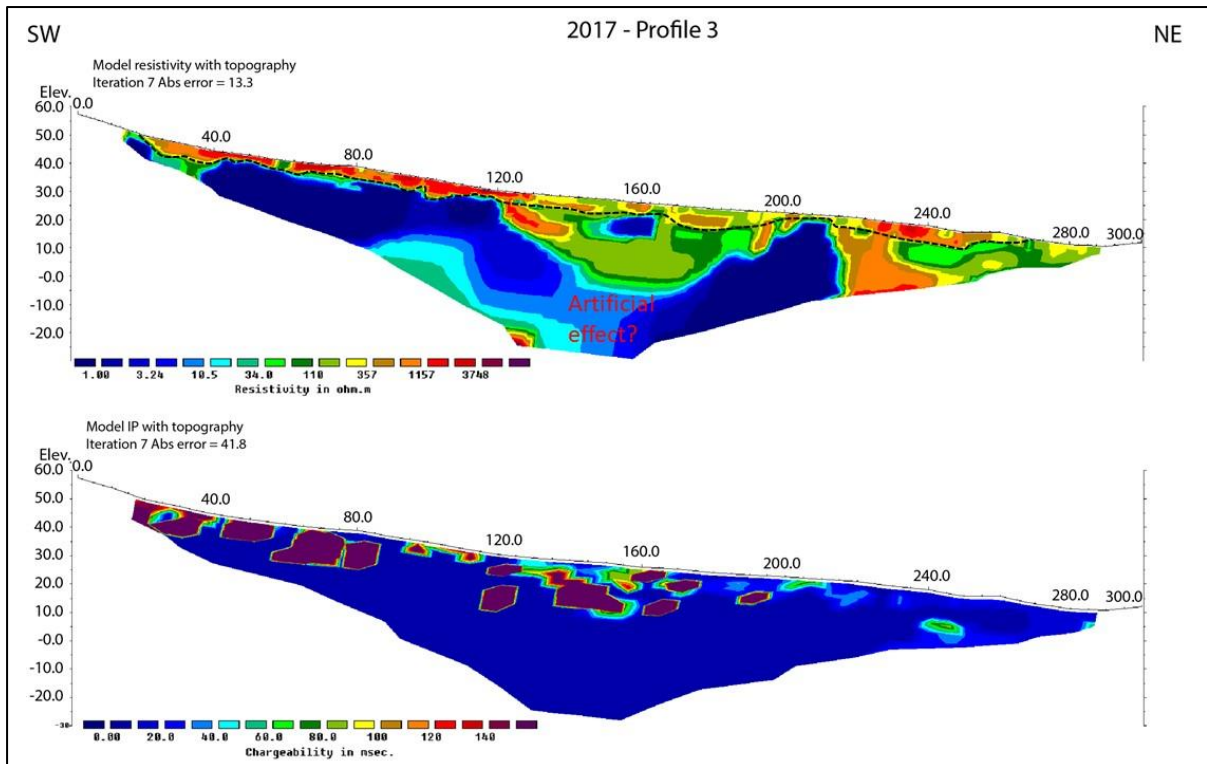


Figure 7.3: The Brenna area. The results from the 2D Resistivity and Induced Polarisation measurements along profile 2017-3. The interpreted soil-bedrock interface is shown as a dotted black line.

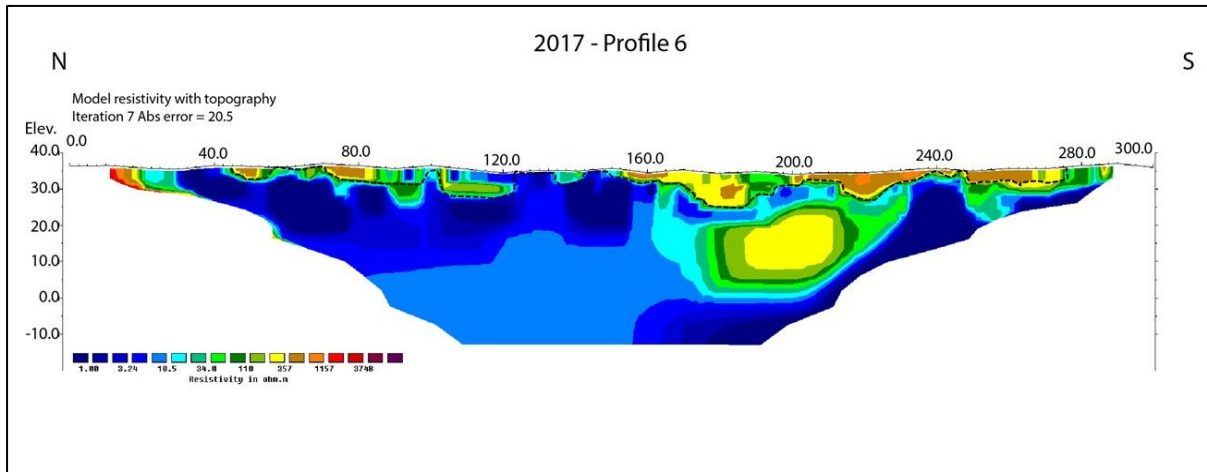


Figure 7.4: The Brenna area. The results from the 2D Resistivity measurements along profile 2017-6. The interpreted soil-bedrock interface is shown as a dotted black line.

7.1.3 Geological work, sampling

A ca. 1.5 km long helicopter-borne EM-anomaly is observed close to the Grønjorda farm west of lake Selnesvatnet, about 2.5 km W of Frøskeland (Figure 7.1) (Rodionov et al. 2013a). The area is almost 100 % soil covered. Graphite is found in some small road cuts along a forest road and in trenches close to the farm in the area. The type and relationship to any country rock is not observed. Sampling and analysis showed the average total carbon content of four samples is 10.1 % TC with a maximum value

30.4 % TC (Gautneb et al. 2017). The size of the anomaly makes this area interesting for more detailed work.

Table 7.2: Total Carbon (TC) data from seven surface samples from the Brenna area.

Brenna	N	Average TC (%)	Max (%)	Min (%)	St. Dev (%)	Median (%)
Grønjordå	7	10.1	30.4	2.4	9.5	8.6

The graphite schist in this area carries a good quality flake graphite with a typical flake grain size that varies from 0.1 mm to >10 mm. However, the almost 100% soil cover makes it uncertain if our samples are representative for the whole occurrence. Trenching or drilling is necessary to give more precise information about the quality of the deposit.

7.1.4 Brenna summary.

EM31 and 2D Resistivity/IP measurements have increased the knowledge of the graphite mineralisation at Brenna. An interpretation of individual structures is presented in Figure 7.5. The total length of these is ca. 2,500 m and their thicknesses are, on average, ca. 15 m (estimated from EM31 data). A potential depth extent of 100 m will give an estimated total volume of 3,750,000 m³.

The graphitic content of total carbon from seven samples shows an average value of 10.1 % and a maximum value of 30.4 %. If this is representative for the entire graphite structures, a total graphite tonnage in the Brenna area can be estimated to ca. 900,000 tonnes. As in other areas, the quality of the graphite is good (flake graphite).

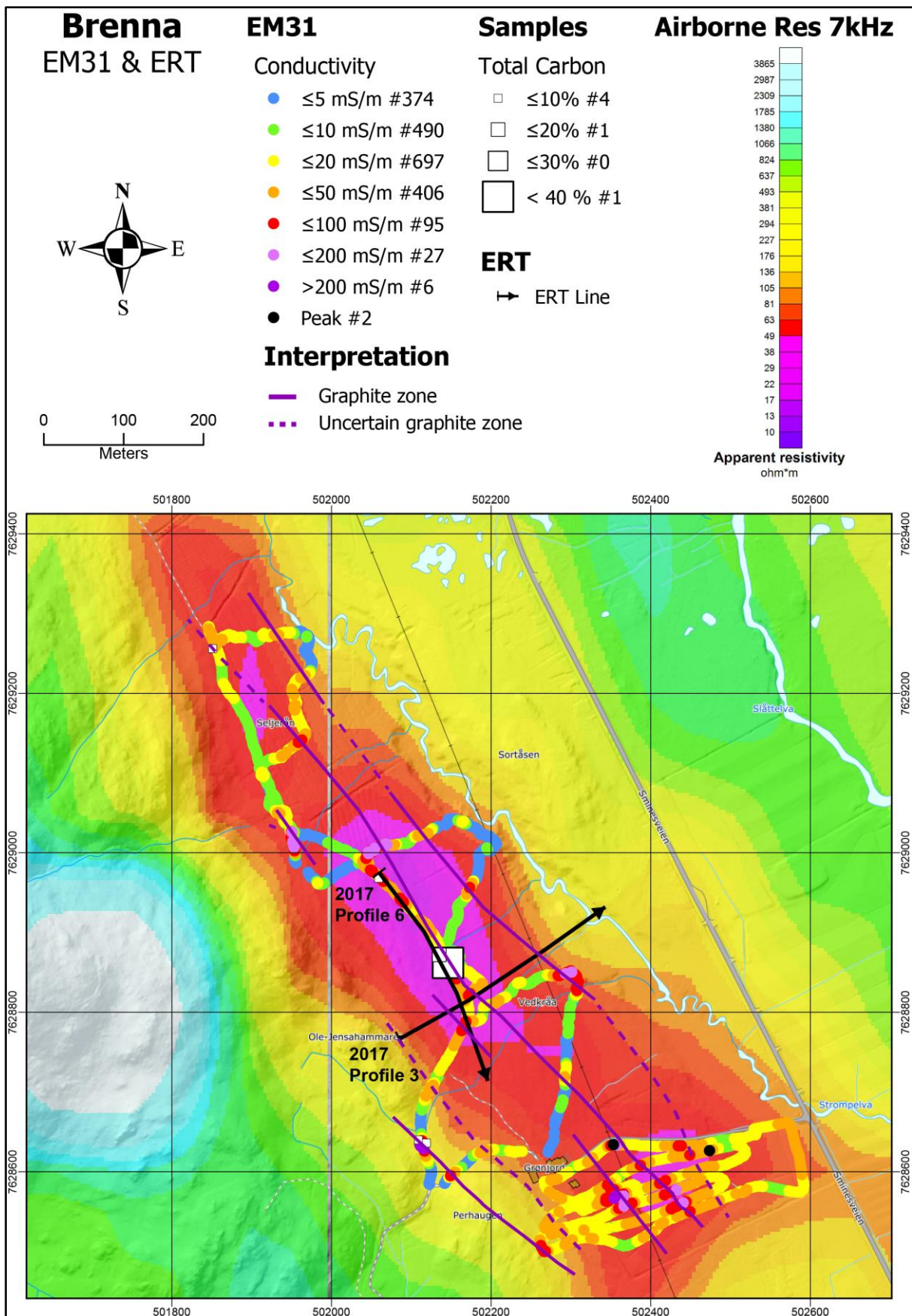


Figure 7.5: The Brenna area. The interpreted near-surface graphite structures are based on exposures, EM31 and helicopter-borne EM data. The locations of graphite samples and their TC content are shown as white squares.

7.2 Ånstad

The graphite occurrence Ånstad, located ca. 2 km north of Sortland, is a known historical mineralisation that has been searched for previously. The mineralisation is hardly seen from the helicopter-borne EM data (Figure 5.2). The apparent resistivity is ca. 200 – 300 Ωm on all frequencies. It is almost not seen in the combined magnetic/electromagnetic analysis either (Figure 5.5). Reconnaissance work in 2018 re-discovered the showing and sampling could be done. In addition, some EM31 profiling was performed. One ERT/IP line was measured to test an uncertain helicopter-borne resistivity anomaly NE of Ånstad in the autumn of 2019.

7.2.1 Geophysical work, EM31

The results of the EM31 measurements are shown in Figure 7.6 together with results from helicopter-borne 7 kHz resistivity data. The apparent conductivity from the EM31 measurements higher than 200 mS/m (apparent resistivity less than 5 Ωm) appear in a ca. 100 m long anomalous area. The strike is oriented close to East-West. EM31 data indicate a total thickness of ca. 10 m but numerous black dots indicate several thin structures with thicknesses < 3 m. Single-peak EM31 values (black dots) outside the mineralised area are most likely caused by metallic installations.

The high electric apparent conductivity measured with EM31 indicates graphite mineralisation. The helicopter-borne measurements show a very weak anomaly in this area (200 – 300 Ωm) which can be explained by several very thin, short and possibly shallow conducting structures.

North and east of the farm Ånstad, an apparent resistivity anomaly less than 10 Ωm appears in the helicopter-borne EM data. This is separated into two areas but is assumed to be continuous. Lack of data in between is caused by flying restrictions in populated areas. The anomaly is 500 m long and 200 m wide, but it does not show the same intensity on all EM frequencies (Rodionov et al. 2013a). The low apparent resistivity at 7 kHz apparent resistivity indicates the presence of graphite mineralisation here as well. One line is measured with EM31 but without interesting anomalies. No anomaly can be caused by a thick soil cover, >10 m.

7.2.2 Geological work, sampling and analysis

Reconnaissance geological work in 2018 re-discovered the old graphite showings called Ånstad. Graphite was sampled in two graphite structures (ca. 0.5 m and 3 m thick) and in a small claim (see Figure 7.7). Coordinates, Total Carbon analysis and Total Sulphur (TS) analysis are given in Appendix 6. The average Total Carbon content of five samples is 36.8 % and the maximum value is 40.6 %. The mineralisation is very rich but unfortunately the deposit appears to be very small.

Table 7.3: Total Carbon (TC) data from five surface samples from the Ånstad area.

Ånstad	N	Average TC (%)	Max (%)	Min (%)	St. Dev (%)	Median (%)
Ånstad	5	36.8	40.6	31.6	3.6	37.6

The high TC content in the Ånstad showings, makes the anomalous zone north-east of Ånstad (see Figure 7.6) more interesting, and follow-up work was recommended. One ERT/IP line, crossing the central part of the anomaly, was acquired in the autumn of 2019.

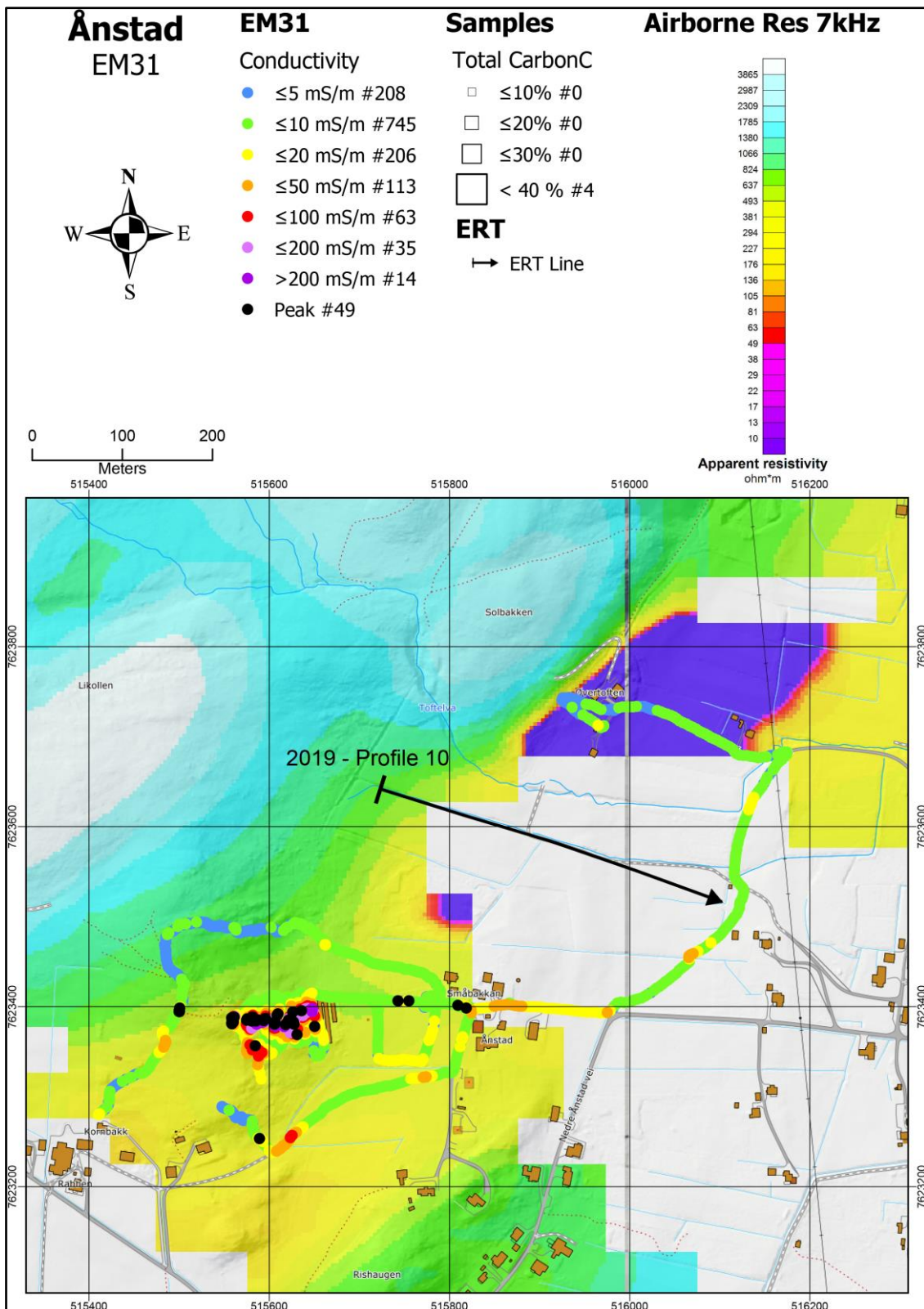


Figure 7.6: Ånstad. The results from the EM31 measurements superposed on apparent resistivity data (EM 7 kHz coaxial coil configuration, Rodionov et al. 2013a). The ERT/IP profile measured in 2019 is shown as a black line.

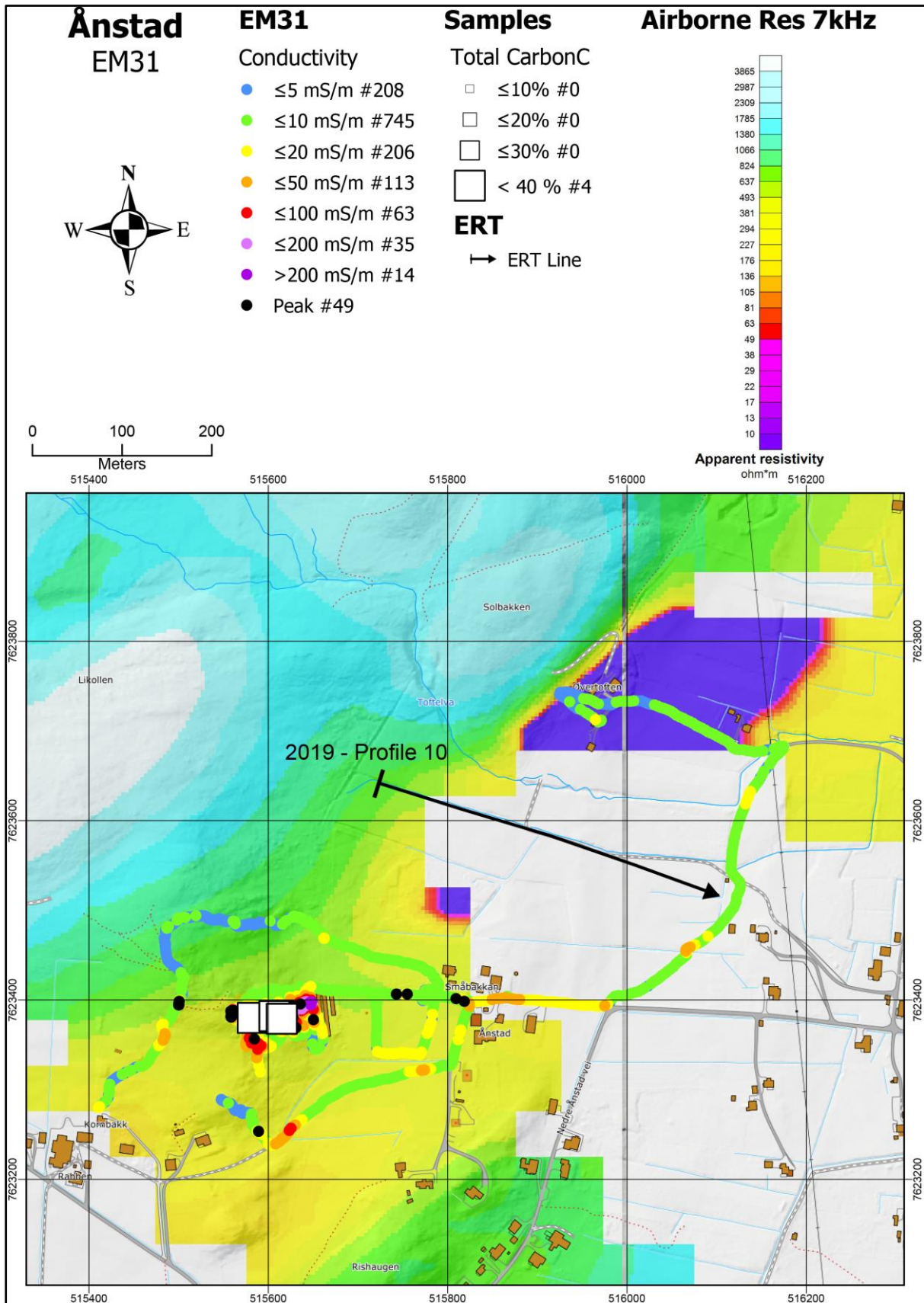


Figure 7.7: Anstad. The results from the EM31 measurements superposed on apparent resistivity (EM 7 kHz coaxial coil configuration, Rodionov et al. 2013a). The locations of graphite samples and their TC content are shown as white squares, an ERT/IP profile as a black line.

7.2.3 Geophysical work, ERT/IP

The location of the ERT/IP profiles at Ånstad is shown in Figures 7.6 and 7.7. The results of the combined 2D resistivity and Induced Polarisation measurements are shown in Figures 7.8. The electrode spacing was 5 m and the other acquisition and inversion parameters are as described in Chapter 4.1.4. The quality of the inverted resistivity and IP data is very good (see Table 7.4).

Table 7.4: Quality of 2D resistivity and IP data at Ånstad. Number of measured, removed and remaining data points for inversion, and observed “Absolute error” from the inversion of resistivity (ERT) and IP data.

Profile name	Location	Measured data points	Removed data points	Inverted points	Abs. error ERT (%)	Abs. error IP (%)
2019-10	Ånstad	1168	0	1168	1.8	1.4

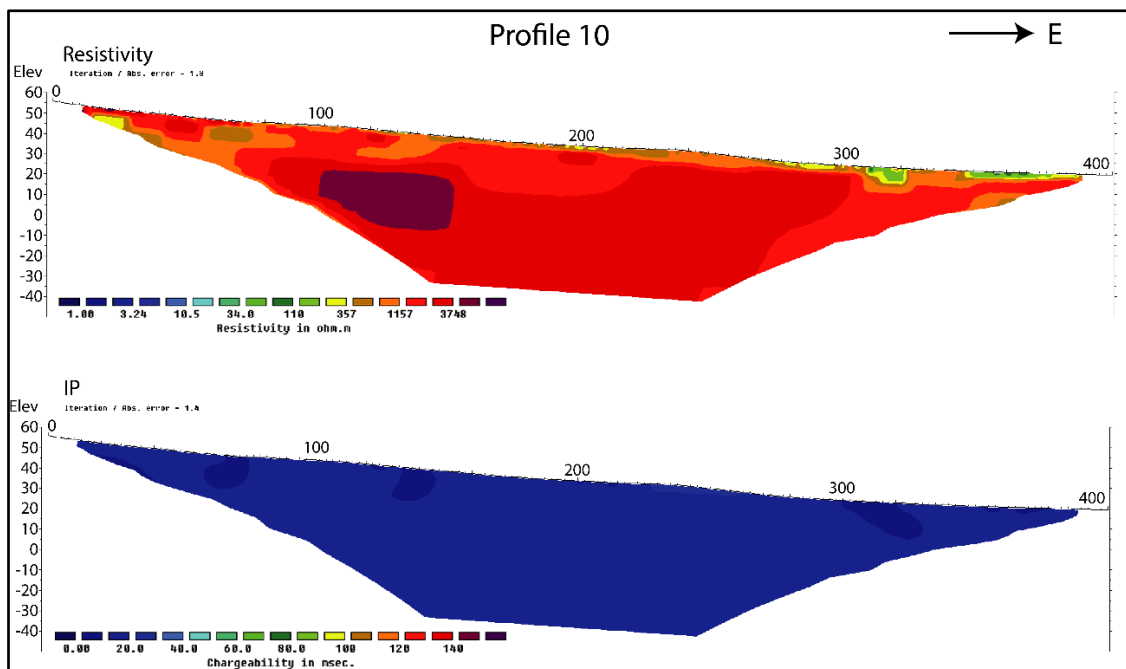


Figure 7.8: The Ånstad area. The results from the 2D Resistivity and IP measurements along profile 2019-2.

The resistivity is high along the entire profile ($> 1000 \Omega\text{m}$) and there is no IP effect. This means that there is no graphite or sulphide mineralisation in the area. The helicopter-borne EM anomaly indicated at the 7 kHz EM frequency seems to be false and is most likely an artificial effect of the data processing. The absence of ERT and IP anomalies corresponds with there being no EM31 anomaly.

7.2.4 Summary Ånstad

The old Ånstad graphite showing is very rich in carbon but is most likely too small to be of economic interest. North-east of the old showing, a 500 m by 200 m resistivity anomaly appears on the helicopter-borne EM data. Follow-up work, one ERT/IP profile, indicated no noticeable mineralisation and the helicopter-borne EM anomaly is most likely an artefact.

7.3 Evassåsen

The graphite occurrence at Evassåsen, ca. 1 km west of Sortland, is also a known historical mineralisation that has not been searched for until in 2018. The mineralisation is hardly visible in the helicopter-borne EM data (Figure 5.2). The apparent resistivity is about 200 - 300 Ωm on all frequencies. It is almost not seen at all in the combined magnetic and electromagnetic analysis either (Figure 5.6). Reconnaissance work in 2018 re-discovered the showing and sampling of the graphite mineralisation could be done. Some EM31 profiling was performed as well. One ERT/IP line was measured in the autumn of 2019 to test an uncertain resistivity anomaly East of Evassåsen, close to Sortland city (Figure 7.9).

7.3.1 Geophysical work, EM31

Results from the EM31 measurements are shown in Figure 7.9 together with apparent resistivity from the helicopter-borne measurements. The latter is moderate (100 – 300 Ωm) which is an indication of little or low-quality graphite. The apparent conductivity from EM31 measurements shows locally apparent electric conductivity higher than 200 mS/m (apparent resistivity < 5 Ωm) which indicates graphite mineralisation.

Both the helicopter-borne EM and the ground-based EM31 results indicate two parallel partly three folded structures (Figures 7.9 and 7.11). The total length of these (Figure 7.11) is ca. 2000 m and the thickness of the structures estimated from EM31 data seems to be ca. 10 m on average.

7.3.2 Geological work, sampling

Reconnaissance geological work in 2018 re-discovered the old graphite showings called Evassåsen. Graphite was sampled at several locations including an old 2 m by 2 m claim and in a 6 - 7 m deep adit (see Figure 7.8). Graphite occurs as disseminated, fine- to medium-sized grains, 0.02-0.5 mm, often in poorly defined 1-5 mm aggregates. The crystallinity appears to be less well developed than at the localities in Bø municipality (presumably due to lower metamorphic grade). Sample details are given in Appendix 6. The average TC content of six samples is 7.6 % and the maximum value is 18.7 % (Table 7.5).

Table 7.5: Total Carbon (TC) data from 6 surface samples from the Evassåsen area.

Evassåsen	N	Average TC (%)	Max (%)	Min (%)	St. Dev (%)	Median (%)
Evassåsen	6	7.6	18.7	1.4	7.0	5.5

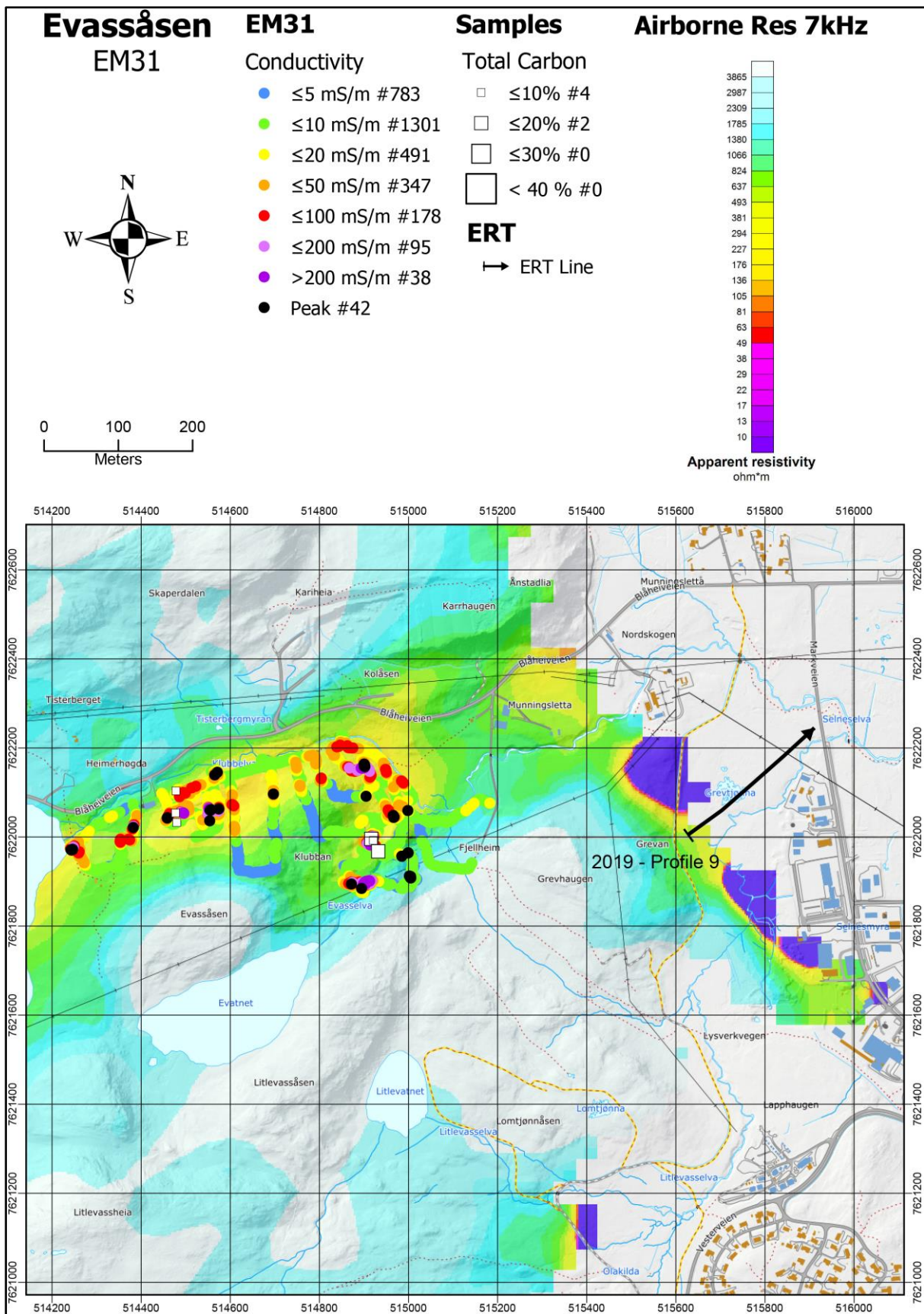


Figure 7.9: Evassåsen. The results from the EM31 measurements superposed on apparent resistivity (EM 7 kHz coaxial coil configuration, Rodionov et al. 2013a). Locations of graphite samples and their TC content are shown as white squares and the ERT/IP profile as a black line.

7.3.3 Geophysical work, ERT/IP

The location of the ERT/IP profile at Evassåsen is shown in Figure 7.9. Results of the combined 2D resistivity and Induced Polarisation measurement are shown in Figure 7.10. The electrode spacing was 5 m and the other acquisition and inversion parameters are as described in Chapter 4.1.4. The quality of the inverted resistivity and IP are good (see Table 7.6).

Table 7.6: Quality of 2D resistivity and IP data east of Evassåsen. Number of measured, removed and remaining data points for inversion, and observed “Absolute error” from the inversion of resistivity and IP data.

Profile name	Location	Measured data points	Removed data points	Inverted points	Abs. error ERT (%)	Abs. error IP (%)
2019-	Evassåsen	1168	15	1153	8.6	6.1

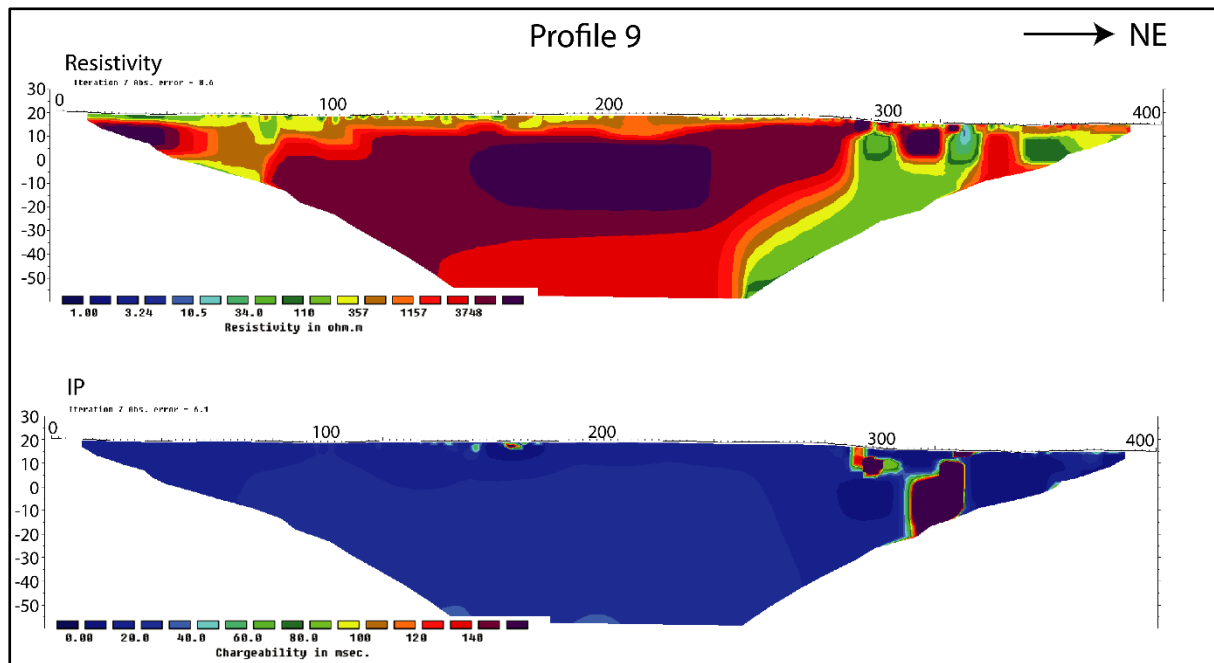


Figure 7.10: The Evassåsen area. The results from the 2D Resistivity and IP measurements along profile 2019-1.

In great parts of profile 2019-1 east of Evassåsen, the resistivity is high ($< 1000 \Omega\text{m}$) and there is no IP effect. There is, in this part, position 105 to 290, no graphite mineralisation. At the end of the resistivity section, at positions 300 and 330, two small low-resistivity structures are seen. These coincide with IP anomalies, and mineralisation of graphite or sulphides is probably to be found. However, these resistivity anomalies are small. The anomalies also coincide with a powerline, and an artificial effect from it cannot be excluded. However, large volumes of graphite are unlikely. In the other end of the profile, a low resistivity anomaly appears at positions 60 to 80. There is no IP anomaly connected to this and the anomaly is probably caused by a fractured zone in bedrock dipping to the west.

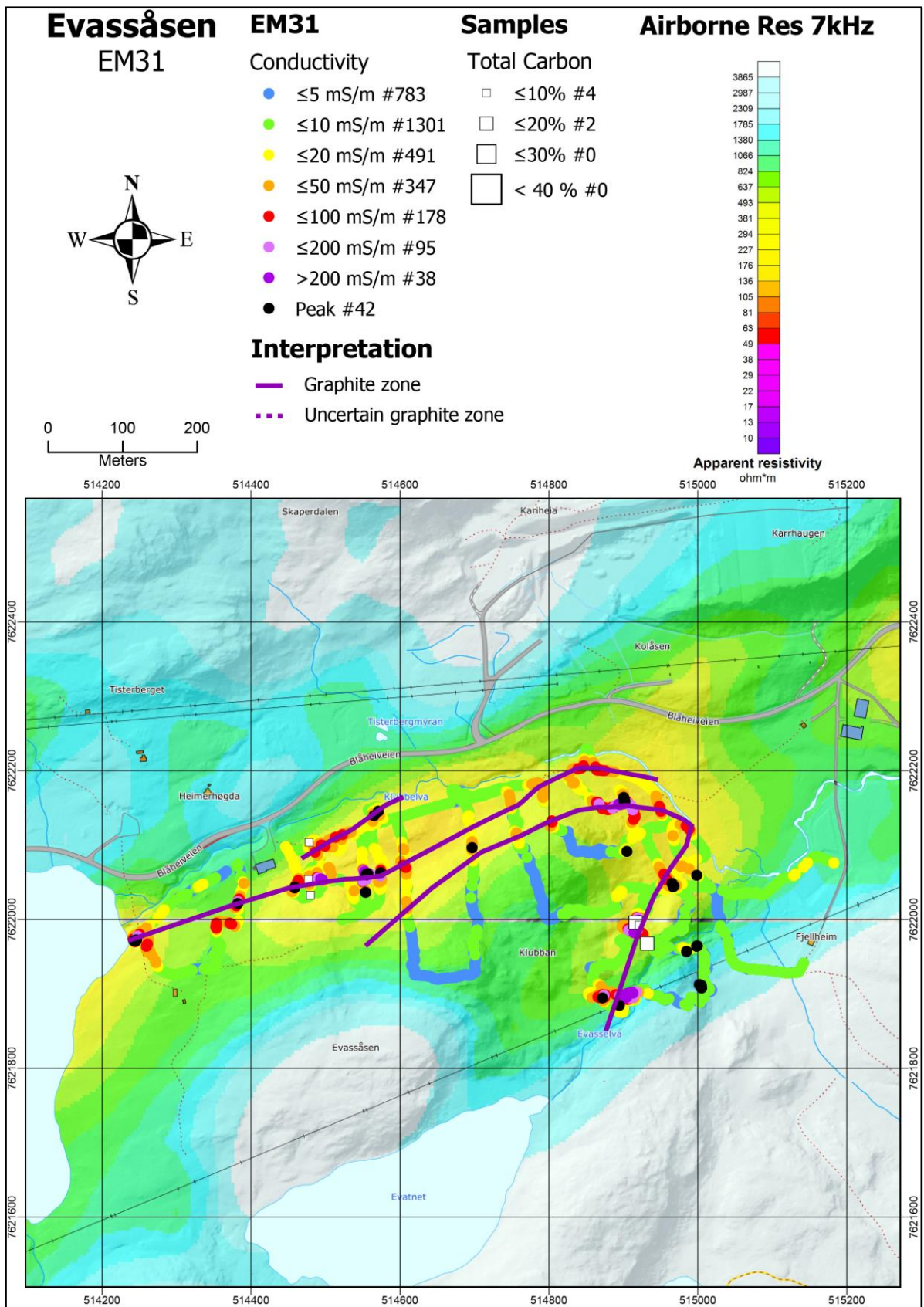


Figure 7.11: Evassåsen interpretation map. The results from the EM31 measurements are superposed on apparent resistivity (EM 7 kHz coaxial coil configuration, Rodionov et al. 2013a) and interpreted graphite mineralisation. Sample locations and TC contents are shown as white squares. Interpreted graphite structures are shown as violet lines.

7.3.4 Summary Evassåsen

A graphite showing at Evassåsen was re-discovered in 2018. EM31 data indicate two (partly three) parallel folded structures with a total length of 2,000 m and an average thickness of ca. 10 m. Flake graphite of interesting grain size is observed. The average total carbon content is 7.6 %. Resistivity anomalies appear in the 7 kHz helicopter-borne EM data east of Evassåsen. Follow-up ERT/IP profiling indicates graphite or sulphide mineralisation but the size of this is probably too small to be of economic interest.

7.4 Vikeid East (Storelvbukta)

No more work was carried out at the eastern part of Vikeid, next to Storelvbukta in 2018. In 2017, one line was measured, using EM31. ERT/IP measurements were undertaken along the same line (Rønning et al. 2018). The data from 2017 are presented here to make information on the Vikeid area complete.

7.4.1 Geophysical work, EM31

At Vikeid East, one profile was measured with EM31 in 2017. The line crosses a ca. 500 m long and 200 m wide resistivity anomaly from helicopter-borne EM measurement. The EM31 results are presented in Figure 7.12, superposed on the apparent resistivity calculated from 7 kHz. No high-conductivity values that could indicate graphite mineralisation were found, despite a very low apparent resistivity from helicopter-borne EM measurements. This is probably caused by thick soil cover (see ERT/IP discussion). For this reason, no further EM31 measurements were undertaken.

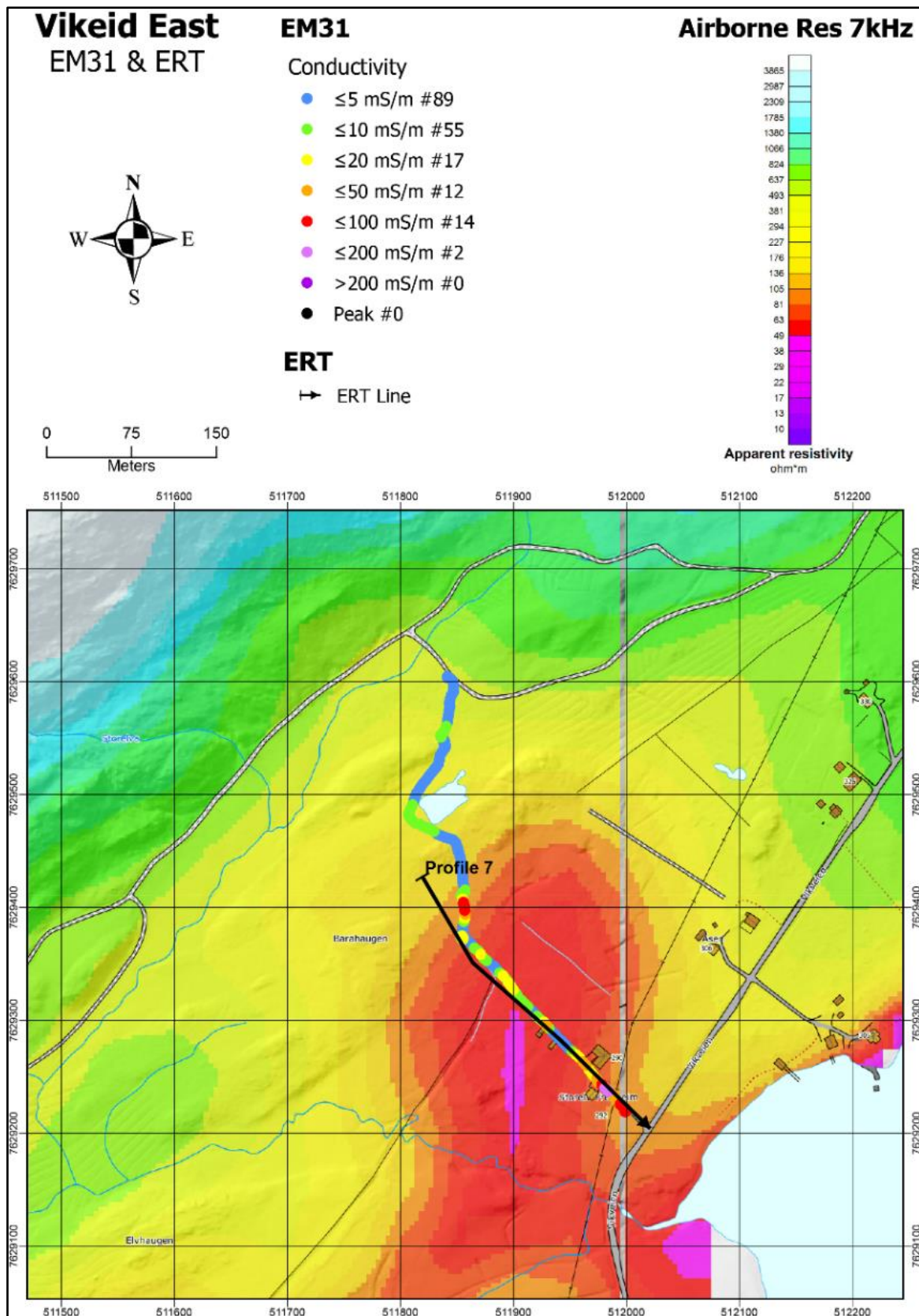


Figure 7.12: The Vikeid East area (Storelvbukta). The results from the EM31 measurements are superposed on apparent resistivity (EM 7 kHz coaxial coil configuration, Rodionov et al. 2013a). Black lines show the location and direction of the ERT/IP profiles.

7.4.2 Geophysical work, ERT/IP

The location of the ERT/IP profile at Vikeid East is shown in Figure 7.12. Results from the combined 2D resistivity and Induced Polarisation measurements are shown in Figure 7.13. The electrode spacing was 5 m and the other acquisition and inversion parameters are as described in Chapter 4.1.4. The quality of the inverted resistivity and of the IP sections are good and acceptable respectively (see Table 7.7).

Table 7.7: Quality of 2D resistivity and IP data in the Vikeid East profile. Number of measured, removed and remaining data points for inversion, and observed “Absolute error” from the inversion of resistivity and IP data.

Profile name	Location	Measured data points	Removed data points	Inverted points	Abs. error ERT (%)	Abs. error IP (%)
2017-7	Vikeid East	676	27	649	6.8	16.3

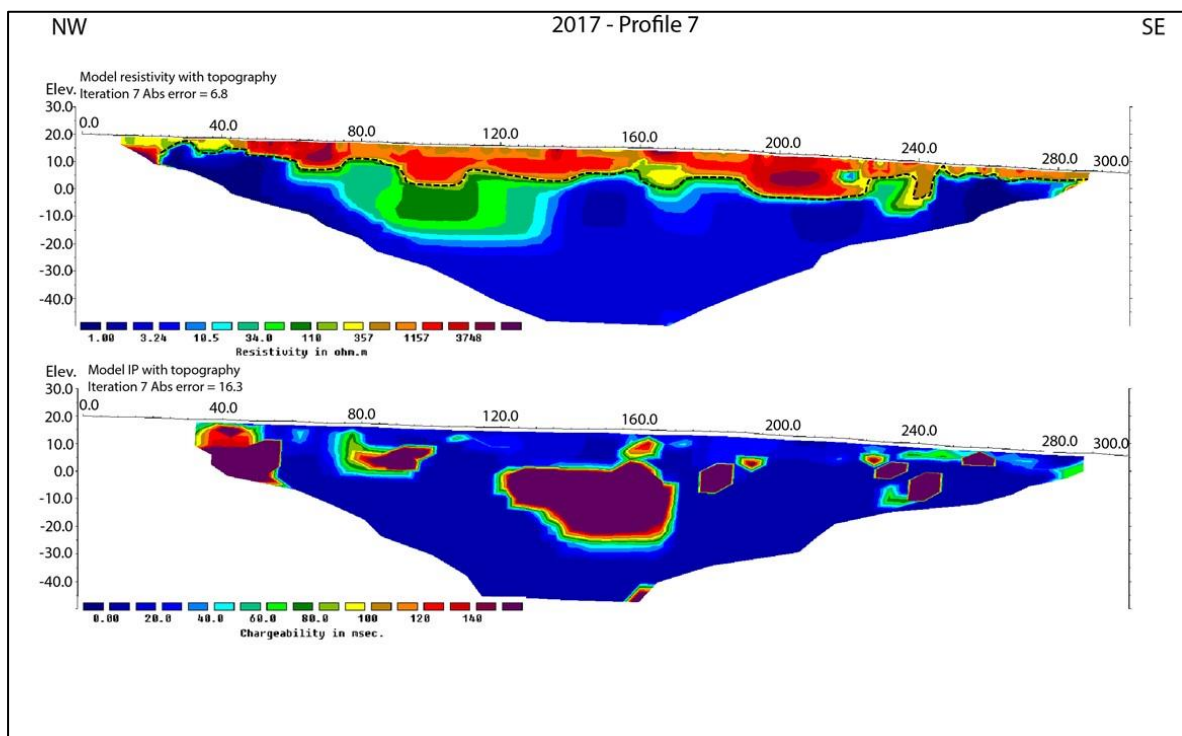


Figure 7.13: The Vikeid East area. The results of the 2D Resistivity (top) and Induced Polarisation (bottom) measurements along profile 2017-7. The interpreted soil-bedrock interface is marked as a dotted black line.

The **ERT/IP profile 2017-7** intersects a ca. 150 m wide low resistive zone observed from helicopter-borne EM data north-west of Storelvbukta in the Vikeid area (see Figure 7.12). The thickness of the soil cover in this resistivity section (Figure 7.13) is from ca. 2-3 m and up to ca. 15 m. The resistivity in this material is somewhat high ($< 1200 \Omega\text{m}$). This may represent more coarse-grained dry soil, but an interpretation of bedrock without mineralisation cannot be excluded.

A resistivity of $< 10 \Omega\text{m}$, and partly $< 3 \Omega\text{m}$, is found underneath this cover along the entire profile of 300 m. Induced polarisation shows locally high values which indicates

disseminated electrically conducting minerals, graphite or sulphide. Modelling has shown that the continuous low resistivity zone consists potentially of at least five subvertical, electrically conducting horizons (Rønning et al. 2014).

The Vikeid East area has few outcrops, and no graphite showings are observed. It is, however, reasonable to believe that since graphite is observed in both the Vikeid Central (Vedåsen) and the Vikeid West areas, graphite mineralisation is also probably to be found in the Vikeid East area.

7.4.3 Summary - Vikeid East

The helicopter-borne EM measurements indicate a ca. 500 m by 150 m anomalous resistivity area. EM31 measurements were tested but the soil thickness in the area is partly too thick to give information on potential graphite mineralisation.

One ERT/IP profile shows a combination of resistivity and IP anomalies which indicate graphite or sulphide mineralisation in a total width of ca. 280 m. Most likely this mineralisation consists of several graphite structures. Unfortunately, no exposures for quality estimations are observed.

7.5 Vikeid Central (Vedåsen)

In 2017, some EM31 profiles and one ERT/IP profile were measured (Rønning et al. 2018). Graphite mineralisation has been known since early 1990 (Gautneb and Tveten 1992). Extended EM31 measurements were undertaken in 2018. The data from 2017 are presented here in order to make the Vikeid Central area complete. The area has earlier been named Vedåsen, which is used as locality name in Table 7.9 and in Appendix 6.

7.5.1 Geophysical work, EM31

Some EM31 measurements were undertaken in 2017 (one line). The EM31 measurements were extended in 2018 in order to map the whole Vikeid Central area. All the results are presented in Figure 7.14.

The helicopter-borne EM measurements indicate low resistivity in a total length of ca. 1.5 km. The EM31 data do not show apparent electric conductivity above 200 mS/m ($< 5 \Omega\text{m}$) which can be an indicator of graphite. This is probably caused by a relatively thick soil cover (see ERT data next section). The EM31 data indicate an average thickness of ca. 20 m for the potential graphite structures. The shape of the helicopter-borne anomaly indicates folded structures.

Graphite is exposed at two locations in the area (Figure 7.14). The eastern exposure lies outside the low resistive (high-conductive) area from helicopter-borne measurements and give little response at the EM31 data. This is most likely a very small mineralisation. The second exposure lies at the eastern rim of the conducting structure and gives some response in the EM31 data. The best conducting part of the helicopter-borne data lies NW of the exposures where the ERT/IP line crosses the

anomaly from helicopter-borne measurements. The best graphite mineralisation is most probably located here.

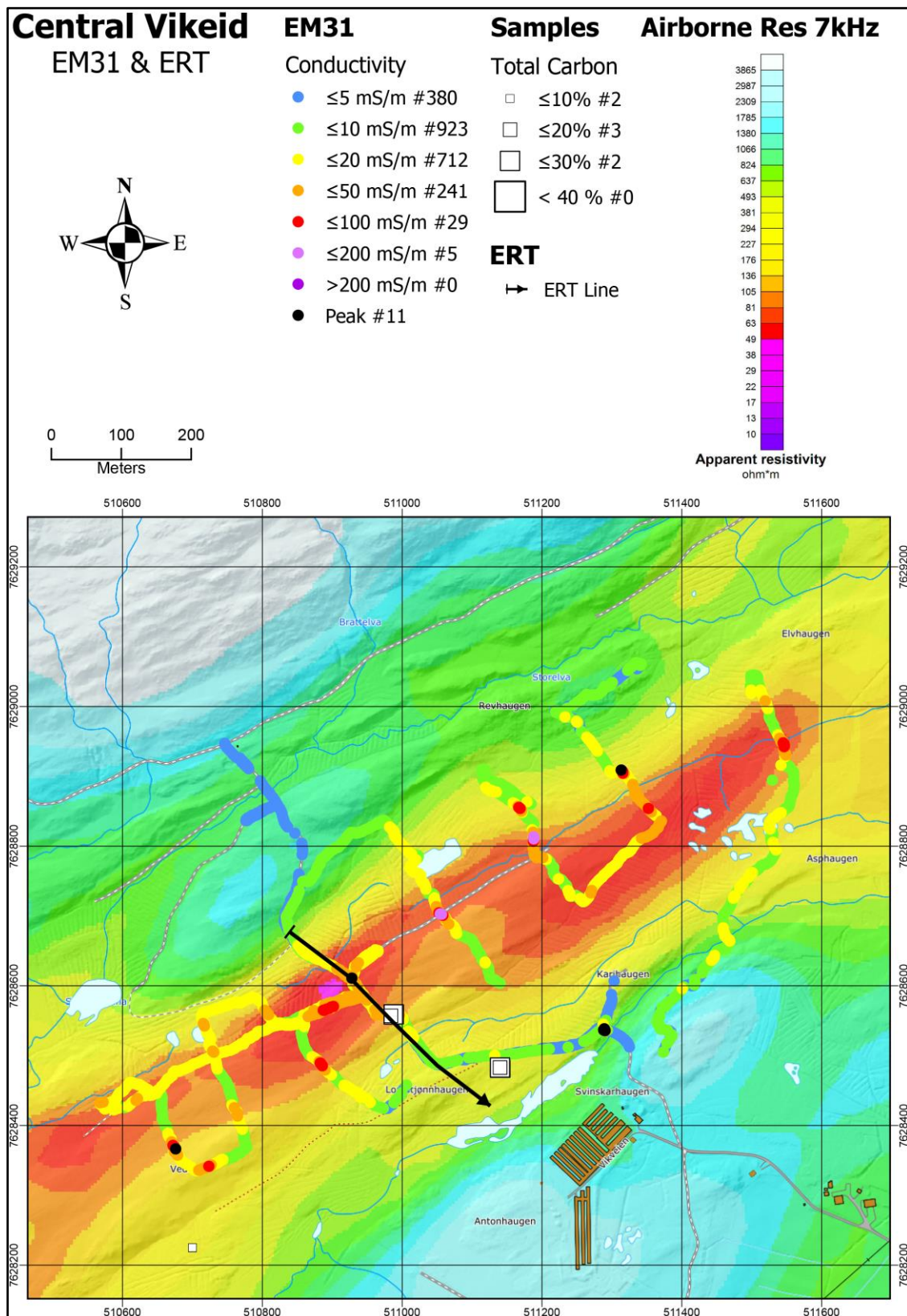


Figure 7.14: The Vikeid Central area. The results from the EM31 measurements are superposed on apparent resistivity (EM 7 kHz coaxial coil configuration, Rodionov et al. 2013a). Black lines show the location of the ERT/IP profile. The locations of graphite samples and their TC content are shown as white squares.

7.5.2 Geophysical work, ERT/IP

The location of the ERT/IP profile at Vikeid Central area (Vedåsen) is shown in Figure 7.14. Results of the combined 2D resistivity and Induced Polarisation measurements are shown in Figure 7.15. The electrode spacing was 5 m and the other acquisition and inversion parameters are as described in Chapter 4.1.4. The quality of the inverted resistivity and IP sections are good and not acceptable respectively (see Table 7.8).

Table 7.8: Quality of 2D resistivity and IP data in the Vikeid Central profile. Number of measured, removed and remaining data points for inversion, and observed “Absolute error” from the inversion of resistivity and IP data.

Profile name	Location	Measured data points	Removed data points	Inverted points	Abs. error ERT (%)	Abs. error IP (%)
2017-2	Vikeid Central	1168	124	1044	7.3	45.6

The **2D Resistivity/IP profile 2017-2** is located west of Svinskarhaugen in the central part of the Vikeid Central area (see Figure 7.14). The resistivity section (Figure 7.15) indicates an area with a 2 m – 10 m thick soil cover. Underneath this cover, a ca. 150 m wide conducting zone is observed (position 40 to position 190). The resistivity is < 10 Ω m, partly < 3 Ω m. South of this zone, (position 190 to 250) the resistivity is also anomalously low, between 10 Ω m and 350 Ω m, the same as in profile 2017-2 in Vikeid West (next section). Further to the south, the resistivity is normal for the host rock in the area (> 700 Ω m). Induced polarisation, despite low quality, shows locally high values in the two most conductive zones indicating electronic conducting minerals, graphite or sulphide. The zone with the lowest resistivity, may represent horizons of massive graphite/sulphide while the moderate resistivity zones are potentially disseminations of the same minerals. Modelling has shown that the continuous low resistivity zone may consist of potentially several conducting graphite horizons (Rønning et al. 2014).

A minor resistivity anomaly appears in the SE end of the ERT/IP profile, at position 360. This resistivity anomaly is not followed by an IP anomaly, and it appears to be a surface phenomenon. Just NE of this anomaly, graphite of fairly good quality is exposed (see Figure 7.16). Almost no signature is found in the helicopter-borne apparent resistivity and the EM31 data, this fits well with the small anomaly at ERT data and this is a strong indication of a sub-economic mineralisation.

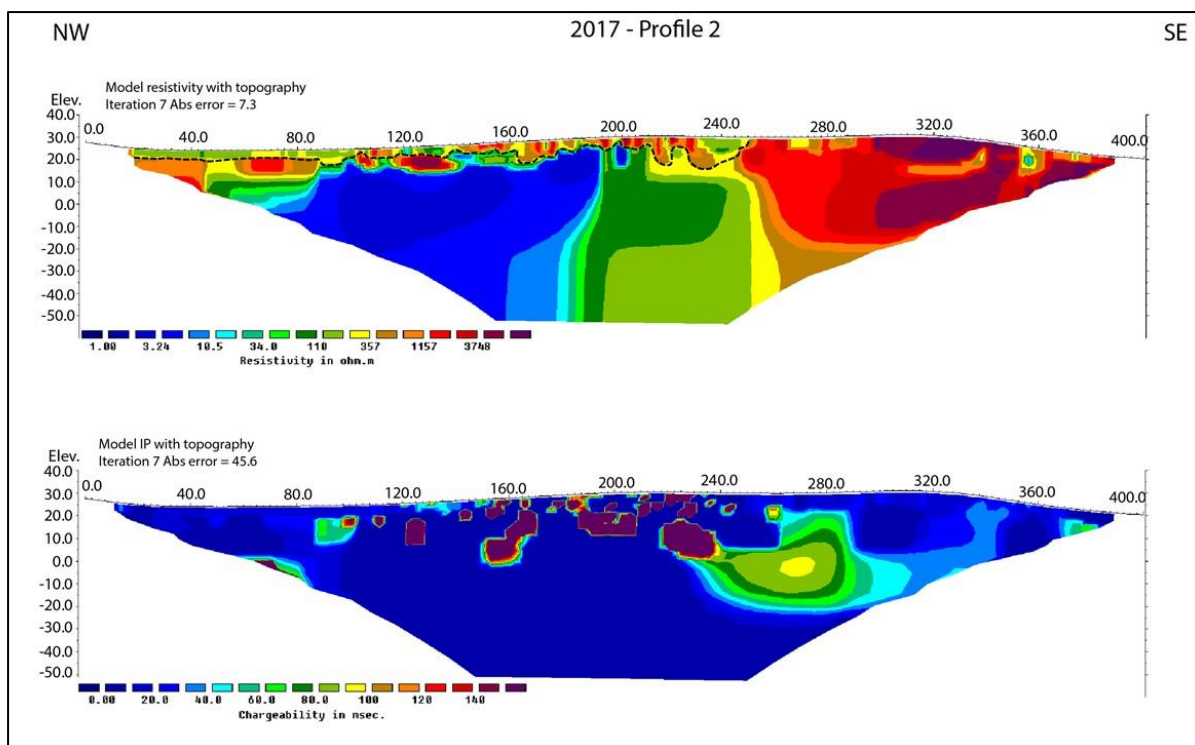


Figure 7.15: The Vikeid Central area. The results of the 2D Resistivity (ERT) and Induced Polarisation measurements along profile 2017-2. The interpreted soil-bedrock interface is marked as dotted black line.

7.5.3 Geological work, sampling and analyses

There are some scattered outcrops of graphite schists in the Vikeid Central area (Vedåsen). We have six samples from this area, showing the following variation in TC (Table 7.9).

Table 7.9: Total Carbon (TC) data from 6 surface samples from the Vedåsen (Vikeid Central) area.

Vikeid Central	N	Average (%)	Max (%)	Min (%)	St. Dev (%)	Median (%)
Vedåsen	6	13.8	24.3	1.7	8.4	13.1

The graphite schist from this locality is the typical flake graphite type, with variable contents of flake graphite and variable contents of quartz and feldspar.

7.5.4 Summary Vikeid Central area

In the Vikeid Central area, named Vedåsen, low resistivity is mapped in a total length of 1.5 km. Graphite of relatively good quality is exposed at two locations, but potentially the best mineralisation is located NW of the exposures. Graphite probably occurs here in a total width of ca. 160 m. This may consist of several individual structures with varying quality. Core drilling is necessary for a good evaluation of the quantity and quality of these potentially good graphite mineralisation. An interpretation of potential graphite structures based on helicopter-borne EM data, EM31 and ERT/IP data as well as graphite exposures is shown in Figure 7.16.

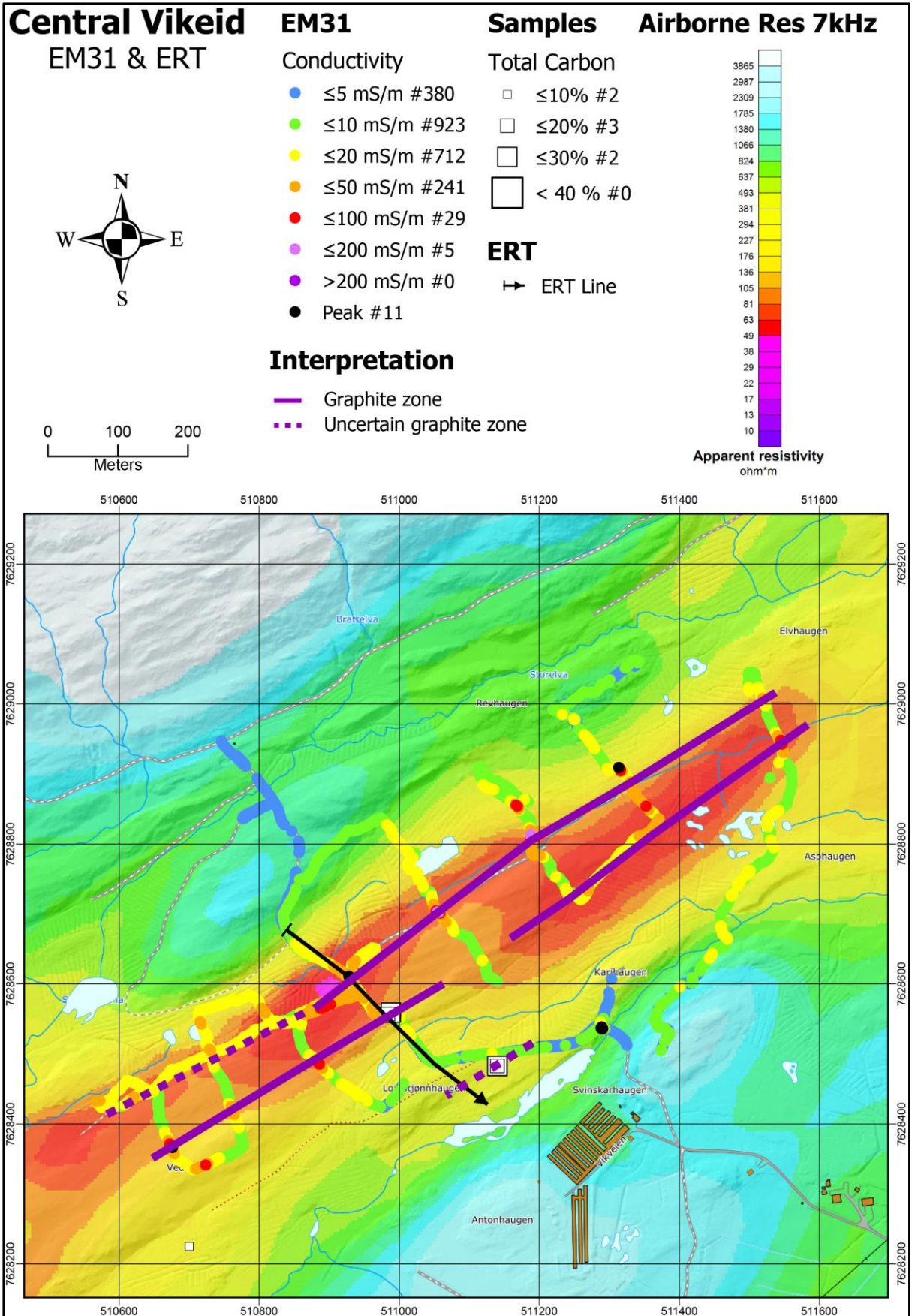


Figure 7.16: The Vikeid Central area. Interpreted graphite structures based on EM31 data, helicopter-borne EM anomalies and exposures of graphite. The locations of graphite samples and their TC contents are shown as white squares.

7.6 Vikeid West (Vikeidet)

The western part of the Vikeid area is the most pronounced regarding the apparent resistivity (Figure 5.2) and the combined magnetic and electromagnetic analysis (Figures 5.5 and 5.6). As a follow-up work of the 1988 helicopter-borne measurements (Mogaard et al. 1988), graphite structures (1 – 2 m) were observed in six trenches in the entire Vikeid area (Gautneb and Tveten 1992). The total carbon content varied from < 1 % to a maximum value of 24.2 %. In 2017, some EM31 profiling and one ERT/IP profile were measured (Rønning et al. 2018). Extensive EM31 and combined CP / SP measurements as well as a 26 m long core drilling was carried out in 2018. To make the Vikeid West area complete, the data from 2017 are presented here, together with the new 2018 data. The general name Vikeidet is used in Table 7.13 and Appendix 6.

As can be seen in Figure 7.17, the area is nearly 100 % soil covered (peat and moraine). Graphite exposures are only observed in drainage channels, by trenching (Gautneb & Tveten 1992) and by core drilling (this report).



Figure 7.17: The Vikeid West area is nearly 100 % soil covered. Graphite is observed in drainage trenches (Illustration from www.norgeibilder.no).

7.6.1 Geophysical work, EM31

All EM31 data is presented on top of apparent resistivity calculated from helicopter-borne 7 kHz EM data in Figure 7.18. Low apparent resistivity from helicopter-borne EM is indicated in a total length of ca. 1.5 km and a width of ca. 650 m. Apparent electric conductivity > 200 mS/m (apparent resistivity < 5 Ω m) was measured using EM31 in a great number of points indicating graphite mineralisation. The highest apparent conductivity from EM31 coincides with the lowest apparent resistivity from helicopter-borne measurements. Several potential graphite structures are indicated within this area, but it is unclear if these are caused by individual conducting structures or by variations in the overburden thickness. In the central part off the anomaly, the

In the outer part of the area of anomalous apparent resistivity, the apparent conductivity from EM31 measurements is lower (< 100 mS/m) and more sparsely distributed, especially towards the north. This may indicate less graphite or lower graphite quality but possibly also increased soil thickness. Exposed graphite (ca. coordinates 509860 – 7628000) with TC between 10 % and 20 % in an area where apparent conductivity is between 10 and 20 mS/m (apparent resistivity between 100 and 50 Ω m) indicates a thin structure.

7.6.2 Geophysical work, ERT/IP

The location of the ERT/IP profile at Vikeid West area is shown in Figure 7.18 (and others). Results of the combined 2D resistivity and Induced Polarisation measurements are shown in Figure 7.19. The electrode spacing was 5 m and the other acquisition and inversion parameters were as described in chapter 4.1.4. The quality of the inverted resistivity and IP sections are good and not acceptable respectively (see Table 7.10).

Table 7.10: Quality of 2D resistivity and IP data in the Vikeid West profile. Number of measured, removed and remaining data points for inversion, and observed “Absolute error” from the inversion of resistivity (ERT) and IP data.

Profile name	Location	Measured data points	Removed data points	Inverted points	Abs. error ERT (%)	Abs. error IP (%)
2017-1	Vikeid West	1168	164	1004	8.1	34.5

The **2D Resistivity/IP profile 2017-1** is located at the eastern flank of the most conductive structure in the Vikeid area (see Figure 7.17). The resistivity section (Figure 7.19) shows a soil cover which is from ca. 2 m to 10 m thick. Underneath this cover, a ca. 120 m wide zone is observed (position 60 to position 185) with resistivity < 10 Ω m, partly < 3 Ω m. This zone coincides with the lowest resistivity from helicopter-borne measurements, and graphite is observed in drill-hole Vikeid Bh1. South of this zone (position 185 to 250) the resistivity is also anomalously low, between 10 Ω m and 350 Ω m. Further south the resistivity is normal for the host rock in the area (> 700 Ω m). At depth, from position 280 and towards the SE, the resistivity is low again but only at a few deep points. This area coincides with the southernmost resistivity anomaly from 7 kHz helicopter-borne measurements and may suggest graphite mineralisation at depth also here.

Induced polarisation shows locally high values in the two most conductive zones, indicating electronic conducting minerals (graphite or sulphide). The zone with the lowest resistivity may represent horizons of massive graphite/sulphide while moderate resistivity can be due to dissemination of the same minerals. Modelling has shown that the continuous low resistivity zone may consist of several conducting zones, potentially graphite (Rønning et al. 2014).

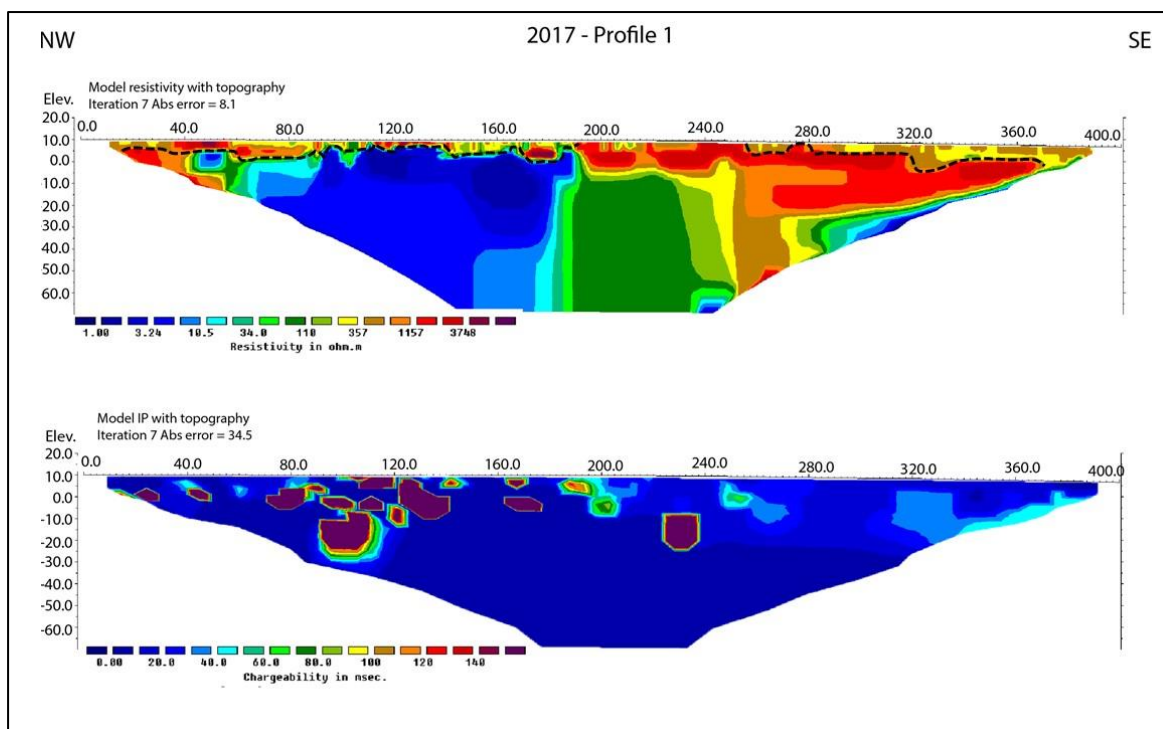


Figure 7.19: The Vikeid West area. The results of the 2D Resistivity (ERT) and Induced Polarisation measurements along profile 2017-1. The interpreted soil-bedrock interface is indicated as the dotted black line.

7.6.3 Geophysical work, CP/SP

In the Vikeid West area, Charge Potential (CP) in combination with Self Potential (SP) measurements were undertaken with one ore grounding point. The locations of the grounding point, current and number of measuring points are shown in Table 7.11 and in Figure 7.20. The results of all CP measurements are shown in Figure 7.20. To visualize the results Geosoft Oasis Montaj software was used for plotting, gridding and contouring the data. A minimum curvature algorithm was used to interpolate between measuring points, and a cell size of 10 m was used for all grids.

Table 7.11: Coordinates (WGS 84, UTM Zone 33), voltage and current for groundings used for CP measurements at Vikeid West. R1 is remote electrodes.

Electrode	Location material	East-coordinate	North-coordinate	Current (A)	No. of measurements
1	Depth 8.5 m in Dh 2018-1	509851	7627758	1.5	581
R1	Local stream	510023	7627393		

The CP data (Figure 7.20) indicate a ca. 1200 m long and ca. 200 m wide conducting structure. This anomaly may consist of several parallel isoclinally folded structures that do have electric contact. Graphite is proven at two locations in trenches central in the anomalous zone, and in the short drill-hole (Bh1, see section 7.6.6). The maximum potential is less than 54 mV, which is an indication of a great downward extent.

Exposed graphite is also found outside the CP anomalous area, approximately at coordinates 509850 – 7628000, 509020 – 7628030 and 508700 – 7627770. This proves that there are several isolated graphite structures in the area, and these are partly confirmed by SP anomalies (red dots in Figure 7.21) and by high apparent conductivity values from EM31 measurements (Figure 7.22). An interpretation of individual graphite structures at Vikeid West is shown in Figure 7.26.

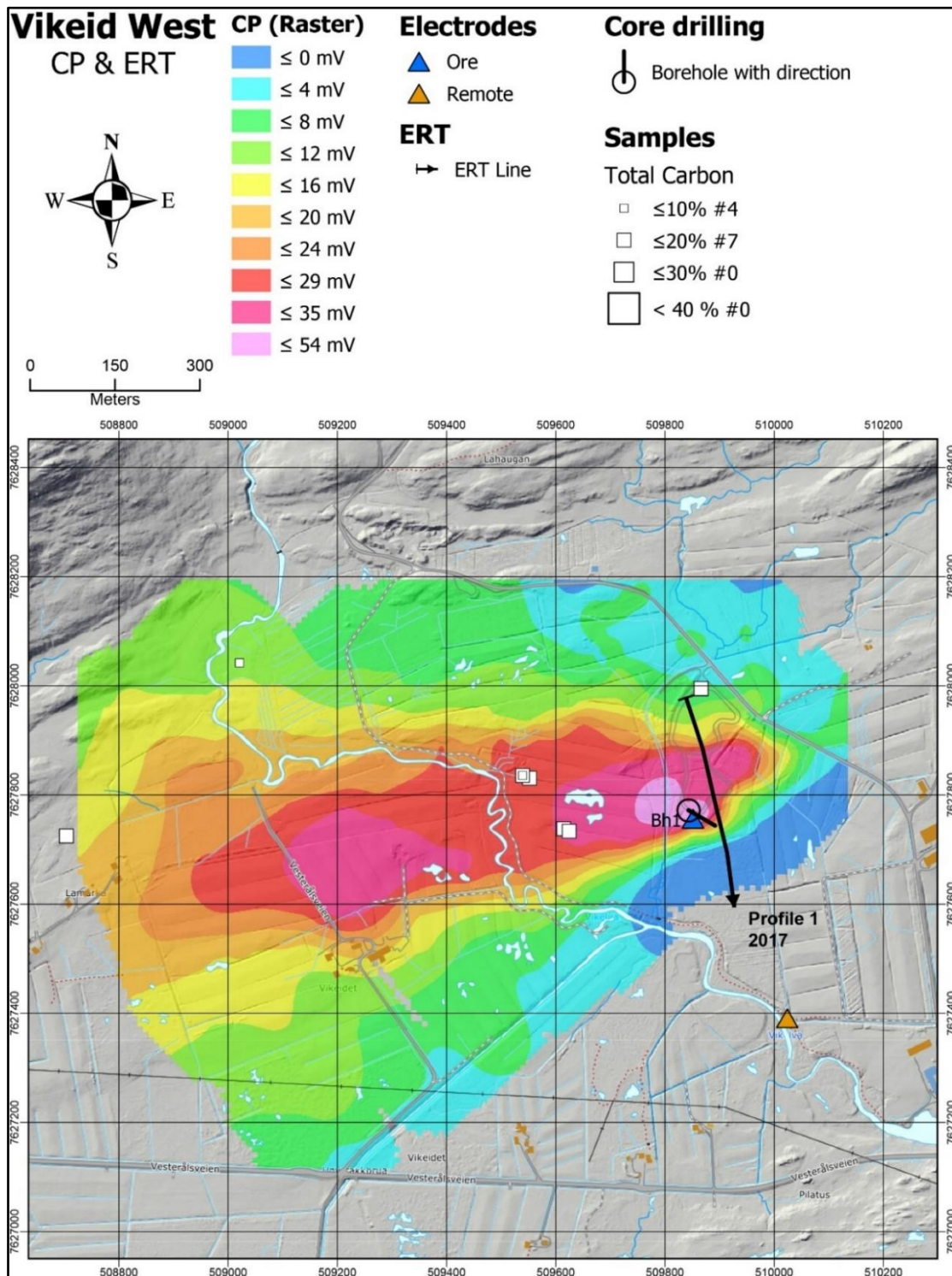


Figure 7.20: The Vikeid West area. Contour map of the CP data. Black lines show the location of ERT/IP profile. The locations of graphite samples and their TC contents are shown as white squares.

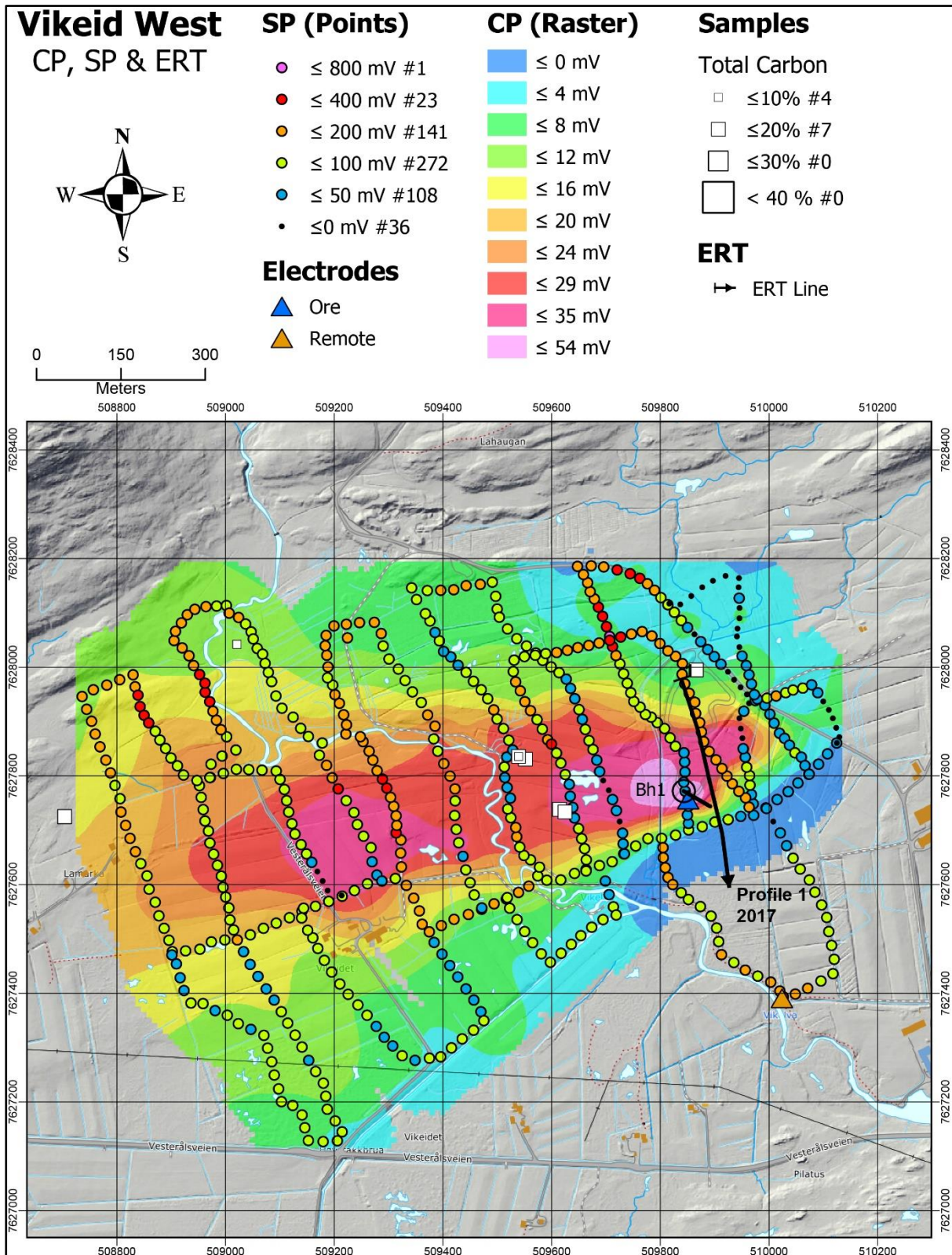


Figure 7.21: The Vikeid West area. SP data superposed on a contour map of the CP data. A black line shows the location of the ERT/IP profile. Locations of graphite samples and their TC contents are shown as white squares.

Table 7.12: Interpreted layers in the 3D resistivity model (top and bottom), plotting level and registered responses on the individual graphite structures shown in Figure 7.26 (Roman numbers). Numbers in brackets indicates a weak response.

Level no.	Top level (m)	Bottom level (m)	Plotting level (m)	Comments
1	0	10	0	Almost no response
2	10	22	10	Response at I
3	22	36	22	Response at I + II + (III) + IV
4	36	54	36	Response at I + II + III + IV + V
5	54	75	54	Response at I + II + III + IV (+V)
6	75	100	75	Response at I + II + III + IV
7	100	130	100	Response at I + II + III + (IV)
8	130	166	130	Response at (I) + (II) + (III) + (IV)
9	166	209	166	Almost no response
10	209	261	209	No response

As shown in Table 7.12 and in Figure 7.24, Level no. 1 does not give a significant response to any graphite structures. The reason for this is probably that this level is dominated by a low conductive soil cover. From Level 2 (10 m) and down to Level 7 (more than 100 m), the graphite Structure I (see Figure 7.26) shows a continuous response. The graphite Structure II and potential graphite Structure IV show up clearly at Level 3 (22 m) while the conductive Structures III and V show up at Level 4 (36 m). Structure V shows up clearly only at Level 4 (36 – 54 m) while the others can be followed down to 100 m or more. The spreading of conductive material (potential graphite) has a maximum at ca. 50 m depth.

The conductive materials completely disappear at ca. 150 m depth. It is also important to mention that lack of response at deeper levels in the 3D model, does not mean that the graphite mineralisation stops at this depth. The lack of responses may be caused by the penetration depth (skin depth) of the individual EM frequencies. In other words, graphite mineralisation in this location may continue to even greater depths.

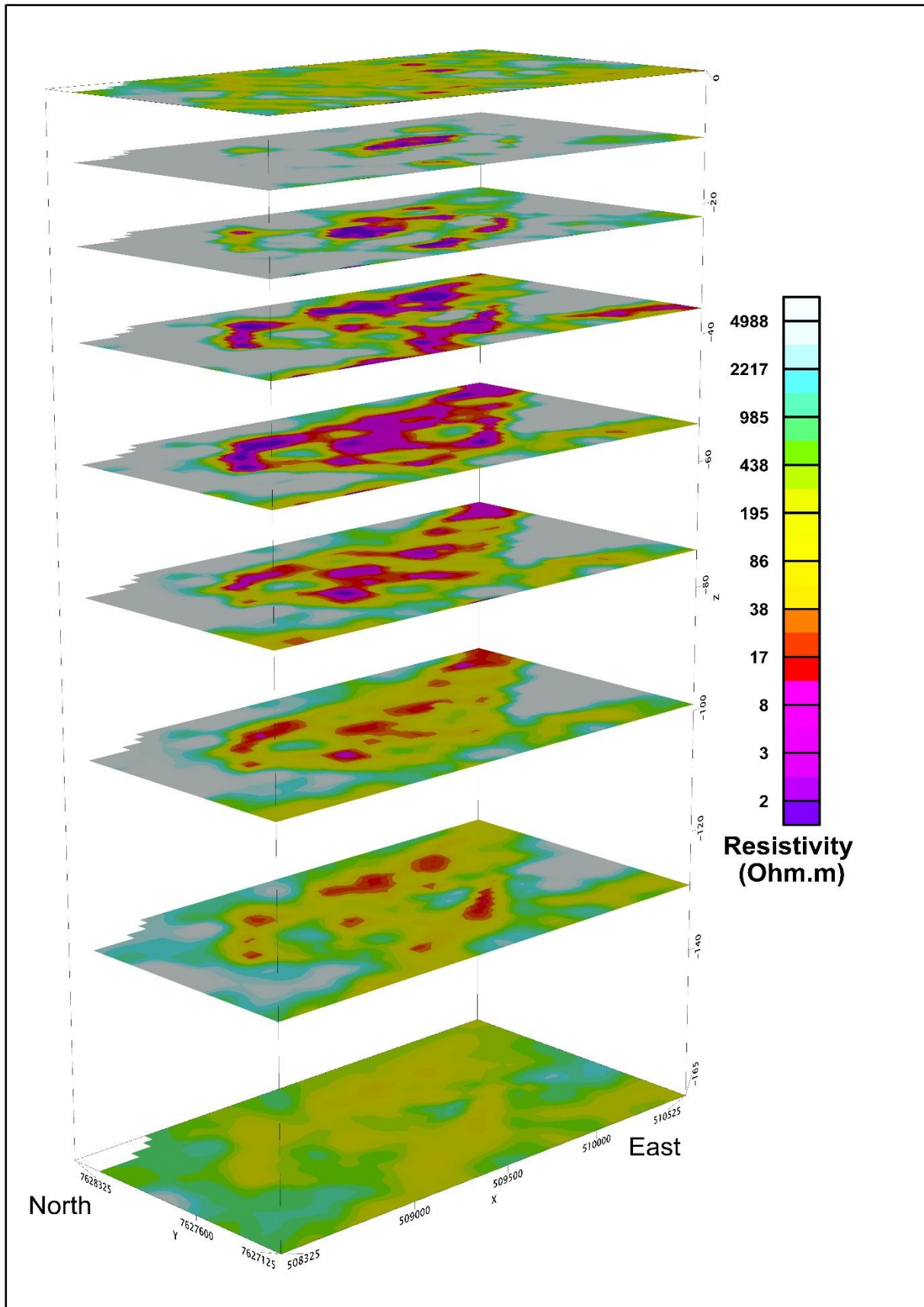


Figure 7.24: The results from 3D inversion of helicopter-borne EM data. Resistivity distributions in individual levels are plotted on top of the levels and represent the resistivity values down to the next level.

7.6.5 Geological work, sampling and analysis

The Vikeid West area is almost 100 % soil covered. Graphite schist was observed in a few drainage channels in 1991 (Gautneb & Tveten 1992). However, neither the relationships to the country rocks, nor the structure and the deformation of the rock can be observed in the field. The drilling (Chapter 7.6.6 and Appendix 2) gave a complete profile through one of the graphite sections at this locality. Analysis of 12 samples from the area show an average TC content of 10.4 % and a maximum value of 16.7 %. The graphite appears as flakes with industrial interesting size (see also Chapter 7.6.6).

Table 7.13: Total Carbon (TC) data from X surface samples from the Vikeid West area.

Vikeidet	N	Average TC (%)	Max (%)	Min (%)	St. Dev (%)	Median (%)
Vikeidet	12	10.4	16.7	0.5	4.8	11.1

7.6.6 Geological work, core drilling

At Vikeid West, one 25.55 m long core drilling was performed. The location of the drill-hole is shown in Figures 7.16 to 7.19 and technical data for this are given in Table 7.14. The electrical conductivity was logged with the equipment described in Chapter 4.1.5 (ABEM 1993). Results from core analyses are given in Figure 7.25. A detailed geological log is presented in Appendix 1, the pictures of the cores are shown in Appendix 2 and analytical data (Total Sulphur (TS) and Total Carbon (TC) Leco analysis) are presented in Appendix 3. In Appendix 4, XRF analysis of the drill-cores are presented.

Table 7.14: Technical data, core drilling at Vikeid West. Coordinates in UTM WGS84 Sone 33.

Area	Drill-hole	UTM E	UTM N	Direction (°)	Dip (°)	Length (m)
Vikeid West	Dh1-2018	509843	7627772	120	45	25.55

The drill-core consists almost entirely of a finely banded quartz feldspar rock, in which the banding is defined by variation in the content of mica (mostly biotite) and the content of graphite. In parts of the core, the graphite content is low but clearly visible. The graphite appears as good-quality flake graphite with a grain size from ca. 0.1 mm to several mm. Massive graphite schist occurs at three levels in the core, at 3 - 4 m, 7- 9 m and 22.0 - 24.5 m. The TC content is ca. 5 – 7 % in the massive graphite schist while the contents in the disseminated parts are ca. 1 % or less. The drill-hole direction is away from the assumed best mineralisation and may not be representative for the entire mineralisation.

The contact to the over- and underlying quartz feldspar rich rock is gradual but quite distinct. The entire 25.6 metres long drill-core is interpreted to be in common graphite bearing rock unit in Vesterålen. We did not observe any country rock such as later intrusions. The core analysis also illustrates what has been described in previous reports (Gautneb et al. 2017, Rønning et al. 2018). Graphite rich parts occur very inhomogeneously and variations in TC from < 1 % to > 10 % appear irregularly and over short distances.

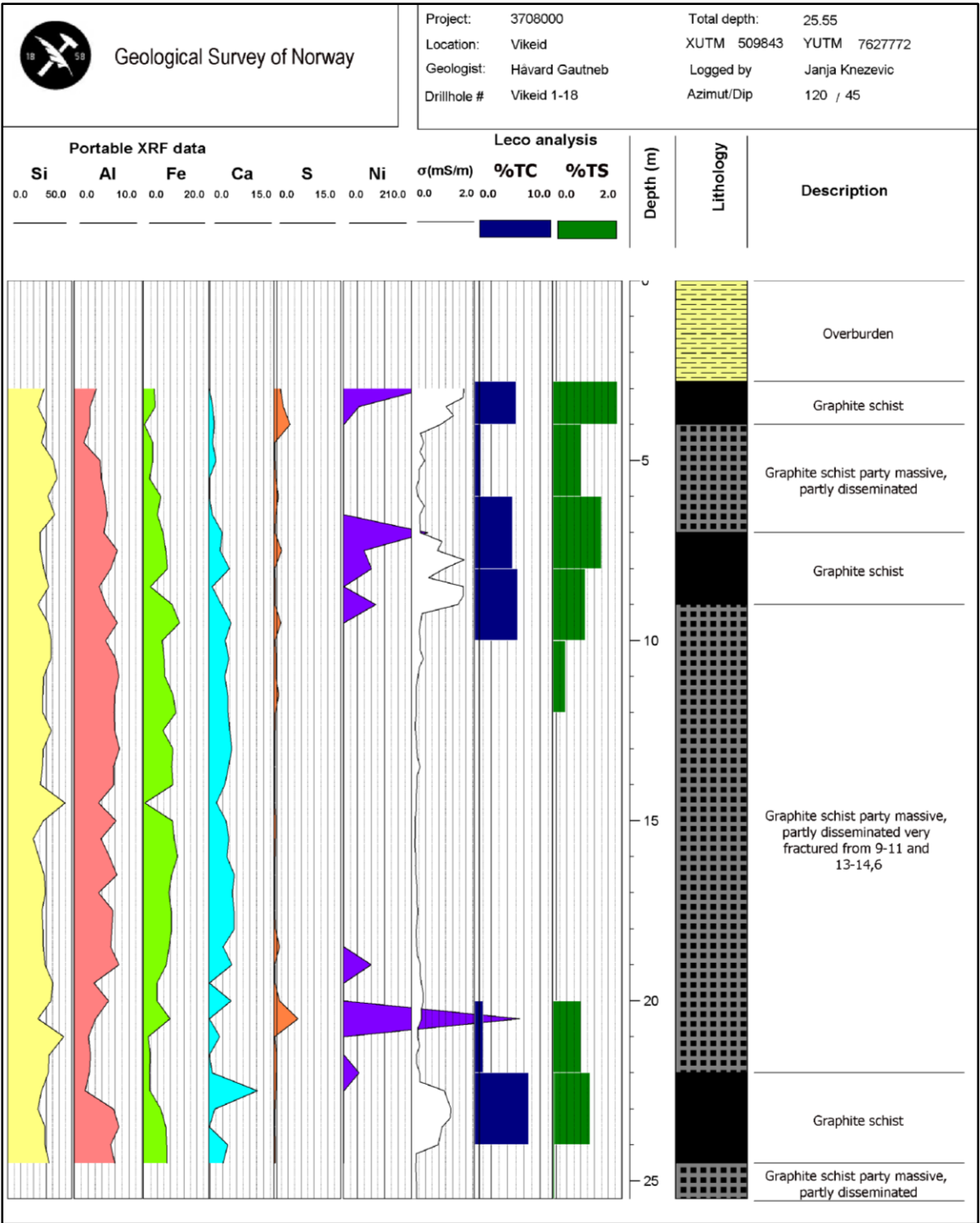


Figure 7.25: Results from the Vikeid Dh1-2018 drill-hole: Portable XRF analyses (Si, Al, Fe, Ca, and S in %, Ni in ppm) at the cores, downhole electric conductivity log (σ), selected Leco analyses of Total Carbon (TC) and Total Sulphides (TS), lithological log and core description.

7.6.7 Summary Vikeid West

Interpretation of individual graphite structures at Vikeid West are shown in Figure 7.16. The interpretation is based on helicopter-borne EM data, ground EM31 data, ERT/IP and CP/SP data.

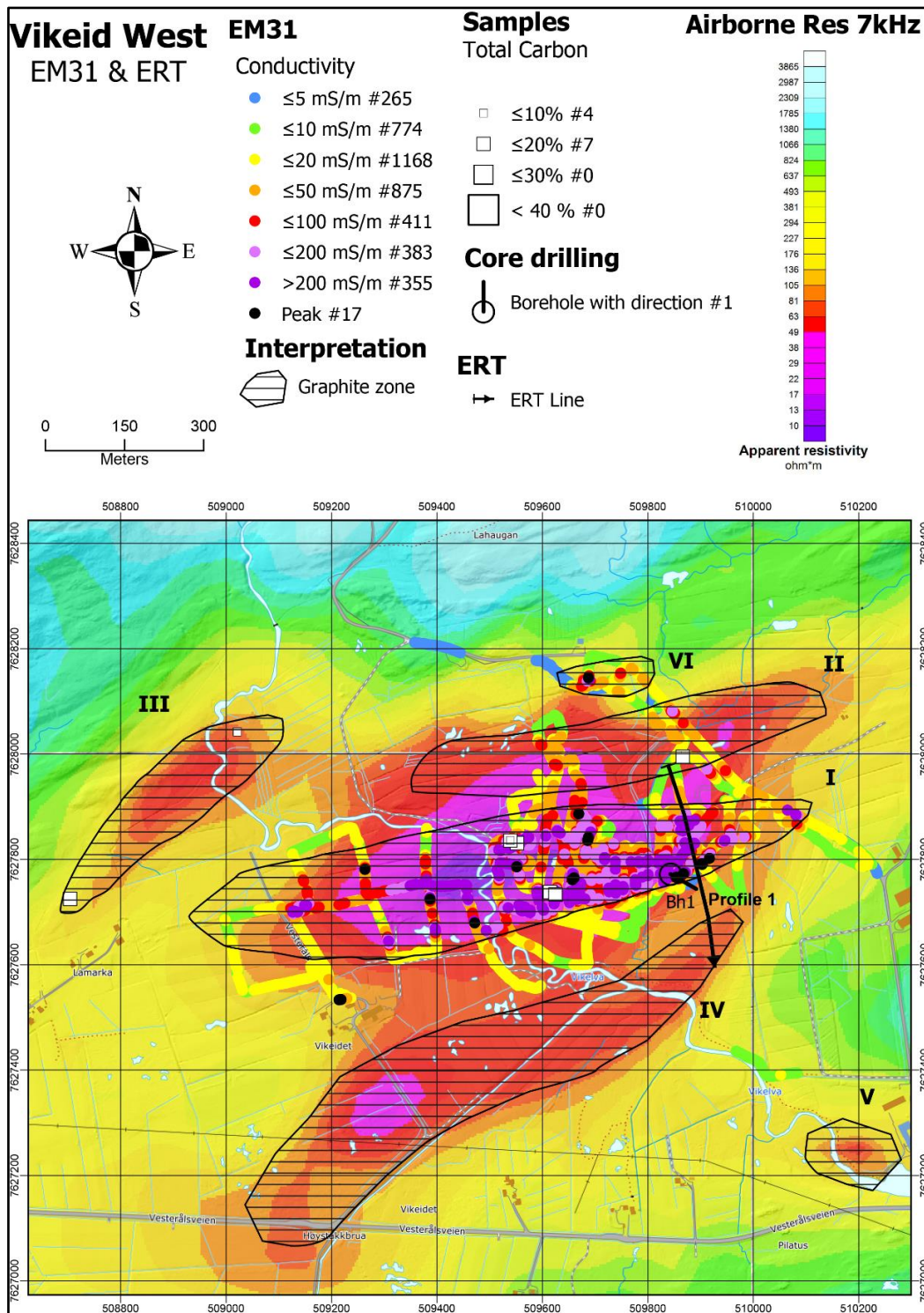


Figure 7.26: Interpreted graphite structures in the Vikeid West area. 3D inversion of helicopter-borne EM data indicates that the Structures I, II, III and IV gives strong responses from ca. 10 m depth and down to 100 m and more. The Structure V shows up at only one resistivity level (36 – 54 m depth) while Structure VI seems to be a small surface phenomenon.

Structure I, exposed at two locations and intersected by a core drilling, appears as a ca. 1200 m long and 200 m wide graphite mineralisation, based on EM31 and the CP measurements. Inversion (3D) of helicopter-borne EM data indicates a depth extent to at least 100 m. Structure II, exposed at one location, is interpreted to be ca. 800 m long and ca. 100 m wide. Structure III is exposed at two locations and seems to be 500 m long. Structure IV is not exposed but is indicated at a depth of ca. 30 m at the ERT/IP line and at the 3D inverted helicopter-borne data. The length of this structure is ca. 1000 m and the width is 10 m or more. Structures V and VI are small and probably without any economic value. In total, the length of the exposed and assumed (not exposed) graphite structures is ca. 3500 m, while the width varies from ca. 10 up to 100 m and potentially more. EM31 readings indicate an average width of ca. 40 m.

The TC content of twelve samples varies from 0.5 % to 16.7 % with an average value of 10.4 %. One drill-hole intersects graphite mineralisation for > 20 m but is directed away from the best conducting part. The TC content in the drill-core is ca. 5 % in massive parts, and ca. 1 % in disseminated parts. However, this drill-hole is located at the rim of Structure I and probably does not describe the real total carbon content in the mineralisation. The graphite appears as good flake quality with grain size from ca. 0.1 mm to several mm. The Vikeid West area (Vikeidet) is among the most interesting graphite mineralisation in Vesterålen.

7.7 Reinsnesøya

The bedrock map Svolveær in scale 1: 250.000 reports a graphite showing at the island Reinsnesøya north-east of Jennestad (Tveten 1978). The host rock is an intrusive granodiorite, and not the normal supracrustal gneisses associated with graphite, but graphite layers as rafts within the intrusion was considered as a possible mode of occurrence. NGU tried to confirm this mineralisation late in 2019.

7.7.1 Geophysical work, EM31

Results from EM31 measurements at Reinsnesøya are shown in Figure 7.27. Extensive measurements all over the small island do not show EM31 anomalies that can be caused by nearly outcropping graphite mineralisation. At three locations the apparent conductivity lies between 50 and 100 mS/m (apparent resistivity between 10 and 20 Ω m) but these locations are close to the sea and may be caused by seawater. However, if these are caused by graphite, the mineralisation will be insignificant. During the 2019 fieldwork, small veins carrying copper minerals were found and sampled at the approximate location indicated for graphite on the 1: 250,000 scale geological map. The reported graphite mineralisation could therefore be a misprint.

7.7.2 Reinsnesøya summary.

The reported graphite mineralisation at Reinsnesøya is most likely false.

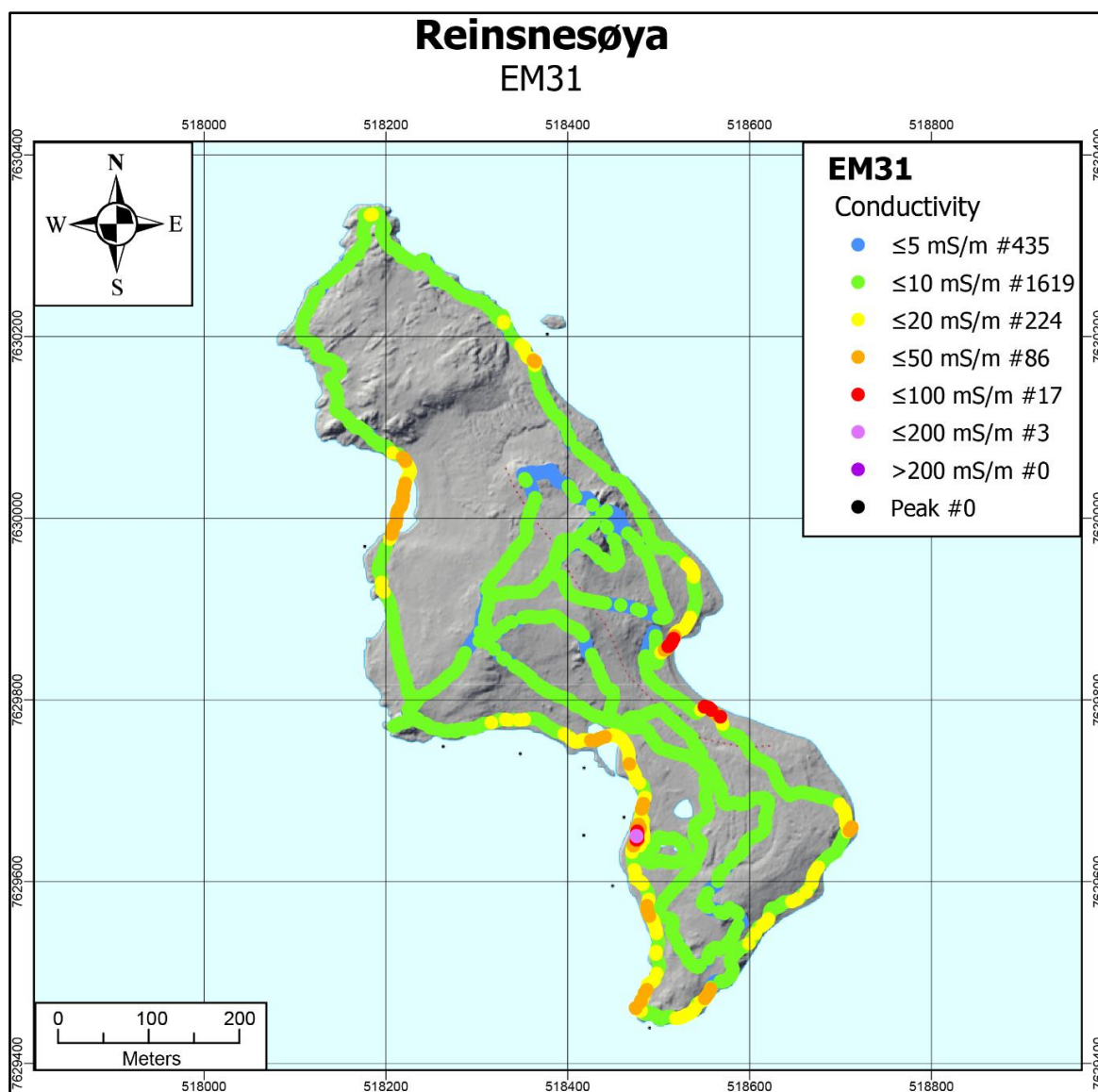


Figure 7.27: Results from EM31 measurements on the island Reinsnesøya.

7.8 Sæterstranda

Graphite was discovered at Sæterstranda, close to Holm on the north-eastern point of Langøya in Sortland Municipality during geological mapping in August 2019. The discovery is situated in the tidal zone, forming a 10 m wide and 40 m long outcrop covered by seaweed. This exposure coincides with a ca. 600 m long EM anomaly turning westwards (Figure 7.28). No geophysical follow-up work has been undertaken.

At this locality, an about 2 m thick layer of coarse-grained (1-2 mm), massive graphitic schist rests upon a fine-grained amphibolite. The overall sequence is of supracrustal origin, also comprising fine-grained rusty rocks with pyrrhotite along strike in a neighbouring area. In map scale, this sequence is connected with the supracrustal rocks of the Alsvåg / Instøya area in the Øksnes municipality (see Chapter 8.5). The sequence is intruded by a gabbroic-dioritic intrusion, occurring just northwest of the locality at Sæterstranda.

The analytical results for three samples from this locality are given in Table 7.15. The Total Sulphur content (TS) is 1 % or less in all samples. Sample details and analysis results are given in Appendix 6.

Table 7.15: Total Organic Carbon (TOC) and Total Carbon (TC) of samples from Sæterstranda.

Sæterstranda, Sortland	N	Sample 1 (%)	Sample 2 (%)	Sample 3 (%)
Sæterstranda TOC	3	12,1	16,2	19,1
Sæterstranda TC	3	12,2	17,7	20,8

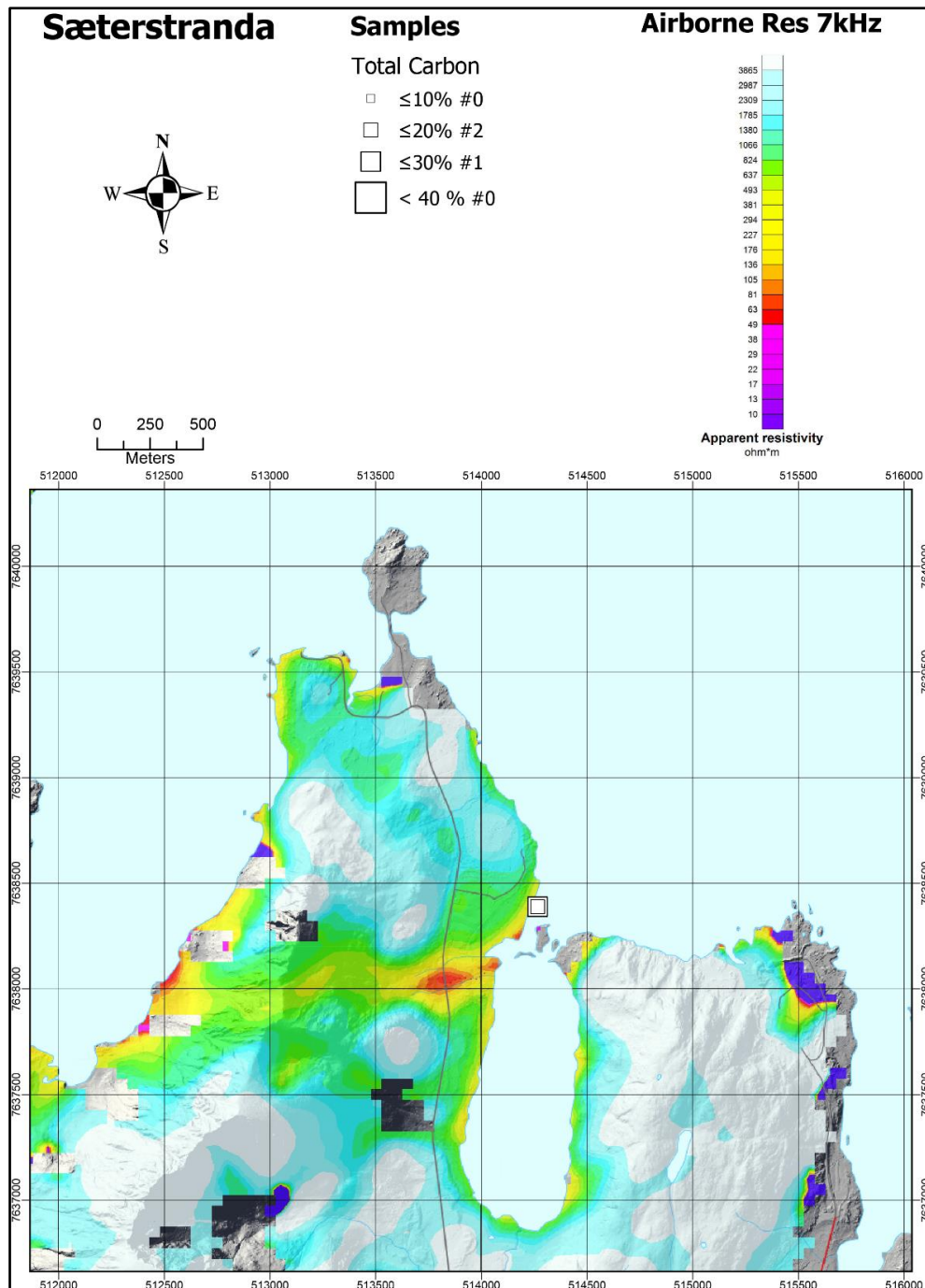


Figure 7.28: Sæterstranda. Apparent resistivity from helicopter-borne 7000 Hz EM data (from Rodionov et al. 2013a). The locations of graphite samples and their TC content are shown as white squares.

8. RESULTS FROM THE FOLLOW-UP WORK IN ØKSNES MUNICIPALITY

During the field season of 2018, NGU performed geophysical measurements and some geological sampling at four areas in the Øksnes municipality: Smines, Romsetfjorden, Steinland and Myre. The area Instøya-Alsvåg-Straumen was discovered and examined in the autumn of 2019. NGU have previously undertaken some geological work at Skogsøya, Svinøya (Gautneb et al. 2017), Rødhamran (Gautneb & Tveten 1992, Gautneb et al. 2017, Rønning et al. 2018) and Lønnskogen (no report).

A brief inspection of the road cuts at Lønnskogen showed no appearance of graphite schist, but rocks quite rich in sulphides.

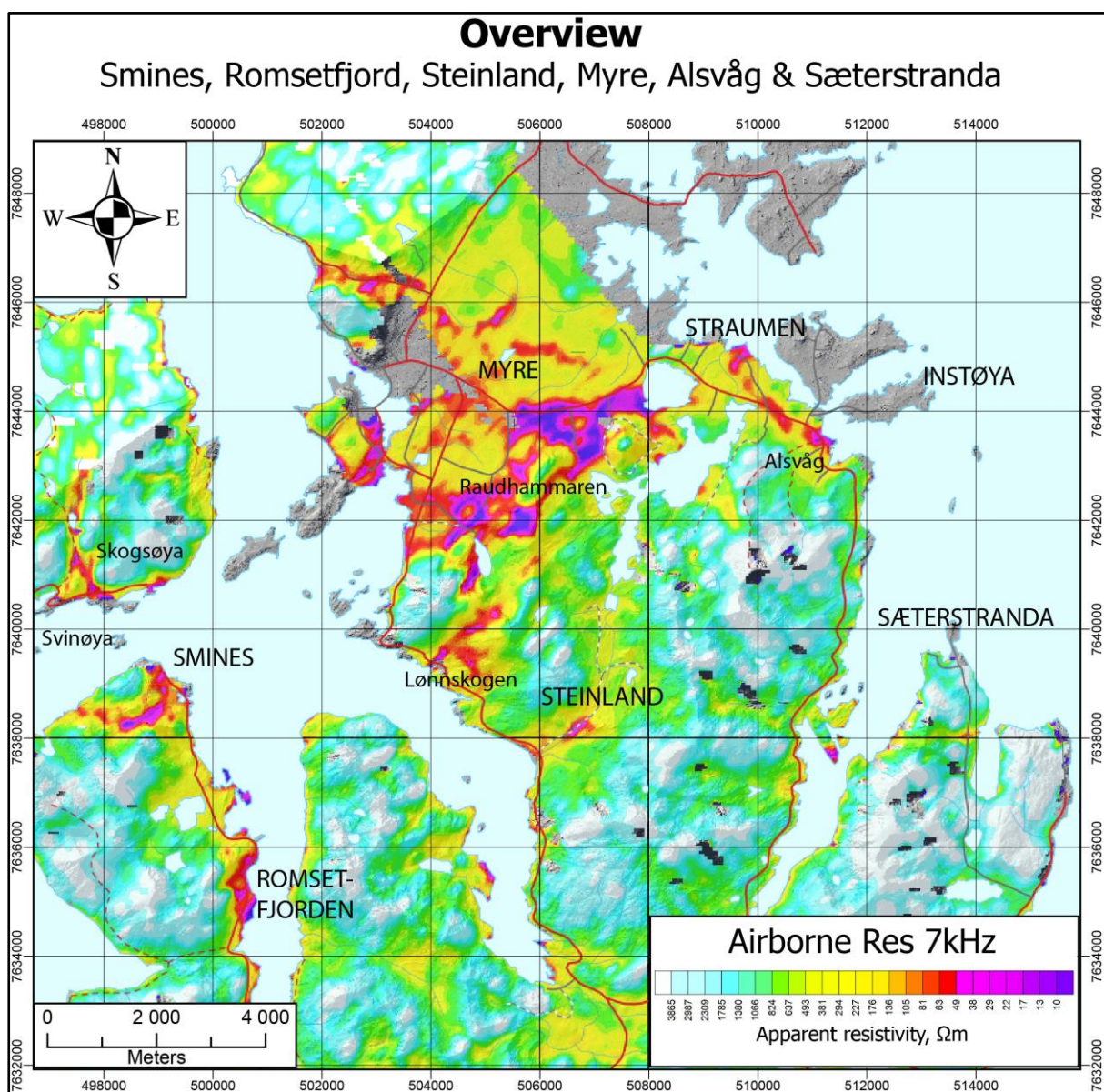


Figure 8.1: Overview map Øksnes and Sortland Municipality. Follow-up work were performed in 2018 in the areas Smines, Myre, Romsetfjorden, Steinland and Myre. In 2019 follow-up work were performed at Alsvåg – Instøya - Straumen and Sæterstranda.

8.1 Smines

The graphite occurrence at Smines was discovered when the 2013 helicopter-borne geophysical data were available. The apparent resistivity maps (Figure 8.2) indicate four individual structures with ca. lengths of (from north towards west) 600 m, 800 m, 400 m and 200 m, altogether ca. 2000 m potential graphite mineralisation. Some geological and geophysical work was performed at Smines in 2015 and 2016 (Gautneb et al. 2017 and Rønning et al. 2017). Some EM 31 measurements were undertaken in 2017 (Rønning et al. 2018). In 2018, these were complemented by SP measurements in areas inaccessible for EM31 measurements. To make the report complete, data from earlier investigations are presented also here.

8.1.1 Geophysical work, EM31

Results from EM 31 measurements in 2017 are presented in Figure 8.2. The helicopter-borne EM measurements show a ca. 1 km long zone of low resistivity ($< 40 \Omega\text{m}$) from Meddagsdalen (UTM 499100 – 7638650) to Rødbergan (UTM 498300 – 7638200) in the eastern part of the Smines area (Figure 8.2). Here, EM31 measurements show numerous apparent conductivity anomalies $> 100 \text{ mS/m}$ (apparent resistivity $< 10 \Omega\text{m}$) and conducting material appears partly in a width of 40 – 60 m. This is most likely the result of graphite mineralisation. Two graphite showings were discovered (UTM 499051 – 7638736 and 498880 – 7638630).

In the central part of the Smines area, between Rotdalen (ca. UTM 498100 – 7638250) and Vikelva (ca. UTM 497850 – 7638500, see Figure 8.2), a ca. 400 m long helicopter-borne EM anomaly appears. The EM31 anomalies are not particularly high despite the relatively low apparent resistivity in the helicopter-borne EM data. No graphite is discovered, but the presence of graphite in this area cannot be excluded since a thicker soil cover may reduce the EM31 anomalies.

In the western part the helicopter EM data suggests a new low resistivity anomaly up to ca. 200 m in strike length. In this area, high apparent electrical conductivity is mapped, and graphite is exposed at two locations at the shoreline.

The electrical properties in the Smines area indicate the presence of graphite mineralisation and graphite is discovered at 7 locations. The most pronounced EM anomaly, from Meddagsdalen to Rødbergan, are not fully mapped with EM31 measurements. Due to steep topography, it was decided to do SP in combination with CP measurements in this area.

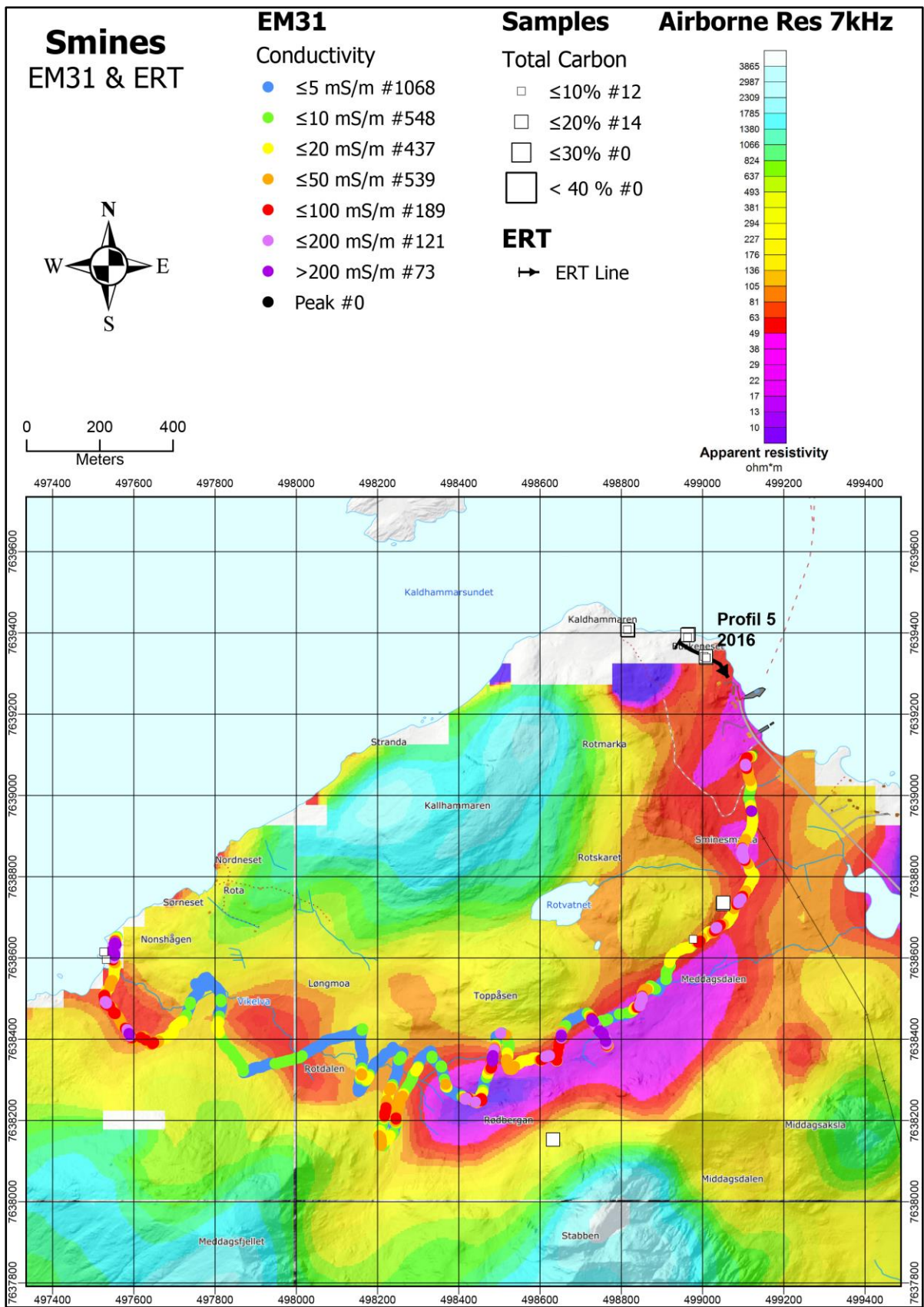


Figure 8.2: Results of EM31 measurements from the Smines area overlain helicopter-borne measurements of apparent resistivity from EM 7 kHz coaxial coil configuration (from Rodionov et al. 2013a). The locations of graphite samples and their TC contents are shown as white squares.

8.1.2 Geophysical work, CP/SP

In 2018, the southern part of the most pronounced EM anomaly between Meddagsdalen and Rødbergan (see Figure 8.2) were covered with SP measurements in combination with CP. In Figure 8.3 all SP data are presented, also data from 2016.

The SP data show numerous anomalies between 400 and 800 mV that can be caused by graphite. Anomalies between 200 and 400 mV can also be caused by graphite but can be of lower quality or lie deeper. In one location, ca. UTM 498620 – 7638160, graphite was discovered at a location of SP anomalies. The SP anomaly pattern is irregular and since few EM31 reading are available, an interpretation of graphite structures is not possible to present.

Charged Potential (CP) measurements were undertaken with one grounding electrode. Technical details are given in Table 8.1.

Table 8.1: Coordinates (WGS 84, UTM Zone 33), voltage and current for groundings used for CP measurements at Smines. R1 is remote electrodes.

Electrode	Location material	East coordinate	North coordinate	Current (A)	No. of measurements
1	Exposure	499051	7638736	2.0	326
R1	Sea	499161	7639126		

The CP measurements gave no conclusive results. The grounding point (exposed graphite) is a small mineralisation and data is not presented due to this.

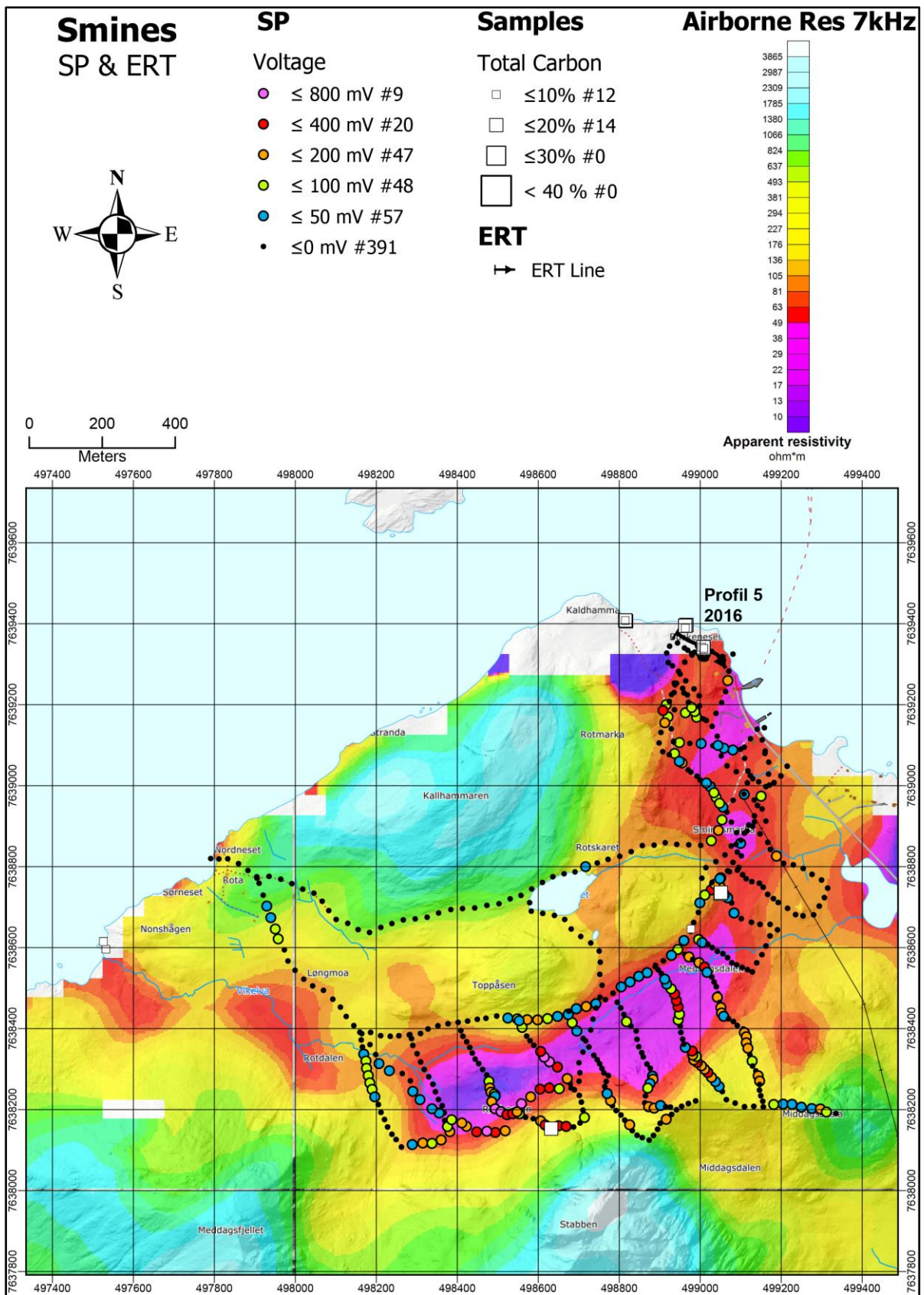


Figure 8.3: Results of SP measurements in the Smines area overlain on top of helicopter-borne measurements of apparent resistivity from EM 7 kHz coaxial coil configuration (from Rodionov et al. 2013a). The locations of graphite samples and their TC contents are shown as white squares, ERT/IP profile as black line.

8.1.3 Geophysical work, ERT/IP

The location of the ERT/IP profile at Smines is shown in Figures 8.2 and 8.3. Results of the combined 2D resistivity and Induced Polarisation measurement are shown in Figure 8.4. Electrode spacing was 2 m and the other acquisition and inversion parameters as described in Chapter 4.1.4. The quality of the inverted resistivity and IP sections are good (see Table 8.2). The profile is partly following a trench where graphite was discovered (Gautneb et al. 2017).

Table 8.2: Quality of 2D resistivity and IP data at Smines area. Number of measured, removed and remaining data points for inversion, and observed “Absolute error” from the inversion of resistivity and IP data.

Profile name	Location	Measured data points	Removed data points	Inverted points	Abs. error ERT (%)	Abs. error IP (%)
2016-5	Smines	1168	28	1140	8.8	9.3

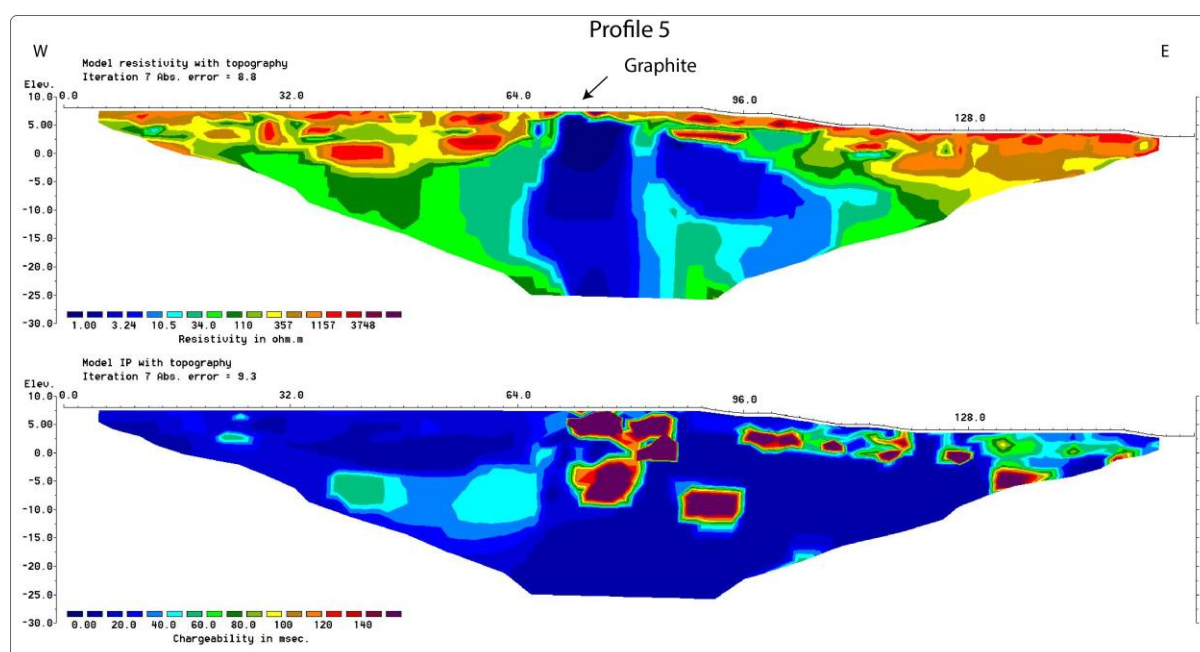


Figure 8.4: The Smines area. The results of the 2D Resistivity (ERT) and Induced Polarisation measurements along profile 2016-5.

In Figure 8.4, a graphite mineralisation shows up as a ca. 10 m wide zone of very low resistivity ($< 5 \Omega\text{m}$) extending from the outcrop all the way down to the bottom of the section. This zone is also detected by IP, but it does not extend to the same depth as indicated by the resistivity. Just east of this structure there is a low-resistivity zone with an apparent dip to the east. It has resistivity that may be caused by graphite. The dip towards east is in agreement with decreasing EM31 response in this direction.

8.1.4 Geological work, outcrops, samples and analysis

The Smines area is poorly exposed. Apart from the outcrops along the shore at Kaldhammaren and Buskeneset in the north and Nonshågen in the west (Figure 8.2), few outcrops of graphite schist are known. During reconnaissance mapping in 2014 one outcrop of graphitic schist was found just north of Meddagsdalen (UTM 499051 – 7638736, Figure 8.2). This outcrop consists of a medium rich graphite schist (Figure 8.5) and was used as a grounding point for CP measurements.

In 2016, EM31 traversing indicated several graphite-bearing conductors under thin cover and a trench was made in the area that was most accessible. Several zones of graphite mineralisation were revealed, and they have a total width in a trench of ca. 6 metres (Gautneb et al. 2017). CP measurement in 2016 showed that this mineralisation has limited length (< 50 m) along the strike (Rønning et al. 2017).



Figure 8.5: Graphite outcrop with 13.2 % TC and 0.33 % TS, sample JK-291517-9, UTM 499051 – 7638736.

Table 8.3 shows a compilation of existing analyses from the Smines area.

Table 8.3: Total Carbon (TC) analysis from the Smines area

Smines	N	Average TC (%)	Max (%)	Min (%)	St. Dev (%)	Median (%)
Kaldhammaren	14	9.6	17.3	1.5	5.3	10.4
Rota	6	2.4	8.6	0.4	3.1	1.2
Smines	4	8.0	14.4	0.3	6.9	8.6
Stabben	1	16.7	16.7	16.7	-	16.7
Stigbergan	3	0.5	0.6	0.4	0.1	0.4
Smines Total	28	7.1	17.3	0.3	6.0	5.0

28 analyses have an average TC of 7.1 % representing both individual point samples and trench samples from Kaldhammaren in 2016, where the latter are described in Gautneb et al. (2017) and Rønning et al. (2017). The Total Sulphur content (TS) is <

1 % in most of these samples, but eight of them have TS values from 2.2 % to 17.9 % (Appendix 6). To make an estimate of graphite volume and tonnage, more data is needed.

8.1.5 Summary Smines

Based on helicopter-borne EM data (Rodionov et al. 2013a), graphite was discovered at Smines in the autumn 2013. The apparent resistivity from the helicopter-borne EM indicate four individual structures of a total length of ca. 2000 m (600 m, 800 m, 400m and 200 m from the north). The terrain made systematic EM31 profiling difficult, and an interpretation map of individual graphite structures was not possible to create. SP in combination with CP did not give conclusive results.

The area is extensively soil covered, but despite of this, graphite was discovered at 7 localities. Average total carbon content of 28 samples from Smines was 7.1 % with a maximum value of 17.3 %. In one trench, graphite of a total width of ca. 6 m was discovered. EM31 data indicates an average thickness of 40 m. If we assume mineable graphite down to 100 m, Smines may contain a potential graphite volume of about 6 mill. m³. More detailed work is needed to confirm this.

8.2 Romsetfjorden

As a result of the 2013 helicopter-borne EM measurements (Rodionov et al. 2013a), graphite mineralisation was discovered in Romsetfjorden in 2016 (see Figure 8.6). The combined low resistivity and low magnetic field analysis (Figure 5.6) makes the Romsetfjorden area a target for follow-up studies.

8.2.1 Geophysical work, EM31

In 2017, a few lines were measured with EM31 (Figure 8.6). In the area of lowest apparent resistivity, around the farm Romset, only one short line was measured with EM31. Four graphite showings are mapped and to delineate the graphite structures in this area, additional EM31 lines were measured in 2018.

All EM31 data next to the farm Romset are presented in Figure 8.7. The helicopter-borne EM anomaly indicates a N-S trending strike along the fjord, but locally the strike is more in NNE-SSW direction. The EM31 lines are partly following the local strike direction and show a confusing image. The apparent resistivity from helicopter-borne measurements is quite low (< 10 Ωm) in the area next to Massvika (Romset farm). This can partly be caused by a response from the conducting seawater, but since the apparent conductivity from EM31 is high (> 200 mS/m, resistivity < 5 Ωm), graphite mineralisation is most likely the cause for the electromagnetic anomalies. In one location north-west of the farm Romset (west of Massvika, see figure 8.7), high conductivity coincides with graphite exposure. Graphite is discovered at four locations,

and partly of high TC content (maximum TC 31.0%) and as shown in Appendix 6, this is mostly organic carbon (TOC 30.7 %).

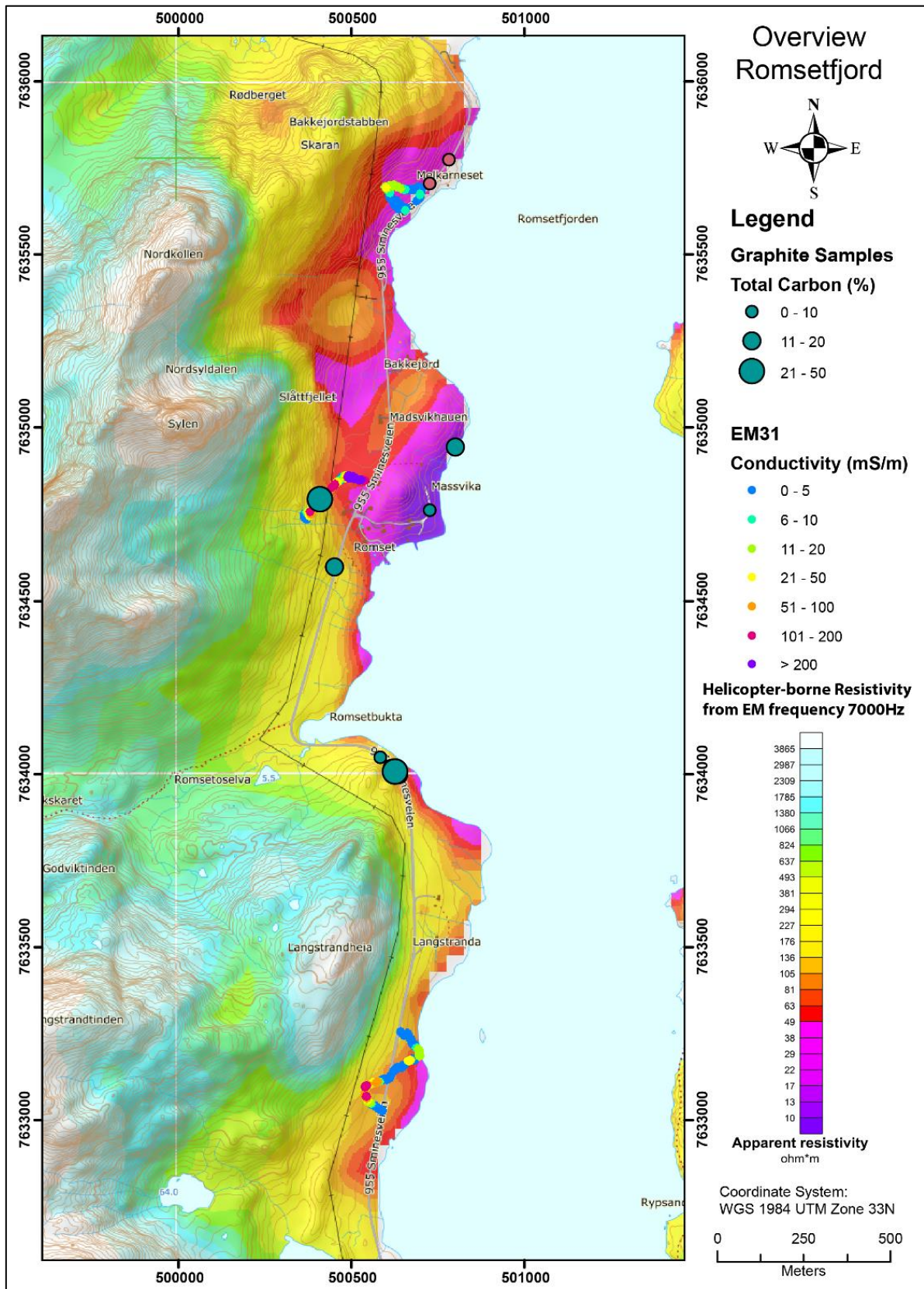


Figure 8.6: Overview map from Romsetfjorden including some EM31 results and graphite showings (green dots) superposed helicopter-borne apparent resistivity from 7 kHz coaxial coil configuration (from Rodionov et al. 2013a). Brown dots represent non-graphite samples.

8.2.2 Geological work, observations, sampling analysis

NGU has collected 16 samples of graphite schist from the three sub-localities Romset, Langstrand and Sæterbukta in the Romsetfjorden area. Statistical data of total carbon (TC) is shown in Table 8.4. The TC content is relatively high, average TC 12.8 %, and the maximum value is 31 %. Data in Appendix 6 shows that this is mostly organic carbon in all samples. Half of the samples has a total sulphide (TS) content < 1 %. In the other half, the TS content varies from 1.1 % to 10.9 % (Appendix 6).

Table 8.4: Total Carbon (TC) analysis from the Romsetfjorden area

Romsetfjorden	N	Average TC (%)	Max (%)	Min (%)	St. Dev (%)	Median (%)
Langstrand	8	13.6	25.6	3.6	7.1	14.0
Romset	5	14.7	31.0	3.9	10.1	14.2
Sæterbukta	3	7.3	20.9	0.5	11.8	0.5
Romsetfjorden, Total	16	12.8	31.0	0.5	8.8	13.4

The helicopter-borne EM data indicate potential graphite mineralisation in a total length of ca. 3 km along the fjord (Figure 8.6). Our field observations show several occurrences of graphite lenses within this area. Many of these lenses are small (Fig. 8.6) but have a high carbon content. The most interesting area is at Romset where EM31 measurements were undertaken in 2018 (Figure 8.7). The quality of the graphite is good and the graphite schist at most localities appears as medium to coarse grained flake graphite.

Figure 8.8 shows typical outcrop of graphite along the road sections in the Romsetfjorden. Graphite schist rich in carbon occur in small lenses mixed with quartz and feldspar bearing country rock.



Figure 8.8: Graphite location in road-cut near Langstrand (UTM WGS84 500625 – 7634012). A sample from this location (hg21-16) showed 25.6 % TC and 4.0 % TS.

Figure 8.9 presents one possible interpretation of graphite structures at Romset (in Romsetfjorden) based on helicopter-borne EM data, ground EM31 data and exposures. This interpretation indicates two parallel folded structures. The EM31 data partly indicates a thickness of several tens of metres, and one of the structures seem to continue under the fjord. The total length of graphite structures may be nearly 2 km, and it looks like the graphite has a considerable width (average of ca. 20 m, EM31 data). NGU wants to stress that the EM31 line pattern is sparse, and other interpretations than shown in Figure 8.9 are possible.

According to the helicopter-borne EM data, graphite may also be present in small locations further to the north, in Bakkejordbukta and at Melkarneset (Figure 8.7) and towards the south (Figure 8.6). Some EM31 profiling is undertaken, but lack of anomalies may be caused by thick soil cover. In other parts, EM31 profiling is missing.

8.2.3 Summary Romsetfjorden

In the Romsetfjorden area, low apparent resistivity shows up as separated lenses in a total length of 3 km along the fjord (Figure 8.6). Graphite is exposed at several localities. The most pronounced of these appears next to the farm Romset. Here, based on EM31 data, graphite is interpreted as two parallel folded structures with a total length of nearly 2 km, and the width of these seems to vary from 10 to 50 m (average value ca. 20 m).

Small outcrops appear along several road sections and along the shoreline. The average total carbon content of 15 % and a maximum value of 31 %. The graphite is characterised as good quality flake graphite.

The area is populated with several residential houses and some industry.

8.3 Steinland

The area called Steinland is situated along the road to Myre, ca. 6 km south of Myre (Figures 5.6 and 8.1). Here, the combined magnetic and electromagnetic analyses indicate structure located from the shore and ca. 2 km towards NNE (Figure 5.6). However, the local low resistivity anomaly is limited to ca. 700 m in length (Figure 8.11). The area is extensively covered, and in spite of bedrock cropping out in the area, no exposures have been discovered that can explain the EM anomaly. EM31 profiling and one short ERT/IP line were therefore measured in 2018.



Figure 8.10: The Steinland area is 100 % soil covered and no exposures are observed. The ERT/IP line follows the forest from left towards the powerline seen to the right.

8.3.1 Geophysical work, EM31

In general, the EM31 measurements do not show apparent conductivity values that indicate graphite mineralisation. Mostly, the apparent conductivity is less than 20 mS/m (apparent resistivity > 50 Ω m). However, at the eastern measured points, at the eastern flank of the helicopter-borne EM anomaly, the apparent electric conductivity is between 20 and 50 mS/m (apparent resistivity 20 – 50 Ω m). This increase in electric conductivity may be caused by deep seated graphite or sulphide mineralisation.

At one location, where the EM31 line crosses the stream, the apparent conductivity is > 200 mS/m. This high value appears only at one point and are most likely caused by a parked car. West of this point, one single reading between 50 and 100 mS/m (red dot) on the road between the houses which also most likely is caused by some technical installation (metallic water pipe?).

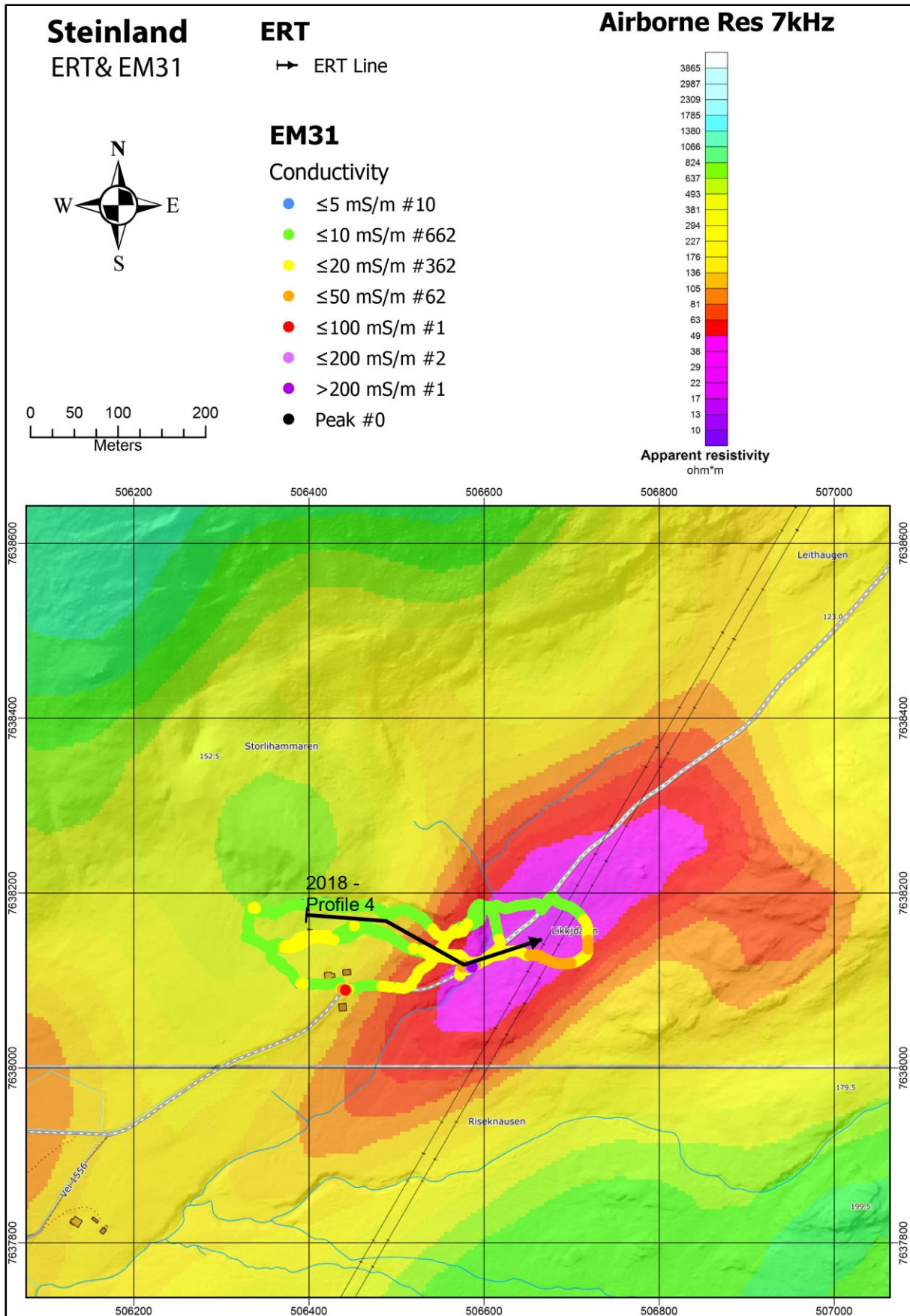


Figure 8.11: Results of EM31 measurements from the Steinland area overlain helicopter-borne measurements of apparent resistivity from EM 7 kHz coaxial coil configuration (from Rodionov et al. 2013a). The location of ERT/IP line is shown as a black line.

8.3.2 Geophysical work, ERT/IP

The location of the ERT/IP profile at Steinland is shown in Figure 8.11. Results of the combined 2D resistivity and Induced Polarisation measurement are shown in Figure 8.12. Electrode spacing was 5 m and the line length 300 m. The other acquisition and inversion parameters were as described in Chapter 4.1.4. The quality of the inverted resistivity and IP sections are good (see Table 8.5).

Table 8.5: Quality of 2D resistivity and IP data at Steinland area. Number of measured, removed and remaining data points for inversion, and observed “Absolute error” from the inversion of resistivity and IP data.

Profile name	Location	Measured data points	Removed data points	Inverted points	Abs. error ERT (%)	Abs. error IP (%)
2018-4	Steinland	676	25	651	8.7	14.2

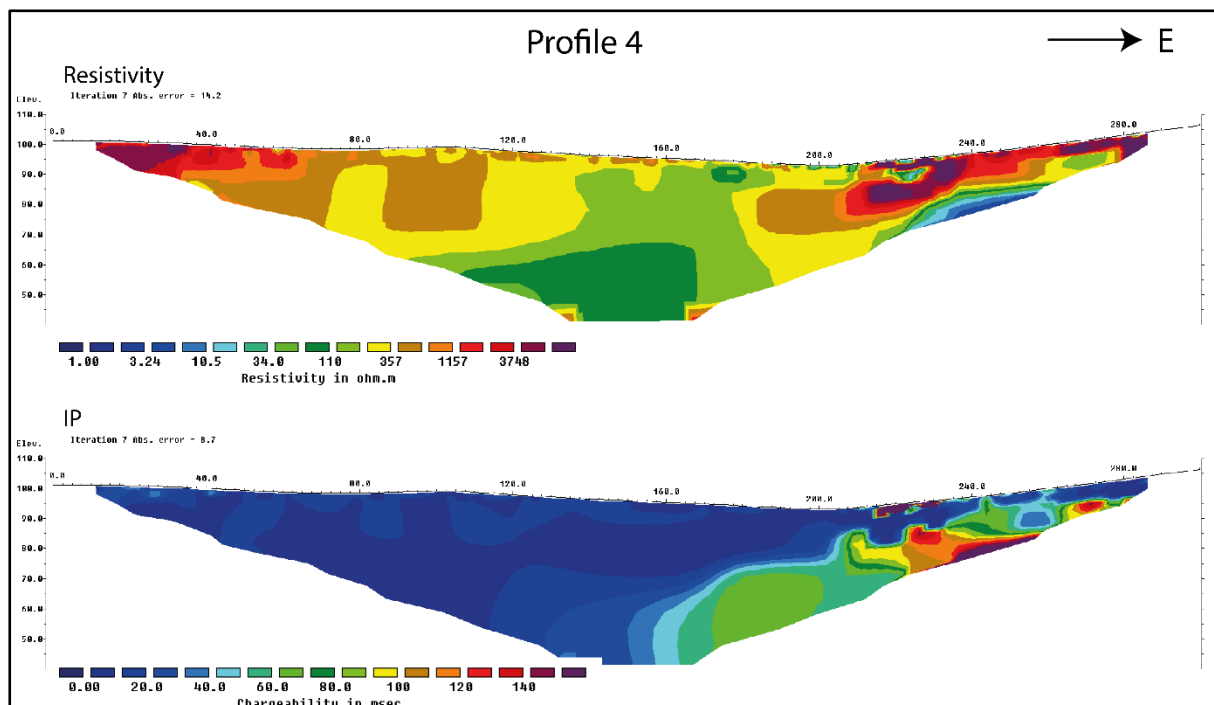


Figure 8.12: Steinland area. The results from 2D Resistivity and Induced Polarisation measurements along profile 2018-4.

In the central part of the resistivity section (upper part of Figure 8.12) the resistivity values are less than 350 Ωm and partly less than 110 Ωm and without any IP effect (lower part of Figure 8.12). This does not explain the EM anomaly from helicopter-borne measurements. Most likely this is fractured bedrock with clay alteration (Rønning et al. 2013). At the end of the profile, at depth from position 220, the resistivity is partly $< 5 \Omega\text{m}$ and it is a marked IP anomaly in the same area. This is a strong indication of sulphide or graphite mineralisation. Unfortunately, the profile is too short to make a complete image of the conductor. The anomaly appears at a depth of ca. 15 m which explains a moderate anomaly at the EM31 measurements.

8.3.3 Summary Steinland

At Steinland, a ca. 2 km long structure was discovered from the combined analysis of helicopter-borne magnetic and electromagnetic data. The area is extensively covered and NGU has no direct information about the mineralisation. Some EM31 profiling and one ERT/IP profile were measured in 2018. The results from these indicate a possible sulphide or graphite mineralisation at ca. 15 m depth. Since the ERT/IP profile was too short and no exposures were found, there is no information on quality and quantity of this mineralisation.

8.4 Myre

East of Myre in the Øksnes municipality, an extensive area of low resistivity is observed on the helicopter-borne EM data (Figures 5.2 and 8.1). This anomalous area was also observed in previous helicopter-borne EM measurements (Mogaard et al. 1988). One EM31 profile was measured north of the anomalous area (Gautneb & Tveten 1992) without any anomaly that may suggest graphite mineralisation. No follow-up work has been performed in the best conducting area. At the harbour of the town of Myre, several low grade graphite showings are registered, but the combined magnetic and resistivity interpretation (Figure 5.6) still indicate a large potential for graphite mineralisation.

To evaluate the EM anomalies from helicopter-borne EM measurements east of Myre, two combined 2D Resistivity (ERT) and Induced Polarisation (IP) profiles were measured in 2017. In 2018, another long ERT/IP profile in combination with EM31 were measured, and based on these three lines, two locations for shallow core drilling were selected. The area mostly consists of bogs and some farmland, with few outcrops (see Figure 8.13). This far, no exposures of graphite are known from in the central part of the helicopter-borne EM anomaly.

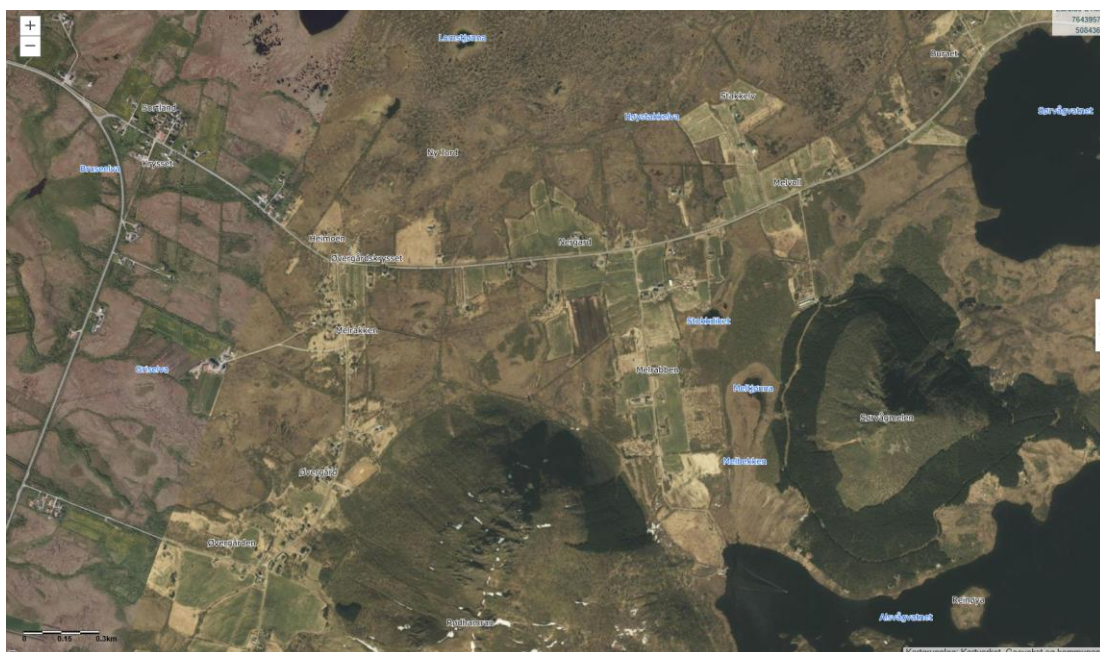


Figure 8.13: The area east of Myre is extensively covered by peat (Downloaded from www.norgebilder.no).

8.4.1 Geophysical work, EM31

EM31 measurements were undertaken only along the ERT/IP profile 2018-1. The results do not indicate any graphite mineralisation since the highest apparent conductivity is less than 100 mS/m (apparent resistivity > 10 Ω m) at the northern end of the profile 2018-1. However, increased electric conductivity shown in Figure 8.14 (orange colour, apparent conductivity between 20 and 50 mS/m) coincide well with the low resistive areas from helicopter-borne EM measurements. This may suggest graphite or sulphides mineralisation at a deeper level (> 10 m).

8.4.2 Geophysical work, ERT/IP

Since EM31 apparently do not reach down to any mineralisation, ERT/IP were chosen as follow-up methods. The location of the ERT/IP profiles at Myre are shown in Figure 8.14. Electrode spacing was 5 m and the other acquisition and inversion parameters are as described in Chapter 4.1.4. The quality of the inverted resistivity and IP sections are mostly good except for IP at profile 2017-4 (not acceptable quality) and resistivity at profile 2018-1 which is an acceptable quality (see Table 8.6). Results of the combined 2D resistivity (ERT) and Induced Polarisation (IP) measurement are shown in Figures 8.15, 8.16 and 8.17.

Table 8.4: Quality of 2D resistivity (ERT) and IP data at Myre. Number of measured, removed and remaining data points for inversion, and observed “Absolute error” from the inversion of resistivity and IP data.

Profile name	Location	Measured data points	Removed data points	Inverted points	Abs. error ERT (%)	Abs. error IP (%)
2017-4	Myre east	1096	72	1168	7.9	63.3
2017-5	Myre west	1132	36	1168	4.5	6.5
2018-1	Myre middle	3904	112	3792	25.9	10.9

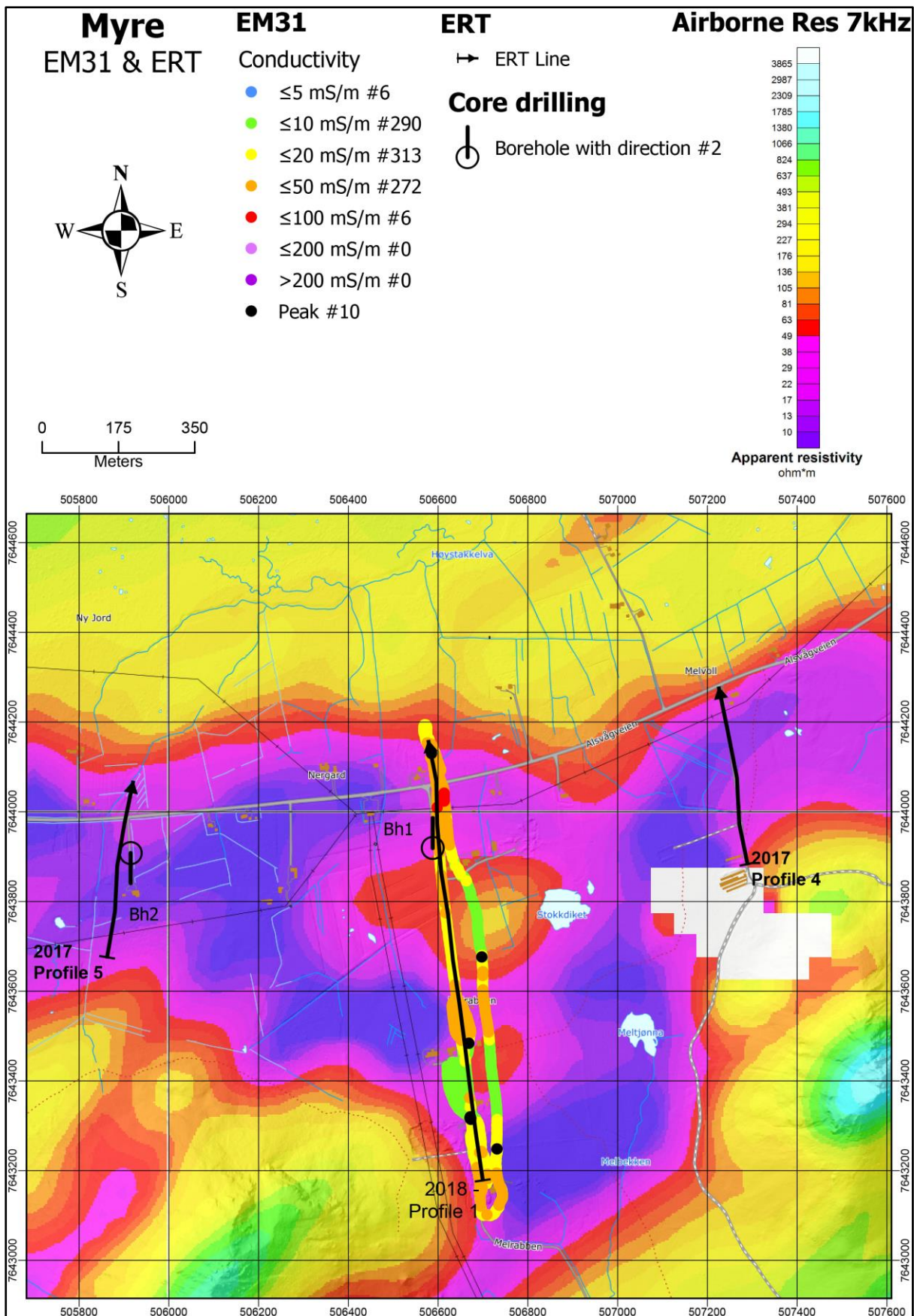


Figure 8.14: The area east of Myre. EM31 results and the location of 2D Resistivity/IP profiles are overlain helicopter-borne measurements of apparent resistivity from EM 7 kHz coaxial coil configuration (from Rodionov et al. 2013a). Location of ERT/IP profiles and drill-holes (Bh1 and Bh2) are indicated in black.

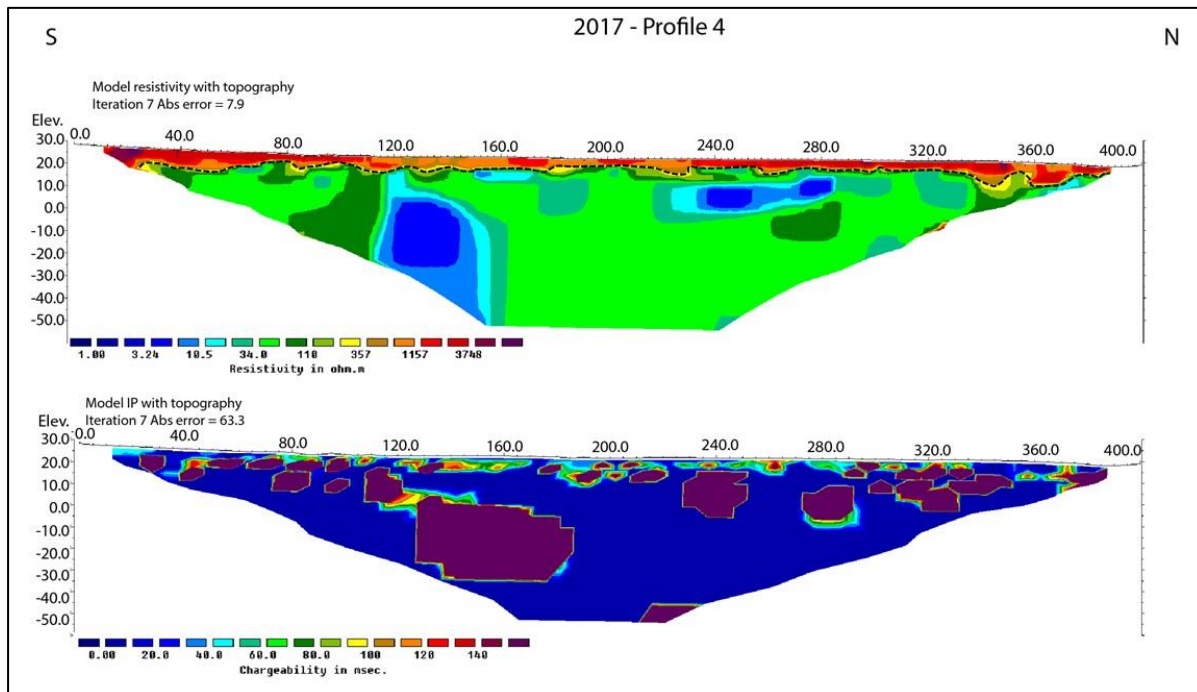


Figure 8.15: East of Myre. The results from 2D Resistivity and Induced Polarisation measurements along profile 2017-4. The interpreted soil-bedrock interface is shown as a dotted black line.

The ERT/IP **Profile 2017-4** is measured 400 m along a local road (Figure 8.14). The resistivity section (Figure 8.15) show an approximately 5 to 10 m thick high resistive layer ($> 350 \Omega\text{m}$) that can be interpreted as soil (road material, peat and possibly moraine). Marine clay can be excluded. Below this layer, the resistivity is in general low, mostly in the interval between 30 and $100 \Omega\text{m}$ which is not representative for the host rock in the area. Locally, the resistivity is $< 10 \Omega\text{m}$ and this may be a result of graphite or sulphide mineralisation. Underneath the soil cover, high IP effects appear along the entire profile. This is an indication of disseminated graphite or sulphide. ERT/IP profile 2017-4 do not indicate obvious targets for shallow drilling.

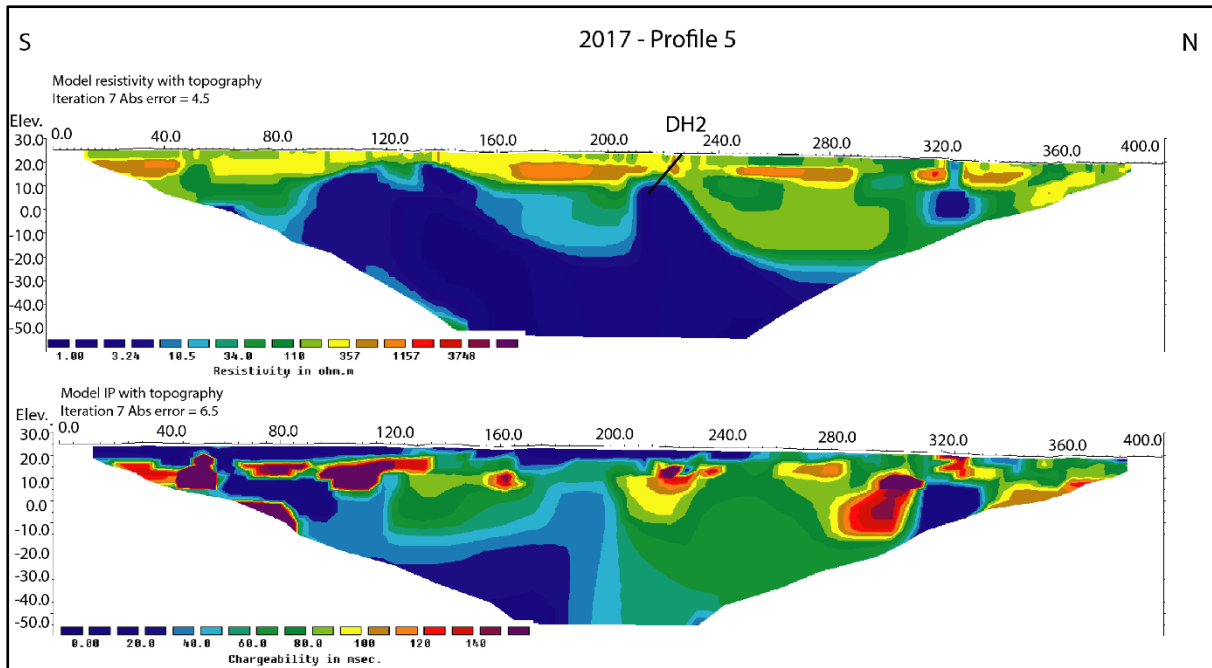


Figure 8.16: The area east of Myre. The results from 2D Resistivity and Induced Polarisation measurements along profile 2017-5. Drill-hole Dh2 is shown as a black line.

The resistivity along **Profile 2017-5** (Figure 8.16) demonstrates different characteristics. This profile was measured partly in open land and partly in cultivated ground. The ca. 3 to 10 m thick top layer shows a resistivity from ca. 100 to 350 Ω m and can be interpreted as peat or possibly moraine material. Marine clay can be excluded as a reason for the helicopter-borne EM resistivity anomalies here. Underneath the top layer the resistivity is partly less than 5 Ω m indicating massive graphite or sulphides. IP effects in parts of the profile are an indication of disseminated mineralisation.

Location for drill-hole 2 was selected based on this ERT/IP data (ca. position 230). Good conducting material seem to be closer to the surface at positions 110 and 120, but this area is not accessible for the truck mounted drilling equipment.

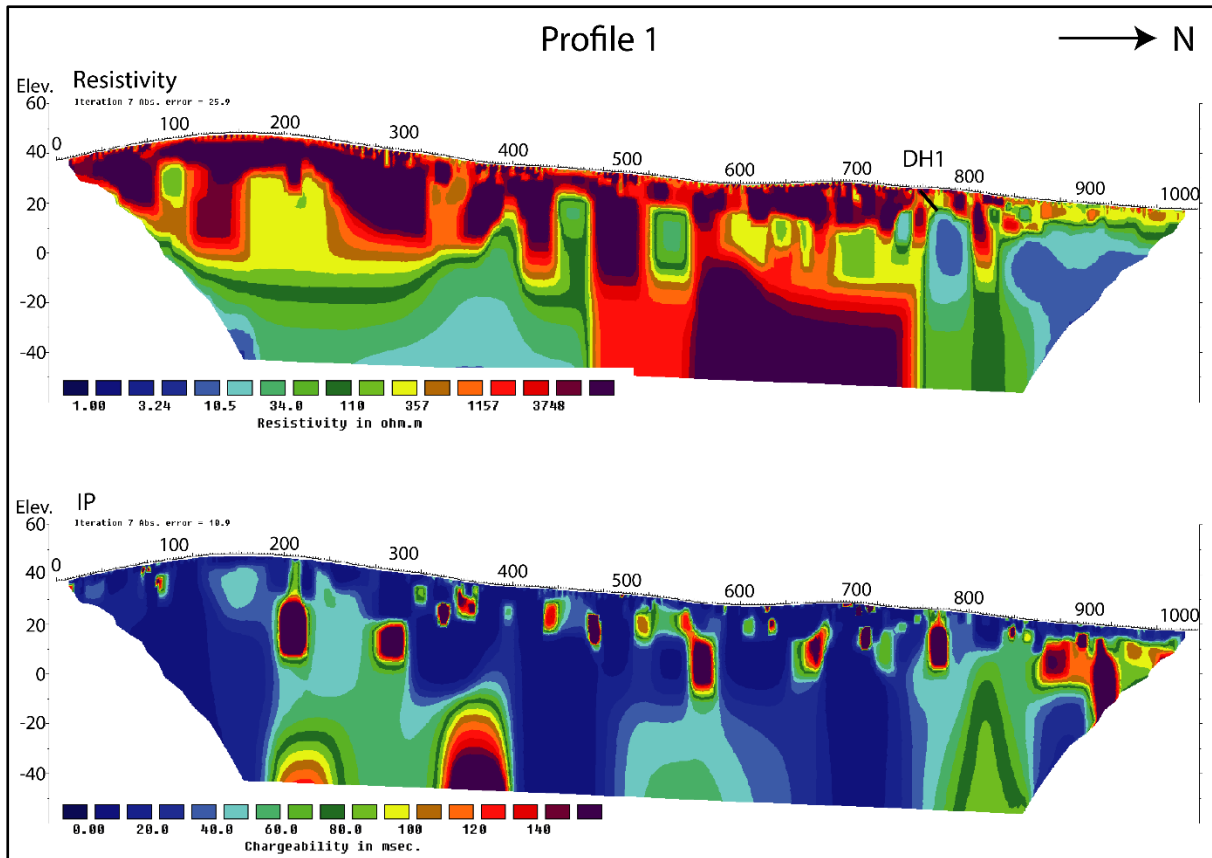


Figure 8.17: East of Myre. The results from 2D Resistivity and Induced Polarisation measurements along profile 2018-1. The soil-bedrock interface is not easy to see in this profile except for the northern part where a soil thickness of 5 to 10 metres is indicated. Drill-hole DH1 is indicated as a black line.

The ERT/IP profile 2018-1 (Figure 8.17) was measured in a total length of 1 km along the road from Melrabben in the south and crossing Alsvågveien (the road to Alsvåg) in the north. Along most of the profile, high resistive ($> 4 \text{ k}\Omega\text{m}$) non-mineralised bedrock is almost outcropping. At the northern end, low resistive material ($< 10 \text{ }\Omega\text{m}$) that may suggest graphite appears at a depth from five to ten metres. In the eastern part, almost the same kind of material (resistivity $< 20 \text{ }\Omega\text{m}$) appears at depths of (from the south) 40 m, 20 m (yellow), 20 m and 10 m (position 450). High IP effects appears in various places, and this is indicating disseminated sulphide or graphite mineralisation. Slightly higher resistivity than in other graphite mineralisation in Vesterålen may suggest graphite of lower quality along this profile.

Location for drill-hole 1 was selected based on this ERT/IP data (ca. position 760). Here, material of low resistivity can be expected at a ca. 10 m depth.

Concluding remarks:

The three ERT/IP profiles east of Myre indicate graphite or sulphide mineralisation. The soil is too thick for trenching (5 to 15 m and locally even more), and core drilling is the only method to obtain information on the type of mineralisation and quality. The soil thickness explains a moderate response at the EM31 measurements.

8.4.3 Geological work, core drilling

To try to find the origin of the extensive low-resistivity anomaly from helicopter-borne EM measurements east of Myre city, two short core drillings were undertaken. Drill-hole sites were selected based on ERT/IP anomalies (see Figures 8.16 and 8.17). The location of the drill-holes is shown in Figure 8.14 and technical data for these is given in Table 8.5. The drilling was much more challenging than expected due to poor rock quality, and the core loss was large. Due to this, the electrical conductivity was not logged.

Table 8.5: Technical data, core drilling at Myre. Coordinates in WGS84 UTM Sone 33.

Area	Drill-hole	UTM E	UTM N	Direction (°)	Dip (°)	Length (m)
Myre	Dh1-2018	506588	7643919	000	45	20.0
Myre	Dh2-2018	505915	7643908	180	45	19.8

Results from core analyses in Dh2 are given in Figure 8.18. In Dh1, the core loss was so great that no core analysis was undertaken. A detailed geological description for Dh1 and Dh2 is presented in Appendix 1, the pictures of the core are shown in Appendix 2 and analytical data (total sulphur (TS) and total carbon (TC) Leco analysis) are presented in Appendix 3. In Appendix 4, XRF analysis of the drill-cores are presented. In both cores the rock was very fractured and broken and difficult to interpret.

As seen in Figures 8.16 and 8.17, the two drill-holes do not reach the best conducting parts of the resistivity sections. The plan was to drill ca. 50 m, but the bedrock was heavily fragmented and technical problems stopped the drilling after ca. 20 m. In addition, since the drilling rig needs road access to the drilling sites, the drill-holes are located at the edges of the strongest helicopter-borne resistivity anomalies (see Figure 8.14). This means that the drilling sites were not optimal to intersect the assumed best parts of a potential graphite mineralisation, and the drilling depth was too short. However, in the most complete log (Myre 2018-2) we see scattered graphite in thin veins irregularly distributed but no massive layers of graphite were found. The TC content was from ca. 0.5 % to ca. 1.1 % in the three analysed intervals. The TS content was from ca. 1.8 to 3.0 % in the same intervals.

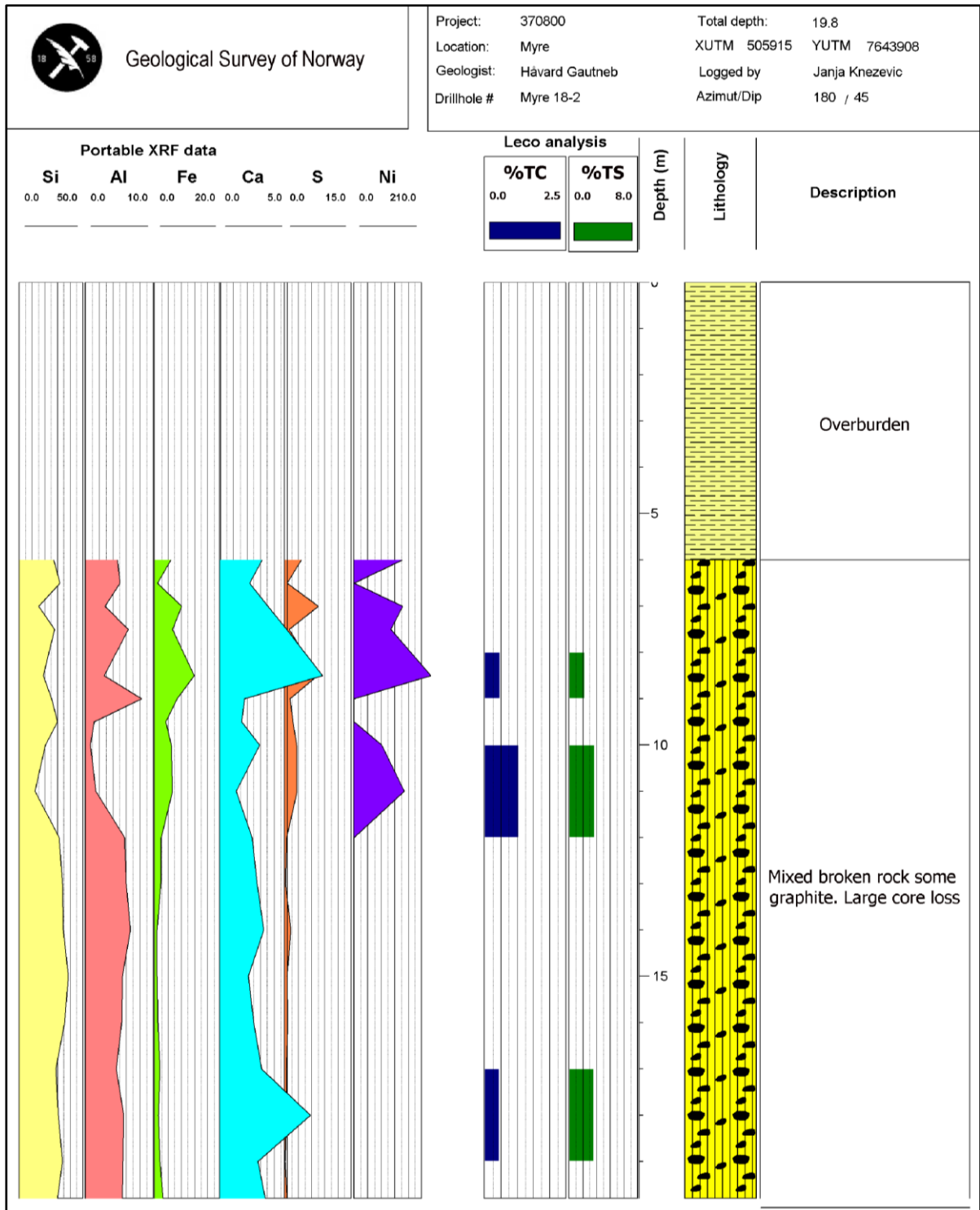


Figure 8.18: Results from the Myre drill-hole Dh2-2018: Portable XRF analyses (Si, Al, Fe, Ca, and S in %, Ni in ppm) at the cores, selected Leco analyses of Total Carbon (TC) and Total Sulphides (TS), lithological log and core description.

8.4.4 Discussion and summary, Myre

The Myre area comprises the largest helicopter-borne EM anomaly in the whole Vesterålen area. Anomalous low resistivity is shown in a total length of ca. 2.5 km in E-W direction, and the thickness varies from ca. 0.3 km to more than 1 km. Several individual structures are likely. The area is extensively covered (mostly peat), and no graphite exposures are discovered except for in the two drill-holes. The drillcore shows the presences of low grade graphite. However, the geophysical ERT profiles indicate the presence of graphite or sulphide deeper than the depth reached by the drilling. Graphite of good quality is discovered at Rødhamran south of the Myre area (Rønning et al. 2018), and to the east at Alsvåg, Instøya and Straumen (see next chapter).

The drilled EM-anomaly east of Myre is connected to anomalies at the south (Rødhamran and Stavadalen) and to the west (Myre harbour). Good quality graphite has been found at Rødhamran (Rønning et al. 2018), but these areas are also the locations for rocks rich in pyrrhotite (cf. analyses in Appendix 6). In particular at Stavadalen southwest of the drilling site, such rocks are well exposed over large parts of the EM anomaly. Similiar mineralisations are also known and described from Sørvågmelen immediately to the east of the drill site, though not expressed as an EM anomaly at this location. The graphite occurrences at Alsvåg, Instøya and Straumen (see these) accomodates less sulphides, but could belong to different strata in the supracrustal sequence, and may not be part of the drilled anomaly.

The Myre area has a great potential for graphite mineralisation, possibly the greatest potential in the Vesterålen area. To evaluate this potential, detailed geophysics and deeper core drilling is recommended.

8.5 Instøya – Alsvåg - Straumen

Graphite was (re)discovered at Instøya close to Alsvåg during geological mapping in August 2019. Old graphite showings (from 1880-1915?) exist on the island Instøya but were not known previously to NGU. Follow-up fieldwork identified graphite also at Alsvåg and Straumen northwest of Alsvåg. Here, conductive zones are observed at the helicopter-borne geophysical mapping from 2013 (Figure 8.19), while Instøya was outside the area covered.

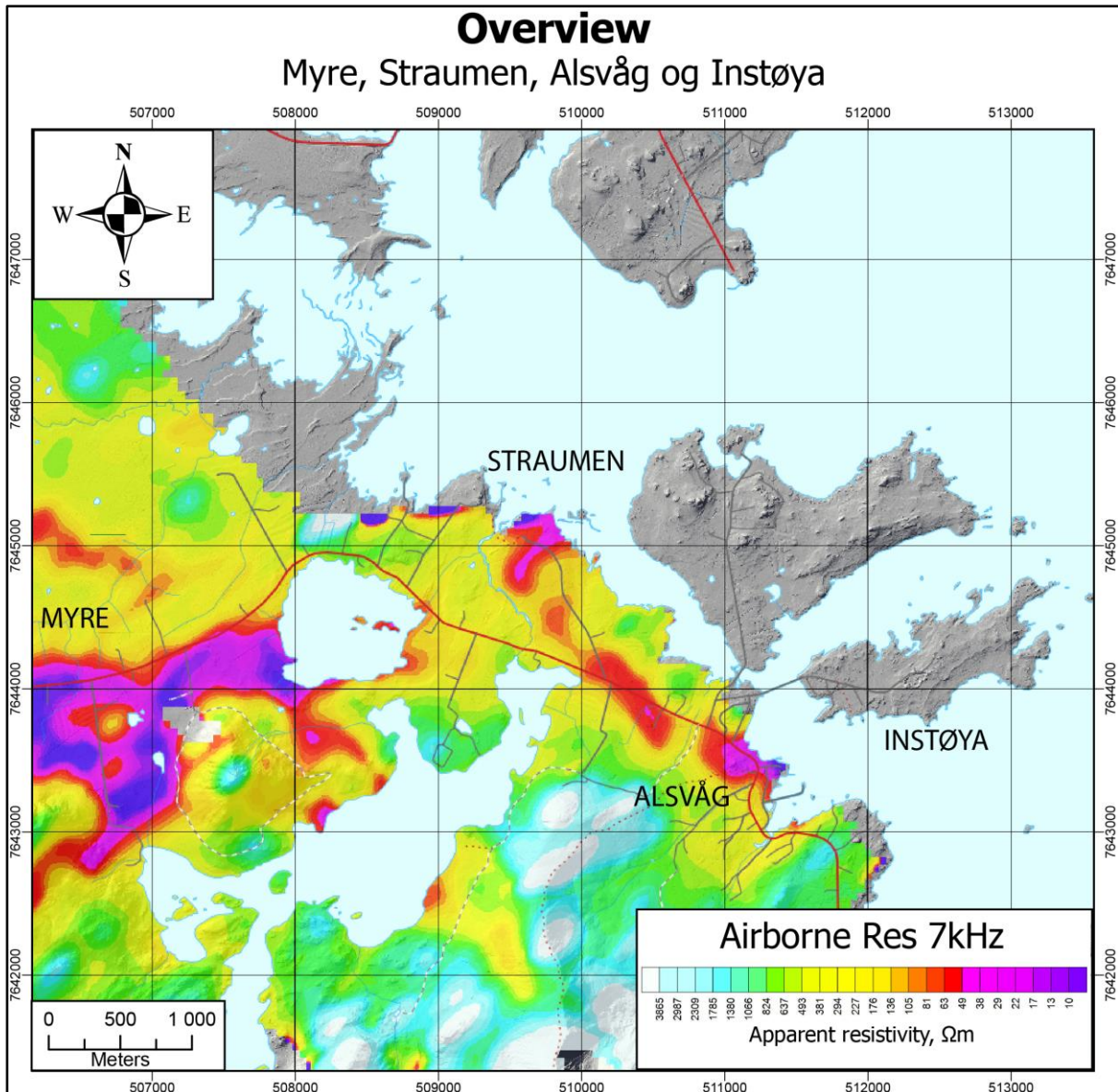


Figure 8.19: Alsvåg – Instøya – Straumen area. Apparent resistivity from helicopter-borne 7 kHz EM data (from Rodionov et al. 2013a). Instøya was not covered with helicopter-borne geophysics.

8.5.1 Instøya

The graphite occurs as several bands of graphitic schists and disseminated graphite in fine- to medium grained felsic gneisses of assumed supracrustal protolith. Fine grained mafic gneisses and minor mica schists are also common in the sequence. Observed graphite bearing zones are typically about 10 m wide, but with individual layers of graphitic schist of 1-2 m. All the rocks display migmatitic features with small medium-grained feldspar lenses containing orthopyroxene, indicating metamorphism at granulite conditions.

On Instøya the supracrustal sequence trends ENE-WSW, following the length of the island. It is bound at the northern side (at Meløya) by medium – to coarse-grained migmatitic rocks of partly igneous origin, while the south-eastern shore of the island is intruded by a gabbroic to dioritic magmatic rock. Intruded (?) into the supracrustals is a pink, foliated granite, also striking along the length of the island. The graphitic rocks occur in two major sequences, exposed on the south-western and north-eastern shorelines, and in a quarry at the middle of the island (see Figure 8.20).

Several locations are sampled. Details and analysis results are given in Appendix 6. The average total organic carbon (TOC) is given in Table 8.6. In total, 28 samples from several locations on the island show an average TOC content of 8.6 % with a maximum value of 21.0 %. The TC values are given in Appendix 6 and in Table 10.1. In hand specimen graphite occurs as flaky grains, up to 1-2 mm.

The discovery has been followed up by profiling using EM-31 and these results are presented in Figure 8.20. Several conducting structures are mapped, and they coincide with graphite exposures. An interpretation of graphite structures is given in Figure 8.21. The total length of three graphite structures is 3500 m, and the width of these varies from ca. 10 m to ca. 100 m. The average width estimated from 22 graphite structure crossings is ca. 20 m. Geological observations indicate variable quality within the structures. Very good conductivity in sea areas to the north and close to the shoreline to the south may be caused by sediments intruded by conductive seawater.

8.5.2 Alsvåg

At Alsvåg the graphitic rocks mostly occur as small outcrops on the shoreline at low tide. However, a helicopter-borne EM anomaly extends onshore, but outcrops are scarce and have not been found. Structural data suggests this is the same graphite as found on Instøya, and then folds and continue northwest towards Straumen. Five samples from the area (see Figure 8.22) show an average TOC content of 8.0 % and a maximum value of 19.8 % (Table 8.6). The TC values are given in Appendix 6 and in Table 10.1.

Follow-up geophysical work is not undertaken in the Alsvåg area, and no detailed information on individual structures exist. The helicopter-borne data indicate graphite structures in a total width of ca. 300 m perpendicular to the strike direction and the length along the strike is ca. 500 m. Most likely the anomalous area consists of several graphite structures, and graphite are exposed at three locations.

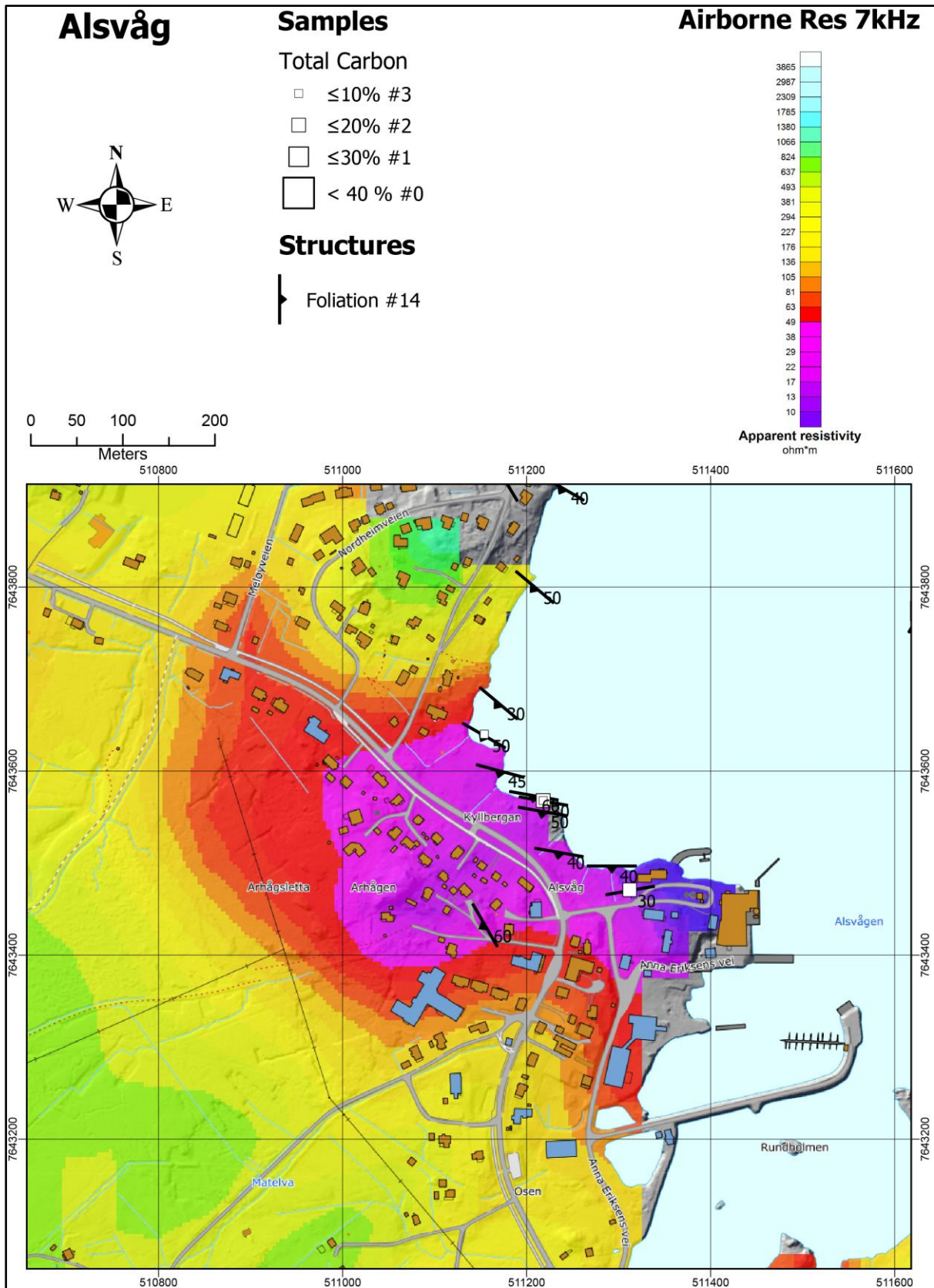


Figure 8.22: Alsvåg. Structural observations superposed on apparent resistivity from helicopter-borne 7 kHz EM measurements (from Rodionov et al. 2013a). The locations of graphite samples and their TC contents are shown as white squares.

8.5.3 Straumen

The graphite discovery at Straumen northwest of Alsvåg is also mostly exposed in the tidal zone as individual outcrops associated fine- to medium grained gneisses of assumed supracrustal origin. Here, 0.5-2 m wide layers of very rich, coarse grained (1-3 mm) graphite can be found as both schistose and massive varieties.

The discovery has been followed up by profiling using EM-31 (Figure 8.23). Apparent conductivity is partly > 200 mS/m (resistivity $< 5 \Omega\text{m}$) and coincide with three graphite exposures at the eastern EM anomaly. A profile further to the south does not show conductivity anomalies of the same order. This may be caused by a thick (< 10 m) soil cover and the three graphite structures most likely continues to the southwest in a length of ca. 500 m. These structures may also continue underneath the sea towards the north.

The helicopter-borne anomaly in the centre of Figure 8.23, shows an EM31 anomaly that indicates graphite mineralisation (> 200 mS/m). However, the size of this structure onshore is shorter than 100 m.

The helicopter EM anomaly to the west (Figure 8.23) shows no conductive structures that can indicate graphite. A graphite structure at depth (10 m – 100 m) may exist but is most likely too small to be of economic interest.

The rock-association, it's general strike, as well as a pinch-and-swell string of EM-anomaly connect this locality as a continuation of the sequences at Alsvåg and Instøya. A possible westward continuation has not been sought for in the field, but outcrops in this area are sparse and the geophysical coverage is limited. On the other hand, there is no obvious connection with the large EM-anomalies trending from Alsvåvatnet and westward to Myre just west of the Instøya-Alsvåg-Straumen structure (see Figure 8.1). The latter therefore could be a parallel structure of different origin and composition.

Since graphite is exposed both at Alsvåg and Straumen, the 700 m long EM-anomaly between these two areas is most probably caused by graphite (see Figure 8.19).

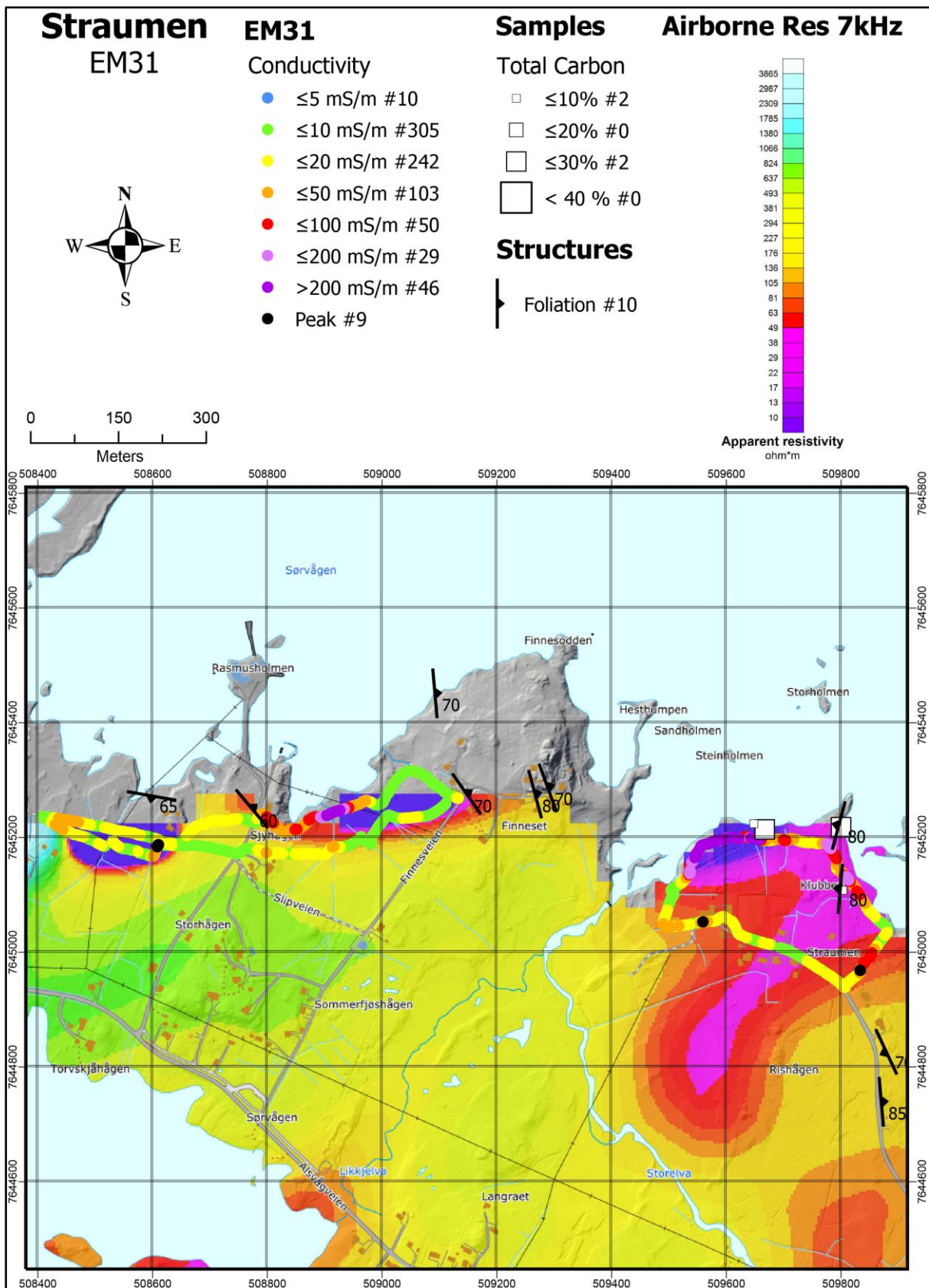


Figure 8.23: Straumen. Strike and dip observations and apparent electric conductivity from EM31 measurements superposed on apparent resistivity from 7000 Hz helicopter-borne EM (from Rodionov et al. 2013a). The locations of graphite samples and their TC contents are shown as white squares.

8.5.4 Summary, Alsvåg – Instøya – Straumen

At Instøya, graphite is exposed at several locations along three structures mapped by EM31 measurements. The total length of these structures is ca. 3.5 km. Flake graphite with grain size up to 1-2 mm is observed in a width of ca. 10 m. EM 31 data indicate thickness from ca. 10 m to ca. 100 m and 22 structure crossings indicate an average thickness of ca. 20 m. Average TOC concentration derived from 28 samples is 8.6 % with a maximum value of 21.0 %. NGU recommend core drilling to evaluate the graphite potential at Instøya.

At Alsvåg, at least three graphite structures are exposed along the shoreline and onshore. In this area, no EM31 measurements have been undertaken. The helicopter-borne EM-anomaly indicate a length of ca. 500 m but no information on the structure width exists. Total Organic Carbon (TOC) data for five samples are listed in Table 8.6.

At Straumen, three potential structures of coarse-grained flake graphite (1 – 3 mm) are exposed. The thickness of these varies from 0.5 m to ca. 2 m and the length is assumed to be ca. 500 m. Total organic carbon content for five samples are listed in Table 8.6. Total carbon concentrations are listed in Appendix 6 and in Table 10.1.

Table 8.6: Total Organic Carbon (TOC) of samples from Instøya, Alsvåg and Straumen area.

Instøya, Alsvåg, Straumen	N	Average TOC (%)	Max (%)	Min (%)	St. dev (%)	Median (%)
Instøya	28	8.6	21.0	1.3	5.4	8.2
Alsvåg	5	8.0	19.8	1.3	8.0	3.3
Straumen	5	11,6	26,9	0,6	12,0	5,3

9. RESULTS OF THE FOLLOW-UP WORK IN HADSEL MUNICIPALITY

During the field season of 2017, NGU performed geophysical measurements, some geological observations and sampling at three localities in the Hadsel municipality; Morfjord abandoned mine, Sommarhus and Sellåter. The work at the old abandoned Morfjord mine was finished in 2017 (Rønning et al. 2018). In 2018 some more work was done at Sommarhus (geophysics and core drilling) and at Sellåter (geophysics). At Korsodden geophysical measurements were undertaken to find the origin of the low resistivity anomaly (Figure 9.1). All four areas show up at the combined magnetic and electromagnetic analysis of helicopter-borne data (Figure 5.10).

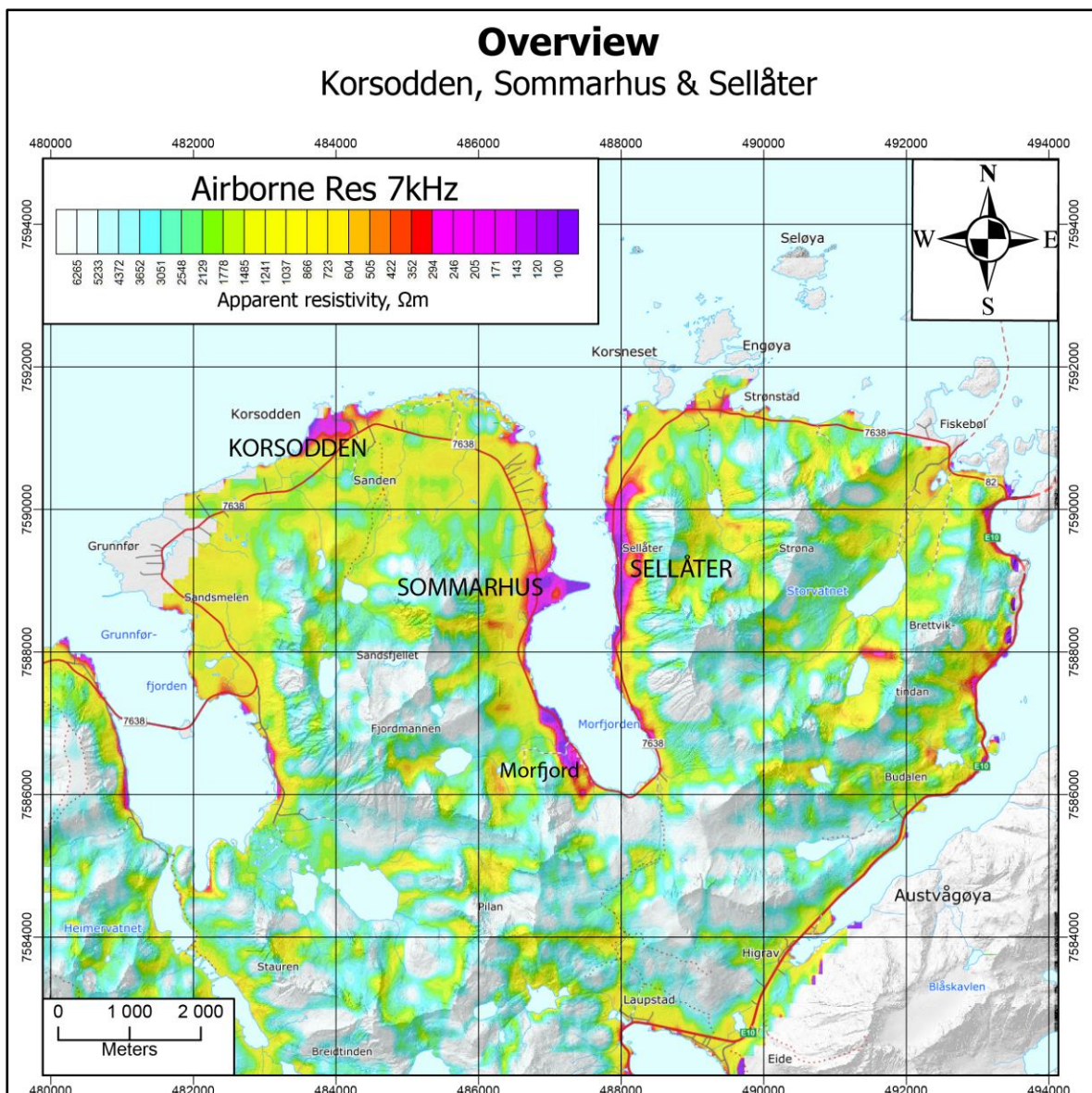


Figure 9.1: Overview map Northern Lofoten, Hadsel Municipality. Follow-up work in 2018 were performed in the areas Korsodden, Sellåter and Sommarhus. The work at the old abandoned Morfjord mine was finished in 2017 (Rønning et al. 2018). Note the colour scale used in this area.

9.1 Korsodden

The Korsodden area is located at the northern part of the peninsula between Grunnfjørden and Morfjorden in Lofoten (Figure 9.1). The farmland is 100 % soil covered, while exposures are present on the shoreline (Figure 9.2). The low apparent conductivity in the area (Figure 9.1) is confirmed by the marked anomaly at the combined magnetic and electromagnetic anomaly (Figure 5.10). With the aim to identify the source for the anomaly, EM31 measurements and one ERT/IP profile were undertaken.



Figure 9.2: The Korsodden area is 100 % soil covered, and no exposures were observed.

9.1.1 Geophysical work, EM31

The helicopter-borne EM data indicate a ca. 400 m x 400 m area where apparent resistivity is $< 300 \Omega\text{m}$, and partly $< 100 \Omega\text{m}$. The latter appears along the shore and may be an effect of conductive seawater. However, the low resistivity more than 200 m from the shoreline cannot be explained only by seawater.

The anomalous resistivity area is covered by several EM31 lines (Figure 9.3). Almost all measured apparent conductivity values are $< 20 \text{ mS/m}$ (apparent resistivity $> 50 \Omega\text{m}$). This is not typical for graphite mineralisation, and most likely, the soil cover can explain these values. To see if graphite is present at a deeper level, one ERT/IP profile was measured.

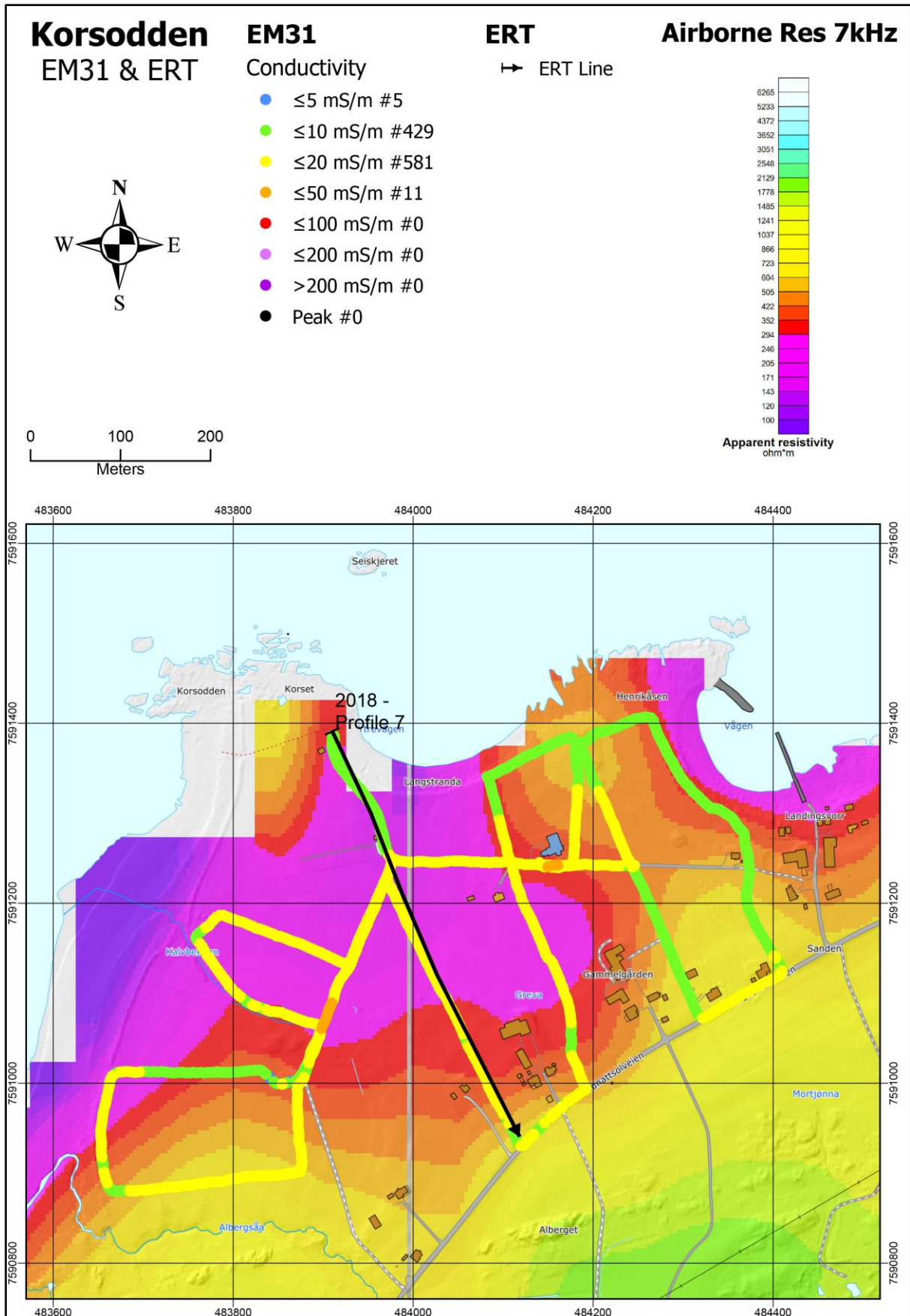


Figure 9.3: The Korsodden area. The results from the EM31 measurements superposed on apparent resistivity (EM 7 kHz coaxial coil configuration, Rodionov et al. 2013b).

9.1.2 Geophysical work, ERT/IP

Location of the ERT/IP profile at Korsodden area is shown in Figure 9.3. Results of the combined 2D resistivity and Induced Polarisation measurement are shown in Figure 9.4. Electrode spacing was 5 m, total profile length 500 m and the other acquisition and inversion parameters are as described in Chapter 4.1.4. The quality of the inverted resistivity and IP sections are good and very good respectively (see Table 9.1).

Table 9.1: Quality of 2D resistivity and IP data at Korsodden. Number of measured, removed and remaining data points for inversion, and observed “Absolute error” from the inversion of resistivity and IP data.

Profile name	Location	Measured data points	Removed data points	Inverted points	Abs. error ERT (%)	Abs. error IP (%)
2018-7	Korsodden	1567	10	1557	7.7	3.4

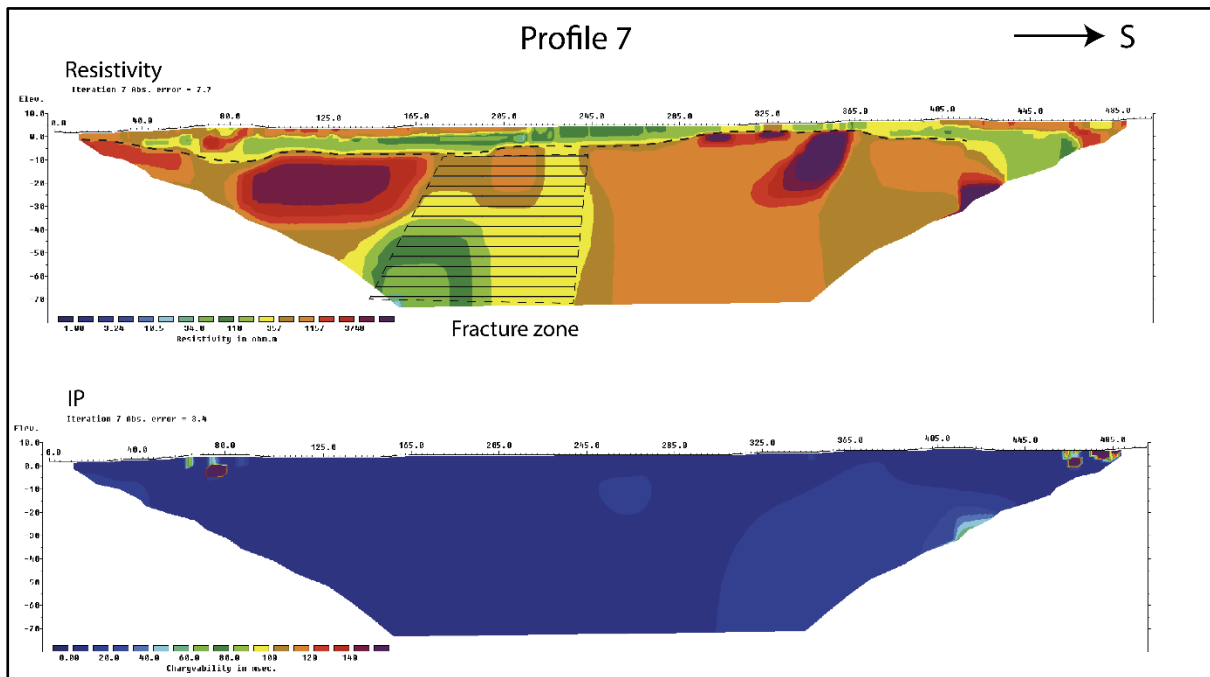


Figure 9.4: The Korsodden area. The results of the 2D Resistivity and Induced Polarisation measurements along profile 2018-7. The interpreted soil-bedrock interface is presented as a dotted black line and a possible fractured zone in bedrock as horizontal line pattern.

The ERT data from Korsodden (upper part of Figure 9.4) indicate a soil cover with thickness from ca. 5 m to ca. 15 m and possibly 20 m. The soil cover consists of two layers, one pretty dry upper layer with resistivities $> 350 \Omega\text{m}$ (brown and partly red colour) and a layer underneath that can be water saturated (resistivity from $20 \Omega\text{m}$ to ca. $100 \Omega\text{m}$). The bedrock underneath the soil cover shows mostly a resistivity level $> 1000 \Omega\text{m}$. From position 150 to position 240, the resistivity in bedrock is $< 350 \Omega\text{m}$ and this is most likely caused by a 90 m wide fractured zone in bedrock. The profile does not display a resistivity and IP combination that indicates any graphite mineralisation. Most likely, the resistivity anomaly from helicopter-borne data is caused by a combination of a thin layer conductive soil, fractured bedrock and partly of seawater.

9.1.3 Summary, Korsodden

The helicopter-borne geophysical data shows a ca. 400 m x 400 m anomalous area that may be caused by graphite. The follow-up work at Korsodden does not show an anomaly combination that indicate graphite mineralisation. Most likely the helicopter-borne low resistivity anomaly is caused by a combination of a thin layer of conductive soil, fractured bedrock and partly of seawater.

9.2 Sellåter

At Sellåter on the eastern side of Morfjorden, a ca. 1200 m long helicopter-borne EM anomaly was discovered along the seaside (Figure 9.1). Partly this can be an effect of seawater, but the anomaly extends into land in a way that indicate some conductive material in bedrock. Geological follow-up work in 2017 discovered graphite mineralisation at the shore (Rønning et al. 2018). To get a better image of the graphite distribution, EM31 profiling was performed in 2018. The Sellåter area is also nearly 100 % soil covered (Figure 9.5). Exposed bedrock (with graphite) is detected along the shore.



Figure 9.5: The Sellåter area is heavily soil covered except for the near shore areas where graphite is exposed.

9.2.1 Geophysical work, EM31

At Sellåter, several lines were measured with EM31 (Figure 9.6). High apparent electric conductivity (> 200 mS/m, apparent resistivity $< 5 \Omega\text{m}$) is proven at several locations and partly these coincide with exposed graphite. The graphite mineralisation seems to be distributed into several isolated lenses. The largest of these is ca. 400 m long and at least 50 m wide. The graphite may also continue underneath the sea and further to the north (outside the area presented in Figure 9.6). An interpretation of graphite structures is shown in Figure 9.7.

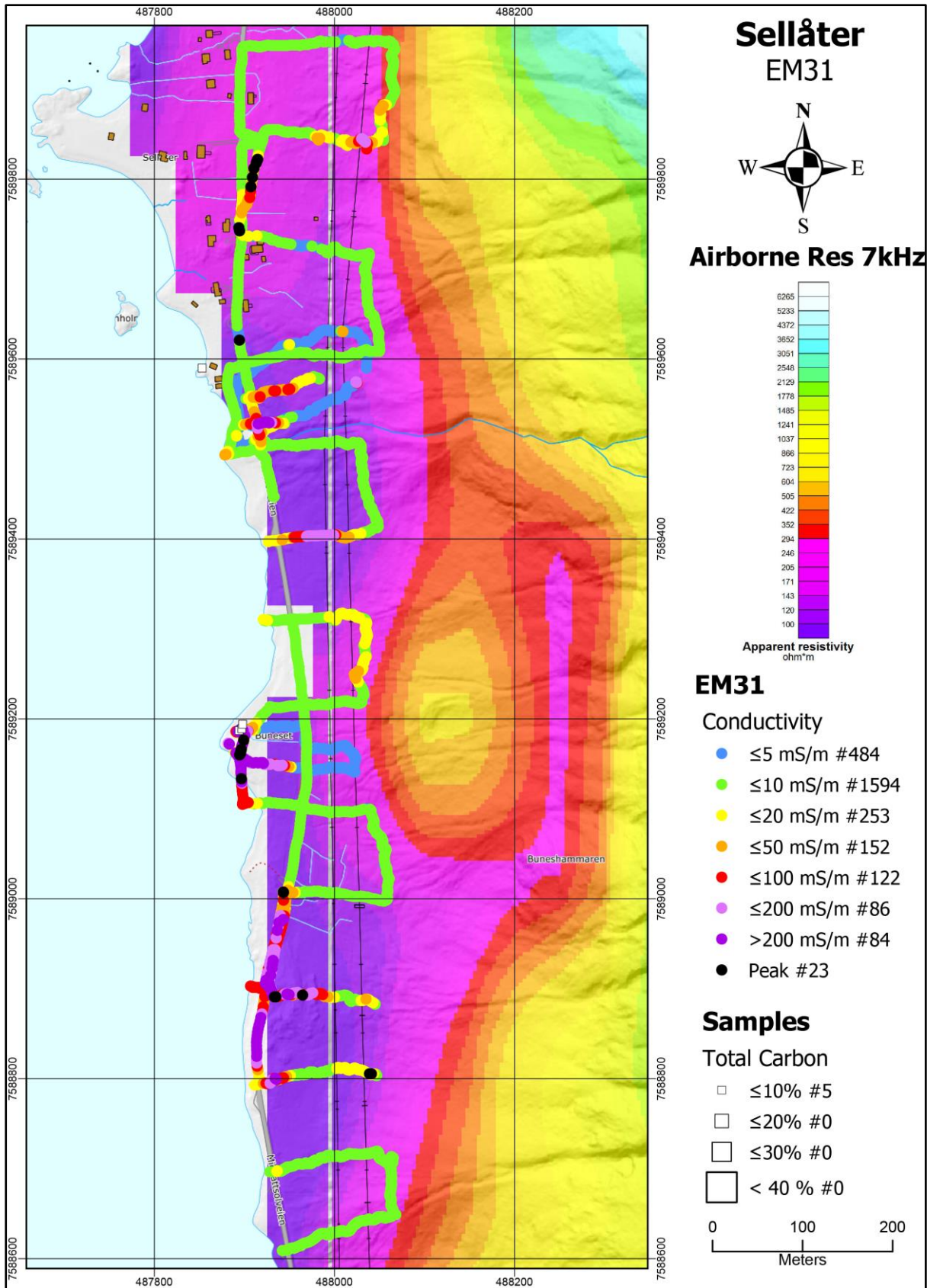


Figure 9.6: The Sellåter area. The results from the EM31 measurements superposed on apparent resistivity (EM 7 kHz coaxial coil configuration, Rodionov et al. 2013b). The location of graphite samples and their Total Carbon content is given as white squares.

9.2.2 Geological work, sampling

Analysis of the total carbon content from the Sellåter area is summarised in Table 9.2. The seven samples show an average TC content of 6.3 % and no samples exceeds 10 % TC.

Table 9.2: Total Carbon (TC) data from 9 surface samples from the Sellåter area.

Morfjorden	N	Average TC (%)	Max TC (%)	Min TC (%)	St. Dev TC (%)	Median TC (%)
Sellåter	9	6.2	7.9	3.7	1.3	5.8

It is possible that the Sellåter occurrence is a part of the same structure as Sommarhus at the western side of Morfjorden and the abandoned Morfjord mine further to the south under the fjord (see Figure 9.1). Due to the conductive seawater, it is impossible to map this.

9.2.3 Summary Sellåter

In the Sellåter area, an anomaly at helicopter-borne EM data show a continuous structure along the eastern shore of Morfjorden in more than 1500 m. Follow-up work with EM31 and geological mapping has discovered several small isolated graphite structures. The largest of these is ca. 400 m long and more than 50 m wide. This structure may continue underneath the fjord. Average TC content of seven samples is 6.2 % and the maximum value is 7.9 %. The graphite bearing rock comprises a coarse-grained rock with abandoned large crystals of zoisite, see Chapter 12.1.1 in Rønning et al. (2018) where the graphite bearing rocks is described in detail.

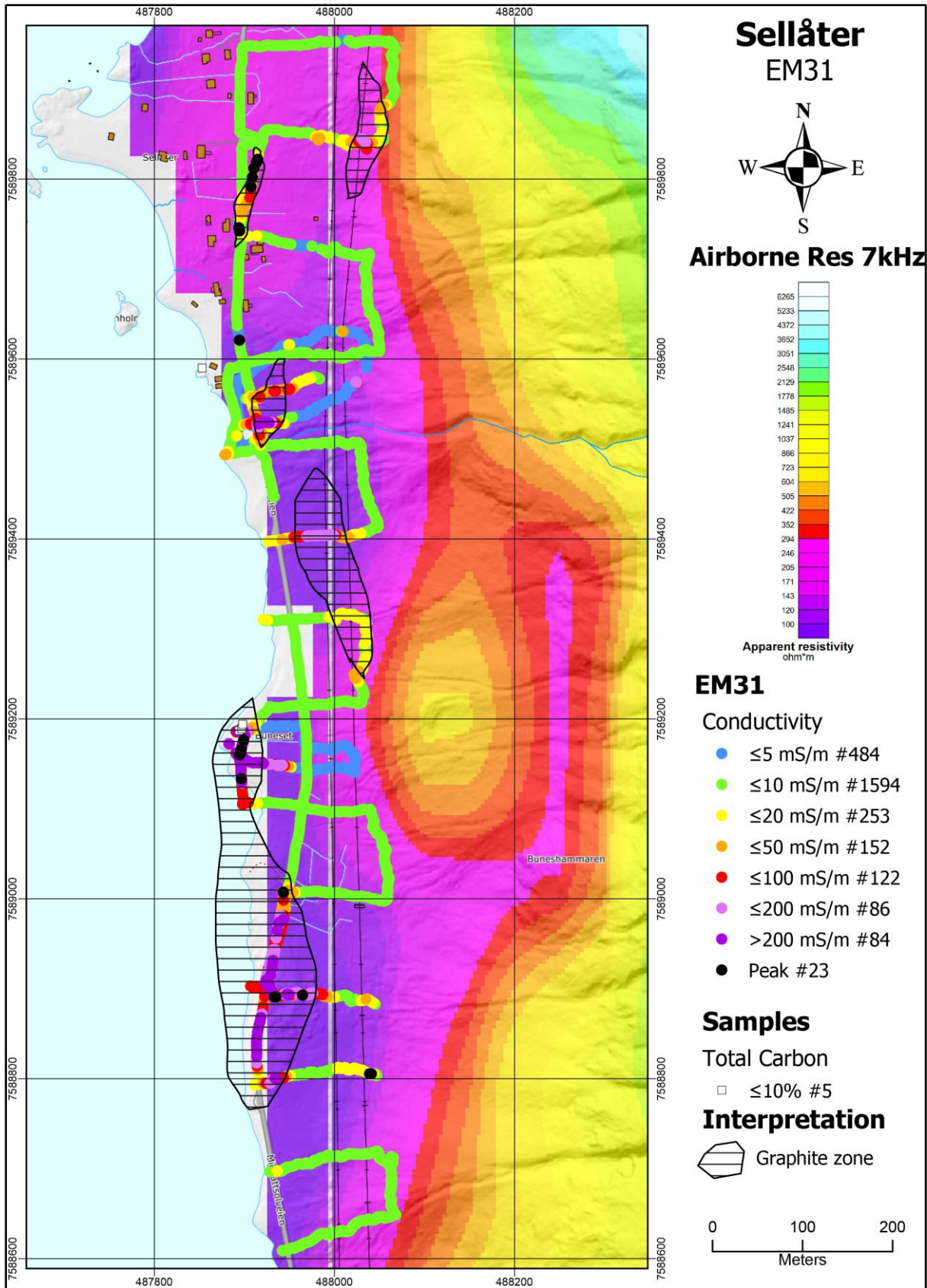


Figure 9.7: The Sellåter area. Interpreted graphite structures based on EM31 data, helicopter-borne EM anomalies and exposures of graphite. The location of graphite samples and their Total Carbon content is given as white squares.

9.3 Sommarhus

At Sommarhus on the western side of Morfjorden, low resistivity was detected at the helicopter-borne EM data in a length of ca. 1 km in E-W direction. This anomaly covers the entire 500 m long peninsula entering the fjord and can here be an effect of the seawater. However, the anomaly lies in the continuation of the abandoned Morfjord graphite mine, and reconnaissance geological work discovered in 2017 graphite mineralisation at two locations as well as an old exploration trench. Sampling and analyses of seven samples show an average TC content of 24.1 % with a maximum value 37.7 % (Table 9.4). To map the graphite mineralisation, some EM31 profiling, one ERT/IP profile and two short core drillings were undertaken in 2018. Except for three heaps of outcropping graphite-bearing bedrock, the area is soil covered (Figure 9.7).



Figure 9.7: The Sommarhus area is 100 % soil covered except for some small heaps where graphite is exposed.

9.3.1 Geophysical work, EM31

EM31 measurements (Figure 9.8) show a ca. 100 m x 100 m area where apparent electric conductivity is > 100 mS/m and partly > 200 mS/m. Within this area, graphite exposures are found in small heaps (see Figure 9.7), and TC is quite high (maximum value 37.7 %, Figure 9.9). Outside this area, the apparent conductivity is also anomalous (20 – 50 mS/m) and graphite may be present also at a depth of more than ca. 10 m.

On the eastern part of the peninsula, apparent resistivity from helicopter-borne EM is anomalous low (< 100 Ω m) and the apparent conductivity from EM31 measurements

is also anomalous (between 20 and 50 mS/m). This can be an indication of graphite at depth (> 10m?) also in this area, but these anomalies can also be caused by seawater either directly or intruded in sediments.

An interpretation of potential graphite distribution is shown in Figure 9.13.

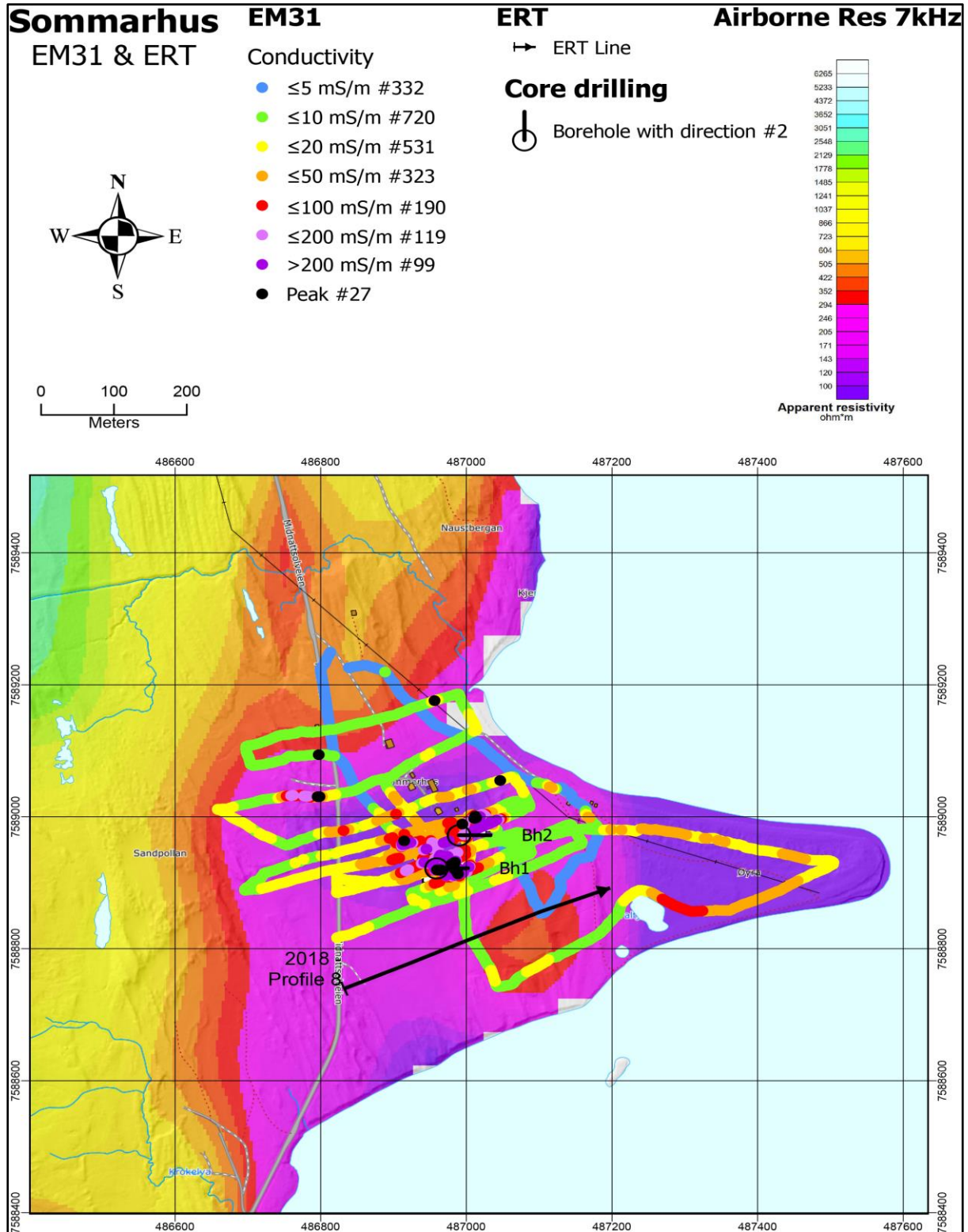


Figure 9.8: The Sommarhus area. The results from the EM31 measurements superposed on apparent resistivity (EM 7 kHz coaxial coil configuration, Rodionov et al. 2013b).

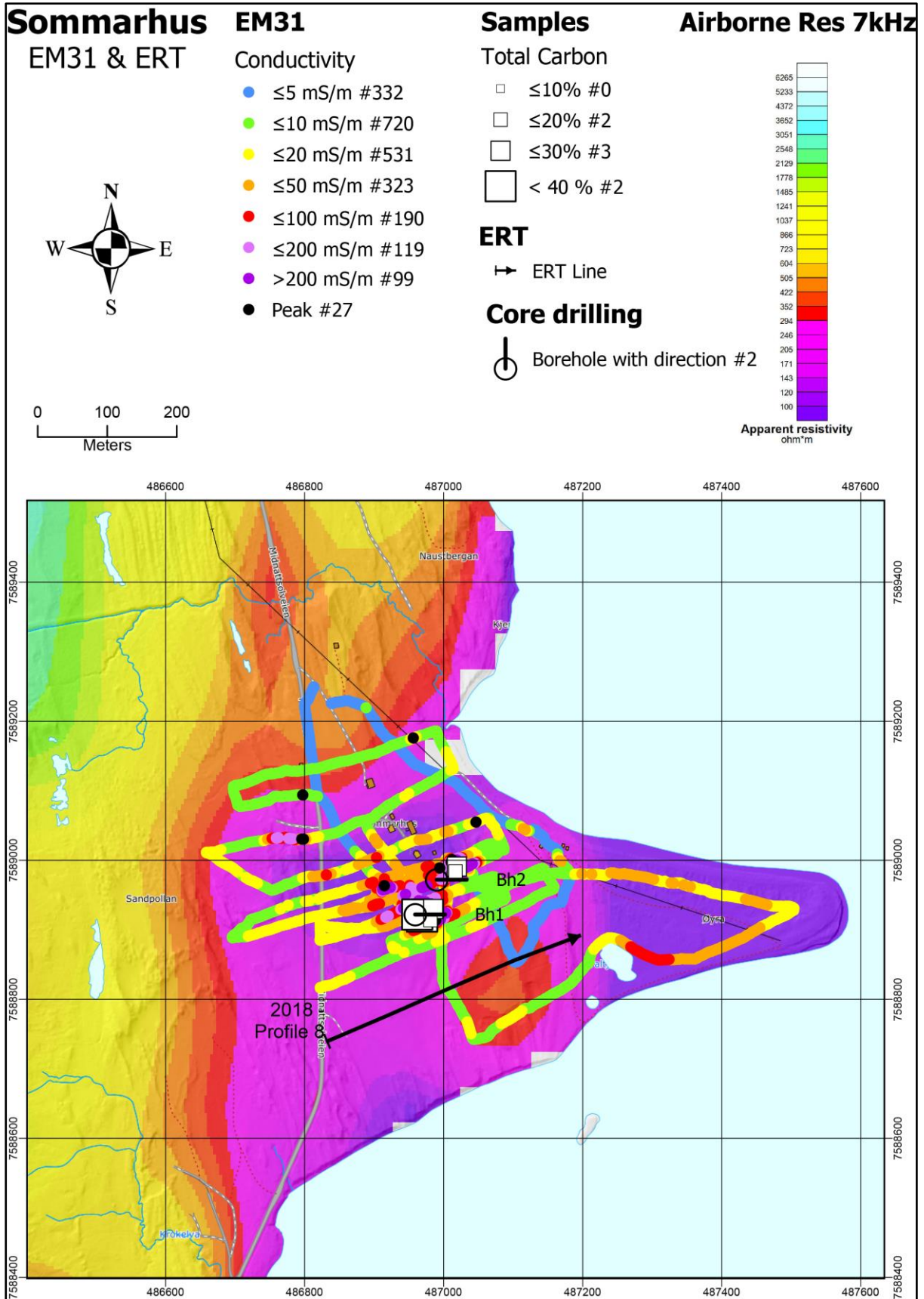


Figure 9.9: The Sommarhus area. The results from the EM31 measurements superposed on apparent resistivity (EM 7 kHz coaxial coil configuration, Rodionov et al. 2013b). The location of graphite samples and their Total Carbon content is given as white squares.

9.3.2 Geophysical work, ERT/IP

Apparent conductivity from EM31 measurements drop rapidly outside the graphite bearing exposures. To see if this is an effect of limited size of the graphite or increased soil thickness, one ERT/IP profile were measured.

Location of the ERT/IP profile at Sommarhus area is shown in Figures 9.8 and 9.9. Results of the combined 2D resistivity and Induced Polarisation measurement are shown in Figure 9.10. Electrode spacing was 5 m and the other acquisition and inversion parameters as described in chapter 4.1.4. The quality of the inverted resistivity and IP sections is very good (see Table 9.3).

Table 9.3: Quality of 2D resistivity and IP data at Sommarhus. Number of measured, removed and remaining data points for inversion, and observed “Absolute error” from the inversion of resistivity and IP data.

Profile name	Location	Measured data points	Removed data points	Inverted points	Abs. error ERT (%)	Abs. error IP (%)
2018-8	Sommarhus	1168	9	1159	3.3	3.5

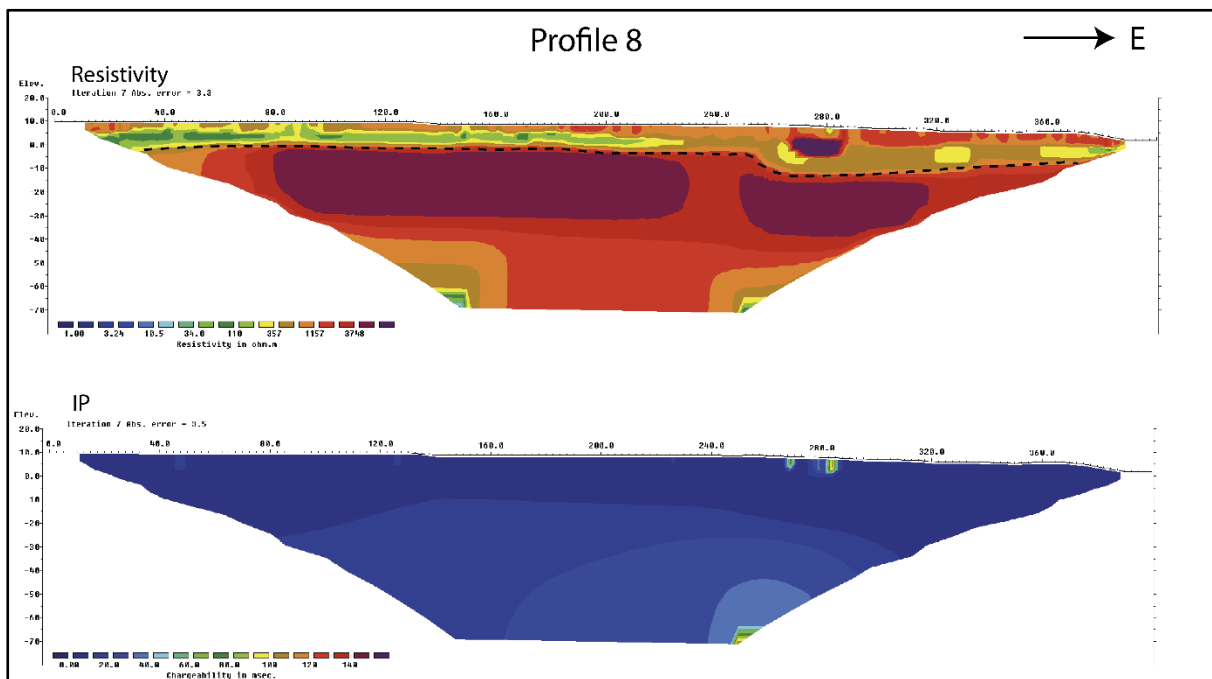


Figure 9.10: The Sommarhus area. The results of the 2D Resistivity and Induced Polarisation measurements along profile 2018-7. The interpreted soil-bedrock interface as dotted black line.

The ERT data from Sommarhus (upper part of Figure 9.10) indicate a soil cover level with thickness of ca. 10 m increasing to ca. 15 m towards the east. The soil cover consists of two layers, one quite dry upper layer with resistivities > 350 Ωm (brown and partly red colour) and a layer underneath that can be water-saturated (resistivity from 20 Ωm to ca. 500 Ωm). Bedrock underneath the soil cover shows mostly a resistivity level > 1000 Ωm, and no IP effect (lower part of Figure 9.10). The profile

does not display a resistivity and IP effect combination that is caused by any graphite mineralisation south of the exposed graphite. Any continuation towards the abandoned Morfjord mine must be at a depth deeper than ca. 80 m which is less likely.

9.3.3 Geological work, sampling

No geological work is reported at the Sommarhus area before 2017. Some EM31 profiling in 2017 discovered two graphite exposures which were sampled (Rønning et al. 2018). Location of the sampling is shown in Figure 9.9. Total carbon content is reported in Table 9.4. Seven samples show an average TC content of 24.1 % with a maximum value of 37.7 %. The total sulphur content is less than 1 % (Appendix 6).

Table 9.4: Total Carbon (TC) data from 7 surface samples from the Sommarhus area.

Morfjorden	N	Average TC (%)	Max TC (%)	Min TC (%)	St. Dev TV (%)	Median TC (%)
Sommarhus	7	24.1	37.7	11.3	9.8	24.7

The graphite schist is coarse grained and rich in flaky graphite. However, we observe a large variation in the graphite content both on outcrop scale and in thin sections.

9.3.4 Geological work, core drilling

At Sommarhus, shallow core drilling was carried out at two sites. The locations of the drill-holes are shown in Figures 9.8 and Figure 9.9 and technical data for these is given in Table 9.5. The electrical conductivity was not logged in these drill-holes due to bad rock quality. In both drill-holes, the water pressure got lost and drilling had to be stopped. Results from core analyses are given in Figures 9.11 and 9.12. Detailed geological logs are presented in Appendix 1. Pictures of the cores are shown in Appendix 2 and analytical data (Leco analysis of total carbon and total sulphur) are presented in Appendix 3. In Appendix 4, XRF analysis of the drill-cores are presented.

Table 9.5: Technical data, core drilling at Sommarhus. Coordinates in WGS 84 UTM WGS84 Zone 33.

Area	Drill-hole	UTM E	UTM N	Direction (°)	Dip (°)	Length (m)
Sommarhus	Dh1-2018	486959	7588922	090	45	39.2
Sommarhus	Dh2-2018	486990	7588972	090	45	25.4

Drill-hole 1 at Sommarhus starts with an almost 6 m thick and compact graphite schist, where the TC content in average over two-meter samples are 11.4, 20.8 and 17.6 % (see Appendix 3). The TS content is ca. 4 %. Further downhole, the bedrock shows a gradual transition into biotite and feldspar rich gneiss with a low content of graphite. From 22 m and down to 28 m, a new horizon appears where TC content is from 7.0 to 8.9 % and where the TS content is lower (0.9 to 2.9 %, see Appendix 3). The rocks are intruded by different monzonitic bodies. The combination of increased Fe, Ni and S content indicate pyrrhotite mineralisation.

Drill-hole 2 at Sommarhus shows a ca. 2.2 m thick massive graphite schist from about 4.6 to 6.8 meters where TC reaches levels of about 18 %. Both above and underneath this unit, the rock is intruded by a white medium-grained meta-granodiorite with some scattered graphite veins.

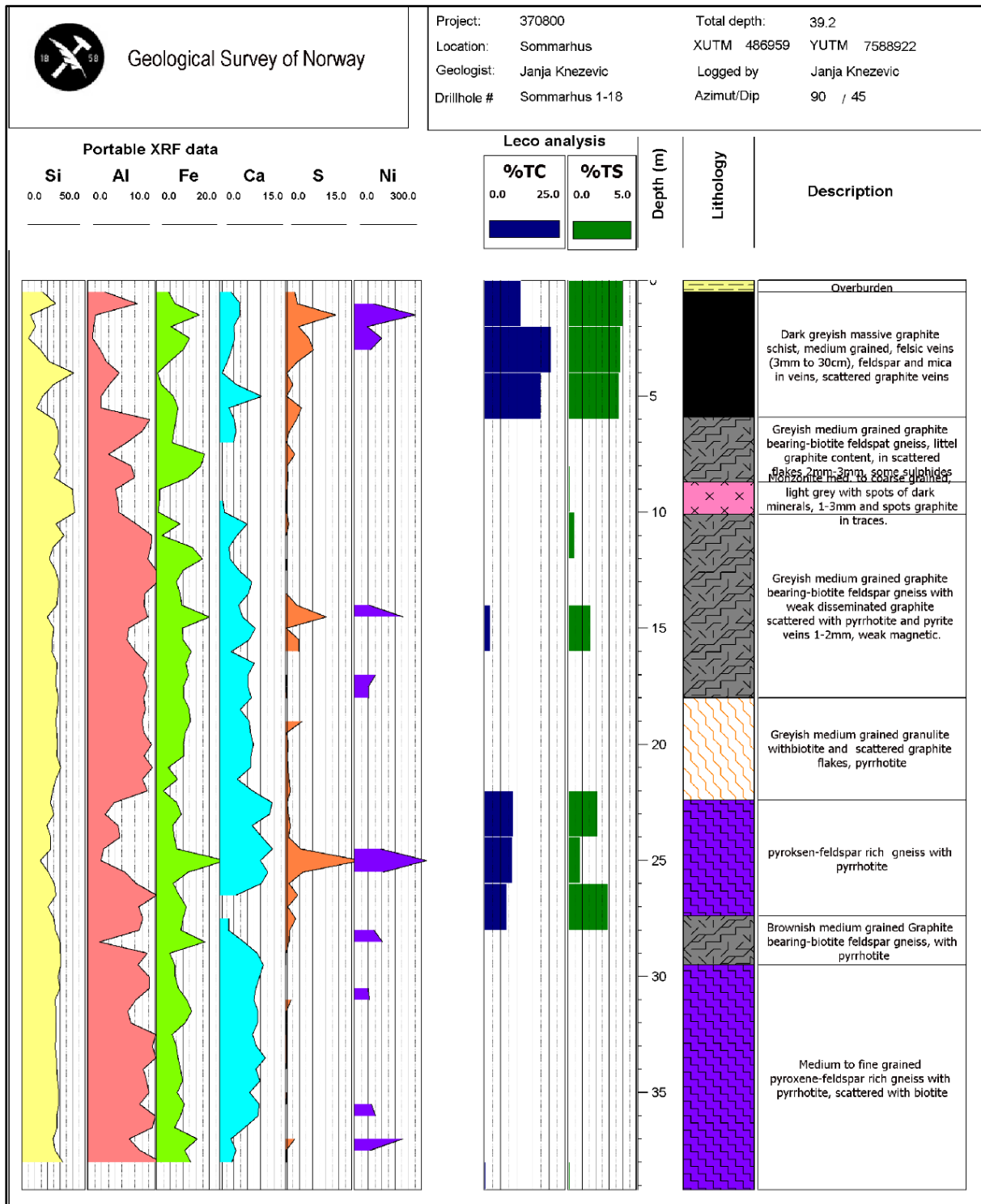


Figure 9.11: Results from the Sommarhus drill-hole Dh1-2018: Portable XRF analyses (Si, Al, Fe, Ca, and S in %, Ni in ppm) at the cores, selected Leco analyses of Total Carbon (TC) and Total Sulphides (TS), lithological log and core description.

The distance between these two drill-holes is only ca. 60 m, despite which there is a remarkable change in the bedrock geology. There is a probability that the outcrops at Sommarhus are the surface exposure of large (house-sized) boulders that are presently in situ which explains the difference in drill-hole geology.

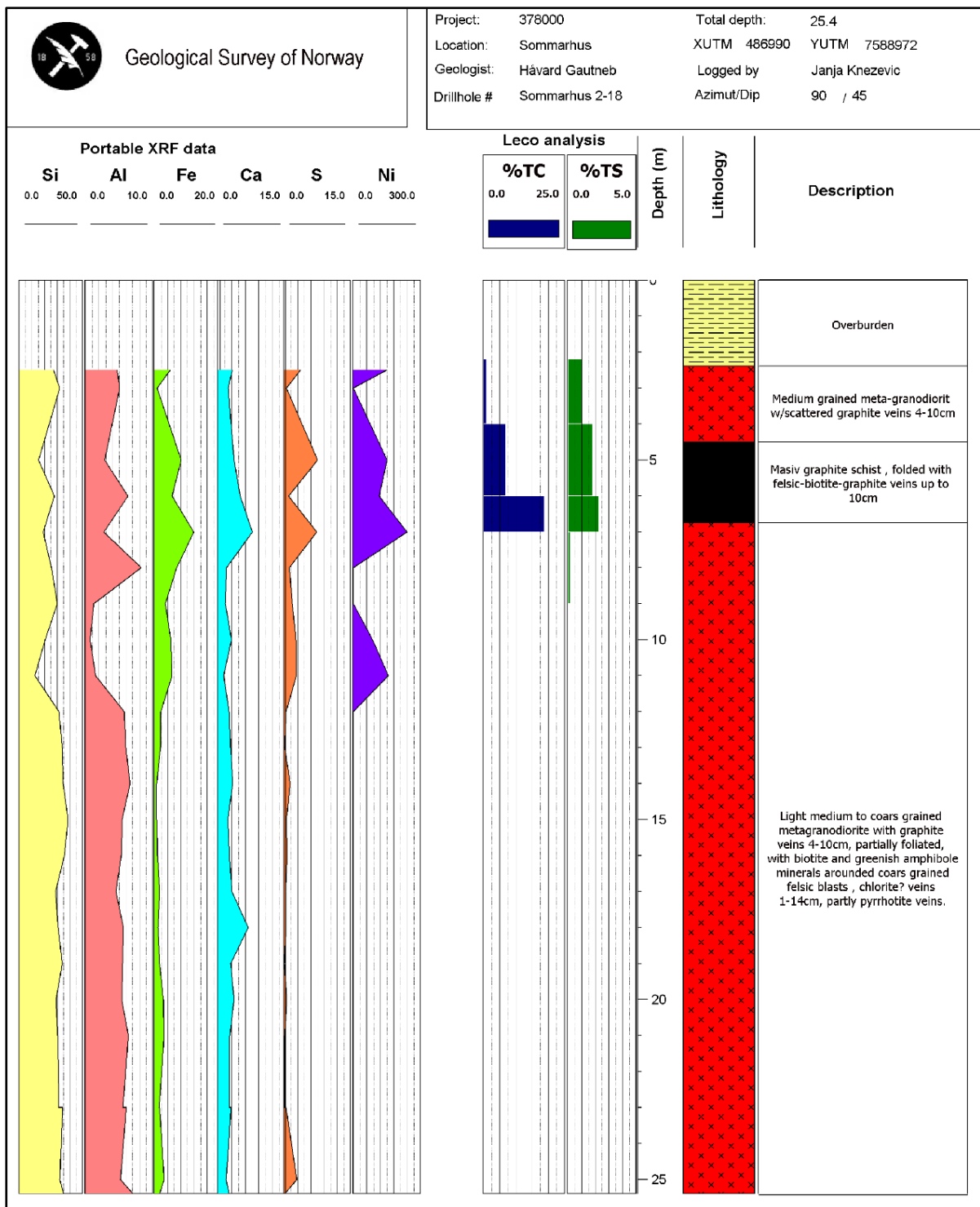


Figure 9.12: Results from the Sommarhus drill-hole Dh2-2018: Portable XRF analyses (Si, Al, Fe, Ca, and S in %, Ni in ppm) at the cores, selected Leco analyses of Total Carbon (TC) and Total Sulphides (TS), lithological log and core description.

9.3.5 Summary Sommarhus

Helicopter-borne geophysical measurements showed a ca. 1 km long E-W trending EM anomaly at Sommarhus. This anomaly followed a ca. 500 m long peninsula in the fjord and could be an effect of highly conducting seawater. However, some EM31 profiling in 2017 discovered two graphite occurrences which proved to be quite rich in graphite (maximum 37.7 %). The area Sommarhus lies in the strike direction of the abandoned Morfjord graphite mine and further investigations was necessary to see the extent of this mineralisation.

Detailed EM31 measurements in 2018 restricted the extend of the Sommarhus occurrence to about 100 m x 100 m with a potential increase underneath a soil cover towards the NW. No connection to the abandoned Morfjord graphite mine was discovered. A combined ERT/IP profile showed that if there is a connection, this must be at a depth deeper than ca. 80 m. Two core drillings towards the two graphite exposures showed quite rich graphite mineralisation (20.8 % and 18 % TC respectively) but the thickness of the structures was less than 6 m.

The graphite occurrence at Sommarhus is situated along strike from the Morfjord mine and is most likely a part of the same zone. However, the highly conductive sea water masks the effect of graphite underneath the seawater. It was suggested that the Sellåter occurrence, at the other side of the fjord, is also connected to Sommarhus under the fjord (Rønning et al. 2018). The graphite occurrences in the Morfjord mine, Sommarhus and Sellåter can be a part of the same mineralised zone where the majority of the deposit is now under sea level. It is also possible that this could have been a continuous mineralisation which is now weathered and has been eroded. On the other hand, the drill-hole logs from the two drill holes at Sommarhus, even though they are quite near each other, shows quite different geology. There is a probability the small outcrops at Sommarhus are the surface exposure of some large (house-size) boulders that are not presently in situ which explains the difference in drill hole geology.

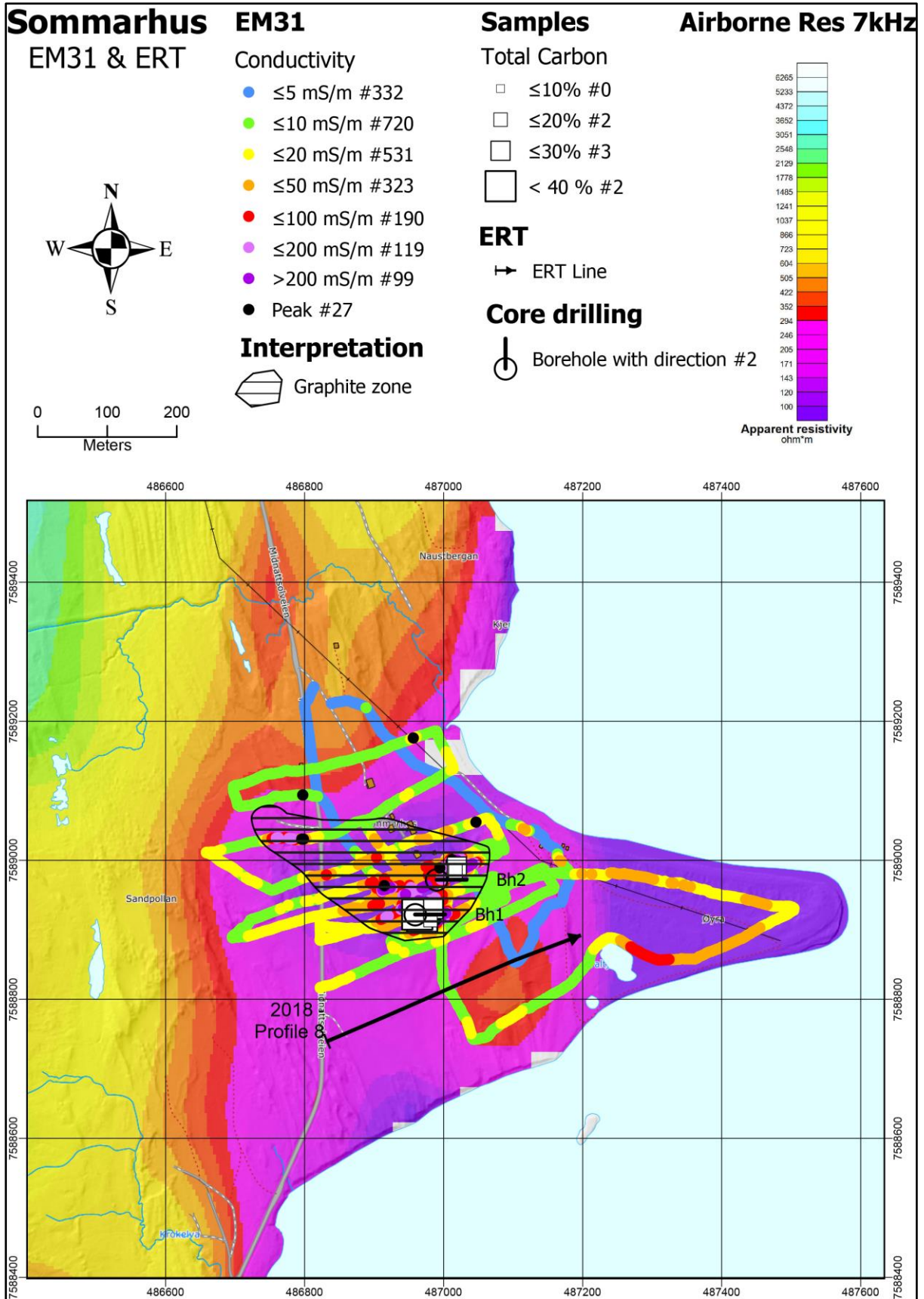


Figure 9.13: Sommarhus. An interpreted maximum extension of graphite based on helicopter-borne EM and ground EM31 data. Both methods indicate good conducting material at the eastern peak of the Øyra peninsula. It is unclear whether this is caused by graphite or salt seawater in sediments.

10. SUMMARY OF GRAPHITE QUALITY AND QUANTITY

In this chapter, the quality (graphite petrography, grain size, total carbon content) and quantity (the total potential volume and tonnage) of the graphite occurrences in Vesterålen are summarised.

10.1 Petrography of the graphite schist and associated rocks

In this chapter we will describe some general features regarding the mineralogy and textures of the graphite-bearing rocks. The compositions of the graphite-bearing rocks at all the localities are approximately similar and Gautneb et al. (2017) gave a brief review of the petrography and mineralogy of the graphite schists using Rødhamran as an example. In this study the understanding of the mineralogy, its variations and its complexity have been improved as a result of drilling at Sommarland and Haugsnes (Rønning et al. 2018), as well as at Sommarhus, Vikeid and Myre (this report). In this section descriptions are constrained to the petrography and mineralogy of the graphite-bearing units, based on selected thin sections. A collection of thin sections is available for examination, on request, by a visit to NGU. Chapter 10.1 is essentially similar to what is reported by Rønning et al. (2018) but is repeated here for completeness.

10.1.1 Examples of thin sections

The graphitic schists usually have a granoblastic texture, frequently with structures displaying ductile deformation. The silicate minerals are dominantly quartz, feldspar and pyroxene with variable amounts of mica, ortho- and clino-pyroxene, and in some cases also clinozoisite (Figure 10.1). If present, mylonitic fabric can be contorted and folded. Recrystallisation is generally pervasive, and potential primary layering is obscured. Figures 10.2 to 10.6 show features typical for the graphitic schists.

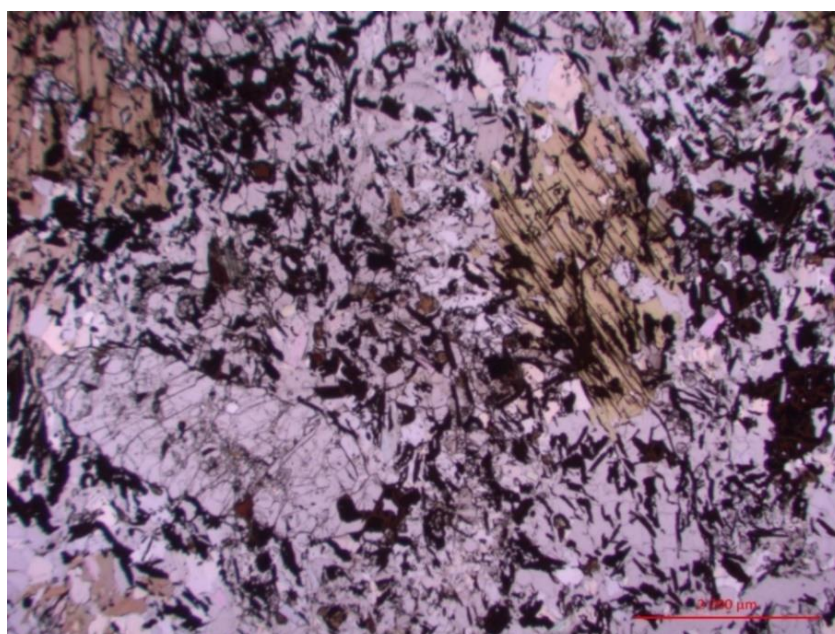


Figure 10.1: Thin section of graphitic schist with a large crystal of clinozoisite in the lower left corner (Hg11-17, From Morfjord, TC = 5.38%).



Figure 10.2: Graphite observed in reflected light, displaying variations in the distribution and grain size of the graphite flakes (thin section JK-2617-1, Sommarhus. TC = 24,7 %).

Figure 10.3 shows graphite flakes that are approximately 3 to 4 mm large, and in rare cases even larger. Graphite crystals occur unevenly distributed in the rock, and there is a large variation both in the grain size and the content of graphite within a small area, in particular at the scale of a thin section. This heterogeneity on microscale is repeated in hand specimen and on outcrop scale and is observed at all graphite localities which are investigated.

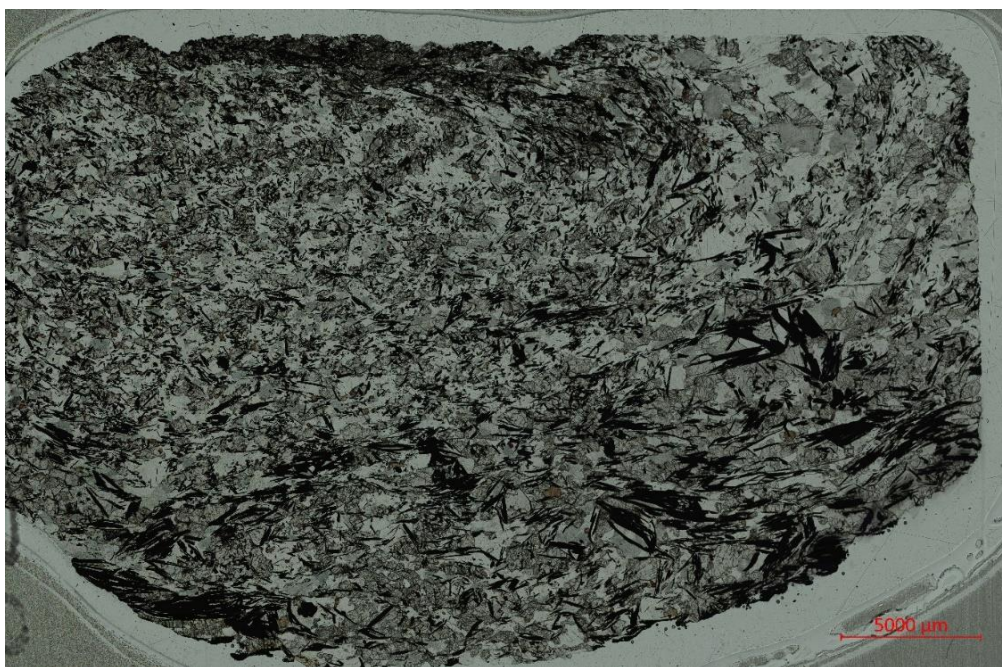


Figure 10.3: Thin section of graphite-bearing rock showing large variations in both grain size and amount of graphite crystals over short distances (thin section JK6617-2, the modal content of graphite is 24.7 vol %).

We also see this type of heterogeneity where we have continuous sections in drill cores, and Rønning et al. (2018) report a number of examples. Often, but not always, the graphite schist is schistose with a well-developed foliation, both at macro- and micro-scales (Figure 10.4).

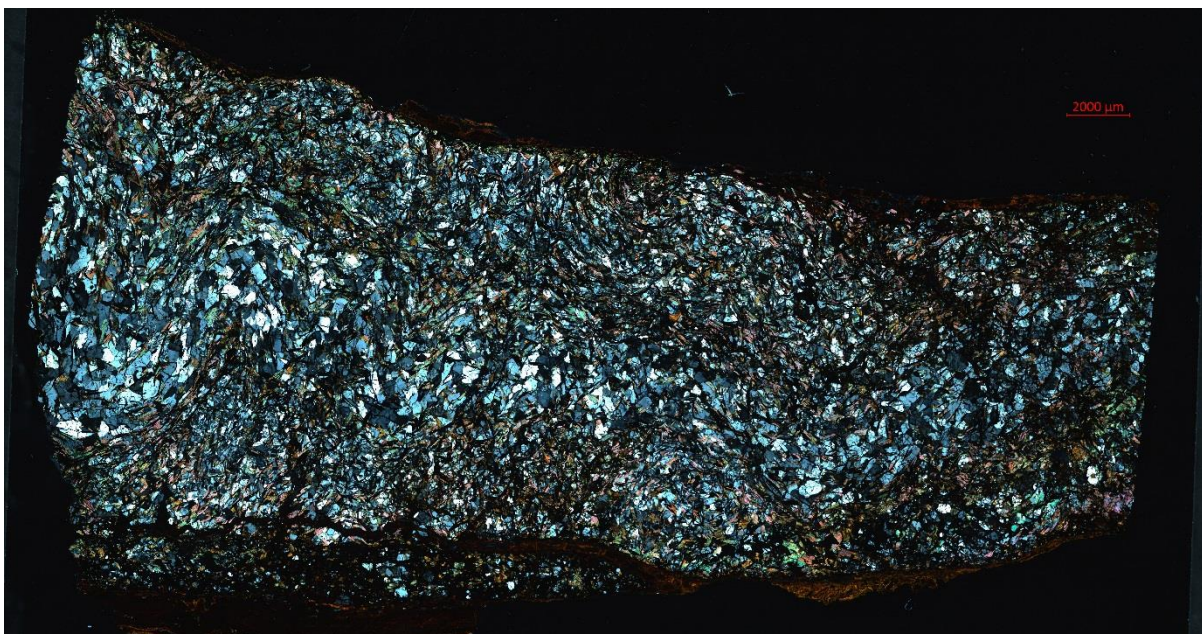
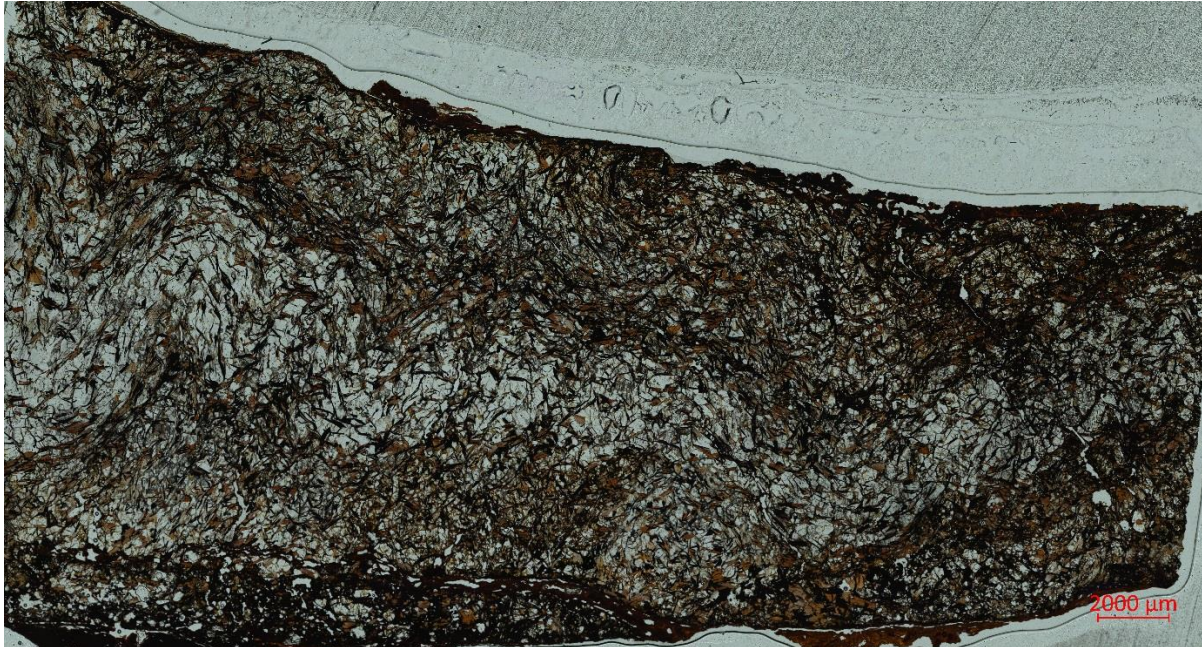


Figure 10.4: Thin section showing a foliated and folded graphitic schist. Transmitted light upper and polarised light lower (thin section JK291517-9).

In some samples (for instance the drill cores at Haugsnes (Rønning et al. 2018)) the graphitic schists can be rich in pyrrhotite. Pyrrhotite is a very ductile mineral which commonly deforms more easily than the surrounding silicate minerals. The result is a rock with a breccia type of texture (Figure 10.5) in which fragments of silicates, often with crystals of graphite, “float” in a matrix of pyrrhotite. This schist texture varies greatly with the relative proportions of sulphides and silicates, combined with the degree of deformation.

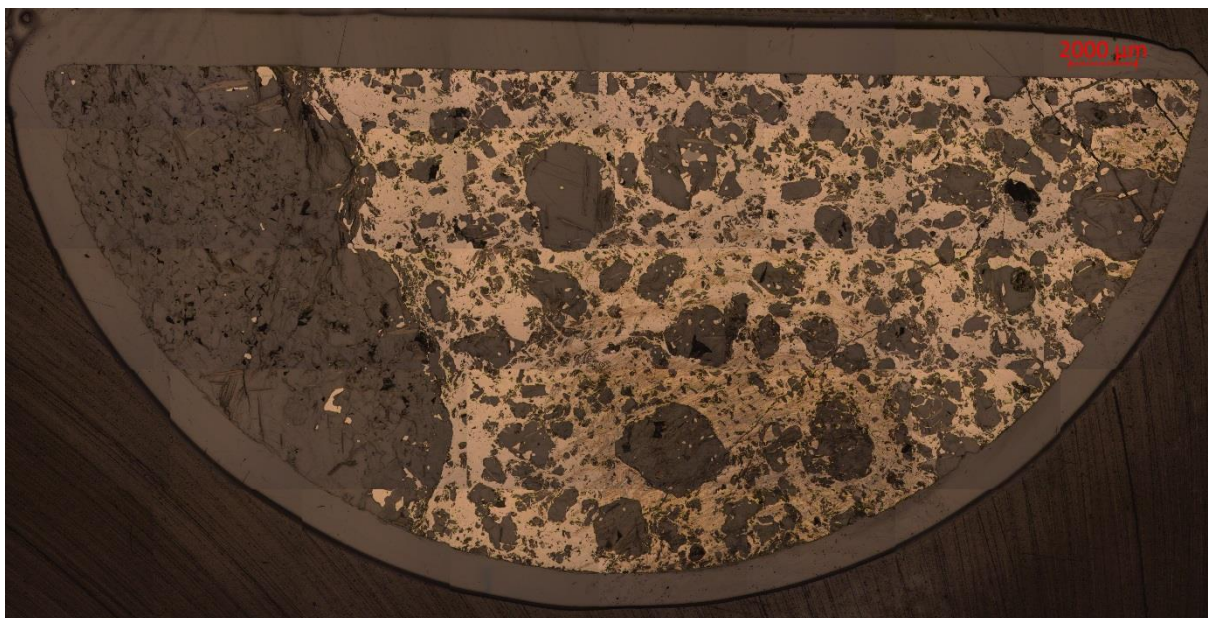
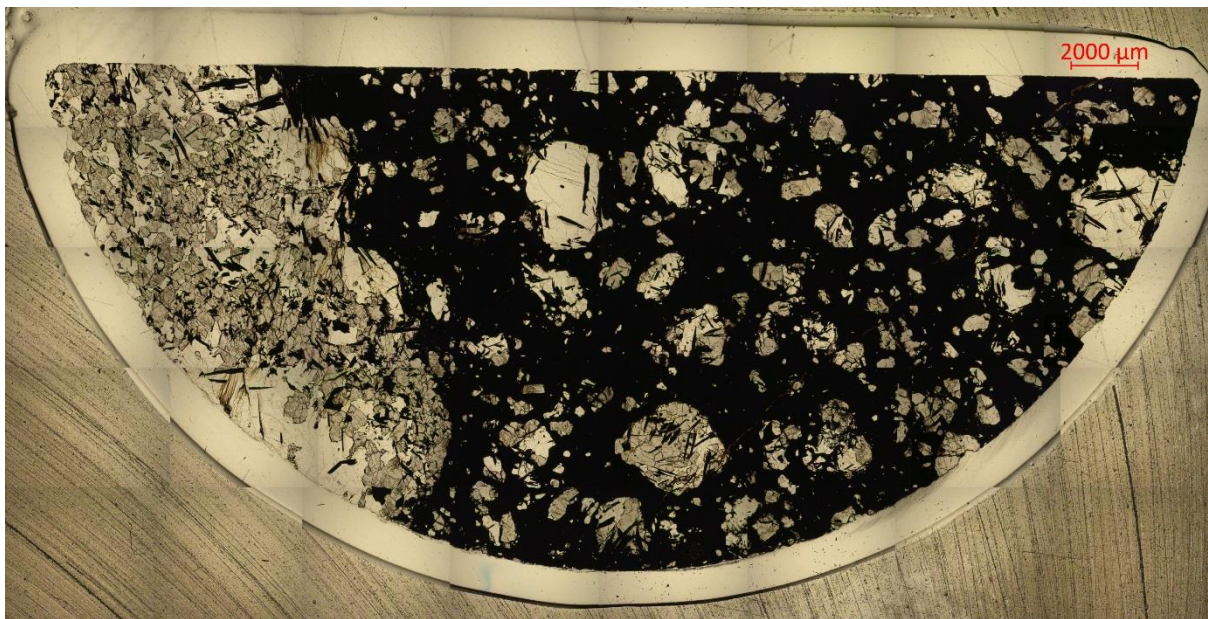


Figure 10.5: Thin section from half of a drill core, showing brecciation of the rock in areas with a high content of pyrrhotite combined with strong deformation. Transmitted light upper and reflected light lower (thin section HG-DhHau1701-6.5).

Typically, the host rock comprises rocks with variable content of feldspars, pyroxene and often with abandoned biotite (Figure 10.6).

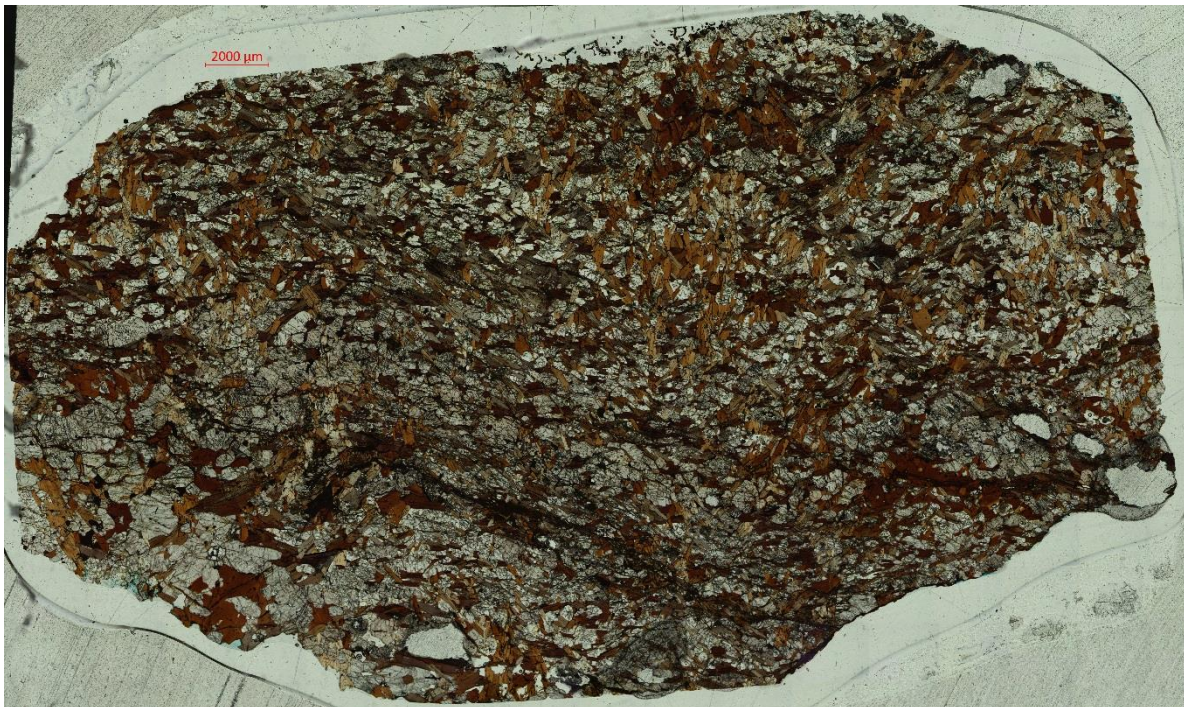


Figure 10.6: Biotite gneiss with graphite in traces, thin section JK-29517-pf7

10.1.2 Particle analysis of graphite crystals

Image processing of selected thin sections was performed in order to get an impression of flake graphite grain sizes. We selected a thin section from a sample with one of the highest contents of total carbon. An image of the measured thin section (HG-Dh Som1702 15.22) is shown in Figure 6.15 in Rønning et al. (2018). The method for particle analysis in thin section is described in chapter 4.2.2

Results

The grain size distribution presented in Figure 10.7 shows a very skewed distribution but also features that are very characteristic for the graphite schist in this area (and in general). Most of the graphite crystals have a grain size of approximately 0.2 to 0.3 mm. Above 0.8 mm the rock consists of a number of large, individual graphite crystals up to a maximum grain size of about 3.2 mm. These large grains represent aggregates of graphite crystals. They also make up the bulk of the areal percentage of graphite. The total areal percentage is 29.0 %. The thin section is from 15.22 metres in the drill core Som1702 (Rønning et al. 2018). The interval from 14-16 metres in this drill core shows an average TC content of 17.2 wt. %. Area (volume) percentage as measured by image processing from a thin section and weight percentage from a bulk rock analysis, are not directly comparable. Theoretically for graphite:

$$\text{Volume \%} = \text{Weight \%} \times 1.7 \quad (\text{Hutchison 1975}).$$

The average TC content of 17.2 % multiplied by 1.7 gives 29.3 %. This is almost equal to the measured areal percentage of 29.0 %. This result is probably coincidental.

These results are considered accurate within the limits and errors given above. However, if a practically usable understanding of the graphite flake size distribution is needed, a mineral liberation study (MLA) should be performed. Here the grain size variation of the graphite flakes is studied after crushing and flotation.

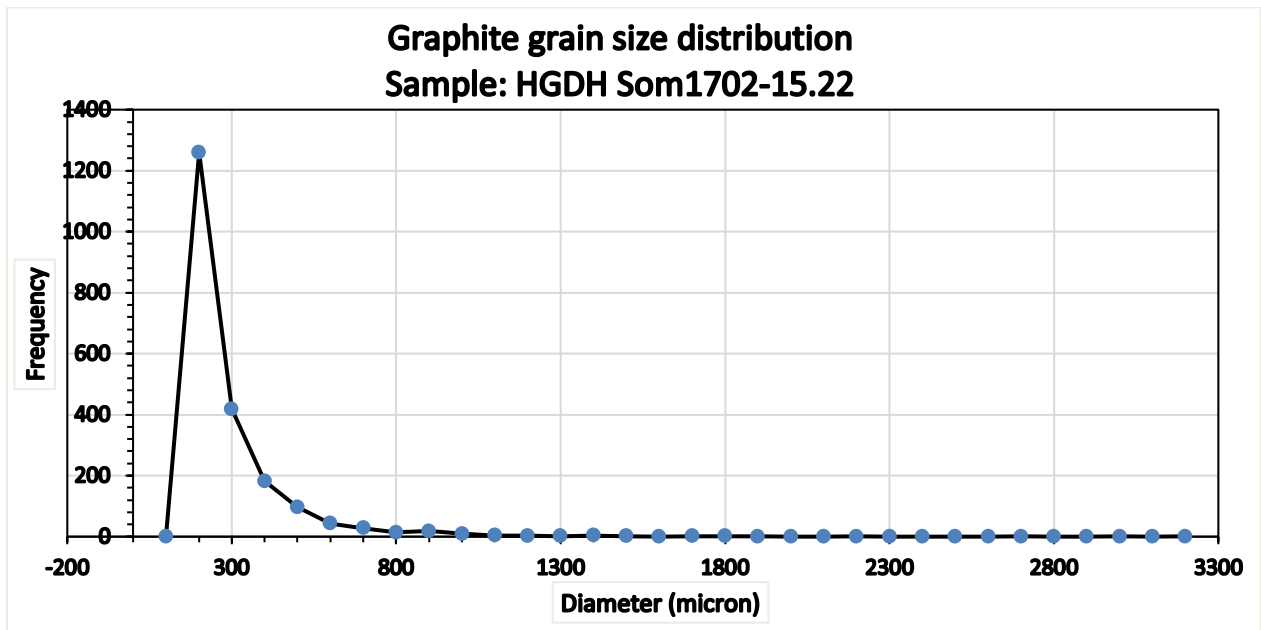


Figure 10.7: The grain-size distribution of graphite crystals in sample HG-DhSom1702 15.22. 1000 microns equals 1 mm.

10.2 Summary of Carbon analyses, updated table

In this chapter an overview of available analyses of total carbon (TC) from all the occurrences investigated between 1990 and 2019 is presented (Table 10.1). Samples from the drill cores are not included. They are discussed in Chapters 6.3 and 7.2 in Rønning et al. (2018) and chapters 7.6.6, 8.4.3 and 9.3.4 in this report. The analyses are grouped into areas and localities. Individual areas usually contain several localities, that can be individual sample localities along strike of a larger body or as several unrelated sampling points in a restricted geographical area. Since our database also includes country rock, we have set a cut-off to 0.5 % TC.

To make this dataset complete, samples from investigations in the 1990-ties are also included, mostly from the Jennestad area. References to these investigations are given in Chapter 3.

As described in Chapter 2, the graphite exploration has been coordinated with geological mapping of the same area. Many of the graphite localities have therefore been found and sampled during bedrock mapping, and later investigated using geophysical methods. However, in some areas no geophysical follow-up work has been conducted, either as a matter of priority or because of little or no anomaly from helicopter-borne measurements. Examples of such localities are: Dvergberg–Skogvoll, Ingelsfjorden, Møysalen and Sørfjorden. The location and total carbon content of samples from these areas, are listed in Appendix 6. A summary of the variation in total carbon content is included in Table 10.1.

In total, 408 samples have been documented for the whole Vesterålen province with a grand total average of 15.5 % and a median of 12.6 % TC. However, there is a large variation in TC from 44.3 % to 0.51 %. The numbers of samples at the different localities are variable, mainly related to the degree of exposure. Persons interested in these data are recommended to request the latest updates from NGU.

Table 10.1: Table showing the variation in total carbon (TC) content at the investigated areas and localities. Data are from 1990 to 2019.

Area Locality	N	Average TC (%)	Max TC (%)	Min TC (%)	St. Dev. TC (%)	Median TC (%)
Alsvåg						
Alsvåg	5	8.9	19.8	1.4	8.4	4.1
Instøya	28	9.3	23.1	1.3	5.7	9.1
Straumen	5	11.7	27.0	0.7	12.0	5.7
Alsvåg Total	38	9.6	27.0	0.7	6.9	9.0
Ånstad						
Ånstad	5	36.8	40.6	31.6	3.6	37.6
Ånstad Total	5	36.8	40.6	31.6	3.6	37.6
Brenna						
Grønorda	7	10.1	30.4	2.4	9.5	8.6
Brenna Total	7	10.1	30.4	2.4	9.5	8.6
Dverberg - Skogvoll						
Haugneset, Saura	1	2.7	2.3	2.3		2.3
Sauradalen	1	14.1	14.1	14.1		14.1
Dverberg - Skogvoll Total	2	8.2	14.1	2.3	8.4	8.2
Evassåsen						
Evassåsen	6	7.6	18.7	1.4	7.0	5.5
Evassåsen Total	6	7.6	18.7	1.4	67.0	5.5
Ingelsfjorden						
Storå	1	10.5	10.5	10.5		10.5
Ingelsfjorden Total	1	10.5	10.5	10.5		10.5
Jennestad						
Golia	8	17.6	32.8	5.7	11.2	14.3
Græva	20	31.4	40.3	1.3	10.4	35.1
Hornvatnet	66	22.7	44.3	1.7	12.3	20.9
Jennestad, shore	5	7.6	15.2	1.2	5.6	7.2
Koven	11	14.9	26.1	0.9	8.6	13.3
Larmarkvatnet	5	9.7	12.7	3.2	4.1	12.2
Lille Hornvatnet	40	13.7	33.1	4.7	6.6	12.1
Jennestad Total	155	19.8	44.3	0.9	11.9	15.9
Kvernfjorden - Haugsnes						
Haugneset	11	19.3	33.8	10.6	9.4	14.7
Kvernfjorddalen	5	9.2	14.2	2.3	5.5	11.7
Kvernfjorden - Haugsnes Total	16	16.2	33.8	2.3	9.5	14.0
Møkland - Sund						
Bjørndalen	10	17.9	32.0	5.9	7.1	16.8
Høgdene	4	16.1	18.3	13.4	2.5	16.4
Skatskaran	17	9.8	22.3	1.1	6.5	8.0
Møkland - Sund Total	31	13.2	32.0	1.1	7.3	14.0

Area Locality	N	Average TC (%)	Max TC (%)	Min TC (%)	St. Dev. TC (%)	Median TC (%)
Morfjorden						
Morfjorden mine	5	13.7	19.7	3.3	7.0	16.8
Sellåter	9	6.2	7.9	3.7	1.3	5.8
Sommarhus	7	24.1	37.7	11.3	9.8	24.7
Morfjorden Total	21	13.9	37.7	3.3	10.1	9.7
Møysalen						
Vestpolltinden	1	27.1	27.1	27.1		27.1
Møysalen Total	1	27.1	27.1	27.1		27.1
Myre						
Myre, harbour	3	1.5	2.4	0.5	0.9	1.7
Rødhamran	14	14.8	25.9	6.7	6.5	12.0
Stavdalen	5	1.5	2.4	0.6	0.7	1.5
Myre Total	22	10.0	25.9	0.5	8.3	9.4
Rise - Kjerkhaugen						
Kjerkhaugen	2	6.5	10.0	2.9	5.0	6.5
Rise	2	7.9	11.1	4.7	4.5	7.9
Rise - Kjerkhaugen Total	4	7.2	11.1	2.9	4.0	7.4
Romsetfjorden						
Langstrand	8	13.8	25.6	3.6	7.1	14.0
Romset	5	14.7	31.0	3.9	10.1	14.2
Sæterbukta	2	10.7	20.9	0.5	14.4	10.7
Romsetfjorden Total	15	13.7	31.0	0.5	8.4	14.2
Sæterstranda						
Sæterstranda	3	16.9	20.8	12.2	4.4	17.7
Sæterstranda Total	3	16.9	20.8	12.2	4.4	17.7
Skogsøya						
Skavlheset	21	20.0	38.4	0.6	13.3	24.5
Svinøya	3	11.7	12.5	11.0	0.8	11.6
Skogsøya Total	24	19.0	38.4	0.6	12.7	20.4
Smines						
Kaldhammaren	14	9.6	17.3	1.5	5.3	10.4
Rota	5	2.8	8.6	0.6	3.3	1.7
Smines	3	10.5	14.4	3.9	5.7	13.2
Stabben	1	16.7	16.7	16.7		16.7
Stigbergan	1	0.6	0.6	0.6		0.6
Smines Total	24	8.2	17.3	0.6	5.9	9.1
Sommarland						
Sommarland	15	12.5	18.2	2.8	5.2	14.6
Sommarland Total	15	12.5	18.2	2.8	5.2	14.6
Sørfjorden						
Sørfjorden	1	29.4	29.4	29.4		29.4
Sørfjorden Total	1	29.4	29.4	29.4		29.4

Area Locality	N	Average TC (%)	Max TC (%)	Min TC (%)	St. Dev. TC (%)	Median TC (%)
Vikeidet						
Vedåsen (Vikeid Central)	6	13.8	24.3	1.4	8.4	13.1
Vikeidet (Vikeid West)	11	11.3	16.7	4.9	3.8	12.1
Vikeidet Total	17	12.2	24.3	1.4	5.7	12.1
Grand Total	408	15.5	44.3	0.5	10.9	12.9

10.3 Summary of geometric information

For some selected localities, a reasonable understanding of the number of graphite-bearing zones and their total strike length has been established from EM31 data. Where these data are missing, strike length is estimated from helicopter-borne EM data (apparent resistivity images, Rodionov et al. 2013a).

Knowledge of the graphite zone width is established from EM31 profiles, trenching or core drilling (two localities in 2017 and two in 2018). In some cases, the thickness is interpreted from ERT data (see Notes in Table 10.2). An approximate average dip is obtained from bedrock mapping. In the volume estimations presented in Table 10.2, the widths are corrected for the dip variations. Assumption of a mineable depth of 100 m allows an estimation of the total volume of graphite ore at different localities using the relationship below (Table 10.2):

$$\text{Volume (m}^3\text{)} = \text{Estimated total strike length (m)} \times \text{average true width (m)} \times 100 \text{ (m)}$$

All calculations in Table 10.2 are, by their nature, uncertain. The total strike length from surface EM31 measurements may be underestimated in cases where the graphite zones are not fully mapped or are situated deeper than the penetration depth of the instrument. In these cases, the total strike length is estimated from helicopter-borne EM data. In areas where the graphite structures are discontinuous, the interpreted total length is reduced.

The depth extent of 100 m is a chosen value that represents a depth that can easily be mined. In this study it has not been possible to evaluate the depth of the individual zones in any area, except for the Vikeid West area. Therefore, an assumed depth of 100 m may be too high or too low.

Observed dip at the various locations vary from 30 to 80 degrees, with 55-60 degree being the common range. Information on the dip is lacking in a few areas.

Table 10.2: Estimations of volume of graphite-bearing rocks from investigated occurrences.

Area Locality	No. of zones	Total length (m)	Depth extent (m)	Average width (m)	Approx. average dip (°)	Estimated volume (m ³)	Comments Background data in NGU Report
Bø Municipality							
Haugsnæs	11	8900	100	4	75	3 438 696	2018.011
Høgmyran	3	1600	100	15	50	1 838 507	No samples/ 2019.031
Kjerkhaugen	2	700	100	20	45	989 949	2019.031
Møkland	6	1700	100	10	55	1 392 558	2017.014 / 2017.015
Sund	0	700	0	0	60	0	No graphite / 2019.031
Olsetvatnet	2	800	?	?	50	?	Uncertain / 2019.031
Rise	1	250	100	4	50	76 604	No geophysics/ 2019.031
Sommarland	5	1000	100	4	60	346 410	2018.011
Øyjorda	0					0	No graphite/ 2019.031
Sortland Municipality							
Brenna	5	2500	100	15	60	3 247 595	2018.011 / 2019.031
Evassåsen	2	2000	100	5	60	866 025	2019.031
Vikeid East	5	2500	100	10	55	2 047 880	No graphite 2019.031
Vikeid Central	4	2100	100	20	60	3 637 307	2019.031
Vikeid West	5	3500	100	40	60	12 124 356	2019.031
Reinsnesøya	0					0	No graphite 2019.931
Sæterstranda	1	600	100	2	40	77 135	2019.031
Ånstad	1	100	100	10	60	86 603	2019.031
Øksnes Municipality							
Alsvåg	3	600	100	2	60	103 923	
Instøya	3	3500	100	20	60	6 062 178	
Myre	1	3000	100	200	45	42 426 407	Uncertain. 2019.031
Rødhamran	4	2000	100	4	45	565 685	2018.011
Romset	2	2000	100	20	80	3 939 231	2019.031
Skogsøya	1	2000	100	3	75	579 555	2017.015
Sminess	5	2000	100	40	75	7 727 407	Uncertain / 2019.031
Steinland	1	500	?	?	30	?	No graphite observed, 2019.031
Straumen	3	200	100	2	80	39 392	
Svinøya	1	200	100	4	60	69 282	2017.015

Area Locality	No. of zones	Total length (m)	Depth extent (m)	Average width (m)	Approx. average dip (o)	Estimated volume (m ³)	Background data in NGU Report
Hadsel Municipality							
Sellåter	5	500	100	20	80	984 808	2019.031
Sommarhus	1	100	30	100	90	300 000	2019.031
Morfjord mine	4	1300	100	2	90	260 000	2018.011

Most graphite occurrences in Vesterålen are soil covered and rarely exposed in their total thickness. Trenching has indicated a good correlation between structure thickness and EM31 anomaly. In most of the areas, the thickness of the occurrences is interpreted from EM31 data. The width of the graphite structures from EM31 readings can be large, up to several tens of metres. This can give a good estimate when graphite is cropping out underneath a thin cover of soil, but quality variations within the structures may not be detected. In some areas the thickness is estimated from ERT/IP data. This may be uncertain since several vertical structures can give a false effect of continuous mineralisation (Rønning et al. 2014). The average width of the graphite zones is also established from core drilling (Sommarland, Haugsnes, Sommarhus and Vikeid). This may provide a good thickness estimate in these areas. However, the drill-holes represent only one point in an occurrence and the thickness away from the drill-hole may differ. In some areas, the width is observed in well exposed bedrock in the field and can be more realistic.

As was established from the drill cores, the quality of the graphite can vary significantly within individual zones. The volume of graphite is therefore an estimate which can be used for individual evaluation, but further investigations are needed to establish a more confident resource knowledge.

10.4 Summary of tonnage estimates

An estimate of the graphite tonnage can be made based on the estimated volume of graphite in the investigated areas (Table 10.2) and on what is known about the total carbon content (Table 10.1). In this estimation, we use a density of the graphite ore of 2.6 t/m³ which is similar to what has been used in graphite exploration in this area earlier (Sletten 2013).

The results are shown in Table 10.3. Based on the estimated tonnage, the individual occurrences are given an importance grade. Grade A is more than 1,000,000 t estimated graphite, grade B between 500,000 and 1,000,000 t, grade C between 200,000 and 500,000 t, grade D between 100,000 and 200,000 while grade E is less than 100,000 t. Areas that most likely do not contain graphite are given grade F.

NGU would like to stress that the purpose of this type of resource calculation is to compare the different graphite occurrences using a common approach. The tonnage calculations must be regarded as tentative resource estimates with a low degree of confidence (inferred resources with low level of significance).

Table 10.3: Estimation of the tonnage of graphite from investigated occurrences (using 2.6 t/m³ as density). See the text for explanation of the occurrence importance classification (Ranking).

Area Locality	Estimated volume (m ³)	Average TC content (%)	Estimated tonnage of graphite ore (t)	Estimated tonnage of graphite (10 ⁶ t)	Occurrence importance (Ranking)	Comments
Bø Municipality						
Haugsnæs	3 438 696	19,3	8 940 609	1,7	A	Many thin structures
Høgmyran	1 838 507	?	4 780 117	?	B	No graphite samples
Kjerkhaugen	989 949	6,5	2 573 869	0,17	D	Only two samples
Møklund	1 392 558	9,0	3 620 652	0,33	C	Many short structures
Sund	0		0	0	F	No graphite
Olsetvatnet	?	?		?	?	Uncertain, graphite?
Rise	76 604	7,9	199 172	0,02	E	Short structure
Sommarland	346 410	12,1	900 666	0,11	D	Many short structures
Øyjorda	0		0	0	F	No graphite
Sortland Municipality	0					
Brenna	3 247 595	10,1	8 443 748	0,86	B	Many structures
Evassåsen	866 025	7,4	2 251 666	0,17	D	Two folded structures
Vikeid East	2 047 880	?	5 324 488		B	No samples
Vikeid Central	3 637 307	13,8	9 456 997	1,30	A	Three structures
Vikeid West	12 124 356	10,4	31 523 325	3,28	A	Five structures
Reinsnesøya	0		0	0	F	No graphite
Sæterstranda	77 135	15,8	200 550	0,03	E	One short structure
Ånstad	86 603	39,1	225 167	0,09	E	One short structure
Øksnes Municipality	0					
Alsvåg	103 923	8,0	270 200	0,02	E	Three structures
Instøya	6 062 178	8,6	15 761 662	1,40	A	Three long structures
Myre	42 426 407	?	?		A	Great area, few data
Rødhamran	565 685	13,7	1 470 782	0,20	C	Four structures
Romset	3 939 231	14,7	10 242 001	1,50	A	Two structures
Skogsøya	579 555	19,0	1 506 844	0,29	C	No ground geophysics
Sminess	7 727 407	7,1	20 091 257	1,40	A	Uncertain, few data
Steinland	?				?	Graphite?
Straumen	39 392	11,6	102 420	0,01	E	Three short structures (?)
Svinøya	69 282	23,4	180 133	0,04	E	Short, under sea?
Hadsel Municipality						
Korsodden	0		0	0	F	No graphite
Sellåter	984 808	6,3	2 560 500	0,16	D	One short structure
Sommarhus	300 000	24,1	780 000	0,19	D	Two bodies?
Morfjord mine	260 000	18,5	676 000	0,13	D	Three structures
Total	93 227 493		132 082 826	13,4		

As discussed above, the volumes of estimated graphite are uncertain. In addition, the uncertainty in the graphite tonnage is increased due to uncertainty in the total carbon

content. At Sommarland (Table 13.2, Rønning et al. 2018), the average TC from surface samples is almost the same as the average from drill cores, thereby reducing the uncertainty. At Haugsnes, the average TC from surface samples is 19.3% while the average from the two drill cores is only 5.2% (Table 13.2, Rønning et al. 2018). In addition, the individual thickness at Haugsnes can be sub-economic as established from the core drilling. The tonnage values in Table 10.3 are therefore an indication of how much graphite the different areas may contain and are probably optimistic estimates.

11. CONCLUSIONS AND RECOMMENDATIONS

Based on helicopter-borne geophysical data, several potential graphite occurrences in Vesterålen have been selected for follow-up work. The purpose for this is to confirm the existence of graphite and next to briefly evaluate the quality and quantity of graphite structures. The goal for the project, which is sponsored by Nordland county administration, is to increase the knowledge of each individual graphite occurrence. By doing so, the interest in graphite prospecting in Northern Norway may increase, effective prospecting can be implemented, and future areal planning may restrict any abuse of areas where potentially economic graphite exists.

During this project (2015 – 2019), NGU has visited 31 potential graphite occurrences in Vesterålen. Eleven of these were previously known and the knowledge of these has increased. 20 new occurrences were discovered and partly mapped. In three locations, low resistivity from helicopter-borne measurements is most likely explained by other reasons than graphite. No work was undertaken in areas where follow-up investigations (detailed geophysics, geological mapping, sampling and drilling) had previously been executed.

In some of these 31 locations, only reconnaissance geological work was performed. Others were mapped by geophysical ground measurements, and in six locations shallow core drilling was undertaken. Based on all the new data, an evaluation of the graphite occurrences has been carried out. Seven occurrences got a grade A (more than one million tons of flake graphite), three got the grade B (between 500,000 and 1,000,000 t), three got the grade C (between 200,000 and 500,000 t), six occurrences got the grade D (100,000 – 200,000 t flake graphite) and six grade E (less than 100,000 t graphite). Most likely, three objects are caused by non-graphitic material (Grade F). NGU would like to stress that this method is for an individual standardized evaluation of the graphite occurrences and is by no means a kind of resource estimation.

Occurrences that got the grades C, D and E are probably not of any economic interest today. Occurrences of grades A and B are interesting, and these are recommended for further and more detailed investigations. This may comprise more geophysical measurements that are able to “see” deeper than the EM31 instrument and deeper core drilling. These investigations are expensive and must be financed by prospecting or mining companies.

12. REFERENCES

- AarhusInv, 2013: Manual for Iversion software ver 6.1, Aarhus, Denmark: Hydro Geophysics Group (HGG), University of Aarhus.
- ABEM 1993: ABEM Terrameter SAS System. ABEM Printed matter n. 93041. ABEM Bromma, Sweden.
- ABEM, 2012: ABEM Terrameter LS. Instruction Manual, release 1.11, Sundbyberg: ABEM Instrument AB, Sweden.
- Corfu, F. 2004: U-Pb age, setting and tectonic significance of the Anorthosite-Mangerite-Charnockite-Granite suite, Lofoten-Vesterålen, Norway. *Journal of Petrology*, 45, 1799-1819.
- Corfu, F. 2007: Multistage metamorphic evolution and nature of the amphibolite–granulite facies transition in Lofoten–Vesterålen, Norway, revealed by U–Pb in accessory minerals. *Chemical Geology*, 241, 108-128.
- Dahlin, T., 1993: *On the automation of 2D resistivity surveying for engineering and environmental applications..* Lund: Department of Engineering Geology, Lund Institute of Technology, Lund University. 187pp, ISBN 91-628-1032-4.
- Dahlin, T. & Zhou, B., 2006: Multiple-gradient array measurements for multichannel 2D. *Near Surface Geophysics, Vol 4, No 2*, April, pp. 113-123.
- Dalsegg, E., 1994: *CP-, SP- og ledningsevne målinger ved grafittundersøkelser ved Hornvannet, Sortland, Nordland*, Trondheim: NGU Report 94.003.
- Davidson, B. & Skår, Ø. 2004: Lofoten and Vesterålen: A Precambrian puzzle. (Abstract). The 26th Nordic Geological Winter Meeting, January 6th – 9th 2004, Uppsala, Sweden. *Geologiske Föreningens Förhandlingar*. Vol 126, 20-21.
- Engvik, A. K., Davidson, B., Coint, N., Lutro, O., Tveten, E. and Schiellerup, H. 2016: High-grade metamorphism of the Archean to Palaeoproterozoic gneiss complex in Vesterålen, North Norway. (Abstract) 32nd Geological Winter Meeting Helsinki, *Bulletin of the Geological Society of Finland*, special issue, 153-154.
- Gautneb, H. & Tveten, E. 1992: Grafittundersøkelser og geologisk kartlegging på Langøya, Sortland Kommune, Nordland. NGU report 92.155.
- Gautneb, H. 1992: Grafittundersøkelser i Hornvannområdet, Sortland, Sortland Kommune, Nordland. NGU report 92.293.
- Gautneb, H. 1993: Grafittundersøkelser i Hornvannområdet, Sortland, Sortland Kommune, Nordland. NGU report 93.134.
- Gautneb, H. 1995: Grafittundersøkelser Hornvann 1994, Sortland Kommune, Nordland. NGU report 95.076.
- Gautneb, H. & Tveten, E. 2000: The geology, exploration and characterization of graphite deposits in the Jennestad area, Vesterålen area northern Norway. *Norges geologiske undersøkelse Bulletin*. 436, 67-74.
- Gautneb, H., Knezevic, J., Johannesen, N. E., Wanvik, J. E., Engvik, A., Davidson, B., Rønning, J. S. 2017: Geological and ore dressing investigations of graphite occurrences in Bø, Sortland, Hadsel and Øksnes municipalities, Vesterålen, Nordland County, Northern Norway 2015 – 2016. NGU Report 2017.015 (70pp.).
- Geosoft 1997: HEM System (Helicopter Electromagnetic data Processing, Analysis and Presentation System), Toronto, Ontario Canada: Geosoft.
- Geonics 1984: Operating manual EM31-D Non-contacting terrain conductivity meter. Revised June 1984, Mississauga, Ontario Canada: Geonics LTD.
- Geotech 1997: Hummingbird Electromagnetic System, User manual, s.l.: Geotech Ltd.

- Griffin, W. L., Taylor, P. N., Hakkinen, J. W., Heier, K. S., Iden, I. K., Krogh, E. J., Malm, O., Olsen, K. I., Ormaasen D. E. & Tveten, E. 1978: Archean and Proterozoic crustal evolution in Lofoten-Vesterålen, N Norway. *Journal of the Geological Society of London* 135, 629-647.
- Helland, A. 1887: Lofoten og Vesterålen. Norges geologiske undersøkelse. Vol. 23, 1-246.
- Heier, K.S. 1960: Petrology and geochemistry of high-grade metamorphic and igneous rocks on Langøya Northern Norway. *Norges geologiske undersøkelse Bulletin* 207, 1-246.
- Hutchison C.S. 1975: The norm its variation, their calculation and relationships. *Schweizerische Mineralogische und Petrographische mitteilungen*, 55, 243-256.
- Keilhau, B. M. 1844: Beretning om en geonostisk reise i norlandene i 1855. *Nyt Magazin for naturvidenskabene*. 11, nr.3.
- Kwiecińska, B. & Petersen, H. I. 2004: Graphite, semi-graphite, natural coke, and natural char classification—ICCP system. *International Journal of Coal Geology*, 57, 99-116.
- Kihle, O. & Eidsvig, P. D., 1978: Nye tolkninger for tolkning av CP-målinger, Trondheim: NGU Rapport 1534.(28 s.).
- Liu Y., Farquharson C.G., Yin C., Baranwal V.C., 2018: Wavelet-based 3-D inversion for frequency-domain airborne EM data. *Geophysical Journal International* 213 (1), 1-15.
- Loke, M. H., 2014: *Geoelectrical Imaging 2D & 3D. Instruction Manual. Res2DInv version 4.0.* <http://www.geotomosoft.com/>.
- Loke, M. H., 2018: *Geoelectrical Imaging 2D & 3D. Instruction Manual. Res2DInv version 4.8.9.* <http://www.geotomosoft.com/>.
- Mogaard, J. O., Olesen, O., Rønning, S., Blokkum, O. 1988: Geofysiske undersøkelser fra helikopter over Langøya, Vesterålen: NGU report 88.151
- Neumann, H. 1952: Dagbok fra Nord-Norge 26.5-19.8 1952 Ba report 7709.
- Palosaari J., Latonen, R.-M., Smått J.-H., Blomquist, R., Eklund, O. 2016: High-quality flake graphite occurrences in a high-grade metamorphic region in Sortland, Vesterålen, Northern Norway. *Norwegian Journal of Geology*, 96, 19-26.
- Rantitsch, G., Lämmeder, W., Fissthaler, E., Mitsche, S. Kaltenbock, H. 2016: On the discrimination of semi-graphite and graphite by Raman spectroscopy. *International Journal of Coal Geology*, 159, 48-56.
- Reynolds, J. 2011: *An Introduction to Applied and Environmental Geophysics*, 2nd edition. Wiley – Blackwell, Oxford UK.
- Rodionov, A., Ofstad, F., Stampolidis, A. & Tassis G. 2013a: Helicopter-borne magnetic, electromagnetic and radiometric geophysical survey at Langøya in Vesterålen, Nordland. NGU report 2013.044.
- Rodionov, A., Ofstad, F. & Tassis, G. 2013b: Helicopter-borne magnetic, electromagnetic and radiometric geophysical survey in the western part of Austvågøya, Lofoten archipelago, Nordland. NGU Report 2013.045.
- Rønning, J. S. 1991: CP målinger ved grafittundersøkelser på Vikeid, Sortland kommune Nordland. NGU report 91.262.
- Rønning, J.S. 1993: CP og SP målinger ved grafittundersøkelser på Vikeid, Sortland kommune Nordland. NGU report 93.018.
- Rønning, J. S., Gautneb, H., Dalsegg, E., Larsen, B. E., & Rodionov, A. 2014: Oppfølgende grafittundersøkelser i Meløy og Rødøy kommuner, Nordland. Trondheim: NGU Report 2014.046.

- Rønning, J. S., Rodionov, A., Ofstad, F., & Lynum, R. 2012: Elektromagnetiske, magnetiske og radiometriske målinger fra helikopter i området Skaland - Trælen på Senja. Trondheim: NGU Report 2012.061.
- Rønning, J. S., Larsen, B. E., Elvebakk, H., Gautneb, H., Ofstad, F. & Knežević, J. 2017: Geophysical investigations of graphite occurrences in Bø and Øksnes municipalities, Vesterålen, Nordland County, Northern Norway 2015-2016. NGU Report 2017.014 (50 pp.).
- Rønning, J. S., Gautneb, H., Larsen, B. E., Knežević, J., Baranwal, J. C., Elvebakk, H., Gellein, J., Ofstad, F. & Brønner, M. 2018: Geophysical and geological investigations of graphite occurrences in Vesterålen and Lofoten, Northern Norway 2017. NGU Report 2018.011 (180 pp.).
- Sato, M., & Mooney, H. M. 1960: The electrochemical mechanism of sulphide self-potentials. *Geophysics*, 25, 226-249.
- Skjeseth, S. 1952: Foreløpig rapport fra geologiske undersøkelser av Jennestad grafitt-felt. Report BA5232, Norges geologiske undersøkelse.
- Sletten, A. M. 2013: Jennestad Graphite Project, Resource estimation. Norwegian graphite, unpublished report.
- Telford, W. M., Geldart, L. P., Sheriff, R. E. & Keys, D. A. 1976: *Applied Geophysics*. Cambridge University Press. Cambridge UK.
- Tveten, E. 1978: Berggrunnskart over Norge; Svolvær 1:250.000. Norges geologiske undersøkelse.
- Tveten, E. 1990: Berggrunnskart 1: 50.000 Sortland. Norges geologiske undersøkelse
- Tveten, E. & Henningsen, T. 1998: Berggrunnskart 1:250.000 Andøy. Norges geologiske undersøkelse.
- UBC 2000: Manual for EM1DFM. Vancouver, Canada: UBC - Geophysical Inversion facility, Department of Earth and Ocean Sciences, University of British Columbia.
- Vokes, F.M. 1954: Rapport over befarings av Jennestad grafitt-felt. Report BA5340, Norges geologiske undersøkelse.

Appendices

Appendix 1: Drill-core geology, log description

Appendix 2: Drill-core pictures

Appendix 3: Analyses of total sulphur (TS) and Total Carbon (TS) on drill-cores

Appendix 4: Portable XRF analyses of drill-cores.

Appendix 5: Electric conductivity (resistivity) from drill-hole logging.

Appendix 6: Complete list of analysed samples for TS, TC and TOC from 1990-2018

Appendix 1: Drill-core geology, log description

Location, Drillhole no.	Depth (m) From-to	LITH- code	Description by Janja Knežević
SOMMARHUS			
SomDh18-1	0 – 0.5	OVERB	Overburden
	0.5 – 5.9	GSH	Dark greyish massive graphite schist medium to coarse-grained, with felsic veins (3mm to 30cm), feldspar decompression, vuggys field with mica 1-2 mm, biotite/phlogopite in coarse-grained graphite and partly segments in vein 3 mm
	5.9 – 8.7	Gr-BFGN	Greyish brownish medium grained graphite-bearing biotite feldspar gneiss with low graphite content, partly graphite flakes 2 mm-3 mm, with weak pyrite
	8.7 – 10.1	MZ	Monzonite intrusion, medium to coarse grained light in colour-light grey with spotted brownish dark minerals 1-3 mm and spotted graphite in traces 1mm
	10.1 – 18.0	Gr-BFGN	Greyish medium grained Graphite bearing-biotite feldspar gneiss with weak disseminated graphite partially with pyrrhotite, pyrite veins 1-2 mm, weak magnetic
	18.0 – 22.4	GRN / Gr-BFGN	Greyish medium grained granulite with partially biotite and graphite flakes, pyrrhotite
	22.4 – 27.5	GRN	Pyroxene-feldspar rich with pyrrhotite
	27.5 – 29.5	Gr-BFGN	Brownish medium grained Graphite bearing-biotite feldspar gneiss, with pyrrhotite
	29.5 – 39-2	GRN?	Medium to fine grained pyroxene-feldspar rich, with pyrrhotite, partially with biotite
SomDh18-2	0 – 2.4	OVERB	Overburden
	2.4 – 4.5	MGD_GV	Light medium grained Meta-granodiorite with graphite veins 4-10cm, with pyroxene and biotite
	4.5 – 6.75	GSH	Massive graphite, folded with felsic-biotite-graphite veins up to 10cm
	6.75 – 25.4	MGD_GV	Light/whiteish medium to coarse grained Meta-granodiorite with graphite veins 4-10cm, partially foliated, with biotite and mafic minerals rounded coarse grained felsic clasts, with greenish amphibole, chlorite? veins 1-14 cm, partly pyrrhotite veins, deformed till 19,8 m with greenish amphibole/pyroxene veins

VIKEID			
VikDh18-1	0 – 3	OVERB	Overburden
	3 – 25	GRN_G	Medium grained greyish-dark greenish granulite with graphite, variable content of graphite, feldspar, pyroxene, biotite, amphibole along drill-core, carbon veins from 5 mm to 10 cm, felsic veins 1 cm-15 cm, sulphides. 21,6-23,4 graphite rich zone with Ca veins, foliated, broken 9-11 and 13-14.6
MYRE			
Myre Dh18-1	0 – 3.0	OVERB	Overburden
	3.0 – 19.8	GRN_G	Greyish medium grained granulite/ pyroxene-feldspar rich rock with graphite (disseminated graphite flakes) with biotite and pyrrhotite + pyrite, pyrrhotite veins -2 mm, felsic veins 3 mm-2cm, felsic veins with graphite and weak biotite. 10 m core loss (8 – 20 m).
Myre Dh18-2	0 – 6.5	OVERB	Overburden
	6.5 - 20	GRN_G	Greyish medium grained granulite / pyroxene-feldspar rich rock with graphite (disseminated graphite flakes) with biotite and pyrrhotite + pyrite, pyrrhotite veins -2 mm, felsic veins 3 mm-2 cm, felsic veins with graphite and weak biotite. Broken and core loss 6.5 – 12 m.

Appendix 2. Drill-core pictures.

Vikeid Dh1-2018. Box 1: 3.0 m – 9.9 m (dry and wet).



Vikeid Dh1-2018. Box 2: 9.9 – 19.7 m (dry and wet).



Vikeid Dh1-2018. Box 3: 19.7 m – 25.8 m (dry and wet).



Myre Dh1-2018. Box 1: 3.0 m – 10.0 m (dry and wet).



Myre Dh1-2018. Box 2: 10.0 m – 20.0 m (dry and wet).
Note: Core loss especially from 10 to 16 m.



Myre Dh2-2018. Box 1: 6.5 m – 10.0 m (dry and wet).



Myre Dh2-2018. Box 2: 10 m – 20 m (dry and wet).

Note: Core loss from 10 to 12 m.



Sommarhus Dh1-2018. Box 1: 0.4 m – 9.9 m (dry and wet).



Sommarhus Dh1-2018. Box 2: 9.9 m – 19.8 m (dry and wet).



Sommarhus Dh1-2018. Box 3: 19.8 m – 29.8 m (dry and wet).



Sommarhus Dh1-2018. Box 4: 29.8 m – 39.2 m (dry and wet).



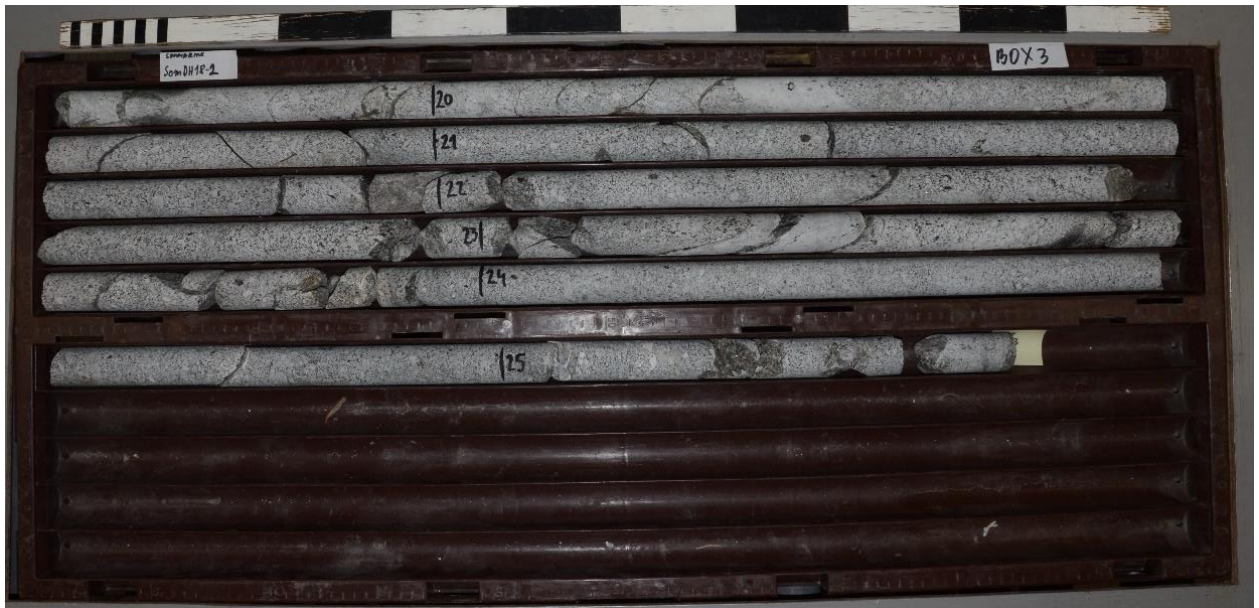
Sommarhus Dh2-2018. Box 1: 2.4 m – 9.9 m (dry and wet).



Sommarhus Dh2-2018. Box 2: 9.9 m - 19.7 m (dry and wet).



Sommarhus Dh2-2018. Box 3: 19.7 m – 25.4 m (dry and wet).



Appendix 3: TS and TC analysis of drill cores

See text for description of methods.

Collar information

Locality	Hole no.	UTM E	UTM N	EOH (m)	AZIMUTH (°)	DIP(°)
Sommarhus	Bh1	486959	7588922	39.2	090	45
Sommarhus	Bh2	486990	7588972	25.4	090	45
Vikeid	Bh1	509843	7627772	25.55	120	45
Myre	Bh1	506588	7643919	20	000	45
Myre	Bh2	505915	7643908	19.8	180	45

Analysis

NGU Lab no.	Drillhole no.	Sample no.	Depth from (m)	Depth To (m)	TS (%)	TC (%)
195032	Sommarhus1	Sommah1 (0-2)	0	2	4.05	11.40
195033	Sommarhus1	Sommah1 (2-4)	2	4	3.87	20.80
195034	Sommarhus1	Sommah1 (4-6)	4	6	3.76	17.60
195035	Sommarhus1	Sommah1 (8-10)	8	10	0.12	0.19
195036	Sommarhus1	Sommah1 (10-12)	10	12	0.47	< 0.06
195037	Sommarhus1	Sommah1 (14-16)	14	16	1.65	1.97
195038	Sommarhus1	Sommah1 (22-24)	22	24	2.17	8.93
195039	Sommarhus1	Sommah1 (24-26)	24	26	0.88	8.69
195040	Sommarhus1	Sommah1 (26-28)	26	28	2.92	7.00
195041	Sommarhus1	Sommah1 (30-32)	30	32	0.04	0.06
195042	Sommarhus1	Sommah1 (38-39.2)	38	39.2	0.13	0.58
195043	Sommarhus2	Sommarh2 (2.2-4)	2.2	4	1.03	1.04
195044	Sommarhus2	Sommarh2 (4-6)	4	6	1.82	6.87
195045	Sommarhus2	Sommarh2 (6-7)	6	7	2.28	18.80
195046	Sommarhus2	Sommarh2 (7-9)	7	9	0.20	0.17
195047	Vikeid	Vikeid (2.8-4)	2.8	4	1.87	5.09
195048	Vikeid	Vikeid (4-6)	4	6	0.82	0.75
195049	Vikeid	Vikeid (6-8)	6	8	1.41	4.69
195050	Vikeid	Vikeid (8-10)	8	10	0.95	5.26
195051	Vikeid	Vikeid (10-12)	10	12	0.36	0.03
195052	Vikeid	Vikeid (20-22)	20	22	0.82	1.05
195053	Vikeid	Vikeid (22-24)	22	24	1.08	6.64
195054	Vikeid	Vikeid (22-25.55)	22	25.55	0.05	0.07
195055	Myre2	Myre2 (8-9)	8	9	1.82	0.48
195056	Myre2	Myre2 (10-12)	10	12	2.98	1.05
195067	Myre2	Myre2 (17-19)	17	19	2.89	0.45

Appendix 4: Portable XRF analysis of drill cores.

The drill core where analysed by a Niton portable XRF, using standard methods, counting time per point was 20 seconds. There were usually 2 points analysed per metre core. Additional information is available upon request. All values are in %.

Drill-hole no.	Depth (m)	Si (%)	Al (%)	Fe (%)	Ca (%)	Ni (ppm)	S (%)
Sommarhus1	0.5	16.22	2.47	3.60	2.44		1.95
Sommarhus1	1	26.33	7.28	5.58	4.44	84.03	2.55
Sommarhus1	1.5	6.56	1.10	12.85	4.36	270.83	11.30
Sommarhus1	2	10.38	0.83	4.35	3.09	55.41	2.87
Sommarhus1	2.5	5.06	0.65	9.99	3.28	120.44	5.20
Sommarhus1	3	14.56	1.82	7.99	2.52	67.68	6.21
Sommarhus1	3.5	21.44	2.71	3.79	1.54		2.68
Sommarhus1	4	40.74	4.64	0.27	0.45		0.22
Sommarhus1	4.5	24.64	3.16	1.36	3.62		1.54
Sommarhus1	5	15.96	1.92	5.08	9.28		0.19
Sommarhus1	5.5	11.12	1.91	6.52	1.97		3.46
Sommarhus1	6	25.23	9.19	5.78	3.15	63.59	2.33
Sommarhus1	6.5	28.74	8.03	5.14	3.48		0.76
Sommarhus1	7	28.56	5.74	4.67	2.93		0.07
Sommarhus1	7.5	25.25	3.04	14.51			2.01
Sommarhus1	8	30.64	6.42	13.37			0.26
Sommarhus1	8.5	25.39	6.90	9.49	2.17	64.06	0.44
Sommarhus1	9	39.88	4.07	0.89			0.16
Sommarhus1	9.5	40.39	4.43	0.71	0.59		0.05
Sommarhus1	10	41.66	4.54	0.53	0.91		0.08
Sommarhus1	10.5	26.49	7.17	7.05	6.03		0.63
Sommarhus1	11	33.14	9.49	1.55	3.67		0.04
Sommarhus1	11.5	24.35	9.30	10.75	1.93		
Sommarhus1	12	21.30	8.88	13.91	2.24		0.04
Sommarhus1	12.5	26.28	10.14	7.92	4.21		0.13
Sommarhus1	13	29.10	10.28	5.96	7.08		
Sommarhus1	13.5	28.41	8.44	7.11	6.25		0.08
Sommarhus1	14	27.45	8.34	7.55	4.08	64.83	2.45
Sommarhus1	14.5	19.65	8.87	16.06	5.04	217.00	9.14
Sommarhus1	15	25.14	6.06	7.74	7.74		0.08
Sommarhus1	15.5	23.69	5.79	8.03	6.47		2.91
Sommarhus1	16	23.46	7.05	10.53	2.38	91.85	2.94
Sommarhus1	16.5	27.71	8.86	8.83	7.60		
Sommarhus1	17	26.97	8.24	9.68	6.19	92.02	0.10
Sommarhus1	17.5	26.93	8.84	8.07	6.17	61.75	0.04
Sommarhus1	18	28.62	8.29	8.22	6.93	62.42	0.15
Sommarhus1	18.5	27.63	8.55	9.90	4.44		

Drill-hole no.	Depth (m)	Si (%)	Al (%)	Fe (%)	Ca (%)	Ni (ppm)	S (%)
Sommarhus1	19	26.62	8.01	10.29	6.47		3.68
Sommarhus1	19.5	27.32	8.32	8.57	6.80		0.12
Sommarhus1	20	27.87	9.47	8.08	7.44		0.60
Sommarhus1	20.5	27.28	8.35	8.17	6.88		0.30
Sommarhus1	21	30.54	9.59	3.39	6.75	53.63	0.51
Sommarhus1	21.5	26.76	8.11	6.39	3.78		0.69
Sommarhus1	22	23.92	8.85	1.91	7.20		0.91
Sommarhus1	22.5	22.41	3.90	6.05	11.57		0.33
Sommarhus1	23	24.91	2.53	7.42	11.04		0.58
Sommarhus1	23.5	19.27	4.44	4.76	7.10		0.94
Sommarhus1	24	22.66	4.75	5.31	9.34		0.56
Sommarhus1	24.5	22.72	2.27	6.03	11.65	114.70	3.34
Sommarhus1	25	14.21	1.90	20.93	8.95	545.61	17.11
Sommarhus1	25.5	20.78	5.48	9.44	10.65	126.32	3.82
Sommarhus1	26	25.27	7.17	4.92	9.16		0.70
Sommarhus1	26.5	26.59	10.17	6.83	3.49		2.67
Sommarhus1	27	20.33	7.55	8.99			0.41
Sommarhus1	27.5	24.87	8.14	8.00	1.90		2.19
Sommarhus1	28	26.36	7.61	7.33	1.89	86.11	0.88
Sommarhus1	28.5	29.95	1.70	14.73	5.32	124.41	0.63
Sommarhus1	29	30.12	8.81	3.92	8.26		0.03
Sommarhus1	29.5	30.66	7.39	5.39	9.62		0.04
Sommarhus1	30	28.20	9.08	5.57	8.79		
Sommarhus1	30.5	29.86	9.13	6.58	7.98	59.36	
Sommarhus1	31	25.88	7.08	9.05	7.52	64.86	1.16
Sommarhus1	31.5	26.62	5.93	10.66	8.44		0.08
Sommarhus1	32	26.74	6.37	8.59	8.37		0.03
Sommarhus1	32.5	27.00	10.07	4.68	7.26		0.06
Sommarhus1	33	26.12	9.58	5.95	8.02		0.16
Sommarhus1	33.5	26.99	10.07	6.40	10.05		0.20
Sommarhus1	34	27.28	8.18	7.17	7.95		0.03
Sommarhus1	34.5	28.07	8.69	7.82	8.90	59.64	
Sommarhus1	35	28.92	9.08	6.21	6.59		0.18
Sommarhus1	35.5	28.97	7.65	8.41	8.73	74.76	0.04
Sommarhus1	36	27.26	9.97	7.20	8.40	92.63	
Sommarhus1	36.5	27.60	9.60	5.38	5.48		
Sommarhus1	37	24.25	6.14	12.26	2.45	215.39	1.94
Sommarhus1	37.5	25.91	7.74	8.50	3.55	67.21	0.05
Sommarhus1	38	32.33	10.95	10.41	2.61		0.07
Sommarhus2	2.5	26.84	4.71	4.80	3.13	149.47	3.66
Sommarhus2	3	32.06	5.06	0.77	2.19		0.48
Sommarhus2	5	15.26	2.82	8.09	3.54	150.36	7.53

Drill-hole no.	Depth (m)	Si (%)	Al (%)	Fe (%)	Ca (%)	Ni (ppm)	S (%)
Sommarhus2	6	27.77	6.32	5.27	4.93	114.18	0.93
Sommarhus2	7	18.87	2.69	11.95	7.59	238.62	7.38
Sommarhus2	8	25.38	8.27	6.66	1.83	-	1.09
Sommarhus2	9	29.84	1.22	3.30	1.59	-	1.83
Sommarhus2	10	20.26	0.67	4.90	2.92	85.67	2.66
Sommarhus2	11	12.04	1.45	5.33	1.21	156.08	2.77
Sommarhus2	12	31.16	5.74	1.92	2.37	-	0.34
Sommarhus2	13	34.02	5.99	1.80	2.74	-	0.08
Sommarhus2	14	34.41	6.62	0.64	3.24	-	1.33
Sommarhus2	15	38.55	5.41	0.59	2.11	-	0.44
Sommarhus2	16	35.67	5.34	0.88	2.49	-	0.63
Sommarhus2	17	28.50	4.48	1.49	3.08	-	0.31
Sommarhus2	18	30.73	5.60	1.05	6.71	-	0.37
Sommarhus2	19	33.84	5.49	1.48	2.82	-	0.03
Sommarhus2	20	28.83	5.38	2.64	3.50	-	0.59
Sommarhus2	21	30.40	6.38	2.89	2.57	-	0.14
Sommarhus2	23	34.17	6.03	1.57	2.89	-	0.34
Sommarhus2	23	31.19	5.58	1.37	2.61	-	0.11
Sommarhus2	25	32.03	5.17	2.94	1.77	-	2.81
Sommarhus2	25.4	34.74	7.01	1.47	2.37	-	0.09
Vikeid1	3	28.31	3.22	3.07	-	256.38	1.35
Vikeid1	3.5	23.38	2.31	3.45	0.78	46.64	1.97
Vikeid1	4	29.89	2.27	0.11	1.15	-	3.52
Vikeid1	4.5	26.46	1.38	2.66	0.70	-	-
Vikeid1	5	35.65	3.78	2.68	1.51	-	0.12
Vikeid1	5.5	38.57	3.95	1.61	-	-	0.24
Vikeid1	6	31.26	4.49	5.07	-	-	0.88
Vikeid1	6.5	36.53	4.80	4.07	0.62	-	0.30
Vikeid1	7	24.97	4.33	5.66	2.90	259.80	0.14
Vikeid1	7.5	25.36	6.30	6.62	2.40	62.21	1.58
Vikeid1	8	27.88	5.33	7.06	4.43	86.12	0.03
Vikeid1	8.5	32.02	3.62	1.91	0.67	-	0.23
Vikeid1	9	23.42	4.60	8.43	2.71	99.00	0.07
Vikeid1	9.5	31.39	6.31	10.70	4.81	-	1.45
Vikeid1	10	33.88	4.56	5.38	3.50	-	0.07
Vikeid1	10.5	33.49	6.03	6.10	4.38	-	0.39
Vikeid1	11	28.01	6.54	6.34	3.41	-	0.32
Vikeid1	11.5	27.43	5.95	8.73	4.07	-	0.98
Vikeid1	12	27.28	5.81	9.62	4.15	-	0.23
Vikeid1	12.5	33.90	5.92	5.73	4.55	-	0.07
Vikeid1	13	27.64	6.58	8.79	4.97	-	0.13
Vikeid1	13.5	27.01	5.74	8.35	4.22	-	-

Drill-hole no.	Depth (m)	Si (%)	Al (%)	Fe (%)	Ca (%)	Ni (ppm)	S (%)
Vikeid1	14	25.18	5.83	8.77	3.42	-	0.13
Vikeid1	14.5	44.70	3.52	0.19	1.54	-	0.02
Vikeid1	15	27.49	6.10	8.56	3.71	-	0.30
Vikeid1	15.5	19.65	3.88	9.06	4.34	-	0.19
Vikeid1	16	24.17	5.15	10.08	3.87	-	0.06
Vikeid1	16.5	28.29	6.21	8.39	5.54	-	-
Vikeid1	17	29.28	3.50	7.42	5.13	-	0.09
Vikeid1	17.5	26.60	5.66	8.27	5.51	-	0.05
Vikeid1	18	27.22	5.52	8.40	5.55	-	0.20
Vikeid1	18.5	27.69	5.32	7.55	3.04	-	1.15
Vikeid1	19	28.95	6.54	6.70	4.97	84.72	0.05
Vikeid1	19.5	35.36	2.81	3.98	-	-	0.05
Vikeid1	20	33.58	4.98	3.93	4.83	-	1.10
Vikeid1	20.5	23.40	3.08	7.87	-	544.09	5.26
Vikeid1	21	43.63	2.05	1.28	2.35	-	0.03
Vikeid1	21.5	32.23	2.37	1.92	-	-	0.51
Vikeid1	22	31.70	2.16	1.61	0.65	46.16	0.34
Vikeid1	22.5	26.47	1.57	1.74	10.63	-	0.32
Vikeid1	23	23.29	5.76	5.09	1.16	-	0.07
Vikeid1	23.5	28.90	6.56	6.61	-	-	-
Vikeid1	24	28.80	5.34	6.81	4.07	-	0.14
Vikeid1	24.5	32.08	5.95	6.99	3.10	-	0.06
Myre2	6.5	30.12	4.73	10.48	5.97	255.00	0.40
Myre2	7	34.14	4.76	2.90	2.55	260.00	1.28
Myre2	7.5	29.49	5.22	3.70	2.50	240.00	0.29
Myre2	8	22.75	5.36	8.24	2.05	230.00	3.05
Myre2	8.5	25.98	5.81	6.37	1.98	-	1.54
Myre2	9	23.59	5.06	9.61	1.61	-	5.56
Myre2	9.5	23.48	5.18	9.01	1.87	86.63	5.64
Myre2	10	28.57	6.26	5.69	2.35	150.00	2.34
Myre2	10.5	30.32	5.96	4.83	1.89	200.00	1.91
Myre2	11	24.20	5.98	8.86	1.60	135.00	3.42
Myre2	11.5	25.78	6.01	5.69	2.18	-	1.96
Myre2	12	30.21	5.22	4.18	2.24	-	1.06
Myre2	12.5	25.54	5.23	6.72	1.46	-	2.15
Myre2	13	34.70	5.08	3.57	1.60	-	1.66
Myre2	13.5	26.29	5.87	9.32	1.59	-	0.30
Myre2	14	27.22	7.25	6.09	2.82	-	0.30
Myre2	14.5	22.10	6.23	13.69	1.99	-	0.40
Myre2	15	30.70	6.80	5.49	2.12	-	0.30
Myre2	15.5	26.31	7.38	9.93	2.00	-	0.30
Myre2	16	24.69	5.80	6.03	2.15	-	1.51

Drill-hole no.	Depth (m)	Si (%)	Al (%)	Fe (%)	Ca (%)	Ni (ppm)	S (%)
Myre2	16.5	35.12	5.82	5.47	2.50	-	3.25
Myre2	17	29.46	7.63	6.91	1.60	-	0.10
Myre2	17.5	37.01	5.61	3.45	2.31	-	0.76
Myre2	18	25.08	6.43	6.53	2.16	-	2.36
Myre2	18.5	24.70	8.55	6.63	2.53	-	2.77
Myre2	19	27.58	5.06	6.99	1.92	-	0.25
Myre2	19.5	26.04	6.87	8.58	1.78	-	0.30
Myre2	20	26.01	6.03	7.22	1.63	-	0.30

Appendix 5: Electric conductivity (resistivity) from drill-hole logging.

Resistivity (electric conductivity) in drill-hole Vikeid, Dh1

R1 to R4 are individual resistance readings, giving Mean R as arithmetic mean.

Coordinates: 509843 East - 7588845 North WGS 84 zone 33, Direction 120°, Dip 45°

Bedrock at 2.4 m.

Depth (m)	R1 (Ω)	R2 (Ω)	R3 (Ω)	R4 (Ω)	Mean R (Ω)	Resistivity ρ (Ωm)	Conductivity σ (mS/m)	Comment
3	6,54	6,45	6,45	6,46	6,48	648	1,54	Casing 2,8 m
3,25	6,57	6,6	6,62	6,65	6,61	661	1,51	
3,5	10,03	9,82	9,78	9,79	9,86	986	1,01	
3,75	8,17	8,15	8,15	8,17	8,16	816	1,23	
4	11,52	11,77	12	12,14	11,86	1186	0,84	
4,25	38,2	38,3	39,9	41,2	39,40	3940	0,25	
4,5	28,3	28,4	28,4	28,4	28,38	2838	0,35	
4,75	42,1	42,2	42,2	42,3	42,20	4220	0,24	
5	27,2	27,3	27,3	27,3	27,28	2728	0,37	
5,25	49,8	49,9	49,8	49,8	49,83	4983	0,20	
5,5	47,7	47,8	47,9	48	47,85	4785	0,21	
5,75	74,6	74,5	74,4	74,3	74,45	7445	0,13	
6	54,3	54,2	54,1	54,1	54,18	5418	0,18	
6,25	27,2	27,8	27,9	27,9	27,70	2770	0,36	
6,5	42,6	42,5	42,5	42,4	42,50	4250	0,24	
6,75	42,6	42,4	42,4	42,3	42,43	4243	0,24	
7	40,4	40,1	40	39,9	40,10	4010	0,25	
7,25	11,16	11,14	11,11	11,09	11,13	1113	0,90	
7,5	13,4	13,32	13,28	13,25	13,31	1331	0,75	
7,75	6,54	6,5	6,47	6,45	6,49	649	1,54	
8	10,49	10,59	10,62	10,63	10,58	1058	0,94	
8,25	20,6	20,6	20,6	20,6	20,60	2060	0,49	
8,5	6,66	6,56	6,51	6,47	6,55	655	1,53	CP Grounding
8,75	6,56	6,53	6,51	6,48	6,52	652	1,53	
9	7,37	7,34	7,32	7,29	7,33	733	1,36	
9,25	33,7	33,7	33,6	33,5	33,63	3363	0,30	
9,5	39,7	39,6	39,6	39,6	39,63	3963	0,25	
9,75	48,4	48,1	47,9	47,8	48,05	4805	0,21	
10	40,4	40,2	40	39,8	40,10	4010	0,25	
10,25	44,2	44	43,8	43,7	43,93	4393	0,23	
10,5	29,2	29,5	28,9	28,9	29,13	2913	0,34	
10,75	48	47,9	47,9	47,8	47,90	4790	0,21	
11	54,3	54,3	54,1	53,7	54,10	5410	0,18	

Depth (m)	R1 (Ω)	R2 (Ω)	R3 (Ω)	R4 (Ω)	Mean R (Ω)	Resistivity ρ (Ωm)	Conductivity σ (mS/m)	Comment
11,25	79,3	79,3	79,2	79,1	79,23	7923	0,13	
11,5	84,1	84,1	84,1	84,1	84,10	8410	0,12	
11,75	84,4	84,3	84,3	84,4	84,35	8435	0,12	
12	83,3	83,8	84,1	84,3	83,88	8388	0,12	
12,25	101,9	101,7	101,6	101,6	101,70	10170	0,10	
12,5	99,9	99,8	99,7	99,7	99,78	9978	0,10	
12,75	77,7	77,4	77,2	77,1	77,35	7735	0,13	
13	71,6	71,4	71,3	71,2	71,38	7138	0,14	
13,25	60,8	60,7	62	62,6	61,53	6153	0,16	
13,5	43,2	43,1	43,1	43	43,10	4310	0,23	
13,75	65,4	65,4	65,3	65,3	65,35	6535	0,15	
14	68,3	68,1	68	67,9	68,08	6808	0,15	
14,25	86,2	86	85,9	85,7	85,95	8595	0,12	
14,5	84,4	84,2	84	83,9	84,13	8413	0,12	
14,75	93,9	93,5	93,3	93,1	93,45	9345	0,11	
15	111,3	111,7	111,9	111,9	111,70	11170	0,09	
15,25	100	100,1	100,2	100,2	100,13	10013	0,10	
15,5	115,7	115,7	115,7	115,7	115,70	11570	0,09	
15,75	115,5	115,4	115,3	115,2	115,35	11535	0,09	
16	96,4	94,2	93,4	93	94,25	9425	0,11	
16,25	100,2	100,1	99,9	99,8	100,00	10000	0,10	
16,5	88,8	88,5	88,3	88,1	88,43	8843	0,11	
16,75	72,7	72,5	72,4	72,3	72,48	7248	0,14	
17	67	67	66,9	66,9	66,95	6695	0,15	
17,25	72,7	72,6	72,5	72,4	72,55	7255	0,14	
17,5	59,1	58,9	58,8	58,8	58,90	5890	0,17	
17,75	64,5	65	66,4	67,2	65,78	6578	0,15	
18	80,5	80,5	80,4	80,4	80,45	8045	0,12	
18,25	74,5	74,4	74,3	74,3	74,38	7438	0,13	
18,5	71,8	71,6	71,4	71,3	71,53	7153	0,14	
18,75	62,6	62,5	62,4	62,3	62,45	6245	0,16	
19	39,7	39,6	39,6	39,5	39,60	3960	0,25	
19,25	41	40,9	40,9	40,8	40,90	4090	0,24	
19,5	36,8	36,7	36,7	36,6	36,70	3670	0,27	
19,75	31,4	31,3	31,3	31,3	31,33	3133	0,32	
20	30,1	30,1	30,1	30,1	30,10	3010	0,33	
20,25	37,5	37,4	37,4	37,4	37,43	3743	0,27	
20,5	34,2	34,1	34	33,9	34,05	3405	0,29	
20,75	59,4	59,4	59,4	59,4	59,40	5940	0,17	
21	60,8	61	61,1	61,1	61,00	6100	0,16	
21,25	46,4	46,3	46,2	46,1	46,25	4625	0,22	
21,5	76,7	76,7	76,8	76,9	76,78	7678	0,13	
21,75	70,1	69,9	69,8	69,7	69,88	6988	0,14	

Depth (m)	R1 (Ω)	R2 (Ω)	R3 (Ω)	R4 (Ω)	Mean R (Ω)	Resistivity ρ (Ωm)	Conductivity σ (mS/m)	Comment
22	45	44,8	44,8	44,7	44,83	4483	0,22	
22,25	42,6	42,7	42,8	42,8	42,73	4273	0,23	
22,5	10,62	10,46	10,36	10,2	10,41	1041	0,96	
22,75	9,55	9,48	9,43	9,4	9,47	946,5	1,06	
23	8,68	8,62	8,58	8,56	8,61	861	1,16	
23,25	8,93	8,86	8,82	8,76	8,84	884	1,13	
23,5	11,16	11,11	11,09	11,08	11,11	1111	0,90	
23,75	11,49	11,82	12,17	12,46	11,99	1199	0,83	
24	13,02	12,96	12,92	12,8	12,93	1293	0,77	
24,25	76,4	76,3	76,2	76,1	76,25	7625	0,13	
24,5	88,2	88,1	88	87,9	88,05	8805	0,11	
24,75	90,5	90,4	90,3	90,2	90,35	9035	0,11	
25	74,9	74,8	74,7	74,7	74,78	7478	0,13	
25,25	73,9	73,6	73,6	73,6	73,68	7368	0,14	
25,5	75,4	75,4	75,4	75,4	75,40	7540	0,13	Mud

Appendix 6: Complete list of analysed samples for TS, TC and TOC from 1990-2019

The database is under continuous update and revision, those interested in these data are advised to request the data in excel format.

Blank cell = not analysed. Values marked with < = below detection limit.

Sampler, all at NGU: HG = Håvard Gautneb, JK = Janja Knežević, BD = Børre Davidsen, NC = Nolwenn Coint, JEW = Jan Egil Wanvik, HS = Henrik Schiellerup, AE = Ane Engvik, FO = Frode Ofstad, OL = Ole Lutro, ET = Einar Tveten.

NGU no.	Year	Area	Locality	Sone	WGS 84 Easting	WGS 84 Northing	Sampler	Sample no.	Text	TS (%)	TC (%)	TOC (%)
	1990	Vikeidet	Vikeidet	33	509 866	7 627 995	HG	90-2c	Graphite schist		13.80	
	1990	Vikeidet	Vedåsen	33	510 700	7 628 225	HG	90-3a	Graphite schist		9.40	
	1990	Vikeidet	Vedåsen	33	510 700	7 628 225	HG	90-3c	Graphite schist		1.36	
	1990	Vikeidet	Vikeidet	33	509 021	7 628 042	HG	90-5a	Graphite schist		9.43	
	1990	Vikeidet	Vikeidet	33	509 021	7 628 042	HG	90-5b	Graphite schist		6.94	
	1990	Vikeidet	Vikeidet	33	509 021	7 628 042	HG	90-5c	Graphite schist		7.48	
	1990	Jennestad	Græva	33	507 225	7 625 671	HG	90-5d	Graphite schist		39.65	
	1990	Jennestad	Græva	33	507 225	7 625 671	HG	90-7a	Graphite schist		8.50	
	1990	Jennestad	Græva	33	507 225	7 625 671	HG	90-7b	Graphite schist		35.86	
	1990	Jennestad	Græva	33	507 225	7 625 671	HG	90-7c	Graphite schist		36.88	
	1990	Jennestad	Hornvatnet	33	507 570	7 625 318	HG	90-8	Graphite schist		1.71	
	1990	Jennestad	Hornvatnet	33	507 570	7 625 318	HG	90-9a	Graphite schist		26.22	
	1990	Jennestad	Hornvatnet	33	507 570	7 625 318	HG	90-9b	Graphite schist		37.23	
	1990	Jennestad	Hornvatnet	33	507 570	7 625 318	HG	90-9c	Graphite schist		39.23	
	1990	Jennestad	Hornvatnet	33	507 570	7 625 318	HG	90-9d	Graphite schist		44.31	
	1990	Jennestad	Græva	33	507 225	7 625 671	HG	90-7c	Graphite schist		36.88	
	1990	Vikeidet	Vikeidet	33	508 704	7 627 725	HG	90-15a	Graphite schist		13.88	
	1990	Vikeidet	Vikeidet	33	508 704	7 627 725	HG	90-15b	Graphite schist		16.66	
	1990	Vikeidet	Vedåsen	33	511 140	7 628 483	HG	90-19	Graphite schist		14.61	
	1990	Vikeidet	Vedåsen	33	511 140	7 628 483	HG	90-20	Graphite schist		24.25	
	1990	Jennestad	Lille Hornvatnet	33	508 592	7 625 860	HG	90-20a	Graphite schist		14.86	
	1990	Jennestad	Lille Hornvatnet	33	508 592	7 625 860	HG	90-21b	Graphite schist		16.57	
	1990	Jennestad	Lille Hornvatnet	33	508 592	7 625 860	HG	90-21c	Graphite schist		25.77	
	1990	Jennestad	Larmarkvatnet	33	510 369	7 625 405	HG	La-1	Graphite schist		12.32	

	1990	Jennestad	Larmarkvatnet	33	510 369	7 625 405	HG	La-2	Graphite schist		12.74	
	1990	Jennestad	Lille Hornvatnet	33	508 592	7 625 860	HG	LH-1	Graphite schist		18.02	
	1990	Jennestad	Lille Hornvatnet	33	508 592	7 625 860	HG	LH-2	Graphite schist		18.18	
	1990	Jennestad	Lille Hornvatnet	33	508 592	7 625 860	HG	LH-3	Graphite schist		14.79	
	1990	Jennestad	Lille Hornvatnet	33	508 592	7 625 860	HG	LH-4	Graphite schist		14.52	
	1990	Jennestad	Lille Hornvatnet	33	508 592	7 625 860	HG	LH-5	Graphite schist		11.95	
	1990	Jennestad	Lille Hornvatnet	33	508 592	7 625 860	HG	LH-6	Graphite schist		12.22	
	1990	Jennestad	Lille Hornvatnet	33	508 592	7 625 860	HG	LH-7	Graphite schist		14.25	
	1990	Jennestad	Lille Hornvatnet	33	508 592	7 625 860	HG	LH-8	Graphite schist		17.68	
	1991	Jennestad	Lille Hornvatnet	33	508 592	7 625 860	HG	911B2	Graphite schist		18.89	
	1991	Jennestad	Lille Hornvatnet	33	508 554	7 625 752	HG	9121a	Graphite schist		12.80	
	1991	Jennestad	Lille Hornvatnet	33	508 554	7 625 752	HG	9121b	Graphite schist		4.65	
	1991	Jennestad	Lille Hornvatnet	33	508 554	7 625 752	HG	9121c	Graphite schist		8.70	
	1991	Jennestad	Lille Hornvatnet	33	508 554	7 625 752	HG	9121d	Graphite schist		11.00	
	1991	Jennestad	Lille Hornvatnet	33	508 554	7 625 752	HG	9121e	Graphite schist		9.23	
	1991	Jennestad	Lille Hornvatnet	33	508 545	7 625 722	HG	9122b	Graphite schist		16.93	
	1991	Jennestad	Lille Hornvatnet	33	508 473	7 625 750	HG	9123a	Graphite schist		21.28	
	1991	Jennestad	Lille Hornvatnet	33	508 473	7 625 750	HG	9123b	Graphite schist		27.41	
	1991	Jennestad	Lille Hornvatnet	33	508 473	7 625 750	HG	9123c	Graphite schist		30.46	
	1991	Jennestad	Lille Hornvatnet	33	508 473	7 625 750	HG	9123d	Graphite schist		33.07	
	1991	Jennestad	Lille Hornvatnet	33	508 448	7 625 722	HG	9125	Graphite schist		7.80	
	1991	Jennestad	Lille Hornvatnet	33	508 427	7 625 680	HG	9126	Graphite schist		9.92	
	1991	Jennestad	Lille Hornvatnet	33	508 438	7 625 617	HG	9128a	Graphite schist		15.90	
	1991	Jennestad	Lille Hornvatnet	33	508 438	7 625 617	HG	9128b	Graphite schist		6.62	
	1991	Jennestad	Lille Hornvatnet	33	508 438	7 625 617	HG	9128c	Graphite schist		7.00	
	1991	Jennestad	Lille Hornvatnet	33	508 438	7 625 617	HG	9128d	Graphite schist		12.58	
	1991	Jennestad	Lille Hornvatnet	33	508 438	7 625 617	HG	9128e	Graphite schist		10.55	
	1991	Jennestad	Lille Hornvatnet	33	508 438	7 625 617	HG	9128f	Graphite schist		6.64	
	1991	Jennestad	Lille Hornvatnet	33	508 438	7 625 617	HG	9128g	Graphite schist		5.64	
	1991	Jennestad	Lille Hornvatnet	33	508 438	7 625 617	HG	9128h	Graphite schist		7.81	
	1991	Jennestad	Lille Hornvatnet	33	508 438	7 625 617	HG	9129	Graphite schist		10.60	
	1991	Jennestad	Lille Hornvatnet	33	508 438	7 625 617	HG	9130a	Graphite schist		9.22	
	1991	Jennestad	Lille Hornvatnet	33	508 438	7 625 617	HG	9130b	Graphite schist		9.80	
	1991	Jennestad	Lille Hornvatnet	33	508 438	7 625 617	HG	9130c	Graphite schist		9.27	

	1991	Jennestad	Golia	33	510 980	7 625 361	HG	9132	Graphite schist		10.20	
	1991	Jennestad	Golia	33	510 980	7 625 361	HG	9136a	Graphite schist		32.78	
	1991	Jennestad	Golia	33	510 980	7 625 361	HG	9138	Graphite schist		32.60	
	1991	Jennestad	Koven	33	510 079	7 625 023	HG	9139	Graphite schist		9.16	
	1991	Jennestad	Koven	33	510 079	7 625 023	HG	9147	Graphite schist		26.13	
	1991	Jennestad	Græva	33	507 225	7 625 671	HG	9148	Graphite schist		38.79	
	1991	Jennestad	Hornvatnet	33	507 570	7 625 318	HG	9153a	Graphite schist		38.42	
	1991	Jennestad	Lille Hornvatnet	33	508 592	7 625 860	HG	9159a	Graphite schist		9.62	
	1991	Jennestad	Lille Hornvatnet	33	508 592	7 625 860	HG	9159b	Graphite schist		10.93	
	1991	Jennestad	Græva	33	507 225	7 625 671	HG	9160	Graphite schist		1.30	
	1991	Jennestad	Larmarkvatnet	33	510 369	7 625 405	HG	9162	Graphite schist		8.13	
	1991	Jennestad	Larmarkvatnet	33	510 369	7 625 405	HG	9164	Graphite schist		3.18	
	1991	Jennestad	Larmarkvatnet	33	510 369	7 625 405	HG	9166	Graphite schist		12.23	
	1993	Jennestad	Græva	33	507 271	7 625 612	HG	9221	Graphite schist	< 0,02	34.63	
	1993	Jennestad	Græva	33	507 271	7 625 612	HG	9221b	Graphite schist	< 0,02	37.71	
	1993	Jennestad	Græva	33	507 271	7 625 612	HG	9221c	Graphite schist	0.51	35.06	
	1993	Jennestad	Græva	33	507 271	7 625 612	HG	9221d	Graphite schist	< 0,02	37.76	
	1993	Jennestad	Græva	33	507 271	7 625 612	HG	9221e	Graphite schist	0.22	38.08	
	1993	Jennestad	Græva	33	507 271	7 625 612	HG	9221f	Graphite schist	0.15	34.89	
	1993	Jennestad	Græva	33	507 271	7 625 612	HG	9221g	Graphite schist	< 0,02	21.31	
	1993	Jennestad	Græva	33	507 271	7 625 612	HG	9221h	Graphite schist	< 0,02	32.31	
	1993	Jennestad	Græva	33	507 271	7 625 612	HG	9221i	Graphite schist	0.06	22.83	
	1993	Jennestad	Græva	33	507 283	7 625 602	HG	9222A	Graphite schist	< 0,02	30.83	
	1993	Jennestad	Græva	33	507 283	7 625 602	HG	9222b	Graphite schist	0.02	28.75	
	1993	Jennestad	Græva	33	507 299	7 625 584	HG	9223	Graphite schist	< 0,02	35.10	
	1993	Jennestad	Hornvatnet	33	507 447	7 625 565	HG	9224a	Graphite schist	3.00	0.06	
	1993	Jennestad	Hornvatnet	33	507 447	7 625 565	HG	9224b	Graphite schist	3.20	7.68	
	1993	Jennestad	Hornvatnet	33	507 447	7 625 565	HG	9224c	Graphite schist	3.50	9.07	
	1993	Jennestad	Hornvatnet	33	507 448	7 625 537	HG	9225a	Graphite schist	3.08	7.37	
	1993	Jennestad	Hornvatnet	33	507 448	7 625 537	HG	9225b	Graphite schist	3.37	7.08	
	1993	Jennestad	Hornvatnet	33	507 448	7 625 537	HG	9225c	Graphite schist	2.36	2.90	
	1993	Jennestad	Hornvatnet	33	507 453	7 625 509	HG	9226a	Graphite schist	0.15	7.80	
	1993	Jennestad	Hornvatnet	33	507 453	7 625 509	HG	9226b	Graphite schist	0.66	7.49	
	1993	Jennestad	Hornvatnet	33	507 477	7 625 456	HG	9227a	Graphite schist	0.80	37.50	

	1993	Jennestad	Hornvatnet	33	507 477	7 625 456	HG	9227b	Graphite schist	0.45	33.89	
	1993	Jennestad	Hornvatnet	33	507 477	7 625 456	HG	9227c	Graphite schist	0.26	40.49	
	1993	Jennestad	Hornvatnet	33	507 477	7 625 456	HG	9227d	Graphite schist	0.07	28.67	
	1993	Jennestad	Hornvatnet	33	507 477	7 625 456	HG	9227e	Graphite schist	0.54	29.91	
	1993	Jennestad	Hornvatnet	33	507 489	7 625 440	HG	9228a	Graphite schist	0.39	38.35	
	1993	Jennestad	Hornvatnet	33	507 489	7 625 440	HG	9228b	Graphite schist	0.15	38.23	
	1993	Jennestad	Hornvatnet	33	507 489	7 625 440	HG	9228c	Graphite schist	0.09	31.68	
	1993	Jennestad	Hornvatnet	33	507 489	7 625 440	HG	9228d	Graphite schist	0.05	39.67	
	1993	Jennestad	Hornvatnet	33	507 521	7 625 411	HG	9229a	Graphite schist	0.20	40.73	
	1993	Jennestad	Hornvatnet	33	507 521	7 625 411	HG	9229b	Graphite schist	0.11	41.68	
	1993	Jennestad	Hornvatnet	33	507 521	7 625 411	HG	9229c	Graphite schist	0.05	32.26	
	1993	Jennestad	Hornvatnet	33	507 521	7 625 411	HG	9229d	Graphite schist	0.23	42.83	
	1993	Jennestad	Hornvatnet	33	507 438	7 625 659	HG	93-1a	Graphite schist	0.58	18.03	
	1993	Jennestad	Hornvatnet	33	507 438	7 625 659	HG	93-1b	Graphite schist	0.24	12.26	
	1993	Jennestad	Hornvatnet	33	507 438	7 625 659	HG	93-1c	Graphite schist	0.36	12.78	
	1993	Jennestad	Hornvatnet	33	507 438	7 625 659	HG	93-1d	Graphite schist	1.30	7.56	
	1993	Jennestad	Hornvatnet	33	507 438	7 625 659	HG	93-1e	Graphite schist	0.50	12.18	
	1993	Jennestad	Hornvatnet	33	507 438	7 625 659	HG	93-1f	Graphite schist	0.18	14.15	
	1993	Jennestad	Hornvatnet	33	507 412	7 625 699	HG	93-2a	Graphite schist	0.20	13.40	
	1993	Jennestad	Hornvatnet	33	507 412	7 625 699	HG	93-2b	Graphite schist	0.20	14.21	
	1993	Jennestad	Hornvatnet	33	507 412	7 625 699	HG	93-2c	Graphite schist	0.60	15.53	
	1993	Jennestad	Hornvatnet	33	507 412	7 625 699	HG	93-2d	Graphite schist	0.20	9.64	
	1993	Jennestad	Hornvatnet	33	507 378	7 625 725	HG	93-3a	Graphite schist	0.18	29.90	
	1993	Jennestad	Hornvatnet	33	507 378	7 625 725	HG	93-3b	Graphite schist	0.34	21.69	
	1993	Jennestad	Hornvatnet	33	507 378	7 625 725	HG	93-3c	Graphite schist	0.28	31.91	
	1993	Jennestad	Hornvatnet	33	507 378	7 625 725	HG	93-3d	Graphite schist	0.12	33.48	
	1993	Jennestad	Hornvatnet	33	507 378	7 625 725	HG	93-3e	Graphite schist	< 0,02	29.55	
	1993	Jennestad	Hornvatnet	33	507 378	7 625 725	HG	93-3f	Graphite schist	0.21	30.72	
	1993	Jennestad	Hornvatnet	33	507 378	7 625 725	HG	93-3g	Graphite schist	0.15	26.44	
	1993	Jennestad	Hornvatnet	33	507 251	7 625 822	HG	93-3h	Graphite schist	0.22	26.73	
	1993	Jennestad	Hornvatnet	33	507 251	7 625 822	HG	93-4a	Graphite schist	0.80	17.42	
	1993	Jennestad	Hornvatnet	33	507 251	7 625 822	HG	93-4b	Graphite schist	0.72	29.36	
	1993	Jennestad	Hornvatnet	33	507 251	7 625 822	HG	93-4c	Graphite schist	0.79	25.91	
	1993	Jennestad	Hornvatnet	33	507 251	7 625 822	HG	93-4D1	Graphite schist	< 0,02	14.52	

	1993	Jennestad	Hornvatnet	33	507 251	7 625 822	HG	93-4e	Graphite schist	0.20	14.05	
	1993	Jennestad	Hornvatnet	33	507 251	7 625 822	HG	93-4f	Graphite schist	< 0,02	9.00	
	1993	Jennestad	Hornvatnet	33	507 192	7 625 886	HG	93-5a	Graphite schist	1.57	10.48	
	1993	Jennestad	Hornvatnet	33	507 192	7 625 886	HG	93-5b	Graphite schist	1.04	10.54	
	1993	Jennestad	Hornvatnet	33	507 192	7 625 886	HG	93-5c	Graphite schist	3.20	8.03	
	1993	Jennestad	Hornvatnet	33	507 192	7 625 886	HG	93-5d	Graphite schist	4.91	12.27	
	1993	Jennestad	Hornvatnet	33	507 192	7 625 886	HG	93-5e	Graphite schist	0.80	13.05	
	1993	Jennestad	Hornvatnet	33	507 192	7 625 886	HG	93-5f	Graphite schist	2.19	6.88	
	1993	Jennestad	Hornvatnet	33	507 173	7 625 918	HG	93-6a	Graphite schist	1.16	22.29	
	1993	Jennestad	Hornvatnet	33	507 173	7 625 918	HG	93-6b	Graphite schist	1.35	19.52	
	1993	Jennestad	Hornvatnet	33	507 173	7 625 918	HG	93-6c	Graphite schist	2.26	19.50	
	1993	Jennestad	Hornvatnet	33	507 173	7 625 918	HG	93-6d	Graphite schist	1.67	20.07	
	1993	Jennestad	Hornvatnet	33	507 173	7 625 918	HG	93-6e	Graphite schist	1.92	11.65	
	1993	Jennestad	Hornvatnet	33	507 173	7 625 918	HG	93-6f	Graphite schist	1.52	17.39	
71951	2012	Jennestad	Golia	33	510 982	7 625 361	HG	HG1-12	Banded graphite schist		9.33	
71952	2012	Jennestad	Golia	33	510 785	7 625 331	HG	HG2-12	High grade graphite schist from bedrock exposure		24.41	
71953	2012	Jennestad	Koven	33	510 079	7 625 023	HG	HG3-12	Weathered but coarse flake graphite schist		23.02	
71954	2012	Jennestad	Koven	33	510 102	7 625 026	HG	HG4-12	Weathered but coarse flake graphite schist		18.89	
71955	2012	Jennestad	Hornvatnet	33	507 225	7 625 670	HG	HG5-12	High grade graphite schist		39.11	
71956	2012	Jennestad	Hornvatnet	33	507 225	7 625 670	HG	HG6-12	High grade graphite schist		36.70	
71957	2012	Jennestad	Lille Hornvatnet	33	508 574	7 625 822	HG	HG7-12	Graphite schist		15.57	
71958	2012	Jennestad	Lille Hornvatnet	33	508 574	7 625 822	HG	HG8-12	Graphite schist		9.01	
71959	2012	Sommarland	Sommarland	33	487 621	7 626 290	HG	HG9-12	Graphite schist		9.26	
71960	2012	Sommarland	Sommarland	33	487 621	7 626 290	HG	HG10-12	Graphite schist		17.13	
71961	2012	Sommarland	Sommarland	33	487 589	7 626 310	HG	HG11-12	Graphite schist		4.05	
71962	2012	Sommarland	Sommarland	33	487 589	7 626 310	HG	HG12-12	Graphite schist		2.83	
71963	2012	Sommarland	Sommarland	33	487 589	7 626 310	HG	HG13-12	Graphite schist		5.44	

71964	2012	Kvern fjorden - Haugsnes	Haugneset	33	488 356	7 619 263	HG	HG14-12	Massive and high grade graphite schist		33.82	
71965	2012	Kvern fjorden - Haugsnes	Haugneset	33	488 356	7 619 263	HG	HG15-12	Massive and high grade graphite schist		14.71	
71966	2012	Kvern fjorden - Haugsnes	Haugneset	33	488 356	7 619 263	HG	HG16-12	Massive and high grade graphite schist		33.68	
71967	2012	Kvern fjorden - Haugsnes	Haugneset	33	488 356	7 619 263	HG	HG17-12	Massive and high grade graphite schist		33.71	
71968	2012	Kvern fjorden - Haugsnes	Haugneset	33	488 238	7 618 895	HG	HG18-12	Massive and high grade graphite schist		14.21	
71969	2012	Kvern fjorden - Haugsnes	Haugneset	33	488 238	7 618 895	HG	HG19-12	Massive and high grade graphite schist		15.17	
71970	2012	Kvern fjorden - Haugsnes	Haugneset	33	488 238	7 618 895	HG	HG20-12	Massive and high grade graphite schist		13.73	
71971	2012	Kvern fjorden - Haugsnes	Haugneset	33	488 274	7 618 822	HG	HG21-12	Massive and high grade graphite schist		12.36	
71972	2012	Morfjorden	Morfjord mine	33	487 144	7 586 575	HG	HG22-12	Disseminated graphite schist		16.80	
71973	2012	Morfjorden	Morfjord mine	33	487 144	7 586 575	HG	HG23-12	Disseminated graphite schist		19.70	
71985	2012	Jennestad	Golia	33	510 982	7 625 362	JEW	JW12-1	Banded graphite schist		7.40	
71986	2012	Jennestad	Golia	33	510 982	7 625 362	JEW	JW12-2	Banded graphite schist		5.69	
71987	2012	Jennestad	Golia	33	510 785	7 625 343	JEW	JW12-3	High grade graphite schist from bedrock exposure		18.37	
71988	2012	Jennestad	Koven	33	510 084	7 625 026	JEW	JW12-4	Weathered but coarse flake graphite schist		21.14	
71989	2012	Jennestad	Koven	33	510 084	7 625 026	JEW	JW12-5	Weathered but coarse flake graphite schist		24.03	
71990	2012	Jennestad	Hornvatnet	33	507 580	7 625 322	JEW	JW12-6	Massive and high grade graphite schist		36.68	
71991	2012	Jennestad	Hornvatnet	33	507 580	7 625 322	JEW	JW12-7	Massive and high grade graphite schist		28.62	
71992	2012	Morfjorden	Morfjord mine	33	486 956	7 587 163	JEW	JW12-8	Disseminated graphite schist		18.86	

82075	2013	Smines	Kaldhammaren	33	498 963	7 639 395	BD	BD Øks 1323B-1	Graphite schist	3.05	15.5	
Externa l	2013	Smines	Kaldhammaren	33	498 963	7 639 395	BD	BD Øks 1323B-2	Graphite schist	0.42	10.3	
82101	2014	Smines	Stigbergan	33	499 596	7 638 408	BD	BD Øks 1403A	Fine grained felsic gneiss	2.29	0.39	0.39
82102	2014	Smines	Stigbergan	33	499 596	7 638 408	BD	BD Øks 1403B	Medium grained felsic vein	1.21	0.55	0.42
82103	2014	Smines	Stigbergan	33	499 621	7 638 475	BD	BD Øks 1404	Fine grained felsic gneiss	0.02	0.40	0.32
82107	2014	Smines	Smines	33	499 050	7 638 733	BD	BD Øks 1410	Fine grained felsic gneiss, rich in graphite	0.69	14.4	14.2
82109	2014	Smines	Smines	33	498 988	7 638 540	BD	BD Øks 1412A	Fine grained felsic gneiss	2.60	0.34	0.32
82120	2014	Smines	Kaldhammaren	33	498 815	7 639 408	BD	BD Øks 1435A	Rusty weathering graphitic schist	2.32	3.44	3.32
82121	2014	Smines	Kaldhammaren	33	498 815	7 639 408	BD	BD Øks 1435B	Rusty weathering graphitic schist	5.92	16.3	17.1
82127	2014	Smines	Rota	33	497 526	7 638 615	BD	BD Øks 1449A	Massive sulphides, with graphite	17.9	2.65	2.70
82128	2014	Smines	Rota	33	497 526	7 638 615	BD	BD Øks 1449B	Massive sulphides, with graphite	19.8	1.73	1.76
82131	2014	Smines	Rota	33	497 402	7 638 507	BD	BD Øks 1451	Fine grained felsic gneiss	1.92	0.66	0.63
82138	2014	Myre	Stavdalen	33	505 360	7 640 904	BD	BD Øks 1458	Rusty zone in fine grained felsic gneiss	7.99	2.39	2.31
82142	2014	Brenna	Grønjorda	33	502 119	7 628 636	BD	BD Øks 1464A	Rusty weathering graphitic schist with sulphides	2.87	8.58	8.77
82143	2014	Brenna	Grønjorda	33	502 119	7 628 636	BD	BD Øks 1464B	Fine grained banded felsic gneiss with sulphides and graphite	1.91	2.41	2.39
82148	2014	Myre	Myre, harbour	33	503 035	7 643 984	BD	BD Øks 1479	Fine grained felsic gneiss, with pyrrhotite	2.61	0.45	0.36

82149	2014	Myre	Myre, harbour	33	503 030	7 643 882	BD	BD Øks 1480A	Fine grained felsic gneiss, with pyrrhotite	1.70	2.38	2.37
82151	2014	Myre	Myre, harbour	33	503 126	7 643 810	BD	BD Øks 1481	Fine grained felsic gneiss, with pyrrhotite	1.24	0.51	0.46
82152	2014	Myre	Myre, harbour	33	503 162	7 643 794	BD	BD Øks 1482	Fine grained felsic gneiss, with pyrrhotite	0.69	0.33	0.31
82153	2014	Myre	Myre, harbour	33	503 125	7 643 723	BD	BD Øks 1483	Fine grained felsic gneiss, with pyrrhotite	6.93	1.66	1.63
82164	2014	Myre	Myre, harbour	33	503 445	7 644 305	BD	BD Øks 1496	Fine grained felsic gneiss	0.04	0.44	0.27
82170	2014	Myre	Stavdalen	33	504 587	7 641 203	BD	BD Øks 14108	Fine grained felsic gneiss, rusty with sulphides	2.81	0.40	0.38
82176	2014	Myre	Stavdalen	33	504 518	7 640 605	BD	BD Øks 14117A	Fine grained felsic gneiss, rusty with sulphides	0.15	0.64	0.55
82178	2014	Myre	Stavdalen	33	504 581	7 640 634	BD	BD Øks 14119	Fine grained felsic gneiss, rusty with sulphides	3.49	0.38	0.34
82180	2014	Myre	Stavdalen	33	504 645	7 640 820	BD	BD Øks 14123	Fine grained felsic gneiss, rusty with sulphides	6.35	1.46	1.44
82181	2014	Myre	Stavdalen	33	505 120	7 640 360	BD	BD Øks 14126A	Rusty weathering gneiss	8.16	1.31	1.26
82182	2014	Myre	Stavdalen	33	505 120	7 640 360	BD	BD Øks 14126B	Rusty weathering gneiss	13.0	1.91	1.87
82184	2014	Skogsøya	Skavlneset	33	498 180	7 640 374	BD	BD Øks 14128A	Rusty zone with sulphides and minor graphite	2.01	2.88	2.75
82185	2014	Skogsøya	Skavlneset	33	498 180	7 640 374	BD	BD Øks 14128B	Rusty zone with graphite	0.54	4.44	4.43
82187	2014	Skogsøya	Skavlneset	33	498 263	7 640 351	BD	BD Øks 14129A	High grade graphitic schist	0.08	31.6	29.1
82188	2014	Skogsøya	Skavlneset	33	498 263	7 640 351	BD	BD Øks 14129B	High grade graphitic schist	0.06	34.9	31.2

82189	2014	Skogsøya	Skavlneset	33	498 263	7 640 351	BD	BD Øks 14129C	High grade graphitic schist	0.17	27.8	25.2
82193	2014	Skogsøya	Skavlneset	33	498 330	7 640 292	BD	BD Øks 14130	Rusty zone with sulphides and minor graphite	2.13	1.29	1.25
82194	2014	Skogsøya	Skavlneset	33	498 336	7 640 300	BD	BD Øks 14131	Rusty zone with sulphides and minor graphite	3.75	0.75	0.74
82200	2014	Dverberg - Skogvoll	Haugneset, Saura	33	542 110	7 670 382	BD	BD And 1452B	Banded metasiltstone with fine grained quartz and graphite	< 0,02	2.26	1.62
92127	2014	Jennestad	Jennestad, shore	33	512 657	7 626 511	BD	BD Jen 1454A	Graphite schist	2.22	3.53	
92132	2014	Jennestad	Jennestad, shore	33	512 767	7 626 493	BD	BD Jen 1460A	Graphite schist	0.15	15.2	
92134	2014	Jennestad	Jennestad, shore	33	512 765	7 626 502	BD	BD Jen 1461A	Graphite schist	0.26	10.9	
92083	2014	Jennestad	Jennestad, shore	33	512 765	7 626 502	BD	BD Jen 1461B	Fine grained qz rich rock	< 0,02	1.17	
92135	2014	Jennestad	Jennestad, shore	33	512 791	7 626 512	BD	BD Jen 1462	Graphite schist	0.46	7.21	
90432	2014	Brenna	Grønjorda	33	502 109	7 628 640	HG	HG31b-14	Graphite schist	4.07	9.90	
90433	2014	Brenna	Grønjorda	33	501 851	7 629 256	HG	HG32a-14	Graphite schist	< 0,02	3.89	
90434	2014	Skogsøya	Skavlneset	33	498 270	7 640 336	HG	HG32b-14	Graphite schist	0.32	29.10	
90435	2014	Skogsøya	Skavlneset	33	498 270	7 640 336	HG	HG33-14	Graphite schist	0.06	19.00	
90436	2014	Skogsøya	Skavlneset	33	498 267	7 640 357	HG	HG34-14	Graphite schist	< 0,02	34.20	
90437	2014	Skogsøya	Skavlneset	33	498 225	7 640 414	HG	HG35-14	Graphite schist	< 0,02	16.70	
90438	2014	Skogsøya	Skavlneset	33	498 139	7 640 440	HG	HG36-14	Graphite schist	1.76	26.40	
90439	2014	Skogsøya	Skavlneset	33	497 813	7 640 671	HG	HG37-14	Graphite schist	0.51	6.46	
90440	2014	Skogsøya	Skavlneset	33	498 345	7 639 890	HG	HG38-14	Graphite schist	0.02	24.90	
90441	2014	Skogsøya	Skavlneset	33	498 345	7 639 890	HG	HG39-14	Graphite schist	0.02	21.80	
90442	2014	Smines	Kaldhammaren	33	498 966	7 639 397	HG	HG40-14	Graphite schist	0.86	13.80	
90443	2014	Smines	Smines	33	498 977	7 638 646	HG	HG41-14	Graphite schist	0.15	3.92	
90444	2014	Smines	Rota	33	497 537	7 638 596	HG	HG42-14	Graphite schist	0.03	0.56	
90445	2014	Kvern fjorden - Haugnes	Kvern fjorddalen	33	488 628	7 622 908	HG	HG43-14	Graphite schist	0.02	0.12	
90446	2014	Kvern fjorden - Haugnes	Kvern fjorddalen	33	488 628	7 622 906	HG	HG44-14	Graphite schist	< 0,02	0.47	

90447	2014	Kvernfjorden - Haugnes	Kvernfjorddalen	33	488 628	7 622 906	HG	HG45-14	Graphite schist	< 0,02	13.70	
90448	2014	Møkland - Sund	Bjønndalen	33	486 633	7 628 877	HG	HG46-14	Graphite schist	< 0,02	16.70	
90449	2014	Møkland - Sund	Bjønndalen	33	486 633	7 628 877	HG	HG47-14	Graphite schist	< 0,02	16.10	
90450	2014	Møkland - Sund	Bjønndalen	33	486 640	7 628 864	HG	HG48-14	Graphite schist	< 0,02	25.70	
90451	2014	Møkland - Sund	Bjønndalen	33	486 640	7 628 864	HG	HG49-14	Graphite schist	0.05	21.10	
106963	2014	Romsetfjordenen	Sæterbukta	33	499 697	7 637 668	OL	OL-14067	Banded felsic gneiss, garnet bearing		0.52	0.50
108051	2014	Myre	Rødhamran	33	506 260	7 643 098	ET	5-14	Fine grained mafic gneiss with rusty weathering and minor sulphides	0.89	0.28	
108056	2014	Skogsøya	Skavneset	33	498 181	7 640 380	ET	36-14	Rusty weathered quartzite	0.41	0.55	
108057	2014	Skogsøya	Skavneset	33	498 376	7 640 309	ET	38-14	Fine grained felsic gneiss	< 0.02	0.22	
90456	2015	Sminess	Kaldhammaren	33	498 817	7 639 406	HG	hg1-15	Graphite schist	1.54	17.30	
90457	2015	Møkland - Sund	Skatskaran	33	486 149	7 627 757	HG	hg2-15	Graphite schist loose boulder	0.52	1.13	
90458	2015	Møkland - Sund	Skatskaran	33	486 154	7 627 755	HG	hg3-15	Graphite schist loose boulder	0.05	6.19	
90459	2015	Møkland - Sund	Skatskaran	33	486 163	7 627 753	HG	hg4-15	Graphite schist loose boulder	0.03	4.48	
90461	2015	Møkland - Sund	Bjønndalen	33	486 631	7 628 873	HG	hg6-15	Good quality graphite schist	0.03	16.90	
90462	2015	Sminess	Kaldhammaren	33	499 008	7 639 342	HG	hg7-15	Graphite schist	0.06	10.50	
90463	2015	Sminess	Kaldhammaren	33	499 004	7 639 342	HG	hg8-15	Graphite schist	2.39	2.71	
90464	2015	Jennestad	Koven	33	510 277	7 625 132	HG	hg9-15	Graphite schist	0.73	13.30	
90465	2015	Jennestad	Koven	33	510 277	7 625 132	HG	hg10-15	Graphite schist	0.26	12.70	
90466	2015	Møkland - Sund	Bjønndalen	33	486 633	7 628 873	HG	hg11-15	Rich graphite schist	< 0,02	17.70	
90467	2015	Møkland - Sund	Bjønndalen	33	486 631	7 628 839	HG	hg12-15	Graphite schist	0.08	0.12	
90468	2015	Møkland - Sund	Bjønndalen	33	486 632	7 628 842	HG	hg13-15	Graphite schist	3.83	0.11	
90469	2015	Møkland - Sund	Bjønndalen	33	486 627	7 628 843	HG	hg14-15	Graphite schist	1.53	0.17	

90470	2015	Møkland - Sund	Bjønndalen	33	486 627	7 628 843	HG	hg15-15	Graphite schist	3.07	< 0,06	
90471	2015	Møkland - Sund	Høgdene	33	486 457	7 628 305	HG	hg16-15	Coarse flaky graphite schist	0.05	14.70	
90472	2015	Møkland - Sund	Høgdene	33	486 454	7 628 298	HG	hg17-15	Coarse flaky graphite schist	0.14	18.10	
90473	2015	Møkland - Sund	Høgdene	33	486 454	7 628 314	HG	hg18-15	Qtz fsp rock with graphite	2.89	0.16	
90474	2015	Møkland - Sund	Høgdene	33	486 456	7 628 313	HG	hg19 -15	Qtz fsp rock with graphite	4.78	0.35	
90475	2015	Møkland - Sund	Høgdene	33	486 453	7 628 307	HG	hg20-15	Coarse flaky graphite schist	0.04	18.30	
90476	2015	Møkland - Sund	Høgdene	33	486 456	7 628 315	HG	hg21-15	Very weathered graphite schist	0.14	13.40	
90477	2015	Møkland - Sund	Høgdene	33	486 463	7 628 307	HG	hg22-15	Amphibolite country rock	0.08	< 0,06	
90478	2015	Kvern fjorden - Haugsnes	Haugneset	33	488 623	7 622 905	HG	hg23-15	Graphite schist	< 0,02	10.60	
90479	2015	Smies	Kaldhammaren	33	499 009	7 639 339	HG	hg24-15	Aggregated trench sample	1.03	12.80	
90480	2015	Smies	Kaldhammaren	33	499 009	7 639 339	HG	hg25-15	Aggregated trench sample	0.78	10.60	
90481	2015	Smies	Kaldhammaren	33	499 009	7 639 339	HG	hg26-15	Aggregated trench sample	3.05	4.38	
90482	2015	Smies	Kaldhammaren	33	499 009	7 639 339	HG	hg27-15	Aggregated trench sample	3.10	1.46	
90483	2015	Smies	Kaldhammaren	33	499 009	7 639 339	HG	hg28-15	Aggregated trench sample	2.15	9.66	
90484	2015	Møkland - Sund	Bjønndalen	33	486 629	7 628 840	HG	hg29-15	Aggregated trench sample	1.58	< 0,06	
90485	2015	Møkland - Sund	Bjønndalen	33	486 629	7 628 840	HG	hg30-15	Aggregated trench sample	2.93	< 0,06	
90486	2015	Møkland - Sund	Bjønndalen	33	486 629	7 628 840	HG	hg31-15	Aggregated trench sample	1.70	0.09	
130707	2015	Møkland - Sund	Bjønndalen	33	486 632	7 628 842	AE	BH1BØ26.30	Country rock	0.950	13.0	15.0
130708	2015	Møkland - Sund	Bjønndalen	33	486 632	7 628 842	AE	BH1BØ26.50	Country rock	3.00	0.38	0.39

130711	2015	Møkland - Sund	Bjønndalen	33	486 632	7 628 842	AE	BH1BØ28.90	Country rock	1.00	5.90	6.10
130713	2015	Møkland - Sund	Bjønndalen	33	486 632	7 628 842	AE	BH1BØ30.10	Massive graphite ore	2.20	14.0	14.0
130714	2015	Møkland - Sund	Bjønndalen	33	486 632	7 628 842	AE	BH1BØ30.60	Massive graphite ore	1.90	32.0	32.0
106468	2016	Ingelsfjorden	Storå	33	511 084	7 594 428	NC	RAF106468	Graphite xenolith in mangerite	5.88	10.5	
92191	2016	Romsetfjorden	Langstrand	33	500 639	7 633 996	BD	BD Øks 1601a	Graphite schist	0.28	17.3	17.2
92192	2016	Romsetfjorden	Langstrand	33	500 639	7 633 996	BD	BD Øks 1601b	Graphite schist	1.12	18.2	18.7
92193	2016	Romsetfjorden	Romset	33	500 412	7 634 791	BD	BD Øks 1602a	Graphite schist	0.03	31.0	30.7
92195	2016	Romsetfjorden	Romset	33	500 412	7 634 791	BD	BD Øks1602c	Pegmatite	0.07	9.80	9.77
92198	2016	Romsetfjorden	Romset	33	500 730	7 634 761	BD	BD Øks 1605	Graphite schist	0.39	3.92	3.98
92200	2016	Romsetfjorden	Romset	33	500 804	7 634 942	BD	BD Øks 1607	Graphite schist	0.52	14.7	14.4
99390	2016	Romsetfjorden	Romset	33	500 454	7 634 597	BD	BD Øks 1609	Graphite schist	0.06	14.2	14.5
97603	2016	Kvernfjorden - Haugnes	Kvernfjorddalen	33	488 625	7 622 904	HS	n.a.	Graphite schist	< 0.02	14.2	14.1
128468	2016	Skogsøya	Skavlneset	33	498 270	7 640 354	AE	140212	Graphite ore	0.05	38.4	38.6
128469	2016	Skogsøya	Skavlneset	33	498 270	7 640 354	AE	140213	Graphite ore	0.03	38.2	37.9
128481	2016	Skogsøya	Svinøya	33	498 342	7 639 890	AE	140225	Graphite ore	0.09	11.6	11.3
128482	2016	Skogsøya	Svinøya	33	498 342	7 639 890	AE	140226	Graphite lenses	0.02	11	11.3
128483	2016	Skogsøya	Svinøya	33	498 342	7 639 890	AE	140227	Graphite lenses	0.05	12.5	12.7
128484	2016	Skogsøya	Svinøya	33	498 342	7 639 890	AE	140228	Graphite lenses	0.95	0.18	0.15
128485	2016	Smines	Kaldhammaren	33	498 963	7 639 389	AE	140229	Graphite ore	7.95	5.36	5.48
128487	2016	Møkland - Sund	Skatskaran	33	486 191	7 627 796	AE	140231	Graphite ore	0.10	3.06	2.96
128493	2016	Jennestad	Koven	33	510 050	7 625 033	AE	140235	Graphite ore	< 0,02	11.9	12.1
128495	2016	Jennestad	Græva	33	507 578	7 625 322	AE	140237	Rich graphite ore	0.12	40.3	39.9
140101	2016	Møkland - Sund	Skatskaran	33	486 140	7 627 616	HG	hg1-16	Rotten weathered graphite schist	0.04	22.30	
140102	2016	Møkland - Sund	Skatskaran	33	486 142	7 627 618	HG	hg2-16	Rotten weathered graphite schist	0.15	12.40	
140103	2016	Møkland - Sund	Skatskaran	33	486 134	7 627 619	HG	hg3-16	Rotten weathered graphite schist	0.13	16.60	
140104	2016	Møkland - Sund	Skatskaran	33	486 132	7 627 617	HG	hg4-16	Rotten weathered graphite schist	0.03	10.60	
140105	2016	Møkland - Sund	Skatskaran	33	486 193	7 627 799	HG	hg5-16	Rotten weathered graphite schist	0.07	7.32	

140106	2016	Møkland - Sund	Skatskaran	33	486 192	7 627 796	HG	hg6-16	Good quality graphite schist	0.10	2.16	
140107	2016	Kvernfjorden - Haugsnes	Kvernfjorddalen	33	486 190	7 627 797	HG	hg7-16	Good quality graphite schist	0.09	11.70	
140108	2016	Kvernfjorden - Haugsnes	Kvernfjorddalen	33	488 618	7 622 873	HG	hg8-16	Disseminated graphite schist	0.03	4.28	
140109	2016	Myre	Rødhamran	33	505 696	7 642 187	HG	hg9-16	Graphite schist loose boulder	< 0,02	25.90	
140110	2016	Myre	Rødhamran	33	505 696	7 642 187	HG	hg10-16	Graphite schist loose boulder	< 0,02	17.10	
140111	2016	Myre	Rødhamran	33	505 770	7 642 183	HG	hg11-16	Graphite schist loose boulder	0.08	19.80	
140112	2016	Myre	Rødhamran	33	505 770	7 642 183	HG	hg12-16	Graphite schist loose boulder	0.04	11.70	
140113	2016	Skogsøya	Skavneset	33	497 896	7 640 656	HG	hg13-16	Low grade graphite schist	2.58	0.40	
140114	2016	Skogsøya	Skavneset	33	497 840	7 640 813	HG	hg14-16	Low grade graphite schist	0.08	6.91	
140115	2016	Vikeidet	Vedåsen	33	510 984	7 628 557	HG	hg15-16	Loose boulder weathered graphite schist	0.03	11.50	
140116	2016	Jennestad	Koven	33	510 039	7 624 973	HG	hg16-16	Medium grade graphite schist	0.09	0.85	
140117	2016	Jennestad	Koven	33	510 039	7 624 973	HG	hg17-16	Medium grade graphite schist	0.06	2.37	
140118	2016	Romsetfjorden	Langstrand	33	500 587	7 634 047	HG	hg18-16	Weathered sulphide rich graphite schist	1.33	3.62	
140119	2016	Romsetfjorden	Langstrand	33	500 587	7 634 047	HG	hg19-16	Weathered sulphide rich graphite schist	1.62	5.44	
140120	2016	Romsetfjorden	Langstrand	33	500 620	7 634 013	HG	hg20-16	Weathered sulphide rich graphite schist	1.20	11.90	

140121	2016	Romsetfjorden	Langstrand	33	500 622	7 634 010	HG	hg21-16	Weathered sulphide rich graphite schist	4.03	25.60	
140122	2016	Romsetfjorden	Langstrand	33	500 625	7 634 004	HG	hg22-16	Weathered sulphide rich graphite schist	10.90	15.40	
140123	2016	Romsetfjorden	Langstrand	33	500 634	7 633 995	HG	hg23-16	Weathered sulphide rich graphite schist	0.16	12.50	
140124	2016	Kvern fjorden - Haugsnes	Haugneset	33	488 563	7 620 431	HG	hg24-16	Medium grade graphite schists	0.07	17.70	
140125	2016	Møkland - Sund	Skatskaran	33	486 190	7 627 797	JK	JK-1	Weathered graphite schist	0.17	13.40	
140126	2016	Møkland - Sund	Skatskaran	33	486 177	7 627 634	JK	JK-2	Amphibolite with graphite and sulfides	4.23	< 0,06	
140127	2016	Møkland - Sund	Skatskaran	33	486 139	7 627 617	JK	JK-3	Weathered graphite schist	0.03	5.76	
140128	2016	Møkland - Sund	Skatskaran	33	486 143	7 627 615	JK	JK-4	Weathered graphite schist	0.05	7.97	
140129	2016	Møkland - Sund	Skatskaran	33	486 141	7 627 615	JK	JK-5	Weathered graphite schist	0.14	18.10	
140130	2016	Møkland - Sund	Skatskaran	33	486 141	7 627 615	JK	JK-5(B)	Weathered graphite schist (wall)	0.02	18.10	
140131	2016	Møkland - Sund	Skatskaran	33	486 188	7 627 795	JK	JK-6	Weathered graphite schist	0.09	2.45	
140141	2016	Møkland - Sund	Skatskaran	33	486 188	7 627 795	JK	JK-6B	Weathered graphite schist	0.10	14.50	
140132	2016	Møkland - Sund	Skatskaran	33	486 190	7 627 797	JK	JK-7	Weathered graphite schist	0.92	0.47	
140133	2016	Kvern fjorden - Haugsnes	Haugneset	33	488 236	7 618 894	JK	JK8	Graphite schist	0.09	12.60	
140138	2016	Myre	Rødhamran	33	505 771	7 642 181	JK	JK9	Graphite schists loose boulder	0.05	18.80	
140134	2016	Myre	Rødhamran	33	505 824	7 642 184	JK	JK10	Graphite schists loose boulder	0.05	7.77	

140135	2016	Myre	Rødhamran	33	505 850	7 642 189	JK	JK11	Graphite schists loose boulder	0.08	12.30	
140136	2016	Myre	Rødhamran	33	505 871	7 642 194	JK	JK12	Graphite schists loose boulder	0.03	24.10	
140137	2016	Myre	Rødhamran	33	505 937	7 642 166	JK	JK13	Graphite schists loose boulder	0.64	11.20	
140139	2016	Skogsøya	Skavneset	33	498 266	7 640 354	JK	JK-14	Well exposed graphite outcrop, 348/80E	0.05	24.50	
140140	2016	Skogsøya	Skavneset	33	498 136	7 640 440	JK	JK-15	Graphite schist, old trench	0.14	29.20	
132750	2017	Sommarland	Sommarland	33	487 674	7 626 459	BD	BD Bø 1796	Graphite schist	< 0,02	15.3	16.4
132751	2017	Sommarland	Sommarland	33	487 534	7 626 234	BD	BD Bø 17100	Medium- to coarse grained granite with graphite as coarse grains and aggregates.			
132753	2017	Sommarland	Sommarland	33	487 713	7 626 405	BD	BD Bø 17105	Graphite schist	0.22	14.6	14.8
132783	2017	Romsetfjordenen	Sæterbukta	33	500 297	7 637 190	BD	BD Øks 1714	Fine grained felsic gneiss, partly rusty	0.66	0.46	0.44
132787	2017	Romsetfjordenen	Sæterbukta	33	500 435	7 637 123	BD	BD Øks 1718	Graphite schist	< 0,02	20.9	20.5
132800	2017	Sørfjorden	Sørfjorden	33	531 769	7 618 051	BD	BD Sor 1702	Graphite schist	< 0,02	29.4	28.4
137157	2017	Sommarland	Sommarland	33	487 668	7 626 464	HG	H3-17	Graphite schist	< 0,02	17.2	
137158	2017	Sommarland	Sommarland	33	487 668	7 626 464	HG	H4-17	Graphite schist	< 0,02	12.4	
137159	2017	Sommarland	Sommarland	33	487 668	7 626 464	HG	H5-17	Graphite schist	< 0,02	16.1	
137160	2017	Sommarland	Sommarland	33	487 722	7 626 399	HG	Hg6-17	Graphite schist	0.36	18.2	
137161	2017	Morfjorden	Sellåter	33	487 897	7 589 189	HG	Hg8-17	Graphite schist	0.69	5.69	
137162	2017	Morfjorden	Sellåter	33	487 897	7 589 189	HG	Hg9-17	Graphite schist	0.32	5.83	
137163	2017	Morfjorden	Sellåter	33	487 894	7 589 187	HG	Hg10-17	Graphite schist	0.96	7.87	
137164	2017	Morfjorden	Sellåter	33	487 898	7 589 194	HG	Hg11-17	Mafic rock for thin section	3.20	5.38	
137165	2017	Morfjorden	Morfjorden mine	33	487 012	7 587 147	HG	hg12-17	Graphite schist	0.99	9.72	
137166	2017	Morfjorden	Sommarhus	33	486 962	7 588 922	HG	hg14-17	Graphite schist	0.34	33.3	
137167	2017	Morfjorden	Sommarhus	33	486 969	7 588 919	HG	Hg15-17	Graphite schist	0.48	37.7	
137168	2017	Morfjorden	Sommarhus	33	487 019	7 588 991	HG	Hg16-17	Graphite schist	0.03	26.6	
137169	2017	Morfjorden	Sommarhus	33	486 985	7 588 930	HG	hg17-17	Graphite schist	0.08	22.0	

137170	2017	Morfjorden	Sommarhus	33	486 981	7 588 914	HG	Hg18-17	Graphite schist	< 0,02	11.3	
137171	2017	Morfjorden	Sommarhus	33	487 017	7 588 984	HG	hg19-17	Graphite schist	0.03	12.9	
137172	2017	Brenna	Grønjorda	33	502 146	7 628 862	HG	hg20-17	Graphite schist	0.03	30.4	
137173	2017	Brenna	Grønjorda	33	502 135	7 628 872	HG	hg21-17	Graphite schist	0.06	10.7	
137174	2017	Brenna	Grønjorda	33	502 059	7 628 968	HG	hg22-17	Graphite schist	< 0,02	5.09	
137184	2017	Morfjorden	Sommarhus	33	487 019	7 588 991	JK	jk2617-1	Graphite schist	0.03	24.7	
137175	2017	Sommarland	Sommarland	33	487 724	7 626 393	JK	JK28517-1	Loose boulder of graphite schist	0.66	9.48	
137176	2017	Sommarland	Sommarland	33	487 712	7 626 405	JK	jk28517-2	Loose boulder of graphite schist	0.02	17.8	
137177	2017	Sommarland	Sommarland	33	487 708	7 626 409	JK	JK28517-3	Loose boulder of graphite schist	0.07	11.0	
137178	2017	Sommarland	Sommarland	33	487 698	7 626 374	JK	JK28517-4	Bolder	0.03	16.4	
137179	2017	Smines	Rota	33	497 532	7 638 596	JK	JK29517-8	Graphite schist	0.03	8.57	
137180	2017	Smines	Rota	33	497 558	7 638 628	JK	JK29517-pf7	mags10pf7/no graphite	0.15	0.37	
137181	2017	Smines	Smines	33	499 051	7 638 736	JK	JK29517-9	Graphite schist, CP grounding point	0.33	13.2	
137182	2017	Morfjorden	Sellåter	33	487 853	7 589 590	JK	JK30517-3	Graphite outcrop-contact sone	0.39	6.29	
137183	2017	Morfjorden	Morfjorden mine	33	487 246	7 586 598	JK	JK30517-5	Morfjord mine graphite schist	0.12	3.30	
137185	2017	Myre	Rødhamran	33	505 880	7 642 242	JK	JK3617-1	Graphite schist	0.12	23.1	
137186	2017	Myre	Rødhamran	33	505 735	7 641 993	JK	JK3617-3	Loose boulders of graphite schist	0.07	9.02	
137187	2017	Myre	Rødhamran	33	505 675	7 641 959	JK	JK3617-5	Loose boulders of graphite schist	0.12	6.71	
137188	2017	Myre	Rødhamran	33	505 653	7 641 935	JK	JK3617-6	Loose boulders of graphite schist	0.02	10.1	
137189	2017	Myre	Rødhamran	33	505 584	7 641 943	JK	JK3617-7	Loose boulders of graphite schist	0.06	9.83	
137190	2017	Vikeidet	Vedåsen	33	510 988	7 628 559	JK	JK5617-4	Weathered supracrustal gneiss with graphite schist	0.13	21.7	

132808	2017	Dverberg - Skogvoll	Sauradalen	33	537 998	7 673 835	BD	BD And 1730	Banded black schist with quartz and fine grained graphite	< 0,02	14.1	15.3
98104	2018	Møysalen	Vestpolltinden	33	523 901	7 600 662	ET	86D2	Graphite schist	< 0.02	27.1	26.9
194505	2018	Rise - Kjerkhaugen	Kjerkhaugen	33	483 963	7 622 248	BD	BD Bø 1813	Weathered graphitic schist	0.07	10.0	10.0
194506	2018	Rise - Kjerkhaugen	Kjerkhaugen	33	484 049	7 622 184	BD	BD Bø 1814	Bluish sand. Stains the fingers	(<0,02)	(2,92)	(2,85)
194520	2018	Kvernfjorden - Haugsnes	Kvernfjorddalen	33	488 589	7 621 775	BD	BD Bø 1840	Pegmatite with graphite	0.07	0.37	0.36
194512	2018	Kvernfjorden - Haugsnes	Kvernfjorddalen	33	488 571	7 622 014	BD	BD Bø 1855	Fine grained felsic gneiss with disseminated graphite	0.03	2.33	2.22
194518	2018	Kvernfjorden - Haugsnes	Kvernfjorddalen	33	488 572	7 621 859	BD	BD Bø 1857	Medium grained intermediate gneiss, small amounts of graphite	1.24	0.34	0.32
194545	2018	Rise - Kjerkhaugen	Rise	33	483 859	7 624 053	BD	BD Bø 18211a	Graphitic schist, with sulphides	5.16	4.70	4.86
194546	2018	Rise - Kjerkhaugen	Rise	33	483 859	7 624 053	BD	BD Bø 18211b	Graphitic schist, with sulphides	17.6	11.1	11.1
194564	2018	Evassåsen	Evassåsen	33	514 932	7 621 968	BD	BD Sor 1801-A	Graphitic schist, with sulphides	15.3	12.3	12.2
194565	2018	Evassåsen	Evassåsen	33	514 921	7 621 992	BD	BD Sor 1801-B	Graphite schist	1.85	2.57	2.50
194566	2018	Evassåsen	Evassåsen	33	514 917	7 621 996	BD	BD Sor 1801-C	Graphite schist	10.1	18.7	19.1
194567	2018	Evassåsen	Evassåsen	33	514 478	7 622 104	BD	BD Sor 1802	Graphite schist	0.08	8.44	8.57
194569	2018	Evassåsen	Evassåsen	33	514 477	7 622 054	BD	BD Sor 1804	Sulphide-rich schist with minor graphite	2.04	1.97	1.94
194571	2018	Evassåsen	Evassåsen	33	514 480	7 622 033	BD	BD Sor 1806	Sulphide-rich schist with minor graphite	2.11	1.42	1.39
194574	2018	Ånstad	Ånstad	33	515 583	7 623 380	BD	BD Sor 1809	Graphite schist	0.02	39.2	39.3
194575	2018	Ånstad	Ånstad	33	515 613	7 623 390	BD	BD Sor 1810	Graphite schist	0.03	40.6	40.6
194576	2018	Ånstad	Ånstad	33	515 607	7 623 382	BD	BD Sor 1811	Graphite schist, massive	0.02	37.6	37.4

194578	2018	Vikeidet	Vikeidet	33	509 552	7 627 831	BD	BD Sor 1815	Graphite schist, thinly laminated	< 0,02	12.1	12.1
194579	2018	Vikeidet	Vikeidet	33	509 539	7 627 836	BD	BD Sor 1816	Graphite schist, thinly laminated	0.18	10.1	10.1
194579	2018	Vikeidet	Vikeidet	33	509 539	7 627 836	BD	BD Sor 1816b	Blue clay	0.235	4.87	4.88
194580	2018	Vikeidet	Vikeidet	33	509 545	7 627 787	BD	BD Sor 1817	Blue clay	0.06	0.47	0.44
194581	2018	Vikeidet	Vikeidet	33	509 615	7 627 738	BD	BD Sor 1819	Graphite schist	4.33	15.5	15.5
194582	2018	Vikeidet	Vikeidet	33	509 625	7 627 734	BD	BD Sor 1820	Graphite schist thinly laminated	< 0,02	13.8	13.7
194598	2018	Smnes	Stabben	33	498 632	7 638 153	FO	FO VE 1801	Graphite schist	0.03	16.7	16.2
194391	2018	Morfjorden	Sellåter	33	487 854	7 589 584	AE	VAE206	Graphite ore	0.418	7.12	7.42
194392	2018	Morfjorden	Sellåter	33	487 854	7 589 584	AE	VAE207	Graphite schist, sulphide rich	0.235	7.64	7.97
194393	2018	Morfjorden	Sellåter	33	487 854	7 589 584	AE	VAE208	Graphite schist, sulphide rich	1.04	3.67	3.52
194395	2018	Morfjorden	Sellåter	33	487 893	7 589 188	AE	VAE210	Graphite w/ zoisite xls	4.55	5.83	5.72
198116	2018	Ånstad	Ånstad	33	515 615	7 623 379	AE	VAE231	Graphite ore	0.05	31.6	32.2
198117	2018	Ånstad	Ånstad	33	515 615	7 623 379	AE	VAE232	Graphite ore	0.03	35.1	35.6
197308	2019	Alsvåg	Instøya	33	512 291	7 644 071	AE	vae247a	Graphite schist	1.14	17.2	17.1
197310	2019	Alsvåg	Instøya	33	512 272	7 644 037	AE	vae248	Graphite schist	1.95	3.59	3.50
197311	2019	Alsvåg	Instøya	33	512 280	7 644 037	AE	vae249	Graphite schist	0.24	19.6	18.9
197312	2019	Alsvåg	Instøya	33	512 280	7 644 037	AE	vae250	Graphite schist	3.95	2.97	2.84
194928	2019	Sæterstranda	Sæterstranda	33	514 266	7 638 389	BD	BD Sor 19147a	Graphite schist	0.22	17.7	16.2
194929	2019	Sæterstranda	Sæterstranda	33	514 266	7 638 389	BD	BD Sor 9147b	Graphite schist	1.03	12.2	12.1
194930	2019	Sæterstranda	Sæterstranda	33	514 266	7 638 389	BD	BD Sor 19147c	Graphite schist	0.71	20.8	19.1
194973	2019	Alsvåg	Hundneset	33	511 848	7 643 253	BD	BD Øks 1958	Fine grained felsic gneiss	< 0,02	0.20	0.17
194974	2019	Alsvåg	Hundneset	33	511 908	7 643 227	BD	BD Øks 1959	Fine grained felsic gneiss	1.49	0.40	0.39
194997	2019	Alsvåg	Instøya	33	511 651	7 643 803	BD	BD Øks 9140a	Fine grained felsic gneiss	1.94	1.33	1.30
194998	2019	Alsvåg	Instøya	33	511 651	7 643 803	BD	BD Øks 9140b	Graphite schist	0.02	15.3	15.4
194999	2019	Alsvåg	Instøya	33	511 651	7 643 803	BD	BD Øks 9140c	Graphite schist	< 0,02	17.6	17.9
195000	2019	Alsvåg	Instøya	33	511 651	7 643 803	BD	BD Øks 9140d	Graphite schist	0.42	9.54	8.81

195001	2019	Alsvåg	Instøya	33	511 628	7 643 774	BD	BD Øks 19141	Graphite schist	0.11	23.1	21.0
195008	2019	Alsvåg	Instøya	33	511 878	7 643 762	BD	BD Øks 19149	Graphite schist	1.89	4.15	4.04
195015	2019	Alsvåg	Instøya	33	513 054	7 644 535	BD	BD Øks19176a	Graphite schist	0.18	8.88	8.37
195016	2019	Alsvåg	Instøya	33	513 054	7 644 535	BD	BD Øks19176b	Graphite schist	0.06	11.6	9.03
195017	2019	Alsvåg	Instøya	33	513 065	7 644 549	BD	BD Øks 19177	Graphite schist	0.18	5.64	5.19
195018	2019	Alsvåg	Instøya	33	513 087	7 644 567	BD	BD Øks 19179	Graphite schist	0.11	13.0	12.0
195019	2019	Alsvåg	Instøya	33	513 164	7 644 631	BD	BD Øks 19180	Graphite schist	0.02	11.6	11.0
195020	2019	Alsvåg	Instøya	33	513 258	7 644 683	BD	BD Øks 19181	Graphite schist	0.21	9.09	7.64
195021	2019	Alsvåg	Instøya	33	513 118	7 644 777	BD	BD Øks19185a	Fine grained felsic gneiss	1.35	7.44	6.37
195022	2019	Alsvåg	Instøya	33	513 118	7 644 777	BD	BD Øks19185b	Fine grained felsic gneiss	0.49	2.66	2.47
195023	2019	Alsvåg	Instøya	33	513 074	7 644 785	BD	BD Øks 9186a	Graphite schist	0.05	11.2	10.2
195024	2019	Alsvåg	Instøya	33	513 074	7 644 785	BD	BD Øks19186b	Graphite schist	0.02	5.19	4.89
195025	2019	Alsvåg	Instøya	33	512 673	7 644 463	BD	BD Øks19192a	Graphite schist	2.81	2.21	2.06
195026	2019	Alsvåg	Instøya	33	512 673	7 644 463	BD	BD Øks19192b	Graphite schist	0.08	4.92	4.83
195027	2019	Alsvåg	Instøya	33	512 766	7 644 584	BD	BD Øks 19198	Graphite schist	0.10	10.6	9.64
195028	2019	Alsvåg	Instøya	33	512 733	7 644 559	BD	BD Øks 19199	Graphite schist	0.92	6.85	6.34
195029	2019	Alsvåg	Instøya	33	512 792	7 644 654	BD	BD Øks 19202	Graphite schist	0.62	13.4	10.6
195030	2019	Alsvåg	Instøya	33	512 778	7 644 656	BD	BD Øks 19203	Graphite schist	0.10	9.88	9.81
195031	2019	Alsvåg	Instøya	33	512 755	7 644 613	BD	BD Øks 19206	Graphite schist	0.04	9.18	8.05
195032	2019	Alsvåg	Instøya	33	512 622	7 644 466	BD	BD Øks 19208	Graphite schist	2.17	2.23	2.11
195045	2019	Alsvåg	Alsvåg	33	511 154	7 643 640	BD	BD Øks19273a	Rusty weathered graphite schist	4.18	1.38	1.30
195046	2019	Alsvåg	Alsvåg	33	511 154	7 643 640	BD	BD Øks 19273b	Rusty weathered graphite schist	4.47	4.13	3.29
195047	2019	Alsvåg	Alsvåg	33	511 218	7 643 568	BD	BD Øks 19276a	Graphite schist	0.06	16.0	13.0
195048	2019	Alsvåg	Alsvåg	33	511 218	7 643 568	BD	BD Øks 19276b	Graphite schist	2.48	3.22	2.73
195049	2019	Alsvåg	Alsvåg	33	511 312	7 643 471	BD	BD Øks 19281	Graphite schist	0.04	19.8	19.8
195053	2019	Alsvåg	Straumen	33	509 967	7 645 025	BD	BD Øks 19295	Graphite schist	1.66	0.69	0.61
195054	2019	Alsvåg	Straumen	33	509 803	7 645 108	BD	BD Øks 19296	Graphite schist	0.33	3.31	3.07
195055	2019	Alsvåg	Straumen	33	509 800	7 645 218	BD	BD Øks 19297	Graphite schist	0.30	27.0	26.9

195056	2019	Alsvåg	Straumen	33	509 667	7 645 214	BD	BD Øks 19299	Graphite schist	0.46	22.3	22.0
195057	2019	Alsvåg	Straumen	33	509 648	7 645 224	BD	BD Øks 19300	Graphite schist	0.90	5.26	5.29



GEOLOGICAL
SURVEY OF
NORWAY

· NGU ·

Geological Survey of Norway
PO Box 6315, Sluppen
N-7491 Trondheim, Norway

Visitor address
Leiv Eirikssons vei 39
7040 Trondheim

Tel (+ 47) 73 90 40 00
E-mail ngu@ngu.no
Web www.ngu.no/en-gb/